Faculty of Science and Engineering

Department of Petroleum Engineering

An Investigation on the Pore Pressure for the Potential Shale Gas Intervals in the Perth and Canning Basins

Abualksim Ahmad

This thesis is presented for the Degree of

Doctor of Philosophy of

Curtin University

August 2015

Declaration

To the best of my knowledge and belief this thesis contains no material previously published by any other person except where due acknowledgment has been made.

This thesis also contains no material which has been accepted for the award of any other degree or diploma in any university.

Signature: 

Date: 13/08/2015

Abstract

The Perth and Canning Basins of Western Australia are still classified as exploration areas for gas shale resources. Amongst other formation characteristics, the shale's pore pressure is an important parameter, particularly when it is studied in conjunction with other shale characteristics such as thermal maturity and total organic content (TOC). Many studies have indicated that the higher the gas saturation in shale formations, the greater the possibility of inducing higher pore pressure. Hence, the ability to host profitable. A combined study of the shale gas parameters would lead to a better understanding and assessment of the candidate formations. Therefore, this may be used for the identification of the sweet spots within the shales. This research involves a broad investigation on the pore pressure for the potential shale gas intervals namely the Kockatea Shale in the Perth Basin and the Laurel Formation in the Canning Basin.

In the Perth and Canning Basins, not many wells were drilled particularly to evaluate gas shale formations. In addition, there are very limited pore pressure measurement data available that can assist in outlining the overall pressure regime. Not only has there been no previous regional experience for estimating overpressure in the Perth and Canning Basins, but the possible origin of overpressure whenever exist has also not been identified in the studied formations. Furthermore, the different tectonic elements (uplifting, erosion and subsidence) of the two basins have influenced their geometry, where they are characterized into compartmentalised regions such as troughs, sub-basins and ridges. However, as some geochemical data (i.e. high thermal maturity) have recently become available, it is significant to study the type of pore pressure regime in place for the candidate formations. Moreover, the effects of the tectonic features on the pore pressure regimes can thus be identified.

This research examined various sets of data including well log, mud log, drilling reports, structural features, seismic interpretation, conventional core images, mineralogical and geochemical data. A detailed study of the aforementioned data was essential to come up with the most suitable correlation between the existence and preservation of overpressure and the local tectonic and structural elements in the

gas shale formations. Indeed, this is a newly established relationship and no previous researchers have addressed this issue**.** This research has also assessed the suitability of the overpressure estimation method, examined the origins of overpressures wherever exist and improved the methodologies that were initially proposed by previous authors.

Based on the results and analysis, overpressure has been observed in certain regions of the studied formations. In contrast, the other regions displayed normal pore pressure in the same intervals. The wells that were drilled in the uplifted and tectonically active areas exhibited normal pressure. On the other hand, the wells that were drilled in areas with less tectonics intensity displayed overpressure gradients. The distribution of overpressure within the studied gas shale layers is attributed to local tectonic activities that have taken place sequentially in the basin. This correlation was observed in the Kockatea Shale in the Perth Basin and was further endorsed by the study on the Laurel Formation of the Canning Basin. In addition, upon testing different values for the x exponent in Eaton's correlation for the overpressure estimation within the studied regions, it was determined that the best fit for Eaton's exponent is the value of 2. Moreover, a thorough multi-disciplinary study was conducted to examine the cause of overpressure in the studied formations. The work comprised of the integration of a large geochemical, geological and mineralogical data with the analysis of the well log data response. The results evidently pointed to clay transformation and lateral tectonic loading being the main overpressure generating mechanisms in the Kockatea Shale of the Perth Basin, whereas compaction disequilibrium and hydrocarbon generations were the possible causes for generating overpressure in the Laurel Formation of the Canning Basin.

Dedication

To my parents, who have been and are my inspiration.

Acknowledgements

First and foremost, I am grateful to God for blessing me with good health and overall well-being, which enabled me to complete this work.

My sincere thanks go to my supervisor, Prof Reza Rezaee, for his continuous support, patience, motivation and enormous wealth of knowledge. His outstanding supervision was critical in helping me through the entire process. I am very appreciative of his time, ideas and guidance; without which, I would not be able get to this point. It has been an honour to be Reza's student.

I am also grateful to the rest of my thesis committee - Prof Brian Evans, Prof Vamegh Rasouli and Dr Ali Saeedi. I would like to take this opportunity to express special thanks and appreciation to all colleagues, friends and staff of the Department of Petroleum Engineering at Curtin University, for their help and support. I also owe thanks to Curtin University for their patience, especially when there were issues with regards to my sponsorship.

In addition, I am grateful to the Western Australia Department of Mines and Petroleum for providing me with full access to the Western Australian Petroleum and Geothermal Information Management System (WAPIMS), which has the necessary database required to conduct this research.

My heartfelt thanks go to my parents for an upbringing grounded in faith. I thank my father Asseni Alwafi, for instilling in me the love of science. My father has always been the main inspiration in my life. I honestly have no words to express the gratitude I feel towards my mother, Fayza Shalaik, for her unwavering support.

Finally, I would like to thank my beloved wife, Suaad Ahmed, for her unconditional support and absolute understanding in the past twelve years. I could not have succeeded without her unwavering love, constant encouragement and sometimes "loud patience". Suaad's support is the foundation upon which my life has been shaped these twelve years. I would like also to thank my beloved children, Yasmene, Youmna and Yazan.

Publications

Parts of this thesis have been published in the following book chapter and journal papers:

Book chapter

1. **Ahmad, A**., Rezaee, R. (2015). Pore pressure prediction for shale formations using well log data. In Fundamentals of Gas Shale Reservoirs, John Wiley & Sons, Inc. First Edition.

Journal papers

1. **Ahmad, A**., Rezaee, R., & Rasouli, V. (2014). Significance of compressional tectonic on pore pressure distribution in Perth Basin. *Journal of Unconventional Oil and Gas Resources*, *7*, 55-61.
2. **Ahmad, A.,** Rezaee, R. (2015). The origin of overpressure in shale gas "Multidisciplinary approach": A case study from the Perth Basin, Australia (Under preparation).
3. **Ahmad, A**., Rezaee, R. (2015). Using seismic interpretation, conventional core images and log data to identify the interrelation between overpressure in shale and tectonic activities (Under preparation).
4. **Ahmad, A.,** Rezaee, R. (2015). Pore pressure evaluation for the Laurel Formation in the Canning Basin, Western Australia (Under preparation).

Table of Contents

List of Figures

List of Tables

List of Abbreviations and Acronyms

Abbreviation	**Log Name (unit)**
CALI	Caliper Log (inch)
C_n	Normal conductivity (1/ohm-m)
C_o	Observed conductivity (1/ohm-m)
CNC	Borehole size Corr-d Compensated Neutron Porosity (%)
ECD	Equivalent Circulation Density (psi/ft)
EDM	Equivalent Depth Method
ESM	Effective Stress Method
d_{co}	Observed drilling exponent
d_{cn}	Normal drilling exponent
Δt_n	Normal sonic transit time (µs/ft)
Δt_o	Observed sonic transit tie (µs/ft)
DRHO/DCOR/DRHB /HDRA/ NRHO/ZCOR	Density Correction (gm/cc)
DMP	Department of Mines and Petroleum
DST	Drill Stems Tests (psi)
g_p	Pore pressure gradient (psi/ft)
g_{ob}	Overburden gradient (psi/ft)
g_n	Normal pore pressure gradient (psi/ft)
DT	Sonic Transit time Log (µs/ft)
DTCO	Compressional Wave Transit time Log (µs/ft)
GR	Gamma Ray (API)
ILD	Induction Deep Resistivity (ohm-m)
K/POTA	Potassium
LLD/HLLD/DLL	Resistivity Log (Deep Laterolog) (ohm-m)
MDT	Modular Formation Dynamic Tester (psi).
Mud wt	Mud Weight Gradient (psi/ft)
NCT	Normal Compaction Trend
NCT_Son	Normal Compaction Trend from Sonic Log (µs/ft)
NGS	Natural Gamma Ray Spectrometry logs
NPHI	Neutron Porosity (%)
NPOR	Enhanced Thermal Neutron Porosity (%)
OBGrad	Overburden gradient (psi/ft)
OBPres	Overburden pressure/stress (psi)
PPG_Son	Pore Pressure Gradient estimated from Sonic Log (psi/ft)
PP_Son	Pore Pressure estimated from Sonic Log (psi)
PEF/PE/PEFZ	Formation Photoelectric Factor (B/E)
PHND	Porosity from Enhanced Density (%)
Res	Resistivity (ohm-m)

Ro or VR	Vitrinite Reflectance (%)
ROP	Drilling rate of Penetration (meter/hr)
RhoGrad	Density estimated by Gardner method (g/cc)
RHOB/DEN/ ZDEN/ RHOZ	Bulk Density Log (g/cc)
RPM	Revolutions Per Minute (rpm)
RFT	Repeated Formation Test (psi)
R_n	Normal resistivity (ohmm)
Ro	Observed resistivity (ohmm)
SN	Resistivity Log (ohm-m)
SP	Spontaneous Potential log (mv)
S_{hmin}	Minimum Horizontal Stress (psi)
S_{hmax}	Maximum Horizontal Stress (psi)
σe	Vertical effective stress (psi)
σob	Overburden Stress (psi)
δ 13 C2	Ethane Isotope
S_v	Vertical Stress (psi)
Th	Thorium
Tmax	Thermal Maturity (°C)
TOC	Total Organic Content
TNPH	Thermal Neutron Porosity (%)
TVD	True Vertical Depth (m)
U	Uranium
USGS	United States Geological Survey
VCLAY	Volume of Clay (%)
VCLGR	Volume of Clay from Gamma Ray (%)
WOB	Weight on Bit (tonne)
XRD	X-Ray Diffraction

Chapter 1 Introduction

1.1 Unconventional Gas Reservoirs

The term ‘unconventional gas reservoir’ is used in the oil and gas industry and refers to a low-permeability reservoir with commercial hydrocarbon accumulation (Naik 2003; Holditch 2006). Several unconventional reservoir**s** that developed in the past were of sandstone; but with the advancement in drilling technology and hydraulic fracturing treatment, gas is now also produced economically from other rocks such as shales.

According to Schenk (2004), the United States Geological Survey (USGS) defined an unconventional gas reservoir to have the following - regional extent, diffuse boundaries, a large in-place resource with a very low recovery factor, a geological sweet spot, a low matrix permeability, reservoir properties generally in close proximity to source rocks, a lack of a traditional trapping or sealing mechanism and to be commonly over-pressured.

Due to the wide availability of conventional gas reservoirs, the unconventional resources have not received proper consideration from operators in the past, and there has been little commercial interest in investing in these resources (Rogner 1997). This negligence is also attributed to the rarity of geologic and engineering information about unconventional resources, the uncertainties associated with evaluating these formations and the market conditions (Schmoker and Klett 1999). Therefore, limited information has become readily available as references when assessing their potential for commercial production (Magoon 1988).

However, the exploitation of conventional reservoirs, together with the increase in price of natural gas, has attracted attention for investment in unconventional gas reservoirs (Rogner 1997; Reeves et al. 2007). Research and development concerning the formation evaluation, geologic controls and production techniques from these unconventional gas resources have been advanced and many new technologies were developed during the last few decades (Ratner and Tiemann 2013). However, due to the complexities and variations in characterization of the unconventional reservoirs, many questions remain unanswered and require further investigations.

Holditch et al. (2007) has summarized the worldwide distribution of unconventional gas resources (Figure 1-1). This includes Tight-Sand Gas, Coal bed Methane and

Shale Gas. Kawata and Fujita (2001) also mentioned that several geologic basins around the world contain unconventional gas reservoirs. For instance, the unconventional gas contributed approximately 10% of the total gas production in the United States in 1990. Nowadays, the figure has risen to over 40% and the estimated supply from unconventional reservoirs is projected to grow rapidly to over 50% by 2020 (Kuuskraa and Stevens 2009). It is important to state that shale gas is driving this growth (Medlock et al. 2011).

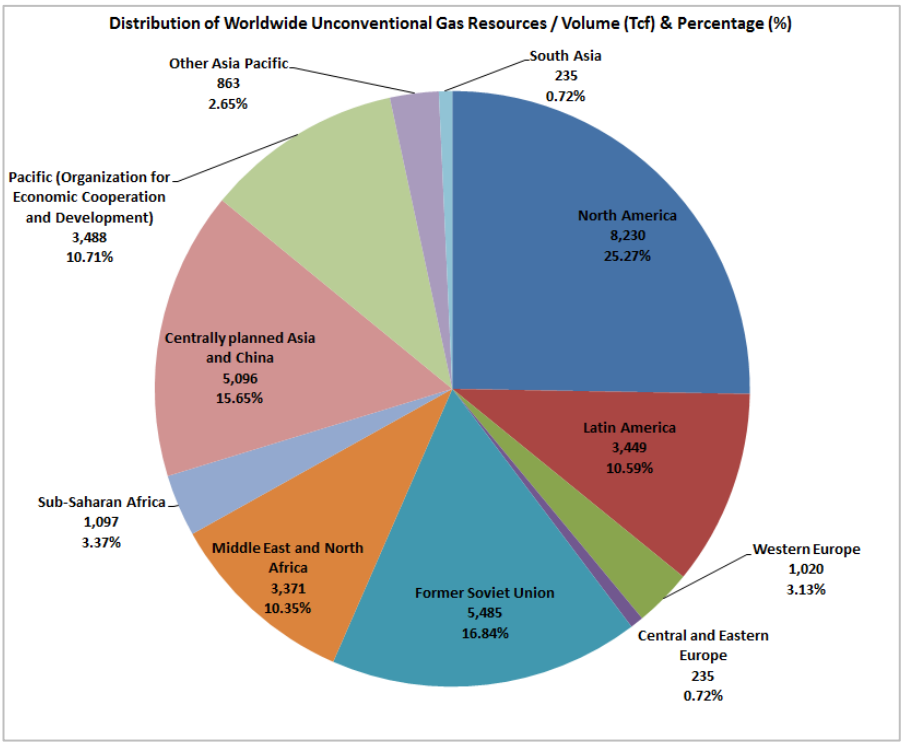

Figure 1-1: Distribution of Worldwide Unconventional Gas Resources, extracted from (Holditch et al. 2007).

1.2 Shale Gas Reservoirs

A shale gas reservoir is defined as an organic rich fine-grained formation that is typically a source rock and also functions as a reservoir rock with continuous hydrocarbon accumulations (Read 1991; Schmoker 1995). In terms of the lithology and reservoir characterizations, several types of shale gas systems exist (Jarvie et al. 2007). These systems include: (1) shales with high thermal maturity such as Barnett Shale in the Fort Worth Basin, (2) low thermal maturity shales such as some of the New Albany Shales in the Illinois Basin, (3) mixed lithology systems comprising shale, silts and sands (intraformational), for example, Bossier Shale in East Texas,

(4) interformational systems in which gas is generated in a high maturity shale and stored in a shale with less maturity, an example being Tertiary Waltman Shale in the Wind River Basin and (5) combination systems that contain both conventional and unconventional reserves (e.g. the Woodford Shale).

Shale gas reservoirs became important resource players in the United States in 2004, accounting for over 14% of the produced gas (Jarvie et al. 2007). Gas in shales can be found in low-matrix-permeability rocks, in the form of free gas within the pore spaces or stored by the adsorption onto organic matters contained within the shales (Schmoker 1995).

The successful gas production from shales in the US has drawn the attention of the world's energy industry. As illustrated in Figure 1-2, there is a significant gas reserve within shale gas resources in various places around the world (Kawata and Fujita 2001).

In Australia, the Perth and Canning basins constitute two major sedimentary basins in West Australia and therein major oil and gas discoveries from conventional reservoirs have already been approved (Geoscience Australia 2003). In recent years (led by the successful gas production from shales in the US), as a result of the advances in technology in the past three decades, as well as the forecasting of Western Australia's domestic gas supply dropping below demand by 2016, several projects have started investigation for possible gas discoveries from several potential shale gas formations in the Perth and Canning Basins (Curtis 2002; Haworth 2013). As illustrated in Figure 1-3, the Perth and Canning Basins contain several prospects for potential shale gas discoveries.

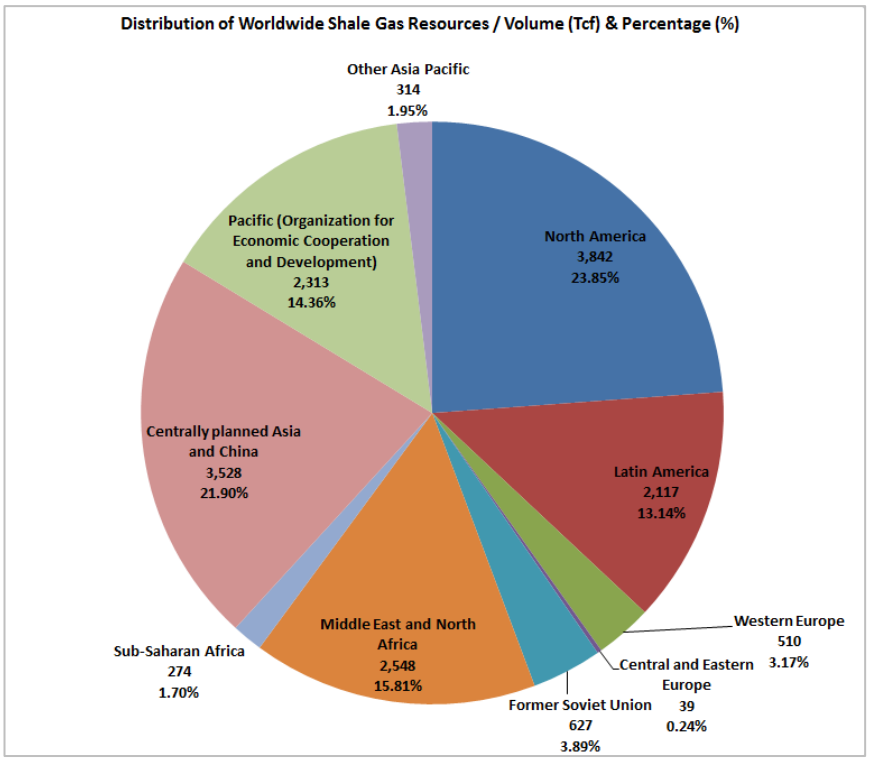

Figure 1-2: Distribution of the Worldwide Shale Gas Reservoirs, extracted from (Holditch et al. 2007).

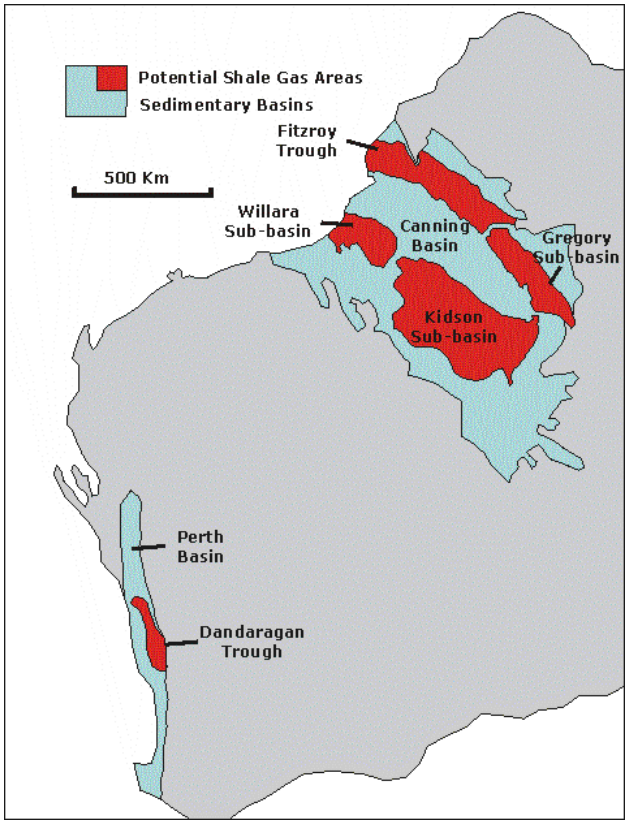

Figure 1-3: Sedimentary basins and potential shale gas areas in Western Australia. Extracted from (DMP 2014).

The recent advances in technology have made the production potential from shales more economically viable through an efficient formation evaluation and appropriate development. As stated in Section 1.1, among other reservoir characteristics, reservoir pore pressure needs to be thoroughly investigated in order to reach a proper formation evaluation outcome. One of the common parameters of the potential shale gas reservoir is being abnormally high pressured (overpressured).

1.3 Motivations and research objectives

Several sedimentary basins around the world display some sort of abnormal pore pressure, particularly abnormal high-pressure (overpressure). The overpressure phenomenon is commonly found in low permeability intervals such as shale formations, as they tend to retain overpressures as compared to other kind of rock types (Osborne and Swarbrick 1997).

Many studies in several parts of the world have indicated with high probability that the higher the gas saturation in shale formations, the greater the possibility of inducing higher pore pressure. Hence, the ability to host profitable hydrocarbon reserves and production capability are greater (Fertl 1973; Chatellier et al. 2011).

As the oil and gas industry evolves, ongoing research investigates the ability for economical production from the unconventional shale gas reservoirs. Shale's pore pressure is an important parameter, particularly when it is studied in conjunction with other shale characteristics such as thermal maturity and total organic contents (TOC). A combined study of shale gas parameters would lead to a better understanding and assessment of the candidate formations. Therefore, this may be used for the identification of the sweet spots within the shales.

In the Perth and Canning Basins, there are limited numbers of wells that have been drilled for the purpose of evaluation of shale gas layers. From the drilled wells, there are very limited measured pore pressure data available that can help to draw-up an overall pressure regime. Moreover, no research has been previously conducted to assess pore pressure in shale formations in these basins. More importantly, in these basins, there are different tectonic features such as uplifting, erosion and subsidence. With some geochemical data (high thermal maturity) that have become available in various regions that have different tectonic elements, it is significant to study what sort of pore pressure regime is in place for the candidate formations and what effects that the tectonic features have on pore pressure regimes. This study will be limited to

studying pore pressure in two potential shale gas formations, namely the Kockatea Shale in the Perth Basin and the Laurel Formation in the Canning Basin. The aim of this research is to address the following objectives:

- evaluate pore pressure in the shale intervals in the Perth and Canning Basins using well log data, mud log data and drilling parameters to understand pore pressure regimes in these formations;
- identify and map any abnormal high pressure (overpressure) encountered in the candidate formations;
- study pore pressure regimes in tectonically stable regions and in regions with intensity in tectonic activities, in conjunction with the geochemical properties such as Thermal Maturity (Tmax) and Vitrinite Reflectance (VR);
- compare the results of the two case studies and evaluate the distribution of overpressure in the areas and establish the most suitable correlation;
- consider how tectonic activities influence pore pressure distribution in shale gas formations (The well log data, seismic characters and conventional core images will be examined to validate the results); and
- investigate the overpressure generating mechanisms, where the analysis includes the response of wireline logs, cross-plots of well logs data, compositional variations study, geochemical and gas composition analysis and stress data.

In accomplishing the above aims, the overall objective is to establish a new theory that correlates the occurrence and preservation of overpressure in the shale to the local tectonic activities. To date, there have been no studies that have addressed this issue and the concepts of such circumstances are not properly understood. Practically, the understanding of such concepts will be of great significance for the well-planning process, in terms of the prospective outcome in penetrating highly viable formation, which can be risky otherwise.

The database includes well logs data, mud log data, well completion reports, limited measured pore pressure data, temperature data, hydrocarbon maturation data, geochemical data, seismic and conventional cores. These data sets were supplied by the Department of Mines and Petroleum (DMP) in Western Australia.

1.4 Thesis outline

In this chapter, an overview of shale gas reservoirs has been provided. The motivations and objectives of this study have also been stated. Chapter 2 includes the geological settings of the Perth and Canning Basins. The theoretical background and methods of work are described in Chapter 3 and Chapter 4 respectively.

Chapter 5 comprises of the analysis of pore pressure in the Kockatea Shale in the Perth Basin. The chapter starts with an overview of the data that are available for the Kockatea Shale. The Kockatea Shale was chosen because it constitutes a uniform lithological section that makes it ideal for analysis. Afterward, the data is analysed and the pore pressure is evaluated in tectonically stable regions (Dandaragan trough and Beharra Springs Terrace) as well as the tectonically active localities (Beagle uplify and Northampton uplift). The role of tectonic activities on pore pressure distribution in shales is then explained. Moreover, a thorough multidisciplinary approach is presented to ascertain the origins of overpressure in the Kockatea Shale.

Chapter 6 comprises of pore pressure and its relation to the local tectonic activities in the Laurel Formation in certain regions of the Canning Basin. The purpose of chapter 6 is to examine whether the theory that was established in the Perth Basin is applicable universally or just locally for the Perth Basin. In Chapter 7, general discussions are provided alongside the concluding remarks.

Chapter 2 Geological settings of the Perth and Canning Basins

2.1 Regional setting of Perth basin

The Perth Basin is a north-northwest trending located in the southwest part of Western Australia. The basin covers approximately 100,000 km^2 on the western coast of Australia. It extends from Geraldton to Augusta (Crostella and Backhouse 2000). The basin comprises of sedimentary sections that vary from Silurian to Pleistocene (Mory et al. 2005). The eastern boundary of the basin is marked by the north-south trending Darling fault, whereas the western end margin extends to the edge of the continental crust, offshore in water depths of up to 4500 m (Iasky and Mory 1993). The Northampton Block constitutes the northern boundary of the basin and separates it from the Carnarvon Basin in the north (Iasky and Mory 1993), while the southern boundaries extend to the edge of the continental shelf (Figure 2-1)

2.2 Basin evolution and structural features

The Basin was initially formed through the rifting and break-up of the Indian and Australian plates that began in the Permian and this was a major structural event in the Perth basin (Crostella 1995). Song and Cawood (2000) expressed that the rifting and sagging which occurred along the western continental margin caused the development of a series of normal faults that dominate the Perth Basin structure. As the drifting took place, the structure was filled by sediments which originated from the Yilgarn Craton during the late Permian through to Cretaceous periods (Iasky and Mory 1994).

The structural history of the Perth Basin is controlled by two major phases of extension. The first is an Early Permian phase that centralizes near the Northampton High (Crostella 1995). A period of uplift and subsequent erosion that occurred in the Late Permian concluded this period of basin development. The second and more widespread phase of extension took place from the Late Jurassic to the Early Cretaceous periods, during the separation of the Australian Plate from Greater India and Africa (Harris 1994).The centre of the second uplifting phase is near the coastal town of Jurien within the Beagle Ridge, where significant sections were removed. According to Song and Cawood (2000), this phase resulted in an extensive uplifting and basin inversion, as well as the development of transfer faults, which affected the geometry and divided the basin into a series of structural terraces that step down

from the centre of the uplifting in the Beagle Ridge to the Dandaragan Trough in the east (Quaife et al. 1994).

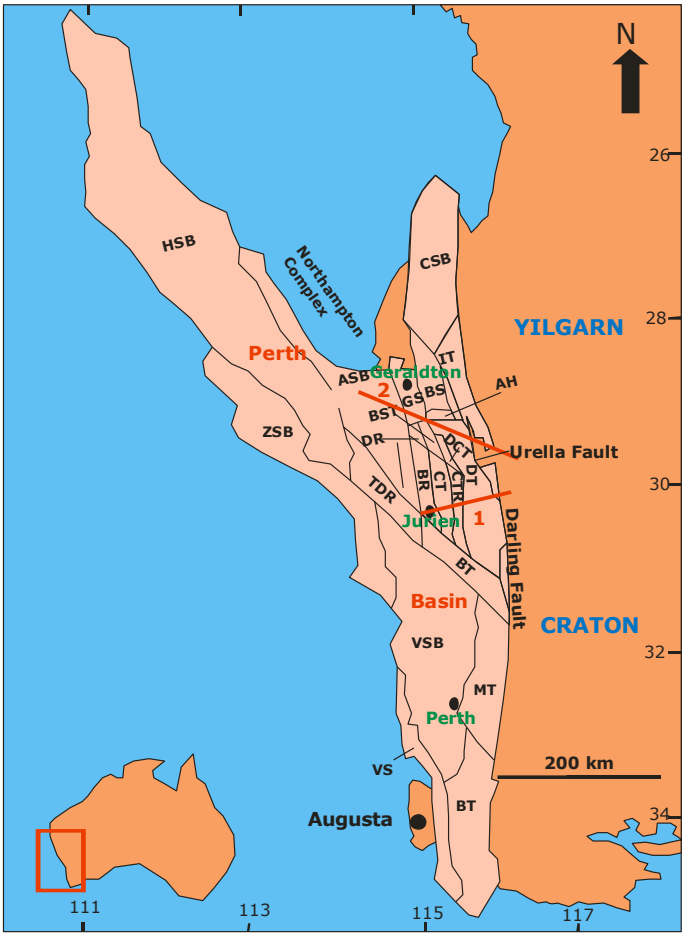

Figure 2-1: The map illustrates the regional setting and structural features of the Perth Basin. Tectonic elements labelled are the Bunbury Trough (BT), Vasse Shelf (VS), Mandurah Terrace (MT), Vlaming Sub-Basin (VSB), Beermullah Trough (BT), Turtle Dove Ridge (TDR), Dandaragan Trough (DT), Coomallo Trough Ridge (CTR), Cadda Terrace (CT), Beagle Ridge (BR), Donkey Creek Terrace (DCT), Baharra Springs Terrace (BST), Dongara Ridge (DR), Irwin Terrace (IT), Allanooka High (AH), Bookara Shelf (BS), Greenough Shelf (GS), Coolcalalaya Sub-Basin (CSB), Abrolhos Sub-Basin (ASB), Houtman Sub-Basin (HSB) and Zeewyck Sub-Basin (ZSB) Modified from (Bradshaw 2003).

According to the data from several wells that were drilled in the Perth Basin, extensive faulting systems were identified within the Kockatea Shale in areas of immediate vicinity to the centres of the two extension phases. This includes the Beagle Ridge and the adjacent Cadda Terrace in the centre of the Basin and the

Northampton High in the Northern Perth Basin. In addition, the severe erosion and uplifting that occurred in these areas have caused the removal of significant parts of the Kockatea Shale. The intensity of faulting within the Kockatea Shale decreases with the increases in distance from the centres of uplift (Figure. 2-2).

2.3 Perth Basin Subdivisions

The aforementioned tectonic evolution influenced the geometry of the basin and further divided it into compartmentalised regions characterized as troughs, sub-basins and ridges of similar structures, producing the current geological structure of the Perth Basin. The structural character and maximum stress direction in the Perth Basin are explained below and illustrated in Figure 2-4.

2.3.1 Beagle Ridge

The Beagle Ridge is characterized as the most uplifted area in the Perth Basin which has a shallow basement. It is important to note that the centre of the second uplifting phase is located within the Beagle Ridge (Figure 2-2). Due to an extensive basin inversion and uplifting, up to 8 km of the section has been removed (Crostella 1995). The ridge is bounded by the Beagle Fault System and the Cadda Terrace to the east, whereas the Geraldton Fault and the Abrolhos Sub-basin bound it to the west. It has 1000 to 3000 m of Permian to Mid-Jurassic sedimentary sections (Mory and Iasky 1996).

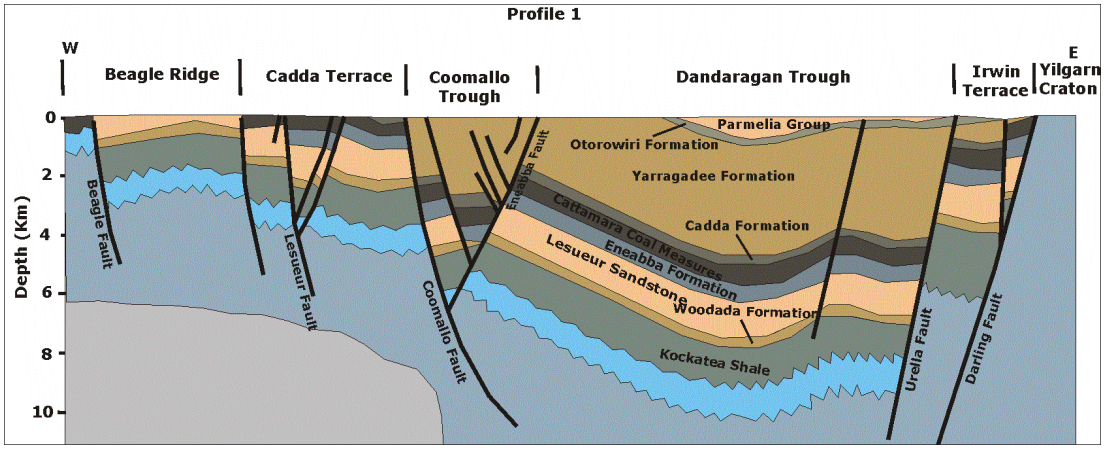

Figure 2-2: East–west structural section across the Beagle Ridge, Cadda Terrace, Coomallo Trough and Dandaragan Trough (Profile 1 as per Figure 2-1) (modified from (Song and Cawood 2000)).

2.3.2 Cadda Terrace

The Cadda Terrace is an intermediate terrace of north-south trending that is situated on the eastern margin of the Beagle ridge in the Northern Perth Basin. The terrace is bounded on the east by the Coomallo Fault and the Coomallo Trough, whilst, the northern boundary is defined by the Abrolhos Transfer Fault. The Cervantes Transfer Fault bounds the terrace on the south. The terrace is classified by a complex faulting system, that increasingly steps down with the depth from the Beagle Ridge (Thomas 1979).

2.3.3 Coomallo Trough

The Coomallo Trough lies between the Cadda Terrace to the west and the Dandaragan Trough to the east. It is bounded by the Abrolhos Transfer Fault to the north and the Cervantes Transfer Fault to the south. The Eneabba Fault bounds the trough to the east and the Coomallo Fault to the west (Iasky and Mory 1994). The features of the Coomallo Trough are intermediate between the characteristics of the Cadda Terrace and those of the Dandaragan Trough. However, the thickness and depth of sediments are comparable with the Dandaragan Trough (Crostella 1995). This implies that the uplifting and subsequent erosion have had insignificant effects on sediments within this region and beyond.

2.3.4 Dandaragan Trough

The Dandaragan Trough is a major depocentre of the Northern Perth Basin which covers approximately 5000 km^2. It is an elongated north-south oriented half-graben defined to the east by the Darling and Urella faults, occupying most of the onshore Perth Basin. It is virtually an unfaulted syncline and has the thickest sediment accumulation of approximately 12000 m (Crostella 1995). The Mountain Bridge Fault forms the western edge of the northern portion of the trough. This fault showed a progressive down-dip that decreases the dip angle from significantly high angles ranges at the top of 65° to 20° at the base of the sedimentary cover (Figure 2-3). The mid-southern section of the trough is defined by the Eneabba Fault that declines in dip from 62° at the surface to 42° at a depth of 10 km (Song and Cawood 2000). The Allanooka Transfer Fault constitutes the northern boundary of the Dandaragan Trough. The fault separates the trough from the Allanooka High to the north. The Urella Fault and the Darling Fault systems form the eastern boundary of the trough,

while the Cervantes Transfer Fault forms the southern boundary of the Dandaragan Trough and separates it from the Beermullah Trough (Figure 2-4).

2.3.5 Donkey Creek Terrace

The Donkey Creek Terrace is located between the Dandaragan Trough to the east and the Beharra Springs Terrace to the west. The Abrolhos Transfer Fault bounds the terrace to the south and it is bounded by the Eneabba Fault to the north and east. The western boundary of the terrace is marked by the easternmost fault of the Beharra Springs-Mondarra - Yardarino trend (Crostella 1995). This small terrace covers a tectonically stable area where no or limited strike-slip movement has taken place. Furthermore, Crostella (1995) expressed that within this terrace, northerly trending faults disappear and the easterly trending faults of the northern and adjacent Allanooka High do not extend into it.

2.3.6 Baharra Springs Terrace

The Beharra Springs Terrace is an intermediate terrace that is located between the Donkey Creek Terrace to the east and the Dongara Terrace to the west and covers approximately 500 km^2. The terrace is bounded by the Allanooka Fault to the north and the Abrolhos Transfer to the south. The western boundary is marked by the Mountain Bridge Fault and to the east, by the easternmost fault of the Beharra Springs – Mondarra – Yardarino trend (Crostella 1995).

The Beharra Springs structure resulted initially from the Permian arching along north-northwest to south-southeast strike direction (Owad-Jones and Ellis 2000). A series of faults with similar orientations were developed during the late Permian, creating a number of structural terraces that step down from the Beagle Ridge in the west to the Dandaragan Trough in the east. These terraces have been accentuated by tectonism during the Early Cretaceous, which revived some of the older faults (Cadman et al. 1994). Further faults that related to this tectonism established a separate system in the younger strata, detached from the older faults by the Triassic formation of Kockatea Shale (Owad-Jones and Ellis 2000).

2.3.7 Dongara Ridge

The Dongara Terrace is an intermediate terrace between the Beharra Springs Terrace to the east and the Beagle Ridge to the south. The eastern boundary of the terrace is defined by Mountain Bridge Fault and it is bounded to the west by the Beagle Fault. The Allanooka Fault constitutes the northern boundary and the Abrolhos Transfer Fault bounds the ridge to the south (Jones and Pearson 1972).

2.3.8 Greenough Shelf

The Greenough Shelf is an area of shallow basement located between the Allanooka High to the east, the Northampton Complex that outcrops to the north and the Dongara Terrace to the south (Crostella 1995). The eastern and southern boundaries are the Mountain Bridge and Allanooka Faults respectively. The shelf contains up to 1500 m of Mesozoic and Permian sediments. Mory and Iasky (1996) stated that the shelf seems to be greatly influenced by the Late Permian phase of extension that centralized around the Northampton High and have caused severe uplift and erosion.

2.3.9 Allanooka High

The Allanooka High is located in the northern of the Dandaragan Trough, between the Greenough Shelf to the west and the Irwin Terrace to the east (Crostella 1995). The basement shallows as we approach the centre of the uplifting to the north. The Urella Fault marks the Allanooka High to the east and the Mountain Bridge Fault forms the western boundary. There is a gradual transition to the Dandaragan Trough to the south, but the Allanooka High is distinguished from the Dandaragan Trough by the change in structural style from northerly striking faults in the latter to east-northeasterly and easterly striking faults in the former (Iasky and Mory 1994).

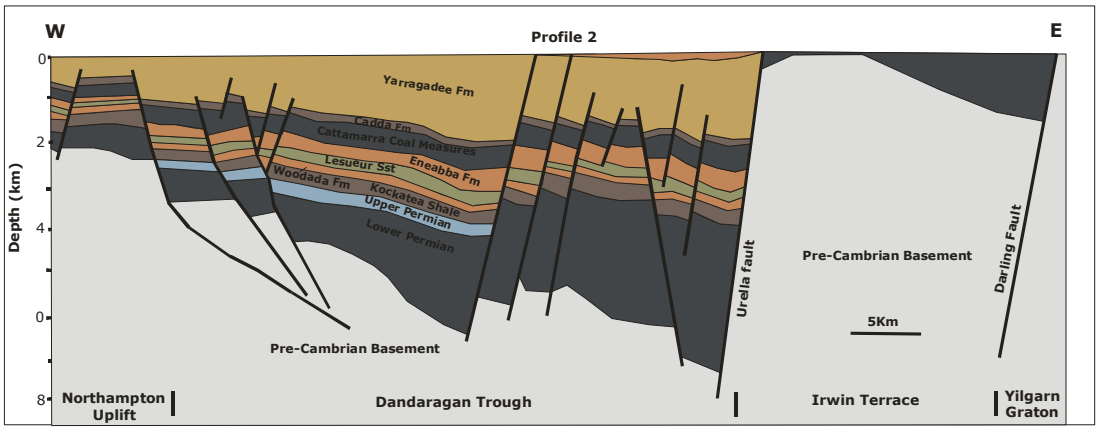

Figure 2-3: East–west structural section across the Dandaragan Trough and adjacent terraces (Profile 2 as per Figure 2-1).

2.4 Stress field in the Perth Basin

Data gained from different sources (Van Ruth et al. 2003; Kings et al. 2008) propose that the Perth Basin is generally in a compressive stress regime. Recent tectonic stress data from the basin signposts that the stress in the Perth Basin is a transitional reverse fault to strike-slip fault stress where $S_{hmax} > S_v \approx S_{hmin}$ (Van Ruth et al. 2003; Kings et al. 2008). However, regardless of the exact state of stress, most stress data indicate that the trajectory of the main stress is horizontal and the main direction of the principa stress axis (S_{hmax}) is east-west oriented (Figure 2-4). The direction of the principal stress is perpendicular to the major north-south and northwest-southeast faults trends. This phenomenon is consistent throughout the basin. Unlike many basins around the world, the stress direction in the Perth Basin is not parallel to the orientation of the regional structure trends (Hillis and Reynolds 2000). It is possible that the stress direction in this part of Australia is induced by the forces applied on the Indo-Australian plate boundary and does not seem to be affected by the regional structure trends.

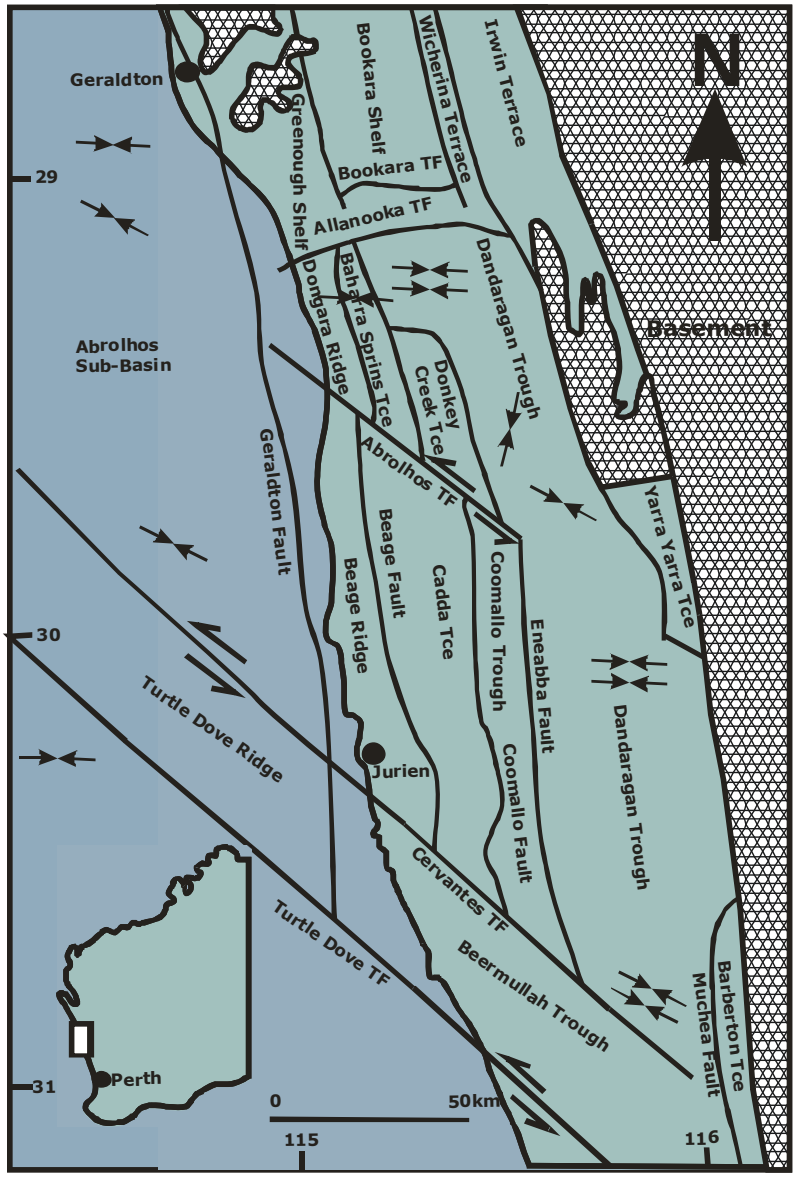

Figure 2-4: Tectonic divisions and structural framework combined with an illustration of maximum stress orientation in the Perth Basin modified from (Mory et al. 2005).

2.5 Perth Basin Stratigraphy and sedimentation

A generalized stratigraphical column for the Northern Perth Basin is illustrated in (Figure 2-5). Following the initial rifting which caused the separation of the Indian and Australian plates, subsequent deformation and deposition occurred sequentially in the basin (Mory et al. 2005). As mentioned in Section 2.2, when the rifting occurred, the structure was filled by sediments during the Late Permian period through to the Cretaceous periods (Iasky and Mory 1994). The rate of sediment accumulation in the Perth Basin during this time frame was rapid and controlled by

the growth of the main regional faults. These faults provided examples of a deformational environment and characterised the Western Australian continental margin prior to and during the break-up (Iasky and Mory 1994). Then, the sediments were lithified into sedimentary rocks that are characterised by sandstone, siltstone and shales (Crostella 1995).

According to Playford et al. (1976), the stratigraphic features of the Perth Basin differ significantly from south to north. The initial rifting formed a series of Permian to Early Triassic depocentres for fluvial and marine siliciclastics with minor carbonates and coals in the north, whereas in the south, fluvial siliciclastics and coals dominated. The most relevant stratigraphic unit to this research was deposited in the Northern Perth Basin. This unit is determined by their extent and significance to be potential shale gas reservoirs and is named as the Kockatea Shale.

2.5.1 Kockatea Shale

The Kockatea Shale was deposited during the Early Triassic period and developed during the tectonic evolution of the basin. This unit forms a major source rock and local cap rock underlying reservoirs and is also thought to be a potential shale gas reservoir (Thomas 1979). The part of the unit with the most source potential is the basal shale. It is rich in sapropel, with an average total organic carbon (TOC) of 2.0%, compared with an overall average for the unit of 0.8% (Hall 1989). The unit consists of dark shale, siltstone, as well as minor sandstone and limestone beds (McWhae et al. 1956) . The unit outcrops consist of thin, red, purple or brown colour ferruginous siltstone or fine-grained sandstone (Crostella 1995). The Kockatea Shale deposition continued over the Northern Perth Basin, with active subsidence in the Dandaragan Trough, where sediment thicknesses in excess of 1000 m were deposited (Iasky and Mory 1994). The permeable Woodada Formation conformably rests on the unit, with an exception to the north of the formation (Figure 2-5). It acts as a thin transitional unit that connects the underlying Kockatea Shale with the overlying Upper Triassic Lesueur sandstone (Mory and Iasky 1996).

Scott (1991) stated that the thickness of the unit generally increases to the south. However, the reduced thicknesses of the Kockatea Shale on the Dongara Terrace and on the Northern part of the Beagle Ridge are attributed to the Early Triassic activities along the Beagle and Mountain Bridge Faults.

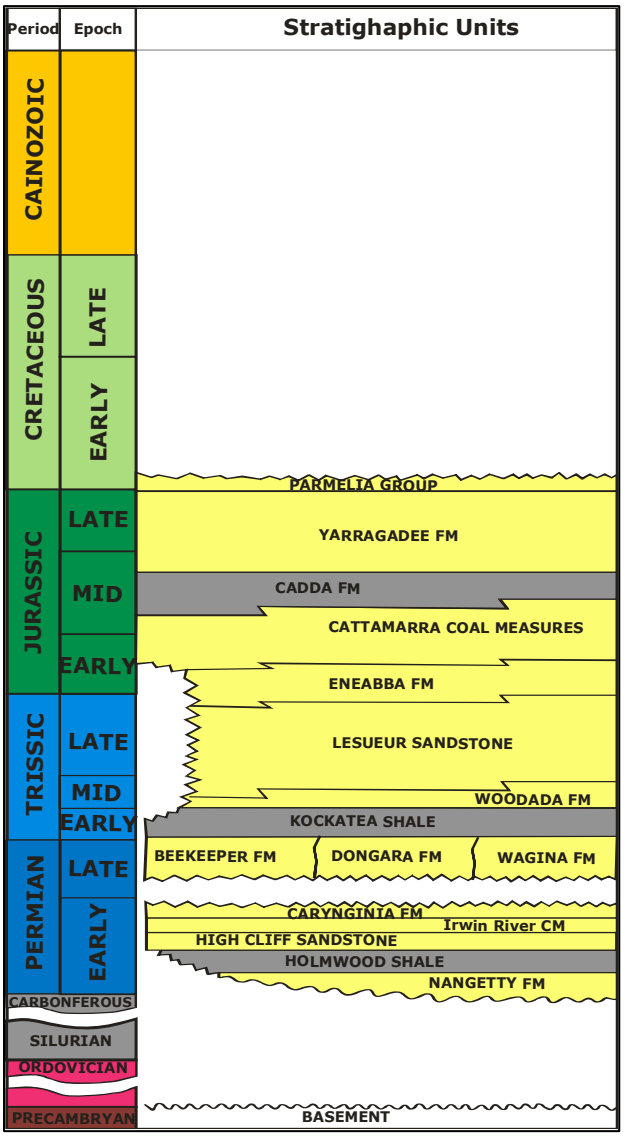

Figure 2-5: Generalized stratigraphy of the Northern Onshore Perth Basin (modified from (Mory and Lasky 1996)).

2.6 Geological Setting of the Canning Basin

The Canning Basin is predominantly an onshore basin that covers an area of about 595000 km^2 in the centre of Northern West Australia and extends offshore in water depths of up to 1000 m (Yeates et al. 1984) . The northern onshore boundary of the basin is defined by the Precambrian Kimberley Block, whilst the Leveque Shelf marks the northern offshore Canning Basin boundary and separates it from the Browse Basin (Figure 2-6). The Pilbara Block bounds the basin to the south (Cadman et al. 1993). The basin is also bounded by an arch of the Upper Proterozoic sediments and the Amadeus Basin to the east. The southern east boundary is defined

by an area of shallow basement (the Warri Arch) that separates the Canning Basin from the Officer Basin (Crostella 1998).

The basin contains complex depositional history ranges from Ordovician to Cretaceous (Forman et al. 1981). At a broader scale, the basin is divided into southern and northern depocentres separated by a mid-basin arch (Figure 2-6). The southern depocentre is subdivided into the Kidson and Willara Sub-basins, whereas the northern depocentre includes the Fitzroy Trough and the Gregory Sub-basin. The central mid-basin arch is divided into the Crossland and Broome Platforms, as well as structural terraces (Haines 2004).

2.7 Canning Basin Evolution and Stratigraphy

A generalized stratigraphical column for the Canning Basin is illustrated in (Figure 2-7). The deposition commenced in the Canning Basin during the Early Ordovician. As a result of transgressions from the northwest, a uniform thickness (approximately 1000 m) of Ordovician sediments have deposited over most of the basin (Veevers and Wells 1961). These sections are characterized as paralic sandstones, intertidal, subtidal shales, siltstones and carbonate (Brown et al. 1984).

The deposition slowed during the Mid-Ordovician and this was driven by the rising of sea floor. During this time, fine grained clastics and carbonate from the Goldwyer Formation and Nita Formation were deposited in shallow marine to sub tidal environments (Forman et al. 1981).

From the Late Ordovician to the Early Devonian, the Fitzroy Trough and the Broome Platform developed as significant tectonic structures. During this period, the evaporitic sequence of the Carribuddy Formation was deposited in the Fitzroy Graben and the Kidson Sub-basin (Brown et al. 1984). The Fitzroy Trough was established as a major depocentre in the Northern Canning Basin as a result of the rifting that took place in the Late Devonian. This fault-bounded and deep trough is flanked by shallow marine terraces (Cadman et al 1993).

The transgression rate increased towards the end of the Frasnian in the Northern Canning Basin, when most features of the Fitzroy Trough were established. Then, a brief regression was followed in the earliest Famennian, which exposed both the entire southern portion of the Fitzroy Trough and the main fault systems on the northern margin (Playford 1989). Subsequent erosion formed the clastic and

carbonate beds of the Napier-Virgin Hills Formation, Clanmeyer shale and Luluigui Formations.

In the Late Famennian, a second cycle of reef building produced the Nullara Limestone (Druce and Radke 1979). A major regression took place in the Early Carboniferous and was associated with subsidence and rapid infill of the trough. During this time, the marine clastics and carbonates of the Laurel and Anderson Formation were deposited.

In the Late Carboniferous to the Early Permian period, uplift and subsidence occurred sequentially in the Fitzroy Trough. A basin-wide erosional unconformity resulting from the uplift and the subsidence was facilitated in the Fitzroy Trough by the faults' growth (Yeates et al. 1984). These faults produced a series of fault blocks and horsts (Passmore 1991).

In the Early Permian, a subsequent transgression resulted in the deposition of the marine Grant Formation (Towner and Gibson 1983). In addition, a periodic tectonism in the Fitzroy Sub-basin preceded the deposition of the Poole Sandstone over a wide area of the Canning Basin (Crowe et al. 1978). The Poole Sandstone was overlain by the marine units of shale, siltstone and calcareous - the Noonkanbah Formation.

In the Early Triassic, the Blina Shale deposited in the Fitzroy Trough as a result of the north-west transgression. The overlying Erskine Sandstone represents a subsequent regression in the Mid Triassic. Between the Late Triassic and Early Jurassic period, a major rifting that took place resulted in an erosional unconformity. According to Brown et al. (1984) , the lateral movements alongside the bounding faults of the Fitzroy Trough created en-echelon anticlinal structures. The break-up between Australia and a previously contiguous mass caused a northwest transgression (Carey 1976; Powell 1976).

The oldest Jurassic sediment found in the Canning Basin is the shallow marine clastics Wallal Sandstone. It is overlain by the tidal shales and sandstones of the Alexander Formation (Brown et al. 1984) . The Late Jurassic to Early Cretaceous Jarlemai Siltstone is conformably overlaying the Alexander Formation (Yeates et al. 1984). The shallow marine Broome Sandstone was deposited over the Jarlemai Siltstone in the Early Cretaceous over most of the Canning Basin. It seems that after the retreat of the Early Cretaceous seas, the features of the Canning Basin have changed little since (Cadman et al 1993).

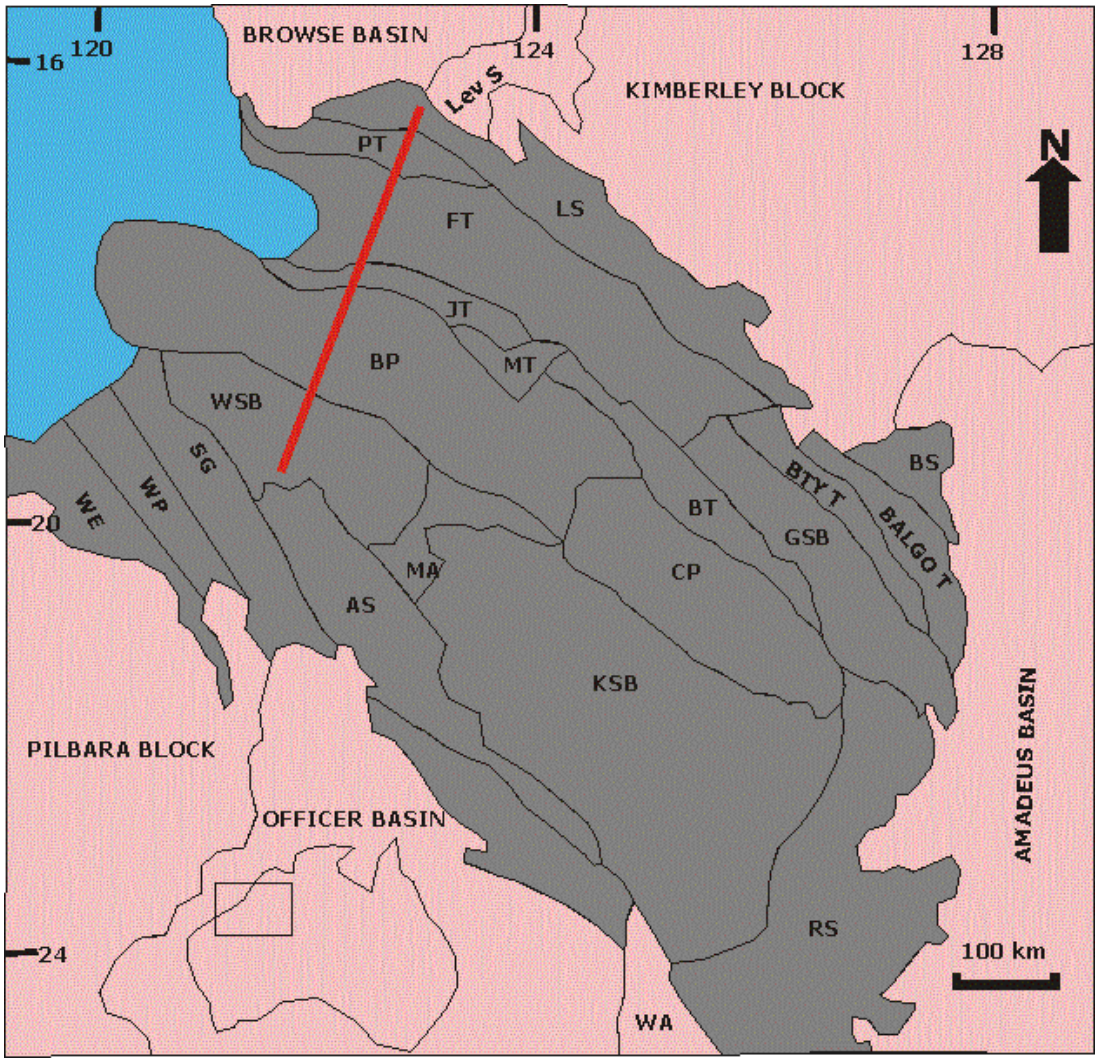

Figure 2-6: Main structural and tectonic elements of the Canning Basin modified from (Haines 2004). Tectonic elements labelled are the Lennard Shelf (LS), Pender Terrace (PT), Fitzroy Trough (FT), Jugurra Terrace (JT), Mowla Terrace (MT), Broome Platform (BP), Willara Sub-basin (WSB), Munro Arch (MA), Samphire Graben (SG), Wallal Platform (WP), Wallal Employment (WE), Anketell Shelf (AS), Kidson Sub-Basin (KSB), Warri Arch (WA), Ryan Shelf (RS), Crossland Platform (CP), Barbwire terrace (BT), Gregory Sub-Basin (GSB), Betty terrace (BTYT), Balgo terrace (BALGOT), Billiluna Shelf (BS) and Leveque shelf (Lev S).

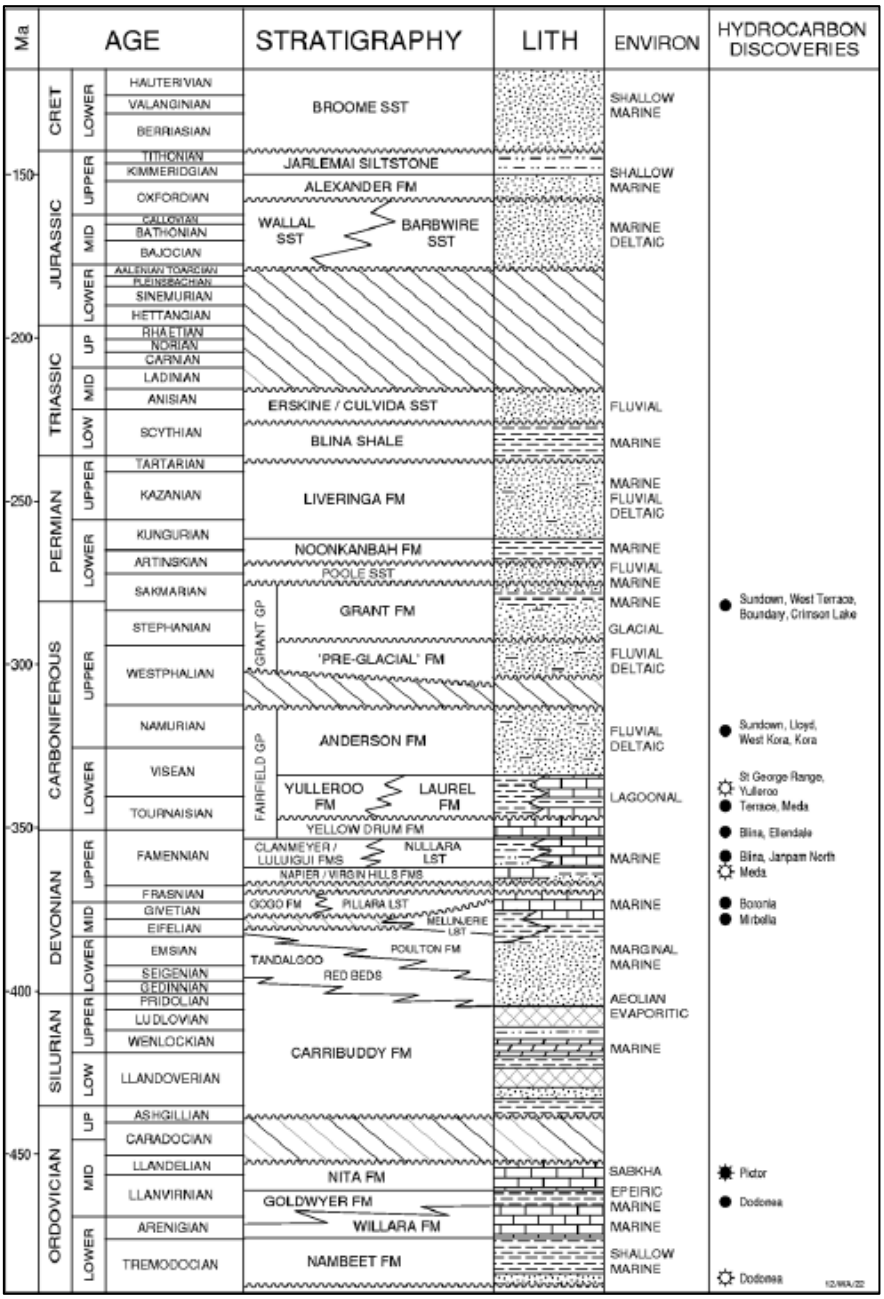

Figure 2-7: Generalised stratigraphy of the Onshore Canning Basin, Western Australia (extracted from Cadman et al 1993).

2.8 Structural features of the Canning Basin

The Canning Basin is divided into a series of platforms, sub-basins troughs, shelves and terraces, bounded by northwesterly–southeasterly trending, syndepositional fault systems (Apak and Carlsen 1997; Jonasson et al. 2001). The study examined areas such as the Fitzroy Trough and Lennard shelf. The divisions and structural framework of the Canning Basin are presented in Figure 2-6.

2.8.1 Fitzroy Trough

The Fitzroy Trough is a major sub-basin that dominates the northern part of the Canning Basin. The Beagle Bay Fault forms the northern boundary of the trough and separates it to the north from an area of relatively shallow basement (less than 4000 m), named the Lennard shelf (Middleton 1991). The Fenton Fault bonds the trough on the south and rifts it from the structurally complex down faulted mid-basin platform (Jonasson et al. 2001). The south-western section of the Fitzroy trough is marked by robust faulting systems along the margin of the Jurgurra and Barbwire Terraces, which flank an area of shallow basement called the Broome Platform.

In some locations, the Fitzroy Trough contains the thickest and probably the most complete, stratigraphic sections in the basin which are estimated at about 15 km. Deep wells such as Yulleroo 1 and Ellendale-1 penetrated thick marine Devonian to Lower Carboniferous (Fairfield Group) strata, e.g. Laurel Formation, overlain by the shallow-marine to deltaic mid to Upper Carboniferous Anderson Formation (Jonasson et al. 2001). These regions have closure at multiple levels, such as the ones observed in the Valhalla prospect. Within the structure, the Fenton Fault is one of the most significant feature that was initiated during the Late Devonian period and continued growing during the Early Carboniferous downthrown to the north-east side (Guppy 1958). According to (Condon and Casey 1958), faulting systems have been established in places alongside the Fenton Fault line.

The asymmetric nature of the Fenton Fault growth accompanied by a further uplift of the northern margin of the Canning Basin has resulted in the maintenance of the considerably thick Laurel Formation (Figure 2-8). Generally, the thickness of the Laurel Formation increases into the major growth depocentre and immediately north of the Fenton Fault. The structural development during the Carboniferous time coincided with the subsidence of the Fitzroy Trough, which provided a further structural growth and significantly influenced the depositional features of the Laurel Formation (Buick, Storkey et al. 2008). As shown in Figure 2-8, it appears that due to the uplifting and subsequent erosion caused by “Alice Springs Orogeny” during the Mid-Carboniferous period, a considerable section of the upper Laurel Formation has eroded (Guppy 1958).

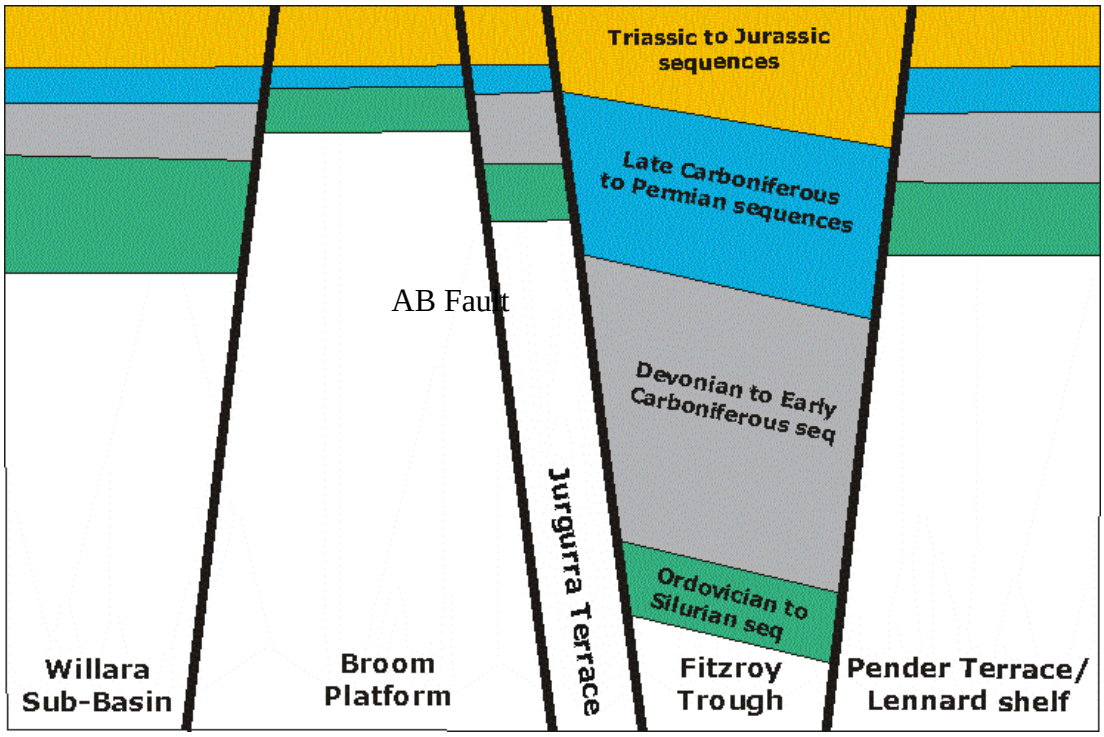

Figure 2-8: Schematic cross section shows relative thickness and age of the sediments in North West of the Canning Basin. This cross section represents a section indicated as the red line in Figure 2.6 (modified from (Strand et al. 2011)).

2.8.2 Pender Terrace and Lennard shelf

The Pender Terrace and Lennard Shelf form the northern margin of the Fitzroy Trough (Figure 2-6). They are comparable with the Jugurra Terrace on the southern boundary (Strand et al. 2011). The Pender Terrace and Lennard Shelf contain sediments of approximately 4000 m, ranging from the Devonian period and younger sections (Figure 2-8). They are structurally controlled by a complex series of northwest fault systems and northeast transfer zones (Crostella 1998). These faults include the Blackstone, Sundown, Meda and Mount Percy Transfer Zones (Middleton 1991). Data from wells that were drilled in these regions of the basin indicate highly fractured sediments.

Chapter 3 Theoretical Background

3.1 Introduction

Pore pressure in any sedimentary formation is defined as the pressure of the fluid contained in the pore space of the rocks, which can be either of normal or abnormal pressure. Abnormal pressure is sub-classified to abnormal high pressure (overpressure) and sub-normal pressure. The knowledge of pore pressure regimes in any sedimentary basins is an integral part of the formation evaluation process in gas shale formations (Gretener 1979). Appropriate evaluation of pore pressure is crucial for drilling and completion planning (Tingay et al. 2003).

In this chapter, definitions of important pore pressure related terms are presented first and then overpressure generating mechanisms are explained in detail, followed by overpressure estimation methods.

3.1.1 Normal pressure

The normal hydrostatic pressure at any depth is defined as the pore pressure equivalent to the hydrostatic pressure, due to an open column of pore fluids that reaches from the surface to the vertical depth of the formation. In normally pressured formations, pore fluids communicate efficiently with the surface during burial. Therefore, the pore fluids are squeezed out by the normal compaction and as a result, a normal hydrostatic pressure regime is established. In normally pressured sediments, the vertical effective stress continues to increase as depth increases. The normal hydrostatic pressure gradient can be calculated by using Equations 3-1 & 3-2 respectively and the graphic illustration of normal pore pressure regime is presented in Figure 3-1.

$$P = \rho_w * g * z \qquad \text{(Equation 3-1)}$$

In terms of pressure gradient:

$$\frac{dp}{dz} = \rho_w * g \qquad \text{(Equation 3-2)}$$

Where P is the pore fluid pressure, ρ_w is the pore water density, g is the gravitational acceleration and z is the vertical depth to the formation. For fresh water with a density of 1 g/cc , the hydrostatic pressure gradient is 0.433psi/ft .

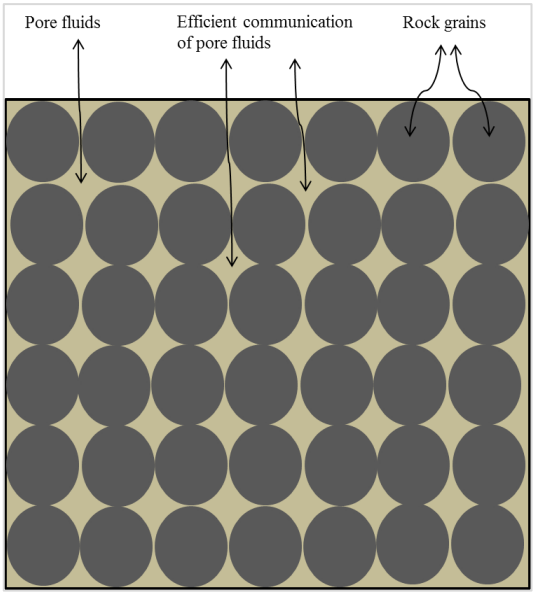

Figure 3-1: Example of a situation where pore fluids communicate efficiently and develop normal pore pressure regime in sedimentary basins.

3.1.2 Overpressure

Overpressure is defined as the formation pressure that is greater than the normal hydrostatic pressure of a column of pore fluids that reaches from the surface to the vertical depth of the formation. Sediments compaction is mainly caused by an increase in overburden stress and the theory of compaction was well described by Terzaghi et al. (1996). The authors established a worldwide accepted equation of equilibrium (Equation 3-3). It was discovered that the overburden stress S is supported by pore pressure P and the effective stress σ. An example of the overpressure situation is when the pore fluids are trapped within the pore space, due to lack of communications (low permeability barriers) between the sediments that are being compacted and the overlying sediments. This process is referred to as compaction disequilibrium or under-compaction.

$$S = \sigma_e + P \qquad \text{(Equation 3-3)}$$

It can be observed from Equation 3.3 that if overburden stress at a certain point increases and water is allowed to escape, the effective stress increases and pore pressure remains constant at hydrostatic pressure. However, if water is not allowed to escape as overburden stress increases, pore pressure increases and the effective stress increases or remains constant depending on the magnitude of overpressure.

Overpressure is also generated by the increase in volume resulting from the expansion of the pore fluids such as hydrocarbon generation, heating and expulsion

and expansion of intergranular water during clay diagenesis. In fluid expansion processes, overpressure develops as the rock matrix restricts the escape of the pore fluids, as the latter increases in volume.

A typical method of plotting pore pressure and stresses versus depth is illustrated in Figure 3-2. As illustrated in this real example, pore pressure *P* increases hydrostatically until the top of the overpressure zone. Then, the pore pressure increases abnormally towards the base of the overpressure zone and returns to the normal trend below the overpressured section. The vertical effective stress σe may increase or decrease depending on the overpressure generating mechanisms. In this particular example, the vertical effective stress decreases due to fluid expansion mechanisms which will be discussed in detail in Section 3.2.2.

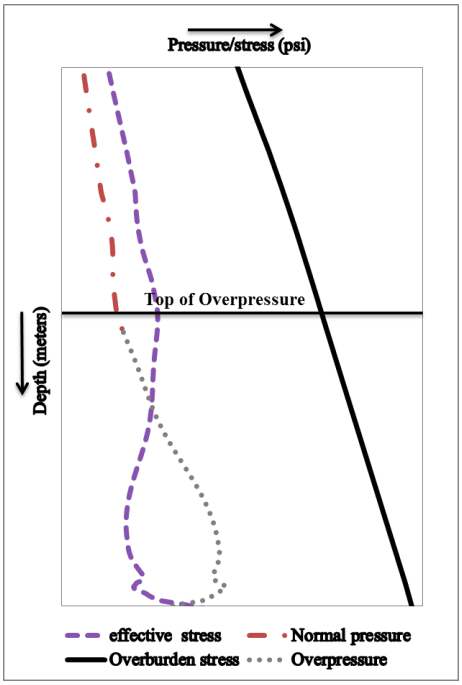

Figure 3-2: A real example of pore pressure and vertical stresses as functions of depth.

3.2 Overpressure generating mechanisms

An accurate prediction of pore pressure involves a proper understanding of overpressure generating mechanisms, as different origins of overpressures have different signatures on petrophysical properties of the formations. The theories of overpressure generating mechanisms have been well described by several authors (Watts 1948; Draou and Osisanya 2000; Cao et al. 2000). The two main generating mechanisms of overpressure in sedimentary rocks can be classified as: (1) loading

mechanisms e.g. under-compaction (compaction disequilibrium) and lateral tectonics compression and (2) unloading mechanisms (fluid expansion) e.g. hydrocarbon generation, clay transformation and aqua-thermal heating. Most researchers have observed that the under-compaction (compaction disequilibrium) accounts for majority of overpressures that were encountered in sedimentary rocks. In under-compaction situations, overpressure results from the rapid loading of sediments, with a lack of communication between the pore fluids and the overlaying sediments. Hence, pore fluids are trapped and became overpressured (Osborne and Swarbrick 1997). The main overpressure generating mechanisms are discussed in detail in Sections 3.2.1 and 3.2.2.

3.2.1 Loading mechanisms

Loading mechanisms involve increasing compressive stresses. They include under-compaction (compaction disequilibrium), where the sediments compact vertically and also include lateral loading (tectonic compression), where the sediments compact horizontally in tectonically active areas.

3.2.1.1 Under-compaction (Compaction disequilibrium)

In normal sedimentary environments, sediments compact and lose porosity as a result of an increase in the effective stress (grain to grain contact). Normal compaction creates efficient communication between the pore spaces and the water-table and some of the pore fluids are squeezed out as a consequence of a normal increase in overburden pressure. Therefore, normal pore pressure regime is established. This pressure trend can be defined by the hydrostatic pressure of the water that is contained in the pores (Draou and Osisanya 2000). However, in many geological settings, compaction is hindered by many mechanical and geological variables that preclude the compaction processes, resulting in pore fluids becoming overpressured. An ideal environment for overpressure generated by under-compaction is when the rate of sedimentation is faster than the rate at which the pore fluids are able to escape. Therefore, the pore fluids are trapped within the pore spaces and the porosity would be greater than it should be in normal compaction situations. As a result, the formation becomes overpressured due to the lack of conduits between the pore spaces and the overlaying formations (Wallace 1965; Eaton 1975). The main difference between overpressured formations caused by under-compaction and

normally pressured ones is that, in overpressured formations, the pore fluids no longer have efficient communication with the water-table.

3.2.1.2 Lateral tectonic loading

Lateral tectonic loading causes an increase in lateral stress as a result of compacting the sediments horizontally, in addition to the vertical compaction caused by an increase in overburden stress. The lateral stress associated with vertical stress causes overpressure, if the pore fluids are not squeezed out by the compaction (Van Ruth et al. 2003) . Another example of overpressure generated by tectonic compression is when a fault moves; the fault plane separates and allows the high pressure zones to communicate with the surrounding lower pressure sand bodies (Figure.3-3). However, when the fault closes, the charged sand releases its pressure into the surrounding shales and develops overpressure (Osborne and Swarbrick 1997). Unlike compaction disequilibrium, lateral tectonic loading can generate high magnitudes of overpressure, which may cause the vertical effective stress to decrease. This is attributed to the fact that in tectonically active areas, compaction is not just controlled by vertical effective stress (Bowers 2002).

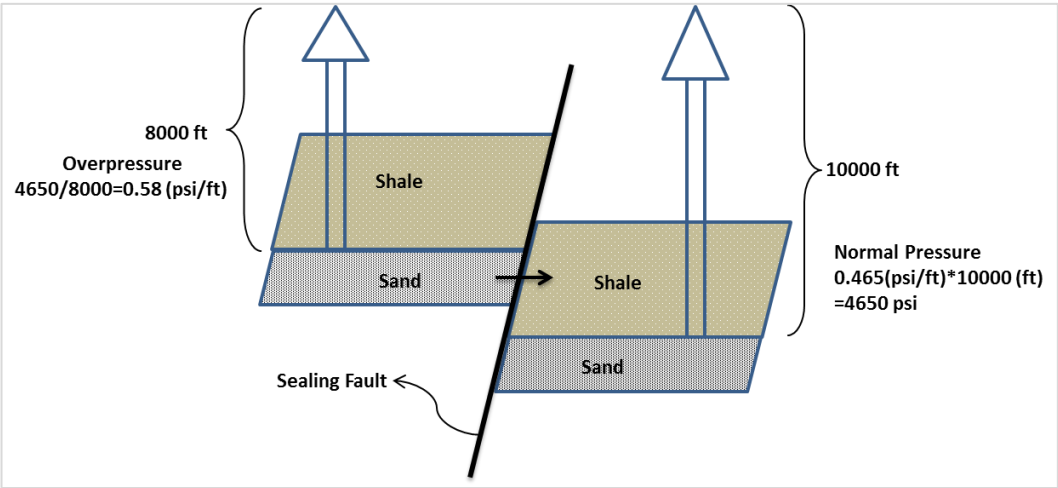

Figure 3-3: A graphic illustration of overpressure generated by lateral tectonic compression.

3.2.1.3 Wireline logs response to loading mechanisms

Normally, the sonic transit time values decrease gradually as depth increases and the density increases as depth increases through the zones of normal pore pressure. However, the responses of wireline logs to overpressure generated by disequilibrium

compaction are constant transit time and density (Ramdhan 2010). The effective stress across the charged interval increases or remains constant (Figure 3-4). Moreover, the magnitude of pore pressure increases due to the undercompaction mechanism being less than or equal to the increase in overburden stress (Hower et al. 1976). In other words, the under-compaction mechanism cannot cause a decrease in effective stress. However, the lateral tectonic loading which generates high magnitudes of pore pressure could cause a reduction in the vertical effective stress as opposed to under-compaction mechanism. All responses for wireline logs mentioned above are for the shale sequence and it is critical to differentiate between shales and other formations prior to analysing the logs' responses.

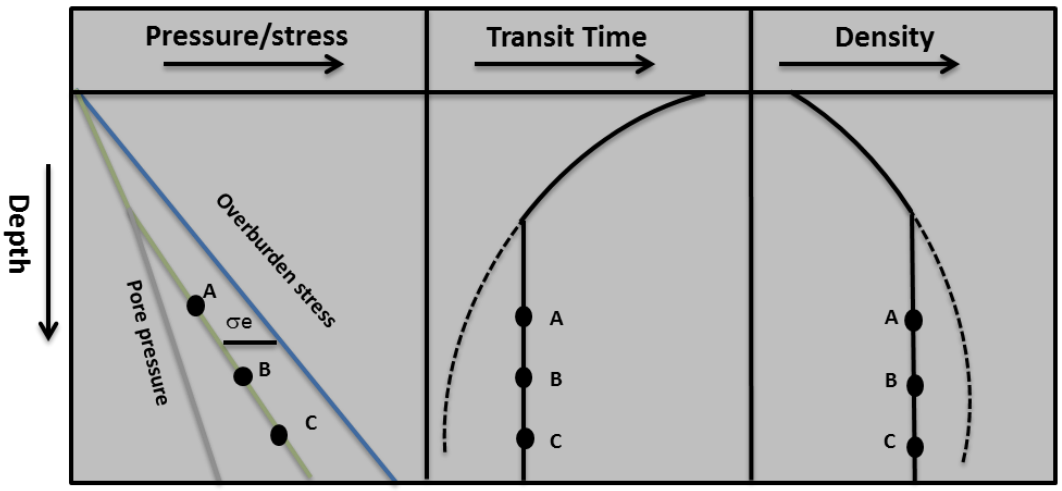

Figure 3-4: A graphic illustration of the response of wireline logs to overpressure generated by under-compaction.

3.2.2 Unloading mechanisms (Fluid expansion)

Overpressure in sedimentary basins can be generated by unloading mechanisms. The process involves either expansion of the contained pore fluids or load transfer into pore fluids, with minimal changes in porosity at rates that do not allow the pore fluids to dissipate. Origins of fluid expansions that are mentioned in the literature include: hydrocarbon generation, cracking of oil to gas, clay transformation e.g. smectite to illite, aqua-thermal heating and cementation and mineral participation (Osborne and Swarbrick 1997). Fluid expansion associated with the transformation of load-bearing framework into pore fluids results in increasing pore pressure when the expanded fluids get constrained by the rock matrix (Hower et al. 1976; Swarbrick et al. 2002; Bowers 1995). Overpressure caused by fluid expansion involves a

decrease of the effective stress as depth increases. This is due to an increase in the volume of pore fluids and the transformation of matrix grains into pore fluids. As a result, some of the loads previously carried out by grains are transferred into pore fluids (Hower et al. 1976). Therefore, the reduction of effective stress resulting from overpressure (generated by fluid expansion processes) forces pore pressure to increase at a higher degree than the increase of pore pressure that is caused by under-compaction process. The increase of pore pressure due to fluid expansion process is faster than the decrease in effective stress and can be greater than the increase in overburden stress (Figure 3-5).

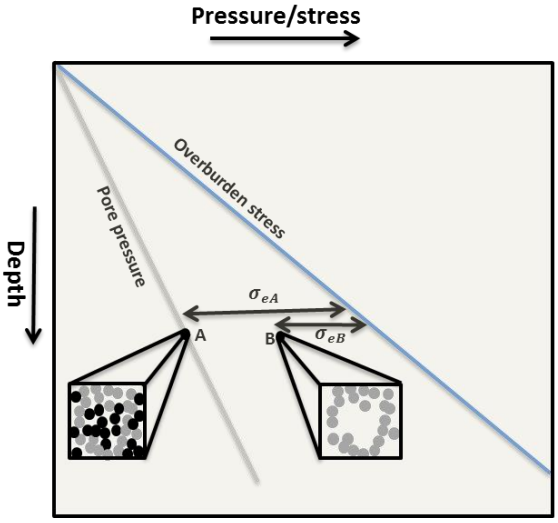

Figure 3-5: A graphic illustration of overpressure generation by unloading mechanisms (e.g. the transformation of load-bearing grains or kerogen (black) into pore fluid (white)).

As mentioned earlier, overpressure generated by unloading mechanisms involves the expansion of the pore fluids or the transformation of the load-bearing framework into pore fluids. The most significant unloading mechanisms presented herein include hydrocarbon generation, clay diagenesis and aqua-thermal heating.

3.2.2.1 Hydrocarbon generation

Hydrocarbon generation processes represent an effective mechanism to generate large magnitudes of overpressure. The processes include cracking from oil into gas and the transformation of kerogen into gas or oil. The volume of the expanded pore fluids during hydrocarbon generation depends on the type of kerogen and the density of the generated hydrocarbon. As mentioned by Hower et al. (1976), out of many

fluid expansion mechanisms, the cracking from oil into gas produces a great magnitude of overpressure as a result of fluid expansion. High magnitudes of overpressure generated by oil cracking into gas occur in source rocks and the generated gas is diluted into the connected pores. Hansom and Lee (2005) also mentioned in their numerical study that the cracking of oil into gas resulted in the generation of high magnitudes of overpressure. The transformation from kerogen into gas or oil involves the processes of load transfer, which was carried out by kerogen into pore fluid in addition to the expansion of pore fluids.

3.2.2.2 Clay Diagenesis

Clay diagenesis includes the transformation of smectite to illite, kaolinite to illite and illitization of mixed layer clay (illite and smectite). The transformation of smectite to illite is broadly known as the clay transformation process that occurs in deeply buried shale formations (Hower et al. 1976). In compacting shales under diagenetic processes, smectite is stable and preserves at least two water layers. There would be no loss of the interlayer water (dehydration) as the temperature of the interlayer water is below the threshold temperature of 71°C (Colten-Bradley 1987). Within a temperature range of 71°-81°C, clay becomes unstable and one of the interlayer water is released. For the other interlayer to be released, it requires a temperature range of 172°-191°C (Hower et al. 1976; Boles and Franks 1979). In other words, the conversion of smectite to illite eliminates a considerable amount of smectite interlayer surface, which was hydrated when the clay was in the smectite phase. As a result, the volume of the shales' intergranular water increases and thereafter increases the pore pressure as well. However, the increase in water volume that results from clay transformation processes cannot generate a high magnitude of overpressure, unless a perfect sealing exists (Osborne and Swarbrick 1997). The related chemical reaction of this transformation produces major changes in the behaviours of subsurface rocks, due to the release of a significant amount of water into the pore system (Draou and Osisanya 2000). The chemical reaction of the transformation of smectite to illite is stated in Equation 3-4 (Boles and Franks 1979).

$$\text{smectite} + K^{+} \rightarrow \text{illite} + \text{silica} + H2O \qquad (\text{Equation } 3-4)$$

All the processes of clay diagenesis are subjected to temperature and create overpressure through the transfer of load-bearing into pore fluids and through the fluid expansion process (e.g. release of water process).

3.2.2.3 Heating

As depth increases, temperature increases and causes the expansion of both the rock matrix and the pores fluids. According to (Miller 1995), the increase of volume resulting from the rock expansion is one order less in magnitude than the increase of volume resulting from the expansion of pore fluids. Hence, the increase in volume resulting from rock expansions can be ignored. If pore fluids are heated while they are efficiently sealed, pore pressure could increase significantly. However, Luo and Vasseur (1992) concluded in their study that the expansion of pore fluids due to heating is not a significant contributor for generating high magnitude of overpressure. They further stated that in order to maintain overpressure generated by heating, the pore fluids must be sealed effectively. However, this condition cannot be met in real situations as there are no formations with zero permeability and when there is a leaking of the fluids in the system, this mechanism is neglected.

3.2.2.4 Wireline logs response to unloading mechanisms

The response of wireline logs to overpressure generated by unloading mechanisms is a decrease of effective stress, which produces a reversal on sonic transit time moving to higher sonic transit time as depth increases. However, there would be no reversal in the density log and it often continues to increase instead. It may also reverse slightly at the bottom of the overpressured section. The response of wireline logs to overpressure caused by unloading are presented in Figure 3-6.

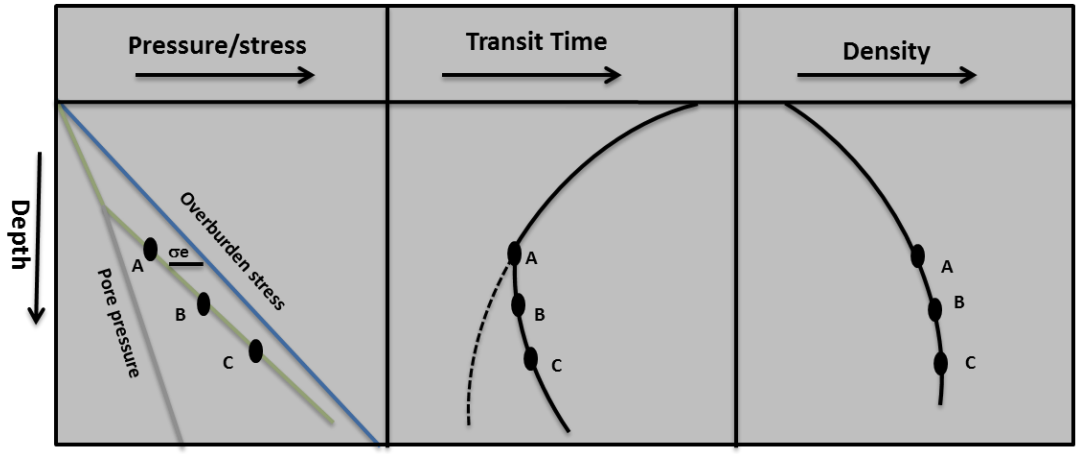

Figure 3-6: A schematic diagram of the responses of wireline logs to overpressure generated by unloading mechanisms.

The pore structures are classified as storage pores (pore spaces) or connecting pores (pore throats) (Bowers and Katsube 2002). The effective porosity is the sum of all the interconnected pores, whereas the total porosity is the sum of the interconnected and isolated pores. The storage pores affect the total porosity and bulk density of a certain formation. These two petrophysical properties are attributed to the total volume of the net pore. Thus, the storage pores are the major porosity contributor of the shale. On the other hand, the connecting pores which control the flow within the pore system have very minor contributions to porosity. When overpressure in the shale is generated by fluid expansion mechanisms, the response of the fluid expansion is basically an elastic opening (widening) of connecting pores as a result of effective stress reduction (Cheng and Toksöz 1979; Bowers and Katsube 2002). This response is due to the fact that connecting pores have a low aspect ratio and they are mechanically flexible and more harmonious than the storage pores. As a result, the porosity increases in very small amounts (Hermanrud e al. 1998). In contrast, the aspect ratio of the storage pores is high and they are mechanically inflexible and scarcely affected by fluid expansion. Moreover, the bulk density is hardly influenced by fluid expansion responding to the low magnitude of porosity increase. Connecting pores have significant impacts on transport properties such as sonic velocity and electrical resistivity, thus affecting sonic transit time and electrical resistivity logs (Bowers and Katsube 2002; Hermanrud e al. 1998). On the other hand, they have insignificant effects on density and neutron porosity logs.

3.2.3 World examples of overpressures

Overpressure exists in almost every geological environment of all ages and appears in all parts of the world. It is believed that the mechanism of under-compaction is the main cause of overpressure in young geological environments that experience rapid sedimentation rates, e.g. US Gulf Coast region (Dickinson 1951). The importance of the unloading mechanisms such as gas generation and clay diagenesis processes has been discussed by many authors. An example of a basin where overpressure was generated by unloading mechanism is the North Sea (Hermanrud e al. 1998). The lateral stress could also play an important role for generating overpressure in relatively old sedimentary basins such as the Cooper Basin in South Australia (Van Ruth et al. 2003).

3.2.4 Overpressure indicators from drilling data

The best technique to detect and assess overpressure is to study and combine all available pore pressure relevant parameters. Depending only on one specific type of data can lead to erroneous interpretations. In conjunction with well log data analysis, mud log data at the surface can also be used as indications for penetrating overpressured formations (Fertl and Timko 1971). These measurements are discussed in detail in the following sections and include the drilling rate of penetration (ROP), gas show at the surface, kicks, mud weight and flow line temperature.

3.2.4.1 Drilling rate of penetration

The evaluation of drilling performance parameters, specifically the rate of penetration, is used to detect overpressure formations (Fertl and Timko 1971). The rate of penetration is inversely proportional to the differential pressure at the bottom hole, between the formation and hydrostatic pressures resulting from the mud weight column. The advantage of using the rate of penetration data over the log data analysis for overpressure detection is the immediate availability during drilling operation (Jorden and Shirley 1966).

Field examples show that the normal trend of the rate of penetration reduces as depth increases, while the other drilling parameters remain constant. Under constant mud conditions, while drilling in normally pressured formations, the bottom hole differential pressure increases as a result of the increase in the formation pressure as depth increases. The effect is a reduction in the rate of penetration. In contrast, when drilling overpressured sections under the same drilling conditions, the bottom hole differential pressure decreases and the rate of penetration increases thereafter (Fertl and Timko 1971). Therefore, under constant drilling conditions, it is believed that the rate of penetration decreases while drilling in normally pressured formations and deviates to a higher rate when encountering overpressured formations.

3.2.4.2 Gas show

There are many possible sources of gas showing in the returned mud to the surface. According to Fertl and Timko (1971), the origins of these gases could be due to: (1) underbalanced conditions when drilling overpressure formation, (2) gas released from the cutting and (3) gas-bearing rocks. The compounds of the returned gas can

be studied and certain components can be related to overpressure. Hence, a sudden increase of connection gas and gas in the mud may indicate overpressured formations.

3.2.4.3 Kicks

Kicks are also considered as overpressure indications when they occur at balanced drilling operations. The advanced drilling technology may require the drillers to adjust the mud weight at a fine line between effective pressure control and the blowout. This may cause a sudden kick when penetrating overpressured formations. Thus, inappropriate pressure balances between the mud weights and formation pore pressures may cause kicks (Fertl and Timko 1971).

3.2.4.4 Mud weight

Kicks may be best avoided by regular checks of the drilling mud properties, particularly for any drop in the mud weight. This can be used as an indication for gas cuttings and kicks.

3.2.4.5 Flow-Line Temperature

Measuring the temperature of the drilling flow line is a useful way to identify changes in temperature while drilling petroleum wells. Several authors such as Lewis and Rose (1970) have reviewed the heat conductivity and suggested that whenever encountering overpressured formations, formation temperatures increase. The observed change is an increase in the flow line temperature by 2 to 10 ° F above the normal temperature, when entering the overpressured environments. However, it is important to bear in mind that the temperature increase can also be due to a change in lithology, presence of salt dome, etc (Fertl and Timko 1971).

3.2.5 Identification of shale intervals

A typical definition of shale can be attributed to three characteristics: (1) clay contents form the load-bearing framework, (2) pore size of the shale which is measured by nanometres scale and permeability which is measured by nanodarcy and (3) the surface area of the shale is large and adsorb water easily. The basic data available for petrophysists for shale identification are well logs data. Shale pore pressure estimation from well logs is based on compaction theory that requires

establishing normal compaction trends within continuous shale and a uniform lithology section. In order to discriminate shale intervals from other lithology sections, the gamma ray log which measures the rocks' radioactivity is generally used to measure the clay contents (Figure 3-7).

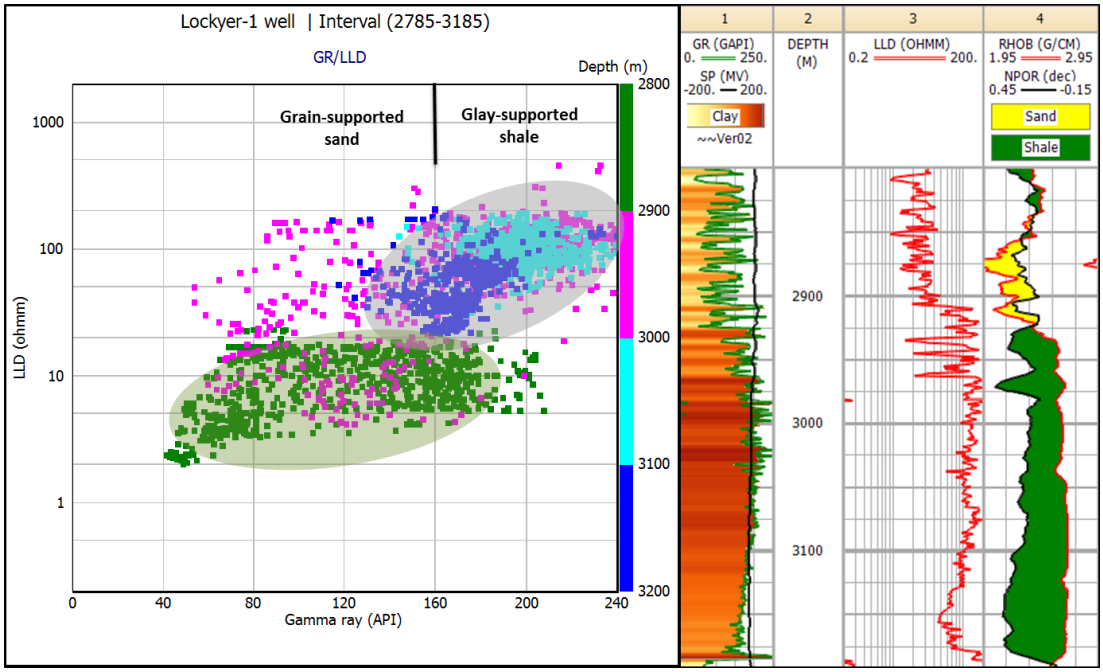

Figure 3-7: Shale discrimination based on the gamma ray log.

The use of the gamma ray for shale discrimination may cause errors as shale radioactivity varies significantly from one shale to another and also, not all shales are radioactive (Fertl 1979). Likewise, sandstone grains may have radioactive materials. Based on rocks petrophysical properties, Katahara (2008) proposed a technique for discriminating shale from sandstone, which is based on the difference between neutron porosity and density porosity. This approach is an appropriate technique for measuring clay contents than using gamma ray. It is also a very simplified model where quartz, clay minerals and water are the only components of shale (Figure 3-8). The shale falls within the triangle constrained by each end point of the three components. The distance from the water-quartz line indicates that the clay contents and clay content are proportional to the difference between neutron porosity and density porosity. However, the difference between neutron porosity and density porosity will remain commensurate with the clay content variations.

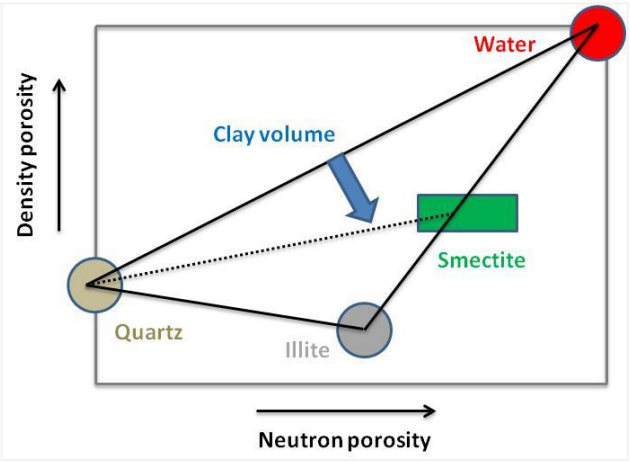

Figure 3-8: A graphic illustration of where the three components of shale stand on the density porosity versus neutron density cross-plot.

This can be better viewed on a cross-plot of density versus (Neutron porosity-Porosity from Density log) (Figure. 3-9 left). The difference between neutron porosity (NPOR) and Porosity from Enhanced Density (PHND) is a measure of the clay content (Katahara 2008). As seen from Figure 3-9, there is a break in the slope which occurs at the threshold between sands and shales and this can be used for shale discrimination. On a log-plot (Figure 3-9 right), the difference between neutron and density porosities which defines shale and sand intervals is illustrated in the green and yellow windows respectively.

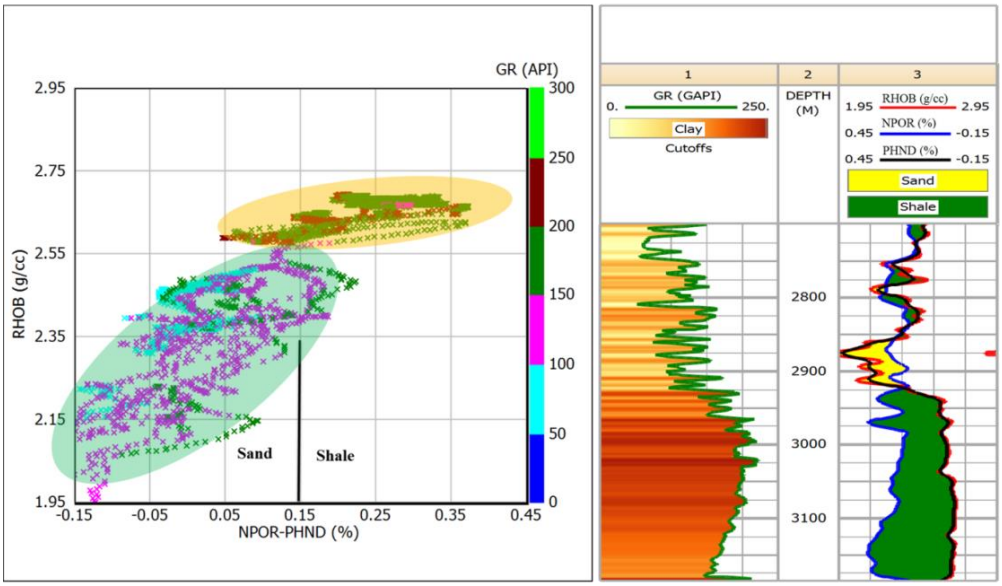

Figure 3-9: Shale identification based on the difference between neutron porosity and density porosity, on cross-plot (left) and log-plot (right).

3.3 Overpressure estimation methods

Techniques used to detect abnormal pore pressure can be classified as: (1) predictive and before drilling methods from offset wells and seismic data, (2) during drilling from mud log data e.g. kicks, drilling rate of penetration (ROP) and flow line temperature and (3) post drilling methods from well logging data (Pikington 1988; Draou and Osisanya 2000).

In other words, formation pressure can be determined by either direct or indirect methods (Lesso and Burgess 1986). The direct pressure measurements provide promising results in permeable formations, where the measurement tool is placed along the formation and allows sufficient time to reach pressure equilibrium. However, pore pressure in very low permeability formations such as shale, cannot be measured by direct measurements. This is due to their associated operational difficulties, such as high cost of rig time as low-permeability formations require a very long time to reach pressure equilibrium. Additional problems associated with the use of direct pressure measurements methods in shales are the risks of differential pipe or tool sticking. Therefore, indirect methods that are based on compaction and porosity dependent parameters concepts such as the applications of well logging and drilling data, where pressure dependent parameters can be used to infer pore pressure (Alixant and Desbrandes 1991; Lesage et al. 1991). According to Tanguy and Zoeller (1981), well logs data provide lithological information and appropriate petrophysical properties needed to estimate pore pressure in shale formations.

As described in Sections 3.2.1.3 and 3.2.2.4, wireline logs respond to normal pressure trends and overpressure phenomenon in different ways. In normally pressured intervals, wireline log parameters follow the normal compaction trends (NCT) as a result of normal sedimentary environments and normal compaction of sediments. On the other hand, in overpressured formations, the responses of wireline logs depart from the NCT, whether the overpressure generating mechanism is loading or unloading. The departure of wireline logs from the NCT is used as a key parameter for the prediction of overpressure in sedimentary rocks. Hence, an appropriate formation of the evaluation process, proper drilling and well completion design can be achieved (Tingay et al. 2003).

In fact, the shale is quite sensitive to compaction process and therefore, it has been used as a key parameter for the determination of pressure profile in sedimentary

rocks (Muir 2013). The most popular prediction methods for pore pressure are: (1) The Effective stress, also called Equivalent Depth Method and (2) Eaton's Method (Figure 3-10). The fundamental concepts for estimating pore pressure in shale formations are: the knowledge of overburden stress, effective stress and the knowledge of porosity dependent parameters (Hower et al. 1976).

Prior explanations of the overpressure estimation methods, an overview of the compaction theory is presented.

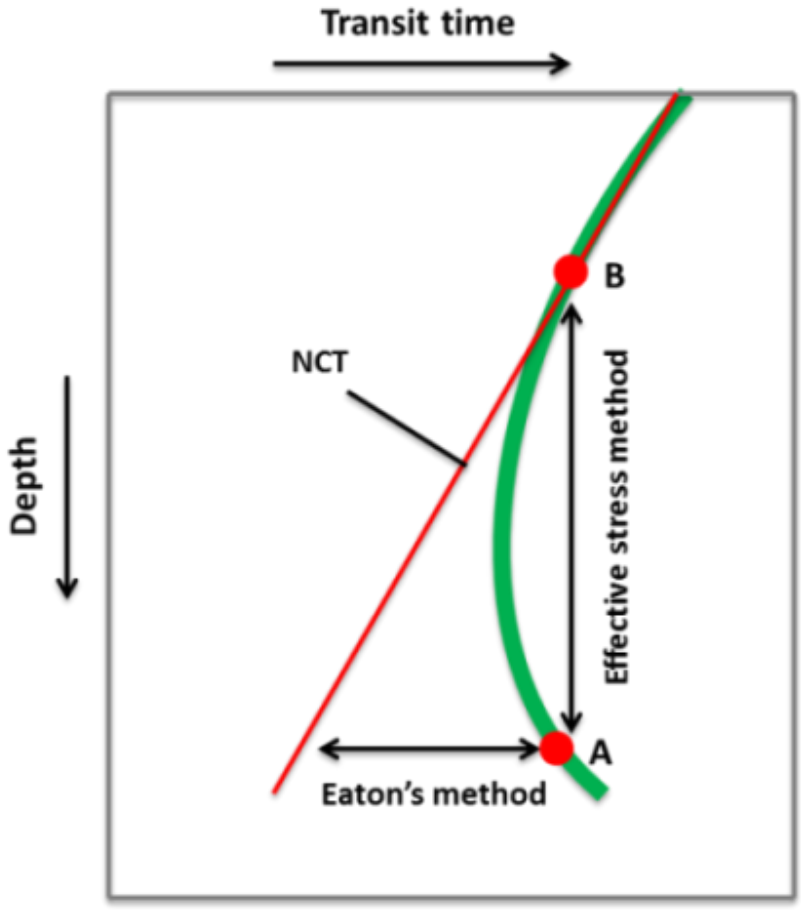

Figure 3-10: A diagram of Eaton's method and the effective stress method.

3.3.1 Overview of the compaction theory

The basic concept of the compaction theory is illustrated in (Figure 3-11). The difference between the pressure exerted by the overburden stress σ_{ob} and the vertical effective stress σ_e is the pore pressure P_p (Terzaghi et al. 1996).

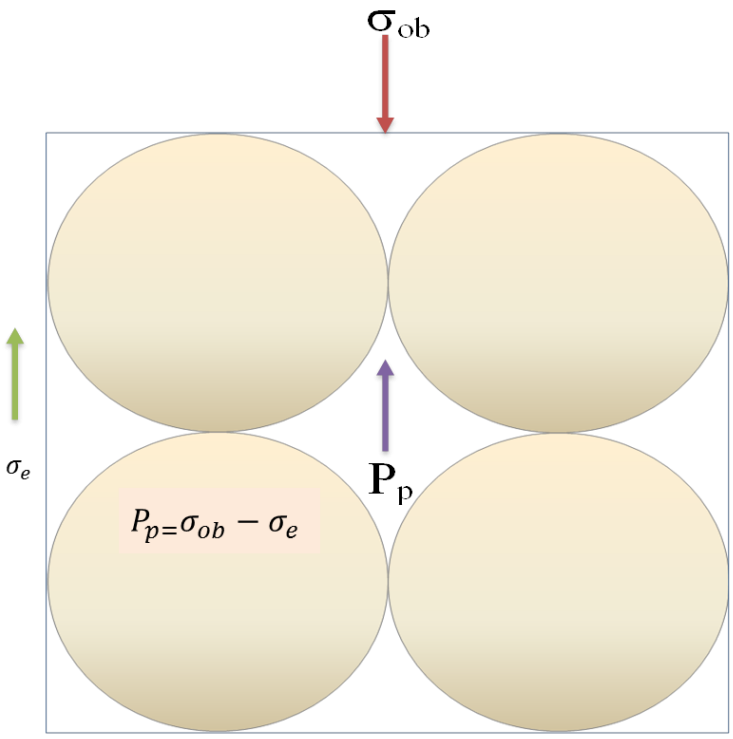

Figure 3-11: Basic concept of the compaction theory and effective stress principle.

According to Alixant and Desbrandes (1991), there are two limitations associated with the application of compaction theory in determining pore pressure: (1) the determination of the normal trend is a subjective task that may be troublesome without a regional experience and (2) an empirical correlation between petrophysical measurements and fluid-pressure gradients must be established on the basis of a regional data set.

Despite these limitations, the use of compaction theory is a general evaluation practice used in the industry to evaluate pore pressure. An overview of the compaction theory is described before an explanation of the overpressure estimating methods.

As depth increases, sediments compact and the result is a reduction of porosity. Many researchers have studied the porosity - depth relationship and many correlations were developed. The most cited experimental relationship between porosity and depth is presented in Equation 3-5 (Athy 1930).

$$\emptyset = \emptyset_0 \, e^{-bz} \qquad \text{(Equation 3-5)}$$

Where $\emptyset_0$ is porosity at the surface, $\emptyset$ is the porosity at any specified depth z, *e* is the base for Napierian logarithms and *b* is an empirical constant attained after fitting the exponential relationship of porosity versus depth.

Athy (1930) did not take into account the high porosity values in overpressured zones resulting from under-compaction. Therefore, Rubey and Hubbert (1959) expanded Athy's relationship to account for the vertical effective stress and remove the effects of high porosity points due to overpressure generated by disequilibrium and they developed Equation 3-6.

$$\emptyset = \emptyset_0 \, e^{-\frac{c}{\rho_b - \rho_w}\sigma_e'} \qquad \text{(Equation 3-6)}$$

Where C is an empirical constant, ρ_b is the bulk density of the formation, ρ_w is the density of the pore water and σ_e' is the vertical effective stress.

It is obvious from Equations 3-5 and 3-6 that as sediments compact mechanically, the porosity decreases as a result of burial or vertical effective stress increase. Ramdhan (2010) stated that mechanical compaction is basically a permanent plastic process, with a minor elastic component. The exponential decrease of porosity with depth (Equation 3-5), or vertical effective stress (Equation 3-6), indicate that the sediments become more resistant to mechanical compaction, when porosity reduces and vertical effective stress increases.

Due to the rare use of the direct measurements for porosity in shale formations, the determination of the normal compaction trend (NCT) is used to infer porosity. Hence, it detects any abnormality of pore pressure within the shales (Athy 1930; Rubey and Hubbert 1959). The NCT obtained from Equations 3-5 and 3-6 are fitted on wireline logs data such as sonic transit time, electrical resistivity and density. Among well logs data, sonic transit time is the most commonly used porosity dependent parameter. This is due to the fact that it is usually available in good quality and is also less affected by the bad borehole conditions compared to other well logs data.

For proper estimation of pore pressure in shales, it is important to establish a reliable NCT. According to Ramdhan (2010), there are three main techniques for defining NCTs from wireline logs, namely (1) direct plots of wireline logs data versus depth, (2) plot of wireline log data versus effective stress and (3) cross-plotting wireline logs data.

3.3.2 Eaton's method

The principle of Eaton's method is the comparison of the wireline logs data and the drilling data with the normal compaction trends (NCTs) at the same depths. Eaton (1975) developed four equations for pore pressure estimation using well logs and drilling data. Among pore pressure estimation methods that use logs data, Eaton's method is the most widely used. This method has been used in the industry for more than 25 years and is found to be fairly reliable. The correlations can be used with different sources of data such as: sonic, resistivity, conductivity and corrected drilling exponent (Equations 3-7, 3-8, 3-9 & 3-10) respectively.

$$g_p = g_{ob} - (g_{ob} - g_n)\left(\frac{\Delta t_n}{\Delta t_o}\right)^x \qquad \text{(Equation 3-7)}$$

$$g_p = g_{ob} - (g_{ob} - g_n)\left(\frac{R_o}{R_n}\right)^x \qquad \text{(Equation 3-8)}$$

$$g_p = g_{ob} - (g_{ob} - g_n)\left(\frac{C_n}{C_o}\right)^x \qquad \text{(Equation 3-9)}$$

$$g_p = g_{ob} - (g_{ob} - g_n)\left(\frac{d_{co}}{d_{cn}}\right)^x \qquad \text{(Equation 3-10)}$$

Where *g* is the pressure gradient, the subscript *n* denotes the value of data parameters at normal compaction trend while the subscript *o* denotes the observed parameters. *ob* denotes overburden, *p* denotes pore pressure and the exponent *x* is Eaton's exponent, which can be adjusted based on regional experiences.

The departure of data from their NCTs is used as a measure of pore pressure within the shale. It should be noted that the above mentioned correlations were derived based on an empirical basis for the Gulf of Mexico data, considering overpressure generating mechanism is disequilibrium compaction. For this reason, it is important to note that this method does not imply the overpressure generating mechanisms, whether loading or unloading. Eaton (1975) also did not mention in his study how to determine the NCT. However, experience indicates that NCT curves can be established for sediments with normal pressure overlying the overpressured sections.

3.3.3 Effective stress method

This method is also called the Equivalent Depth Method (EDM) and it further stresses the importance of the normal compaction trends (NCTs) in shales. The principle of the Effective Stress Method (ESM) is that, the overpressured shale have the same effective stress value as a normally pressured shale that has the same porosity (Mouchet and Mitchell 1989). Figure (3-10) illustrates the application of the effective stress method. It is important to note that the method is only applicable when the overpressure generating mechanism is the disequilibrium compaction and the lithologies at the two points of interest are the same. If overpressure is generated by unloading mechanisms, then the effective stress will be overestimated and the pore pressure will be underestimated. Thus, the EDM will fail due to deviation of porosity- effective stress relationship from the normal trends.

With reference to Figure (3-10), the sonic transit time at point A is the same as the sonic transit time in point B, which has normal pressure gradient. Implementing the principle of the ESM, the effective stress at point B is the same as the effective stress at point A.

$$\sigma_{e(A)} = \sigma_{e(B)}$$

$$\text{Since} \quad \sigma_e = \sigma_{ob} - P_p$$

$$\text{Then} \quad \left(\sigma_{ob} - P_p\right)_A = (\sigma_{ob} - P_n)_B \qquad (\text{Equation } 3-11)$$

$$\text{Rearrange 3-11} \quad P_{p(A)} = P_{n(B)} + \left(\sigma_{ob(A)} - \sigma_{ob(B)}\right) \qquad (\text{Equation } 3-12)$$

3.3.4 Bowers' method

Bowers (1995) modified the Equivalent Depth Method to estimate pore pressure where overpressure is generated by either the loading or unloading mechanisms. This author developed a useful tool to predict overpressure, where the velocity versus effective stress relation is the key element that is used for overpressure estimation. Bowers further explained how the velocity-effective stress relationships can be used to identify overpressure generating mechanism in the area of study, whereas all the other methods do not take into account the cause of overpressures.

The normal relationship between effective stress and acoustic velocity is proportional. As depth increase the effective stress increase and the acoustic velocity increases (Khaksar and Griffiths 1996). Under normal compaction with normally pressured sediments, sonic velocity increases and effective stress continues to increase. The velocity-effective stress relationship will be referred to as the virgin curve (Figure 3-12 left). Overpressure generated by undercompaction mechanisms will also be on the virgin curve because undercompaction cannot cause the effective stress to decrease. The most under-compaction can do, is to make the effective stress remain constant at a fixed value, which causes the velocity to be at a fixed value on the virgin curve. In contrast, unloading mechanisms cause overpressure to increase at a higher rate than overburden stress, resulting in a decrease in effective stress as depth increases as well as a velocity reversal. As a result, the data inside the velocity reversal follow a different path, which is called unloading curve; whereas the data outside the velocity reversal stays on the virgin curve (Figure 3-12 right). In case of subsequent increase in effective stress, the velocity will track the unloading curve returning to the virgin curve (Bowers 1995).

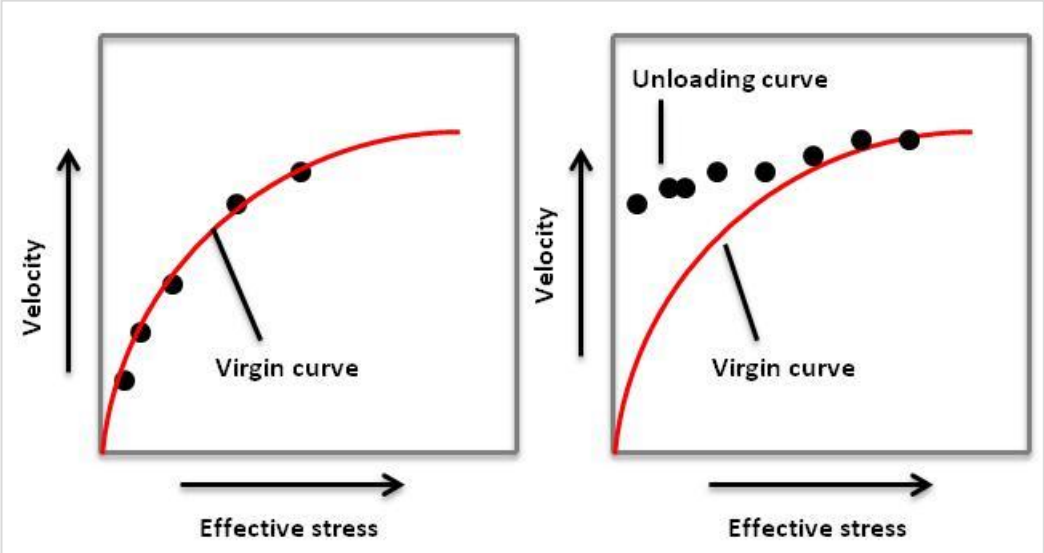

Figure 3-12: Velocity-effective stress relationship and shale behaviour- virgin curve (left) and unloading curve (right).

The following relationships between vertical effective stress and velocity were developed by Bowers:

1. Virgin Curve: Bowers developed the virgin curve velocity-effective stress relationship for shale (Equation 3-13) based in-situ data of effective stress.

$$v = 5000 + A{\sigma_e}^B \qquad \text{(Equation } 3-13\text{)}$$

Where A, B are virgin curve parameters obtained from fitting velocity-effective stress relationship and calibrated with offset velocity-effective-stress data, σ_e is the effective stress psi and v is the sonic velocity ft/sec.

2. Unloading Curve: Bowers proposed also the empirical velocity-effective stress relationship (Equation 3-14) for the unloading curve:

$$\sigma'_e = \sigma'_{e_{max}}\left(\frac{1}{\sigma'_{e_{max}}}\left(\frac{v-5000}{A}\right)^{1/B}\right)^U \qquad \text{(Equation } 3-14\text{)}$$

$$\text{With} \quad \sigma_{ec} = \left(\frac{v-5000}{A}\right)^{1/B} \text{ and re-arrange (Equation } 3-15\text{)}$$

$$\frac{\sigma'_v}{\sigma'_{max}} = \left(\frac{\sigma_{vc}}{\sigma'_{max}}\right)^U \qquad \text{(Equation } 3-16\text{)}$$

Where A, B are constants as previously defined and U is the unloading curve parameter (Bowers 1995), σ_{ec} is the effective stress at which the velocity intersects with the virgin curve given in psi, $\sigma'_{e_{max}}$ is the maximum vertical effective stress given in psi. In the absence of major lithology changes, $\sigma'_{e_{max}}$ is usually taken to be equal to the effective stress at which the velocity reverses.

Pore pressure caused by unloading can then be computed by deducting the vertical effective stress from the overburden stress.

Chapter 4 Research methodology

A generalized research workflow is presented in Figure 4-1. Generally, there are several data sets used to conduct this research; well log data, mud log data, geochemical data, drilling reports, seismic characters, conventional core images, geological structure data and limited pressure data. The results were incorporated and analysed to produce pore pressure profile, analyse the cause of overpressure and study the effects of tectonic activities on overpressure distribution for the potential shale gas intervals in the Perth and Canning Basins. All depths used in this thesis are in true vertical depth (TVD) meters.

4.1 Well log data

A typical illustration of plotting pore pressure is presented in Figure 4-2. As shown in this real example, the pore pressure gradient rises hydrostatically, 0.433 psi/ft, to a depth of 3200 m and then increases with depth and reaches 0.6 psi/ft at depth 3680 m.

Based on the available data, the proposed methodology to conduct this study was to implement the normal compaction trend method (NCT) to predict the pore pressure in the two potential gas formations located in the Perth and Canning Basins of Western Australia. Well log and mud log data formed the base of this study, along with other data gathered from 43 wells in the Perth Basin and 19 wells in the Canning Basin. Pore pressures were inferred indirectly using Eaton's Equation (Eaton 1975), (Equation 4-1) from sonic logs utilizing the Interactive Petrophysics software.

$$g_p = g_{ob} - (g_{ob} - g_n)\left(\frac{\Delta T_n}{\Delta T_o}\right)^x \qquad (4\text{-}1)$$

Where g_p is the pore pressure gradient, g_{ob} is the overburden pressure gradient & g_n is the normal hydrostatic pressure gradient. The subscript n & o denote the normal & observed sonic transit time ΔT and the exponent x is Eaton exponent, which can be adjusted according to regional experience.

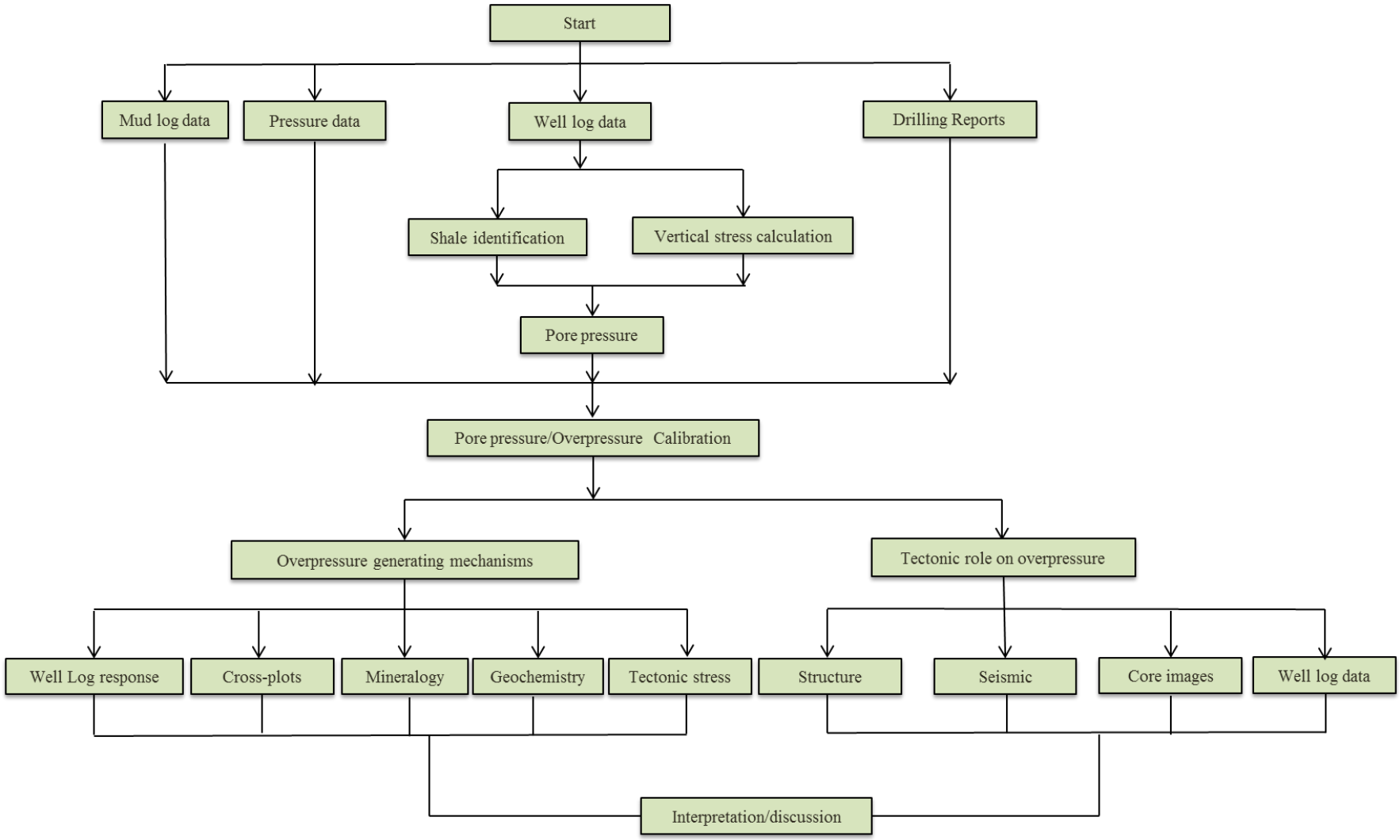

Figure 4-1: Generalized research workflow.

Well log data that were analysed include sonic, neutron, density, resistivity, and gamma ray logs. For pore pressure estimation, two main steps, which are the overburden stress gradient calculations and shale identification, are necessary.

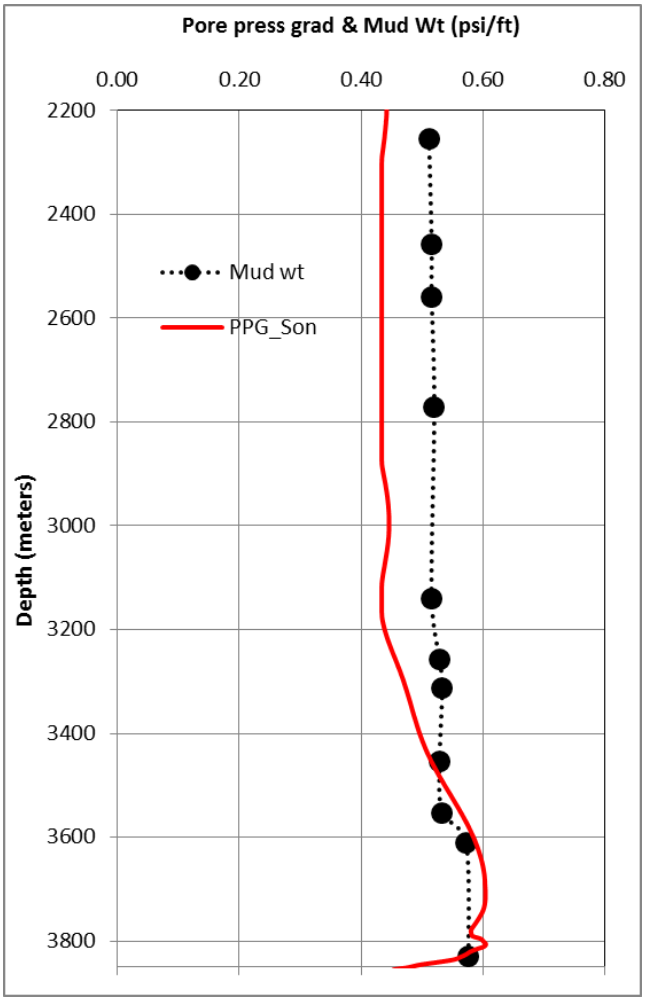

Figure 4-2: Real example of pore pressure profile as a function of depth from the Redback-2 well.

4.1.1 Overburden stress calculation

The overburden stress is calculated from the density log that measures the bulk density value every 0.15 m. Therefore, the computing of the overburden pressure and stress is made at every depth step. The overburden stress is computed by using the Equation 4-2.

$$\sigma_v = \sum_{i=1}^{n} \rho_b g \, dz \qquad (4-2)$$

4.1.2 Shale Identification

The gamma ray log was the core log used to recognize the top and bottom of the potential shale gas intervals. It is primarily used to measure the clay contents of a certain formation. However, Katahara (2008) indicated that the gamma ray is susceptible to error due to the fact that not all shales are radioactive and that not all other rocks lack radioactivity. Therefore, he suggested a simple shale discrimination model as having three constituents - clay minerals, water and quartz (Figure 4-3). The clay content of a certain formation is greater under the quartz–water line. On a cross-plot, points within the triangle are defined by the percentage of the three components (Figure 4-4). Katahara (2008) mentioned that this technique is more reliable than the gamma ray technique for shale discrimination.

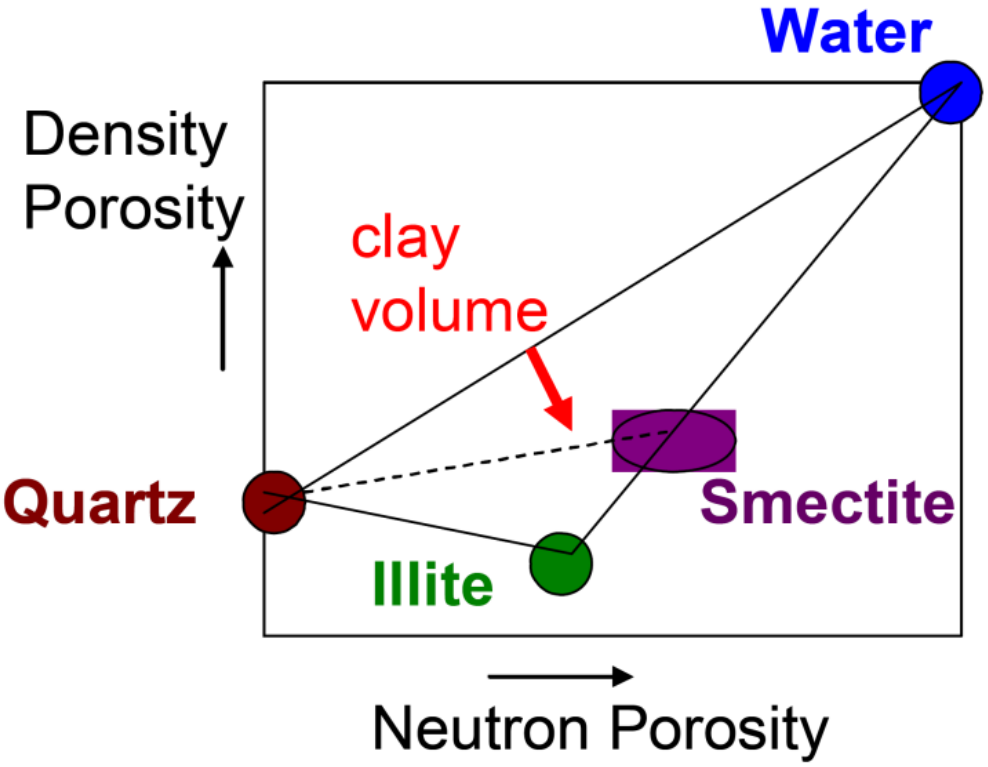

Figure 4-3: A schematic illustration of where the three components of shale stand on neutron density versus density porosity (Katahara 2008).

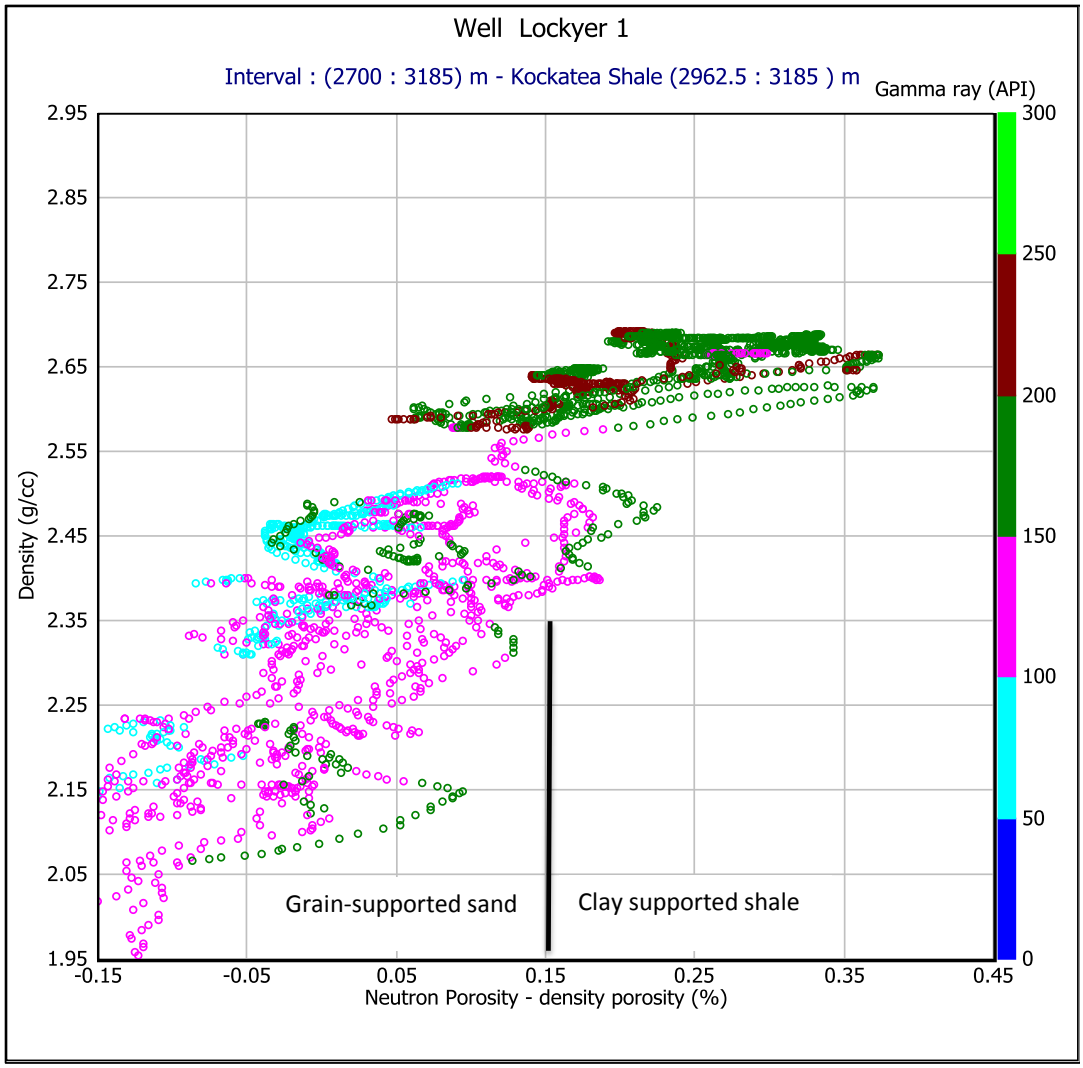

Figure 4-4: Shale discrimination based on the difference between neutron porosity and density porosity.

In order to ensure the quality of the data across the shale intervals, the quality was cross-checked with other data sources, including the Photoelectric, Calliper and Gamma ray logs. The results demonstrated good quality data of the studied boreholes as illustrated in Figure 4-5. To illustrate, the calliper histogram shows that the standard deviation is small and average value is close to 8.5 inches, since the diameter of the target interval is 8.5". This means the borehole is in good shape. In addition, the GR and PE within the target interval show consistency within the same range values with no major deviations.

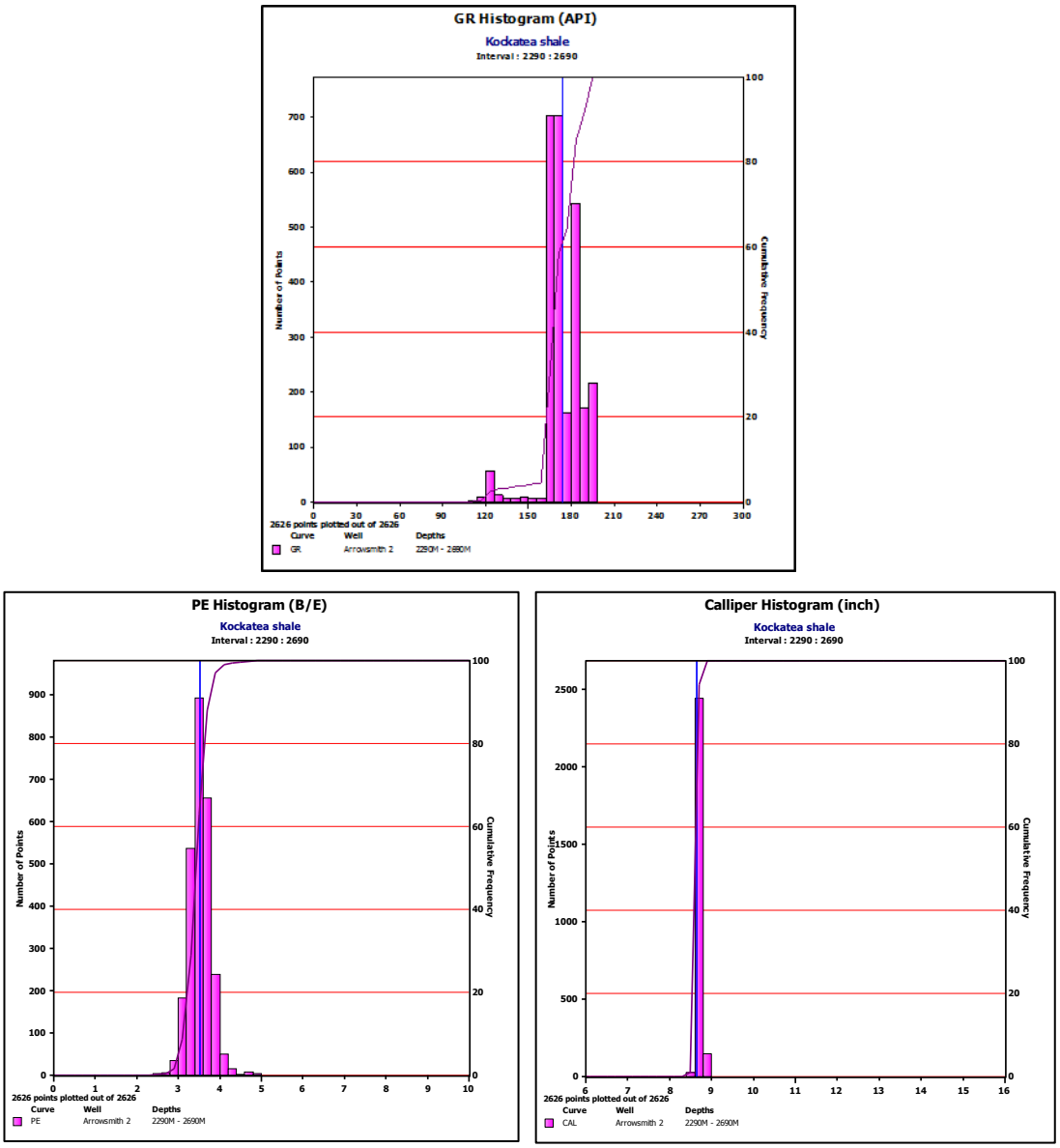

Figure 4-5: Data quality checks across the shale gas potential interval (Kockatea Shale) in the Arrowsmith-2 well, Gamma ray log (top), Photoelectric log (PE) (bottom-left) and Calliper log (bottom-right).

4.2 Mud log data

Mud logging data such as mud weight, equivalent circulating density (ECD), drilling rate of penetration (ROP), kicks and real pore pressure measurement where available, were used to validate the estimated pore pressure. The mud log data replaced the direct pressure measurement (e.g., MDT, DST, RFT) when the direct pressure measurements were not available for the formations under examinations.

Direct pressure measurements have also been approved not to be in practical use in low permeability formations such as shale because of their associated operational

difficulties, such as the high cost of rig operation and risk measurement tools sticking (Alixant and Desbrandes 1991; Bigelow 1994).

The compaction trend method utilizing Eaton's Equation (Equation 4-1) was first used with Eaton's exponent n=3 as proposed by (Eaton 1975). The results of pore pressure gradients were compared with the used gradients of mud weight and Equivalent Circulating Density (ECD) and were found to be mismatched, as the predicted pore pressure gradients were much higher than the used mud weight and ECD gradients. After testing different values for the Eaton's x exponent, the best match was found when using a value of 2 for the x exponent.

For the overpressure analysis to be performed, the well log data for the shale intervals were plotted versus depth. In regions where there were deviations from normal compaction trends (NCT) within the shale intervals, the cause of the deviations were examined against two criteria: (1) change in lithology and (2) change in pore pressure profile. Gamma ray, Photoelectric Factor (PEF), and Calliper logs were combined with the drilled cutting description.

These factors were the main tools to identify lithology. The deviations from NCT were also examined by analyzing the observed mud logging data that were used as qualitative overpressure indicators such as increase in: (1) mud weights, (2) drilling rate of penetration (ROP) and (3) total gas units across the examined intervals. Emphasis was also given to other drilling parameters such as surface and bit speed (RPM), weight on bit (WOB) and mud flow rates. Geochemical data such as ethane isotope were also used to validate the occurrence of overpressure, were the real pressure measurements are not available.

4.3 Other data

In regions where there are confirmed overpressures, results were analysed to determine the overpressure generating mechanisms. In order to do so, several data sets were analysed. This includes well log responses, data cross-plots, mineralogical study and stress data. Pore pressure gradients were also mapped to have an overall view and therefore to characterize basins' pore pressure profile.

The pore pressure profiles were then correlated to the tectonic activities which have driven the present complicated geology of the studied areas. The focus on the Perth Basin was to study pore pressure in the Kockatea Shale in three areas - two of which have similar tectonic characterizations as both have experienced severe tectonic

activities. These include the localities of Beagle uplift and Northampton uplift. The other studied area in the Perth Basin which has not been affected by those phases of extension includes the Dandaragan Trough and its adjacent Beharra Springs Terrace of similar characterizations.

In the Canning Basin, the pore pressure profile was studied in the Laurel formation in the Fitzroy Trough and Leonard Shelf. The implications of tectonic features were also examined and correlated to the occurrence of overpressure.

Structural features, seismic characters, core images and well log data were analysed to validate the correlations.

Chapter 5 Pore pressure Evaluation in the Perth Basin

Some materials presented in this chapter were published in the Journal of Unconventional Oil and Gas Resources (Ahmad et al., 2014) and significant portions of the results discussed herein were published as a book chapter by John Wiley & Sons (Ahmad and Rezaee 2015).

The primary objective of this chapter is to present pore pressure profiles in the Kockatea Shale (Perth Basin). The chapter highlights the pore pressure regimes in this shale formation in every compartmentalised region that are characterized as sub-basins, ridges, troughs and terraces. The other purpose is to examine whether pore pressure regimes exhibit the same trends all around the basin or if there are some pore pressure abnormalities in certain regions. The results were analysed in the light of the geological and tectonic variables (Chapter 2) and theoretical background (Chapter 3), together with the proposed methodology (Chapter 4), to come up with the most suitable correlation.

The desired outcome of this chapter is a broad understanding of pore pressure distribution in the potential shale gas interval of the Kockatea Shale in the Perth Basin and the relation between pore pressure and the tectonic activities that have taken place in the concerned regions. The chapter starts with a section on the background information and data that are available for the Kockatea Shale in Section 5.1. Thereafter, the observation of pore pressure is discussed in Section 5.2. After which, the data is analysed in Section 5.3. In Section 5.3, pore pressure is evaluated in tectonically stable regions (Dandaragan trough and Beharra Springs Terrace) as well as the tectonically active localities near the centres of the two major phase of uplifting. The effect of tectonic activities on pore pressure distribution in shales is explained in Section 5.4. Furthermore, a thorough multidisciplinary approach is discussed in Section 5.5, to confidently identify the grounds giving rise to the overpressure generation in this region of the Perth Basin.

Further study was conducted on the shale gas formation of the Laurel formation in the Canning Basin to examine whether the theory that was established in the Perth Basin is applicable universally or just locally for the Perth Basin. A detailed interpretation of these results will be given in Chapter 6.

5.1 The Kockatea Shale

Perth Basin is still classified as exploration areas for gas shale resources. Thus, no real pore pressure data have yet been released for the potential shale gas reservoirs. The unavailability of such pressure measurements might also be attributed to the lack of such data, as these kinds of tests are associated with several difficulties particularly when performed in shale intervals. Therefore, the analysis of pore pressure in this study will be inferred indirectly from the well log data, mud log data and drilling reports, combined with analysis of geochemical data.

Geologically, the top depth of the Kockatea Shale varies significantly from one part of the basin to another. This is exclusively driven by the excessive tectonic activities that occurred sequentially in the basin. A detailed explanation of these phenomena was provided in Chapter 2, Section 2.2. Figures 5-1, 5-2 and 5-3 show prospective structural view of Northern Perth Basin, average thickness and top depth of the Kockatea Shale respectively.

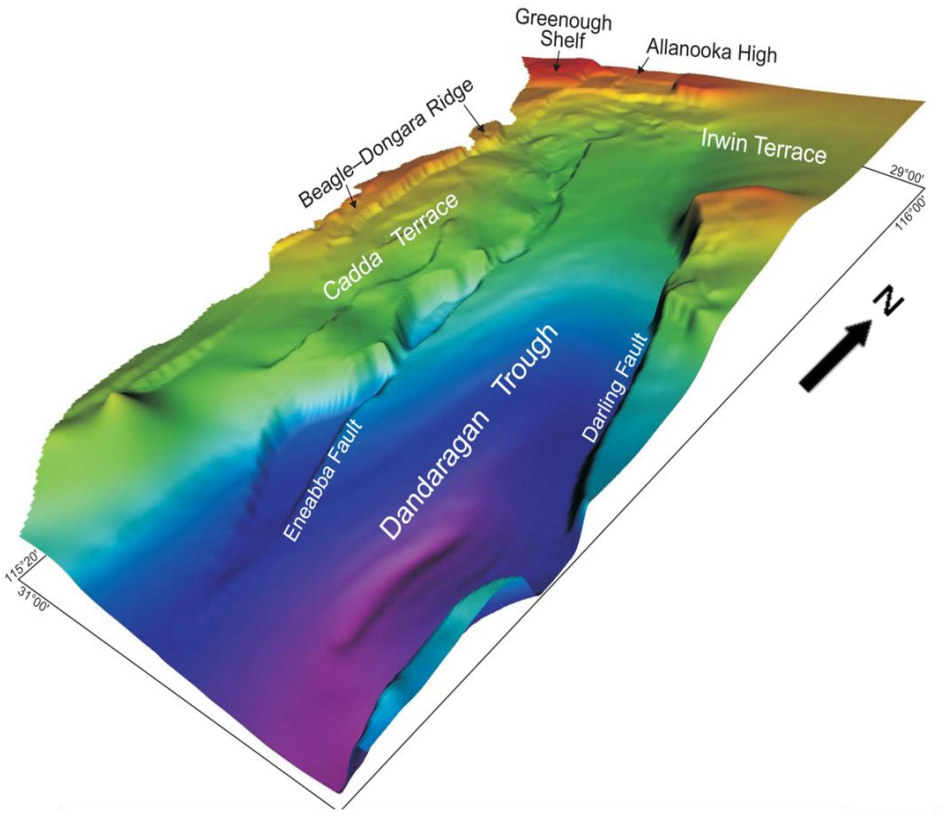

Figure 5-1: Prospective view the northern Perth Basin extracted from (D'Ercole et al. 2003).

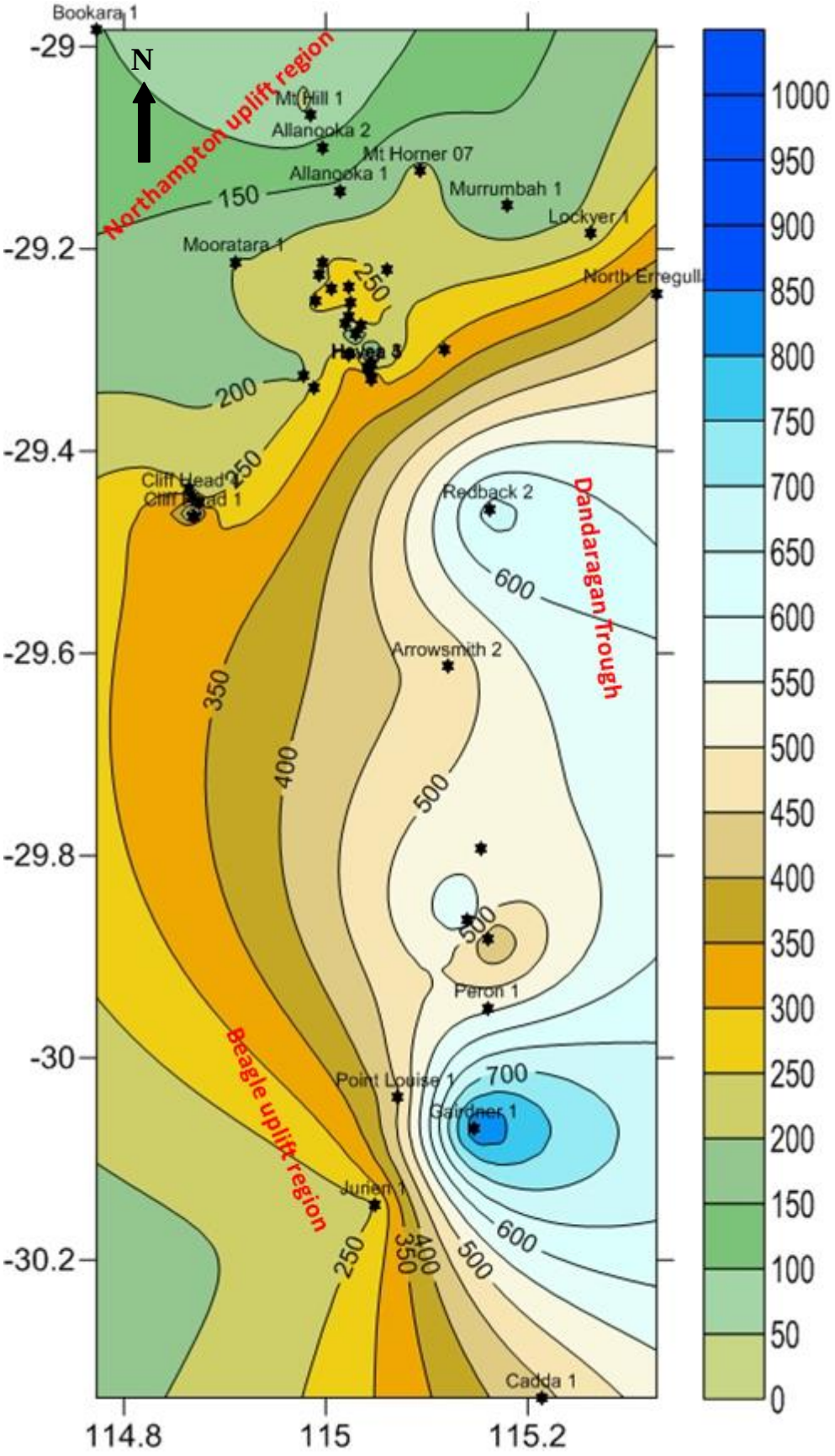

Figure 5-2: Isopach map for the Kockatea Shale in the Northern Perth Basin (depth is given in meters)

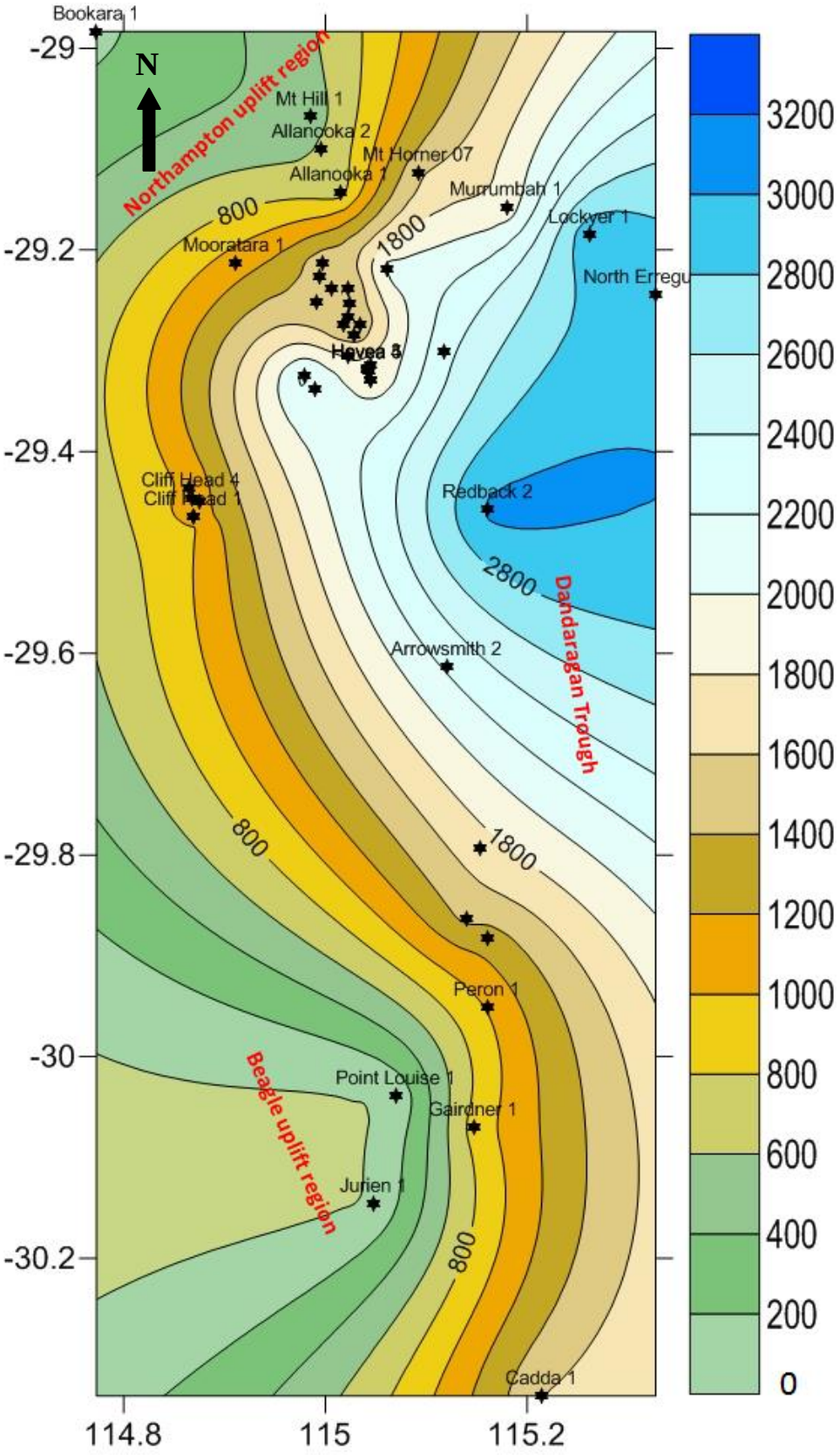

Figure 5-3: Depth contours of the top of Kockatea Shale in the Northern Perth Basin (depth is given in meters)

Generally, there are more than 200 wells that have been drilled in the Perth Basin. However, many of these boreholes neither have good quality data nor intersect with the Kockatea Shale. On average, 43 wells in the Perth basin were useful because they had good quality well log and mud log data. These wells constitute the database of this study and were significantly examined to determine the pore pressure distribution and overpressure generating mechanisms.

5.2 Observation

The well log data suites that were available for analysis came from 35 wells. The identification of shale formations was made by cross-plotting the density log against the difference between neutron porosity and density porosity, using a technique established by Katahara (2008). In this research, the data displayed a clear difference in the slope. A threshold value of 0.15 was selected for the difference between neutron porosity and density porosity ($\Phi N - \Phi D > 0.15$) to guarantee that the overpressure analysis was performed in shales (Figure 5-4).

5.2.1 Overburden stress calculation

The density log was used to compute the overburden stress in the region using Equation 4-2. An illustration from the Redback-2, Woodada-9 and Arrowsmith-2 wells is shown in Figure 5-5 and examples for the calculations are presented in Table 5-1.

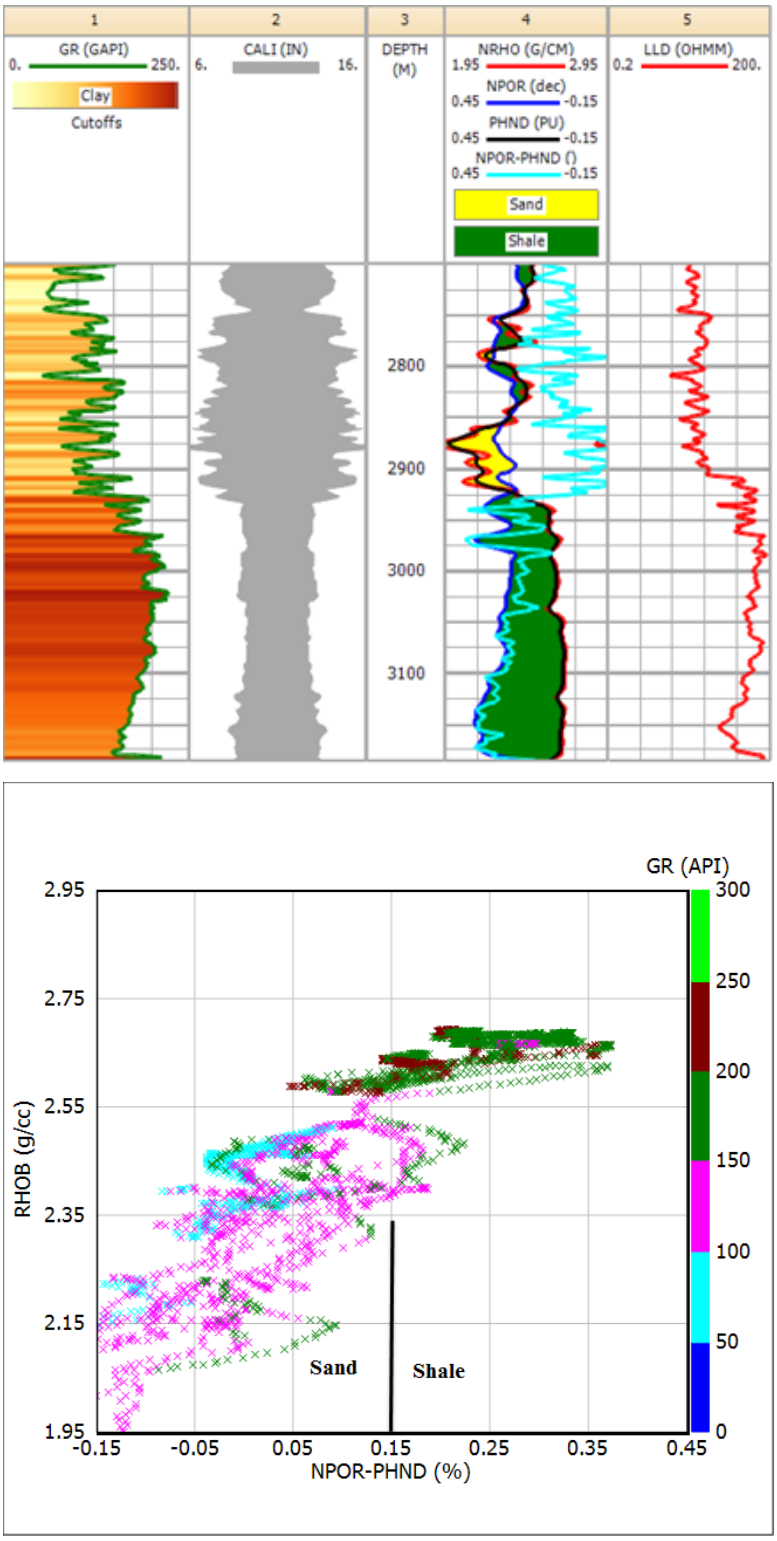

Figure 5-4: Cross-plot of shale discrimination on the basis of the difference between the neutron porosity and density porosity for the Lockyer-1 well (Perth Basin).

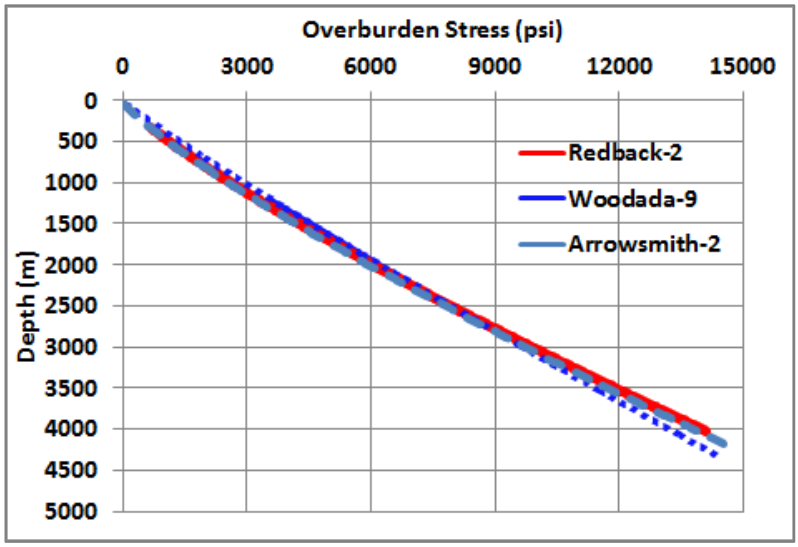

Figure 5-5: Examples of vertical stress in the Redback-2, Woodada-9 and Arrowsmith-2 wells.

Table 5-1: An example of overburden stress gradient calculation in the Redback-2 well.

TVD (m)	RHOB (g/cc)	dz (m)	dσv (psi)	σob (psi)	OB Grad (psi/ft)
2054.447				6237.591	0.926
2054.599	2.0734	0.1524	0.448	6238.039	0.926
2054.751	2.0953	0.1523	0.452	6238.491	0.926
2054.903	2.1167	0.1521	0.456	6238.947	0.926
2055.056	2.1376	0.1524	0.462	6239.409	0.926
…	…	…	…	…	…
3576.200	2.6463	0.1521	0.570	11692.695	0.997
3576.353	2.6463	0.1526	0.572	11693.267	0.997

5.2.2 Compaction trend and overpressure estimation

As discussed in Section 3.3.1, sonic transit time is most widely used as a porosity indicative factor. Therefore, it is more reliable to establish regional compaction trend using sonic transit time versus depth. Normally, the sonic transit time values decrease gradually as depths increase through the zones of normal pore pressure. The normal compaction trend was established by fitting the sonic data linearly to hydrostatically pressured formations that overlay the Kockatea Shale as shown in the example presented in Figure 5-6.

As shown in Figure (5-6), the sediments continued to compact normally and density continued to increase while sonic transit time decreased until a certain depth within the Kockatea Shale. This depth varies from one well to another depending on the top depth of the Kockatea Shale. At this depth, the well log data started to deviate from the normal compaction trend. The sediments return to normal trends below the shale interval of Kockatea.

In addition, mud logging data showed the same normal and abnormality within the lower section of the Kockatea Shale. The results were interpreted as the lower section of the Kockatea Shale being overpressured. The top of the overpressure zone is picked where the porosity and vertical stress dependent parameters divert from their normal trends.

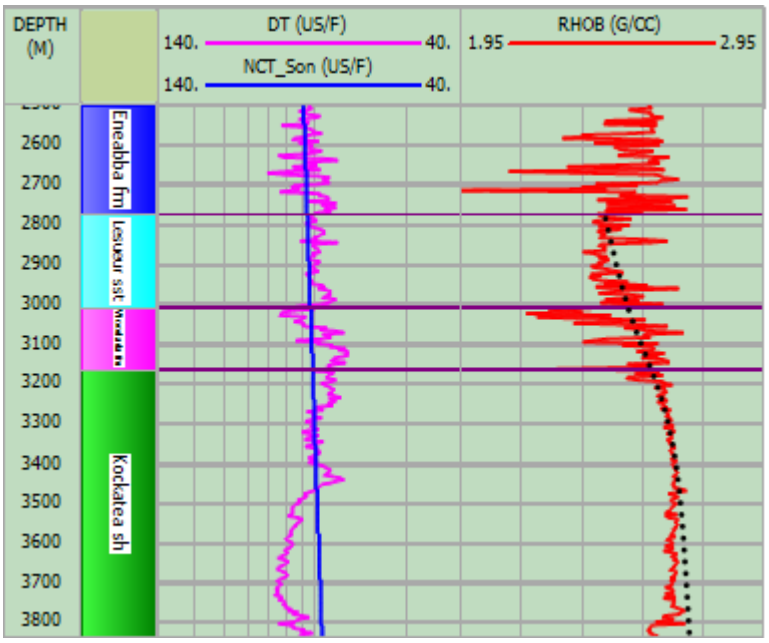

Figure 5-6: Composite sonic and density logs for the Redback-2 well (Perth Basin). The blue and black-dashed lines are the compaction trends for sonic and density respectively.

The pore pressure has been inferred indirectly using Eaton's Equation with sonic logs (Eaton 1975) (Equation 4-1), employing the Interactive Petrophysics Software. Overpressures have been detected by the departure of the porosity-dependent parameters such as sonic transit time, resistivity and density logs, from their normal trends. The sonic log was favoured for shale pore pressure estimation primarily

because the sonic log is usually less influenced by bad borehole conditions as compared to other logs e.g. resistivity and density logs (Bois et al. 1994).

After testing different values for the *x* exponent in Eaton's correlation (Equation 4-1), it was determined that the best match between the estimated pore pressures and other relevant pore pressure parameters such as drilling data and mud log data is found when using a value of 2 for the *x* exponent.

The complete well log data responses for the shales in all wells from the Perth Basin are provided in Appendixes 1. For the purpose of overpressure analysis, the data from the wells, Arrowsmith-2, Lockyer-1 Redback-2 and Hovea-5 are presented to depict the finding on wells that exhibit overpressure. The wells, Arrowsmith-2 and Redback-2, were selected as representative examples for the wells that have the thickest sections of the Kockatea Shale. They were drilled away from any identifiable faults within an area of low incidence of fracturing or possible erosion. Hence, a full section of the targeted shale intervals can be penetrated and examined effectively. These two wells were drilled in the northern part of the Perth basin in the Dandaragan Trough and Baharra Springs Terrace respectively, mainly to evaluate the unconventional shale gas potential formations. As such, high quality data were available for analysis. The wells, Lockyer-1 and Hovea-5, were chosen because the sediments within this area were deposited in a similar environment, but the Kockatea Shale is less thick. Therefore, a comparison can be made with the response of well log data from the wells, Arrowsmith-2 and Redback-2. The Lockyer-1 well also has a variety of data which makes them ideal boreholes for analysis.

Furthermore, the data from the wells, Point Louise-1, Cadda-1, Cliff-Head-1, Mooratara-1, Gairdner-1, and Peron-1 are presented to show the results on wells that exhibit normal pore pressure in the Kockatea Shale.

5.3 Data analysis

5.3.1 Pore pressure of the Kockatea Shale in tectonically stable regions (Dandaragan Trough & Adjacent terraces -Perth Basin)

This area is classified as the deepest region with the thickest sedimentation column in the Perth Basin. The date from these regions is presented first because of their tectonic nature, as the tectonic activities is less intense compared to the other parts of the Perth Basin. The other reasons are the burial depth of the Kockatea Shale and the

high quality of the wirelines log data available in this region. Structurally, these areas form the major depocentres in the Perth Basin (D'Ercole 2003). A broader discussion of tectonic influences on pressure profiles is given in Section 5.4.

A comparison was made between two sets of wells that were drilled in these regions. This comparison was based on the variations of the thicknesses, formation tops and pore pressure profiles as well as the geographical positions of the representative wells.

5.3.1.1 The Dandaragan Trough

The Dandaragan Trough is a major feature that has the thickest section of sedimentary rocks in the onshore Perth Basin (Crostella 1995). According to Cadman et al (1994), the subsiding Dandaragan Trough was developed in response to rifting which originated in the Early Permian and concluded in the Early Cretaceous, in the final separation of India and Australia. Up to 15000 m of Silurian to Cretaceous sediments were deposited in the region. To the west and south, the trough is flanked by a series of faults and the shallow basement of the Beagle Ridge and Harvey Ridge respectively.

The top of the Kockatea Shale deepens towards the centre of the depocentre and reaches 7000 m (Figure 2-2). The trough has limited tectonism and virtually an unfaulted syncline (Figure 2-2). However, as the sediments approach the axis of the Beagle Ridge from the centre of Dandaragan trough, the faulting intensity increases (Crostella 1995).

Stratigraphically, the nature of the Dandaragan Trough provides thick and clean shale intervals (Playford et al. 1976). The average thickness of the major source rock and potential shale gas formation Kockatea Shale is 400 m around the edges and the thickness increases up to 1000 m near the centre of the trough (Figure 5-2).

The data that has been analysed in the Dandaragan Trough includes well log data, mud log data, drilling data and geochemical data. There is only one well with Ethane isotope data in the Perth Basin, i.e., Arrowsmith-2 (Figure 5-7). The Ethane isotope data shows consistency with the well log data analysis. An illustration of this consistency is presented in (Figure 5-7). Normally, the isotope increases as depth increases. However, there is a deviation of isotope from the normal trend at the same depth 2425 m where well log data parameters deviate.

In order to study the cause of overpressure, a temperature survey was conducted. The temperature data derived from 18 wells drilled in the Northern Perth Basin shows that the geothermal gradient is around 3.42°C/100 m, with the temperature at the surface being around 21°C (Figure 5-8). Based on the geothermal gradient, this part of the Perth Basin is relatively warm.

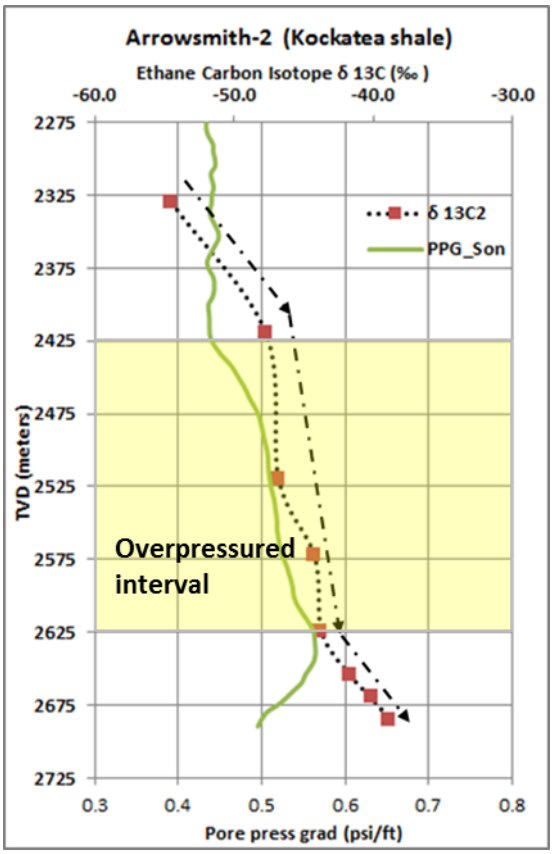

Figure 5-7: Ethane Isotope analyses and pore pressure profile for the Kockatea Shale in the Arrowsmith-2 well.

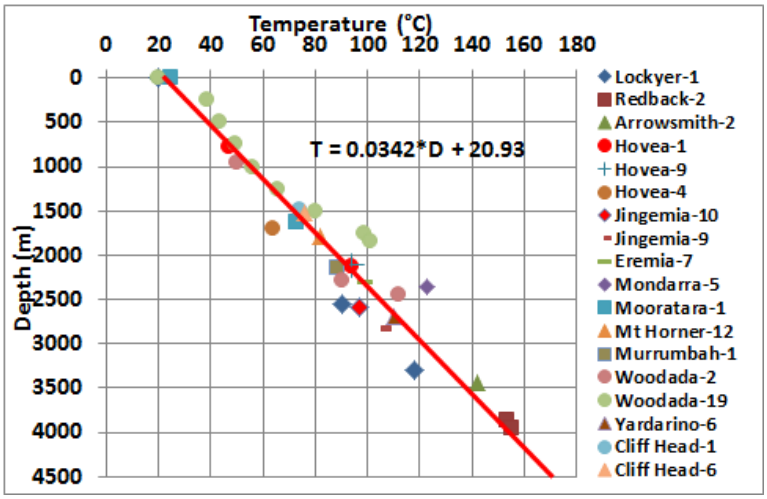

Figure 5-8: Thermal gradients in the Northern Perth Basin (DMP-WA 2012).

For overpressure analysis, the data from the wells, Arrowsmith-2, Lockyer-1, are presented to illustrate the findings.

5.3.1.1.1 Log data

5.3.1.1.1.1 Arrowsmith

The Arrowsmith-2 well was chosen as a typical example to present the finding because of the wide range of data that is available from it. Geographically, this borehole was drilled in the Northern Perth Basin in the Dandaragan Trough. It was vertically drilled to a total depth of 3340 m to primarily evaluate the unconventional shale gas potential formations. At this well, typical onshore Northern Perth Basin sedimentary sections were encountered. The well intersected 465.5 m thickness of the Kockatea Shale at depths of 2226.0 – 2691.5 m. The lithological section of the Kockatea Shale consists of interbedded claystone, sandstone and minor limestone. Well log data from this well exhibited overpressure. There is a clear reversal in sonic transit time and resistivity logs, whilst the density log remains approximately constant. The pore pressure gradient at the well continued to be normal at around 0.44 psi/ft. The upper section of Kockatea Shale exhibits normal pore pressure gradient. However, at the depth of 2425 m, pore pressure gradient increased gradually with depth and reached 0.56 psi/ft at the depth of 2630 m true vertical depth (TVD) (Figure 5-9).

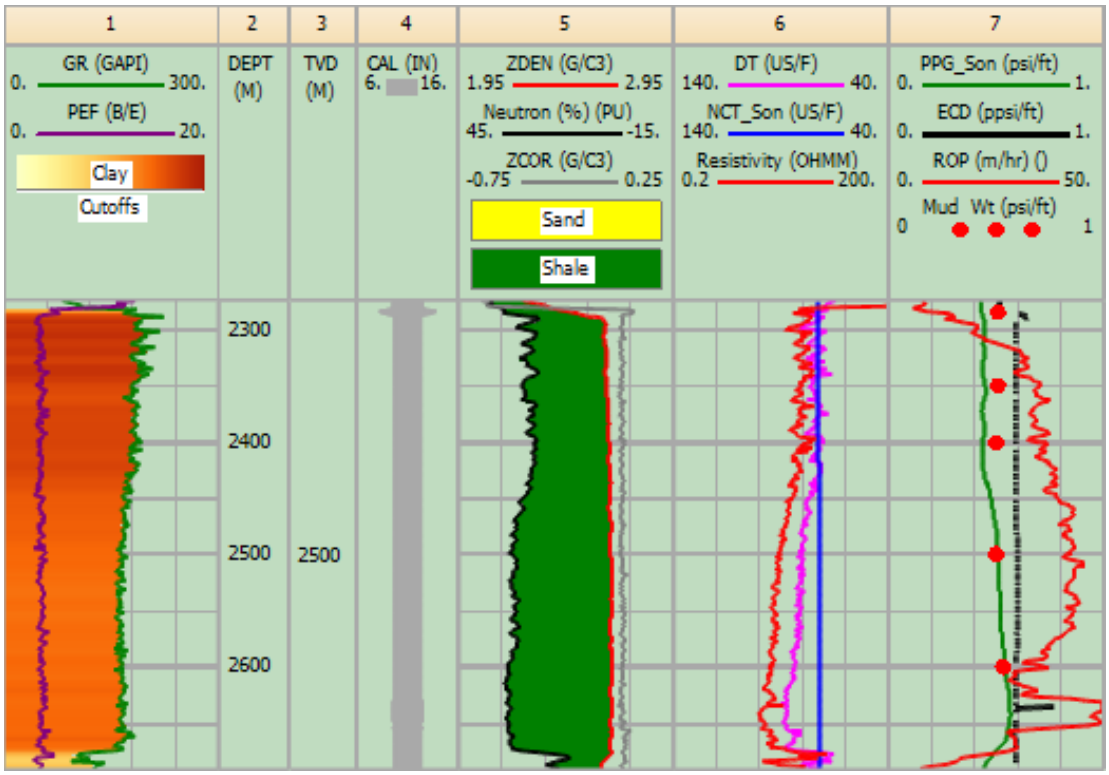

Figure 5-9: Estimated pore pressure gradient, mud weight gradient, Equivalent Circulation Density and well log data versus depth in the Kockatea Shale for the Arrowsmith-2 well (Dandaragan Trough – Perth). Eaton's method is with an exponent of 2.

There is a correlation between the reversals of well log data (sonic transit time, neutron porosity and resistivity) and the overpressure related parameters such as a continuous increase in drilling Rate of Penetration (ROP). In addition, despite the Equivalent Circulation Density (ECD) being higher than the predicted overpressure, several attempts were made to increase the mud weight in response to the gas flowing to the service while drilling the borehole as illustrated in Figure 5-9. The simplified lithological column also shows consistency all through the Kockatea Shale with very good borehole quality as shown in Calliper Log (Figure 5-9, Track 4).

As opposed to sonic, neutron and resistivity logs, the density log shows no noticeable reversal. Instead, it continued to increase until the depth of 2425 m TVD and then remains fairly constant across the lower section of the Kockatea Shale. This response is explained further in Section 5.5.1.

Cross-plots of neutron porosity versus sonic transit time and density-sonic transit time as well as density-neutron porosity are shown in Figure 5-10 with the TVD

colour–coded in the Z axis. The plot reveals that the overpressured section data points fall within the high density, high transit time and neutron porosity portion of the figure. This can be explained that even though the sonic transit time and neutron porosity have deviated from the normal trend at the lower section of the Kockatea Shale and showed increased transit time and neutron porosity in the depth range 2425-2690 m, the density log responded to overpressure differently by remaining at higher values and staying constant as opposed to the response of other well log data parameters. The illite compaction trend was established based on the empirical correlation established by (Dutta 2002). The overpressured data points fall away from the illite compaction trend. This is presented by the circled data (purple, light green and navy points) in Figure 5-10. The purpose of plotting these is to identify what mechanisms stand behind the overpressure generation, which will be discussed further in detail in Section 5.5.

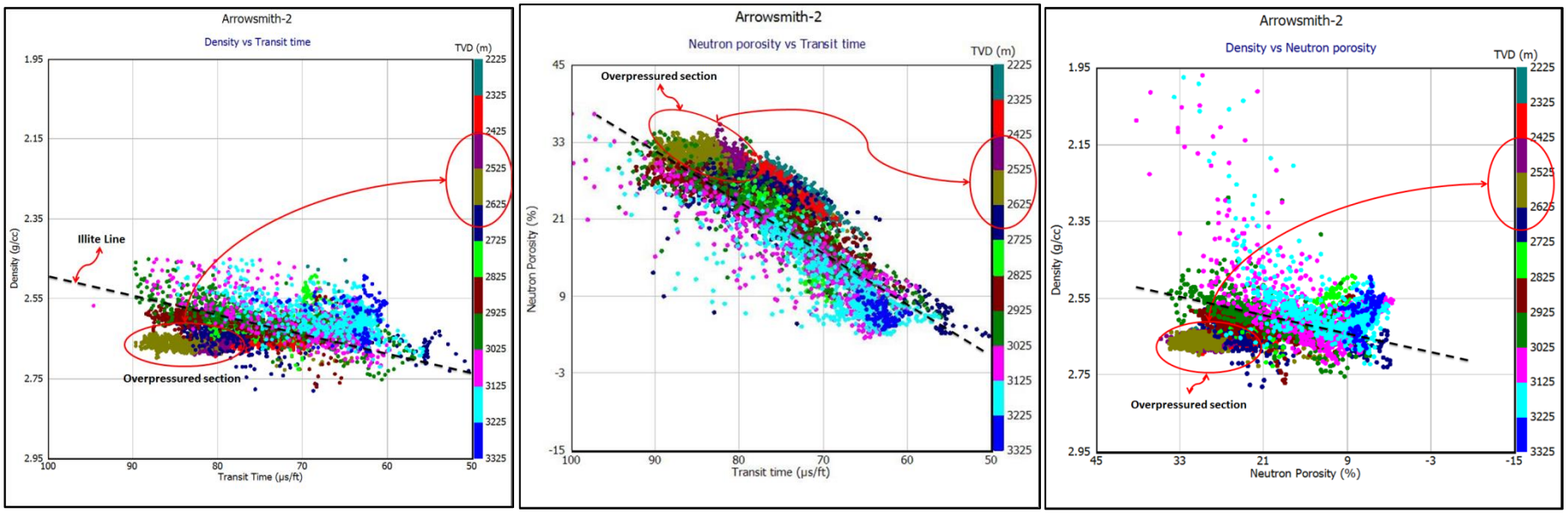

Figure 5-10: Cross-plots of density versus sonic transit time, neutron porosity and neutron porosity versus sonic transit time for the Arrowsmith-2 well (Perth Basin

5.3.1.1.1.2 Lockyer-1

This well was also drilled in the Northern Perth Basin in the Dandaragan Trough. It was chosen because the sediments within this area were deposited in a similar environment. However, the thickness of the Kockatea Shale is significantly lesser than the Kockatea Shale interval observed in the Arrowsmith-2 well. Therefore, a comparison of the responses of well log data can be made. The well intersected 223 m of Kockatea Shale consists of interbedded claystones, siltstones and sandstones.

Overpressure was observed from well log and mud log data in the Kockatea Shale (Figure 5-11). However, DST was conducted at the bottom of the Kockatea Shale at 3183, but failed to record pressure build-up. The tightness of the formation explains the failure of recording overpressure within this interval. Similar results were obtained from the North Erregulla-1 well, which was drilled within the same structure. Results are shown in Appendix 1a.

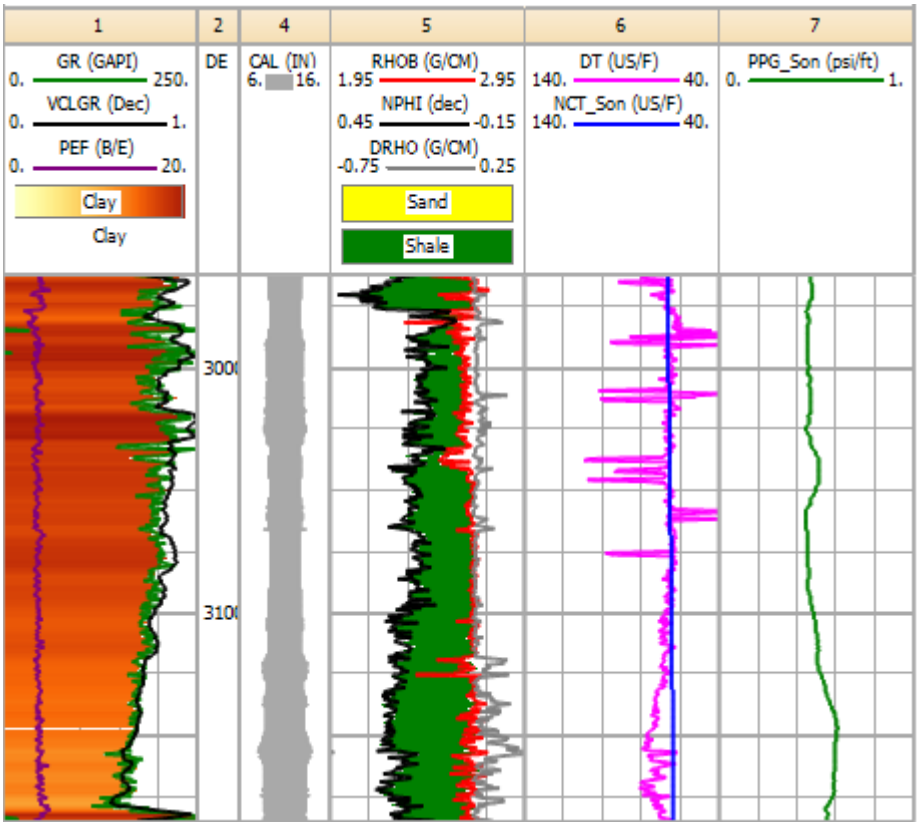

Figure 5-11: Estimated pore pressure gradient, and well log data versus depth in the Kockatea Shale for the Lockyer-1 well (Dandaragan Trough – Perth).

Cross plots of well logs data from the Lockyer-1 well show the same abnormalities as observed in the Arrowsmith-2 well, with indication of the lower section of the Kockatea Shale as being overpressured (Figure 5-12).

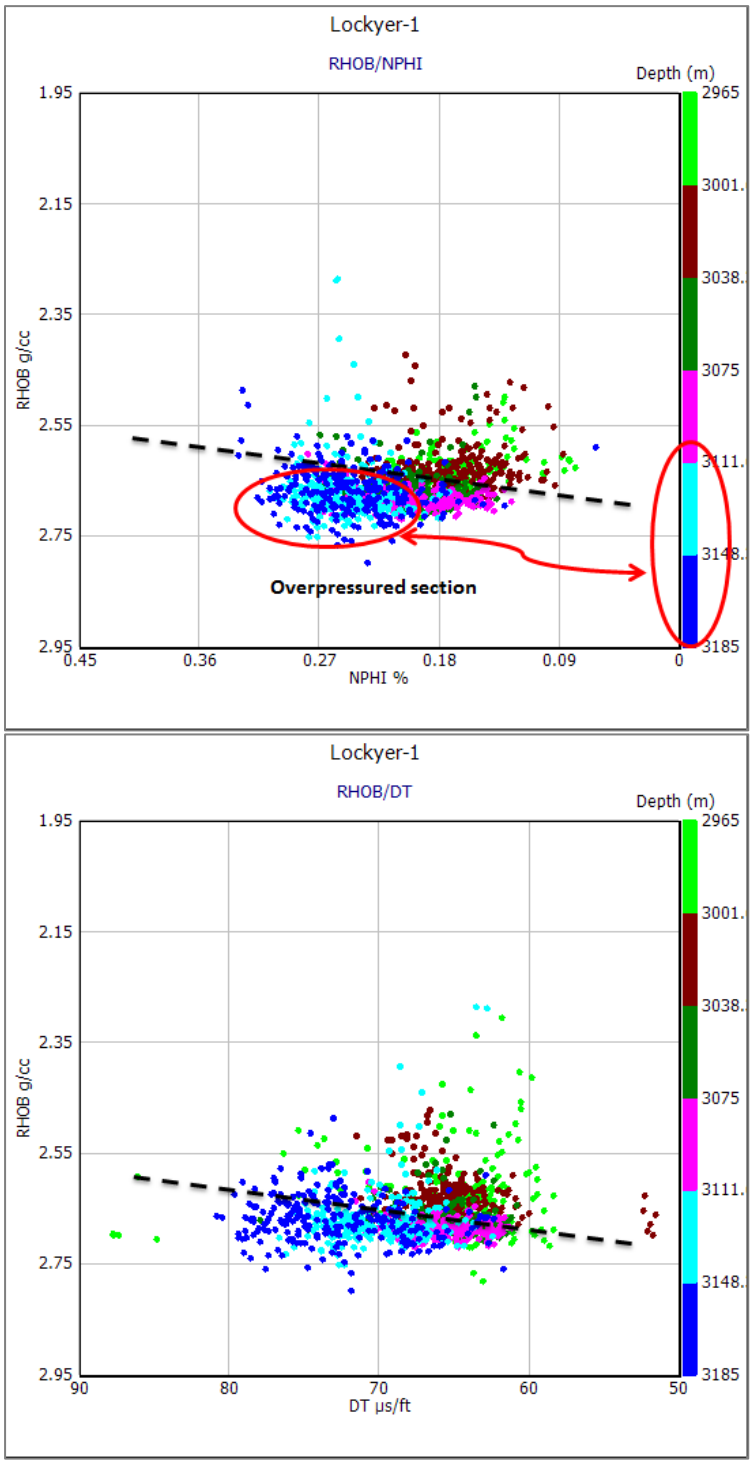

Figure 5-12: Cross-plots of density versus sonic transit time and neutron porosity for the Lockyer-1 well (Perth Basin).

5.3.1.1.2 Gas Geochemistry

As overpressure has been observed from the well log and mud log data analysis and with the absence of the real pore pressure data in the shale to calibrate the estimation of pore pressure, an alternative approach was used to look for evidence of

overpressure. In light of the above, geochemical gas compositions from chromatography were used for overpressure calibration. The data were interpreted in the form of an isotope (free gas).

Unfortunately, there is only one well with isotope analysis data for the Kockatea Shale in the Perth Basin, i.e. Arrowsmith-2. A remarkable match has been observed between the top of overpressure as observed from the well log data parameters and the Ethane isotope from their normal trends (Figure 5-7). The trend of the isotope is increasing linearly with depth in the normally pressured zone. However, it deviates at approximately the same depth 2425 m, where the sonic transit time diverts from its normal trend. Within the overpressure zone, the isotopic values remain fairly within the same range value as opposed to what they supposed to be if they follow the normal trend. However, the values return to the normal trend when the pore pressure profile reverses back to normal.

According to Chatellier et al. (2011) and Ferworn et al. (2008), the diversion of Ethane isotope from its normal trend within the shale demonstrates that overpressure has been encountered. These authors stated that overpressured systems can be observed by gas carbon isotope signatures.

5.3.1.2 The Beharra Springs Terrace

The Beharra Springs Terrace is a north-south trending block that is bounded to the west by the Mountain Bridge Fault and the Beharra Springs Fault to the east. As stated in Section 2.3.6, the terrace is located between the Dongara Terrace to the west, and the Dandaragan Trough and Donkey Creek Terrace to the east (Crostella 1995). Owad-Jones and Ellis (2000) stated that the Kockatea Shale in this region acts as a detachment between the older faults and the faulting system in the younger strata. Since the Kockatea Shale in this region has not been affected by the two periods of faulting, pore pressure was studied and compared with pressure profiles in the Dandaragan Trough, so that a valid conclusion can be drawn.

5.3.1.2.1 Log data

5.3.1.2.1.1 Redback-2

The Redback-2 well is drilled in the Northern Perth Basin, approximately 33 km south-southeast of the township of Dongara. The well was directionally drilled in the

Beharra Springs Terrace to test the hydrocarbon potential of the Redback structure. The Redback Terrace is located in the hanging wall of the Beharra Springs Fault. Typical onshore Northern Perth Basin sedimentary sections were encountered. The Kockatea Shale is a thick interval intersected between 3043-3714 m TVD and dominantly comprises of claystones and siltstones.

The pore pressure gradient exhibits normal gradient at 0.44 psi/ft until the depth of 3340 m TVD. After that, the pore pressure gradient slowly increased with depth and reached 0.6 psi/ft at the depth of 3600 m TVD (Figure 5-13).

The drilling and mud logs data from this well show every indication for overpressure. Good gas shows have been recorded in the Kockatea Shale from 3172 m TVD. Below the top overpressured section at depth of 3340 m TVD, there was an increase in background and connection gases. The mud weight was increased several times in response to the high pumps of gases. The maximum recorded mud weight was 0.58 psi/ft, which is slightly less than the maximum overpressure. However, the Equivalent Circulating Density is still higher than the maximum overpressure gradient. An additional overpressure indicative parameter is the increase in drilling Rate of Penetration (ROP) at the lower section of the Kockatea Shale (Figure 5-13).

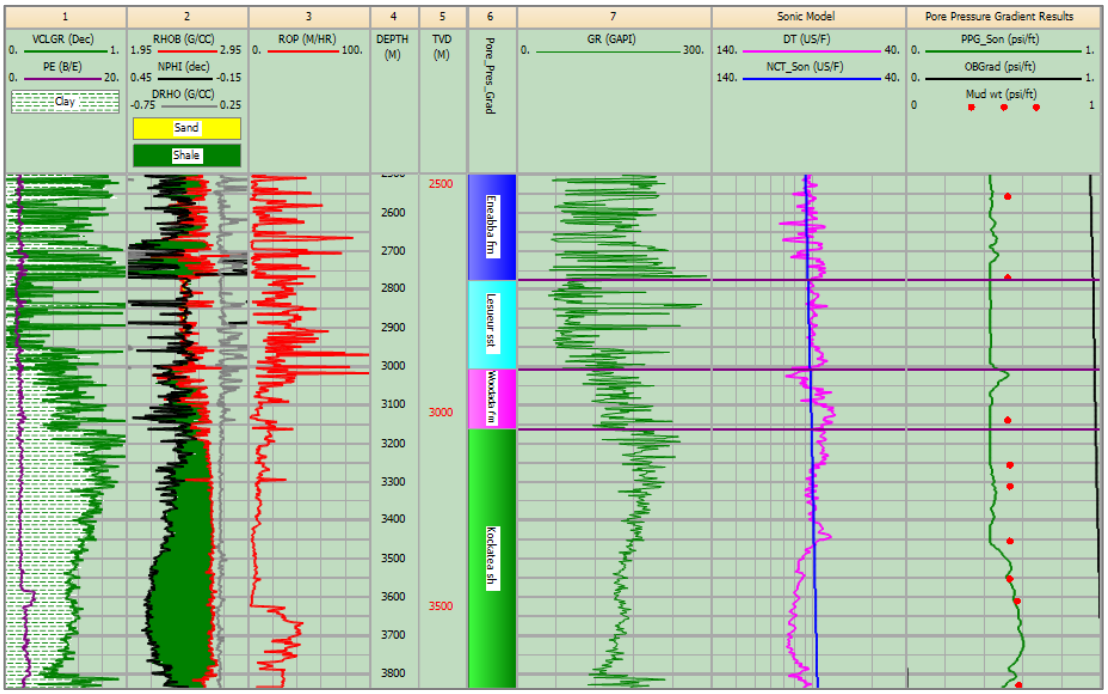

Figure 5-13: Estimated pore pressure gradient, mud weight gradient and well log data versus depth in the Kockatea Shale for the Redback-2 well (Beharra Springs Terrace – Perth Basin).

Cross-plots of density versus sonic transit time and neutron porosity and neutron porosity versus sonic transit time are shown in Figure 5.14 with the TVD colour-coded in the Z axis. Similar responses are observed in the Arrowsmith-2 well (Figure 5-10) and the interpretation is given in Section 5.5.2.

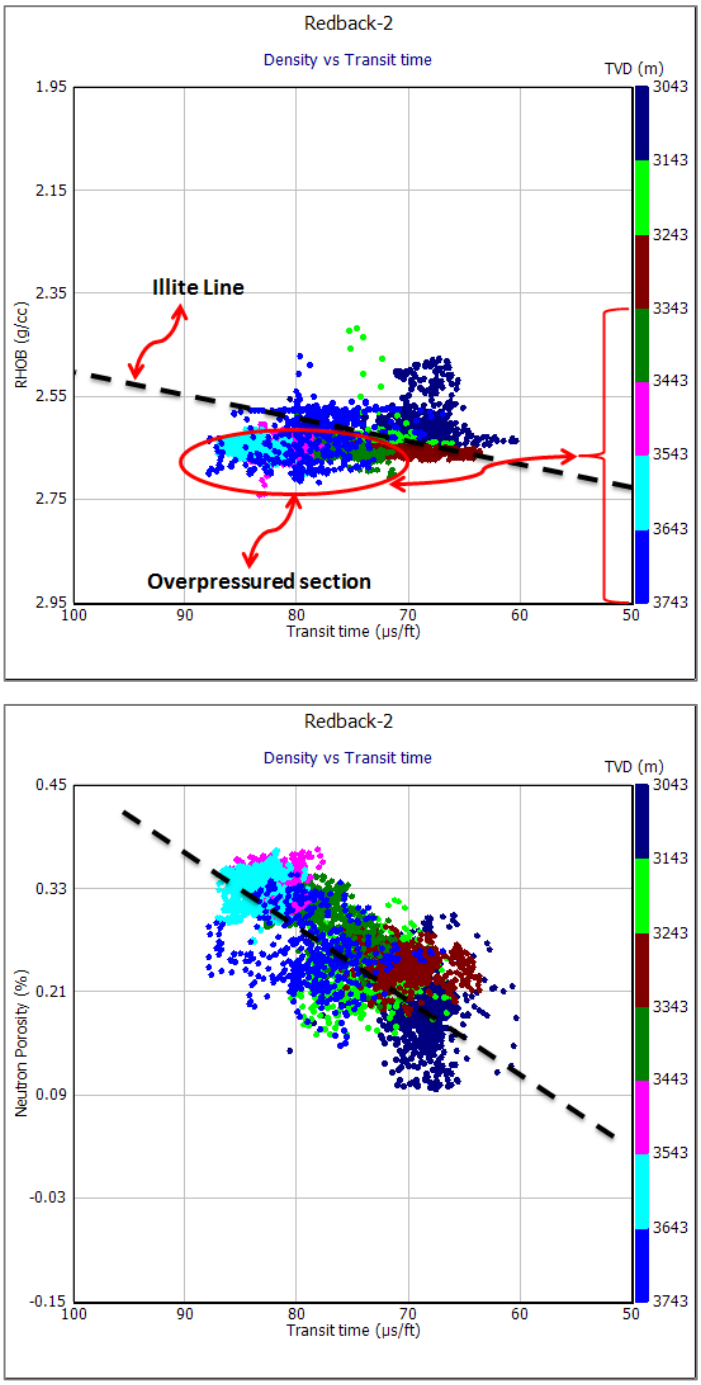

Figure 5-14: Cross-plots of density versus sonic transit time and neutron porosity and neutron porosity versus sonic transit time for the Redback-2 well (Perth Basin).

Similar responses were clearly observed in several wells drilled within the same region (Appendix 1a).

5.3.1.2.1.2 Hovea-5

The Hovea-5 well was drilled in the western portion of the onshore Northern Perth Basin in the Beharra Springs Terrace on the eastern side of the Mountain Bridge Fault and northwest of the Central Dandaragan Syncline.

The dominant structural feature of the Hovea structure is the north-south orientated, east-dipping Mountain Bridge Fault, which bounds the structure to the east and to the north by an east-west trending north-dipping fault. The activities that occurred in the Early Triassic along the Mountain Bridge fault have affected the structure and formed a local depocentre near the Beharra Springs filed (Mory and Iasky 1996). The well intersected 233 m of the Kockatea Shale, as opposed to 671 m in the Redback-2 well. This region has not been subjected to erosions due to the two rift cycles that took place in the Permian to Triassic and Jurassic age.

Well logs and mud logs data analysis from the Hovea-5 well show every indication for the lower section of the Kockatea Shale to be overpressured (Figures. 5-15 and 5-17). Sonic transit time (DT) diverted from the normal trend and increased at depth 1826 m TVD with good borehole quality. The porosity increased also in the interval of interest and there was a decrease in resistivity at the same depth.

It can be seen that there was no significant increase in mud weight within this interval. This can be due to the fact that the well has been drilled in overbalanced drilling conditions in a reasonably short time. These drilling conditions would not allow pore pressure and associated thin beds for the shale to build up. Therefore, overpressure was not noticed while drilling the borehole, considering the fact that the shale is impermeable and will need a long time to build up pressure and reach pressure equilibrium. However, the equivalent circulation density (ECD) is 0.54 psi/ft, which is quite close to the predicted pore pressure gradient in the overpressured section of 0.56 - 0.6 psi/ft.

Generally, drilling rate of penetration (ROP) decreases as depth increases as shown in Figure 5.15, Track 8. However, ROP increased at the same depth where sonic, resistivity and porosity logs deviated from their normal trends. This is an additional indicator for overpressure supported drilling report data which showed no changes in

rotary speed and constant RPM (Figure 5-16). It has been noted that there was also an increase in total gas units at the lower section of Kockatea Shale in this well.

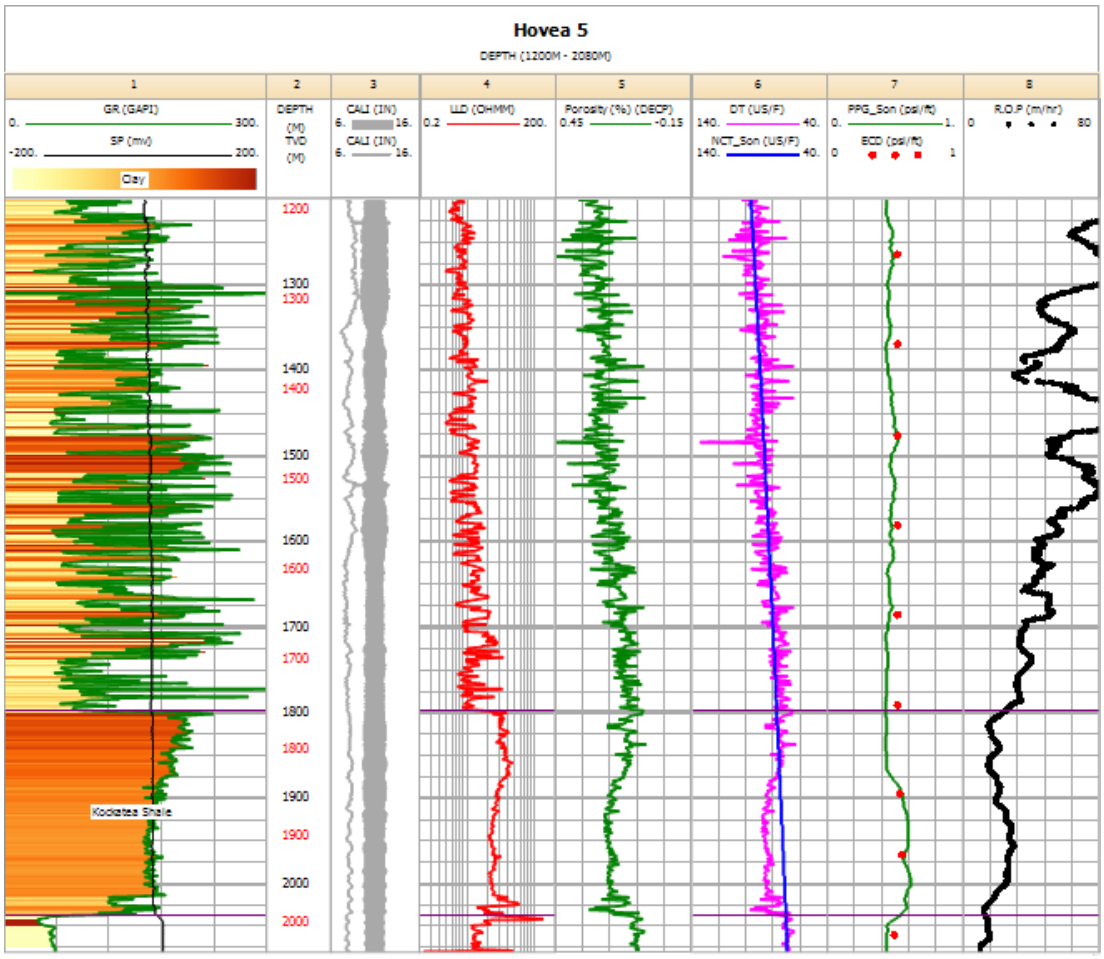

Figure 5-15: Estimated pore pressure, Equivalent Circulation Density gradients as well as log data against depth over the Kockatea Shale in the Hovea-5 well (Dandaragan Trough – Perth).

Figure 5-16 shows cross-plots of data taken from the Hovea-5 well that are shown RPM in the Y axis and ROP in the X axis with depth in the Z axis (TVD), pore pressure gradient, and mud flow pump respectively. The relationship between RPM and ROP for this well is that: ROP increases while RPM fairly remains constant in the overpressured section 1760-2000 m TVD, with no change in Z axis variables.

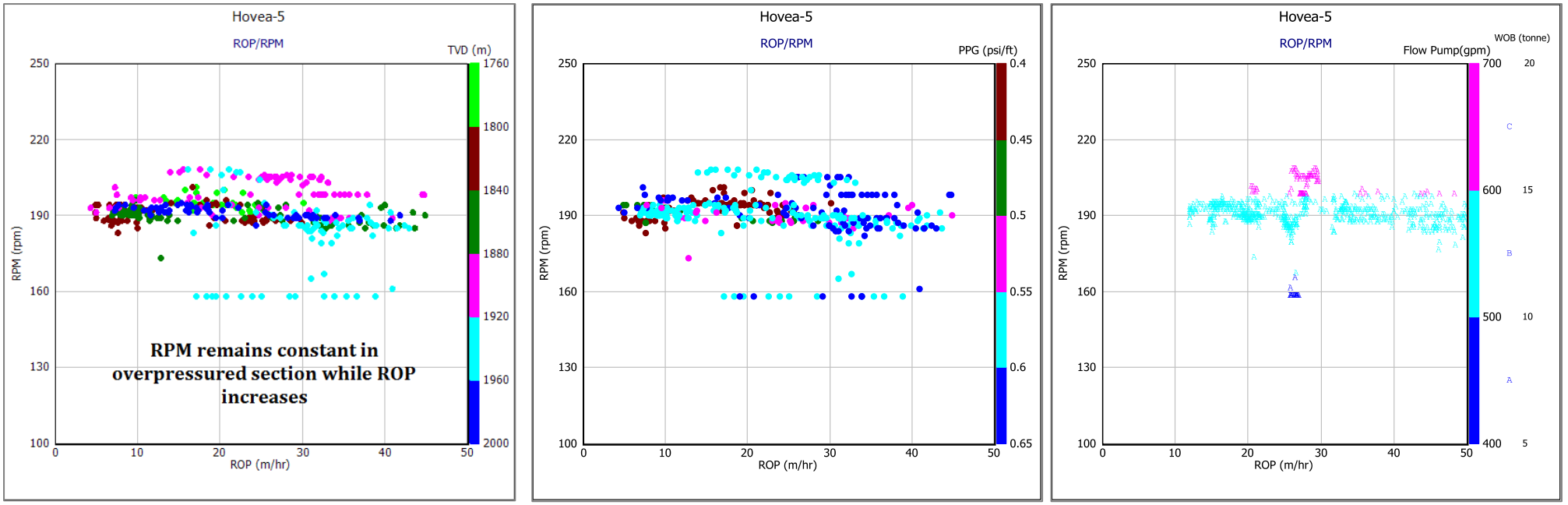

Figure 5-16: Cross plots of mud logs data from the Kockatea Shale in the Hovea-5 well (Perth Basin).

5.3.2 Pore pressure of the Kockatea Shale in tectonically active regions

The pore pressure results from these regions are analysed to make a comparison with the pore pressure profiles that have been observed within tectonically stable regions. The nature of these regions has been faulted and the tectonic activities that were experienced are more intense as compared to the other parts of the Perth Basin.

As mentioned in Section 2.2, the structure of the Perth Basin is controlled by two major phases of extension. The first is an Early Permian phase that centralizes around the Northampton High, whilst the second and more extensive phase occurred in the Late Jurassic to the Early Cretaceous periods (Harris 1994). The centre of the second uplifting phase is near the coastal town of Jurien within the Beagle Ridge.

In this section, pore pressure profiles in these two areas are studied and the tectonic influence on pressure profiles is explained. Then, a comparison between the two study cases of the Perth Basin is provided, by broadly analysing several data sets to ensure the validity of the comparison.

5.3.2.1 Beagle uplift

This area of the Perth Basin is classified as a faulted area. It is highly influenced by the Late Jurassic to the Early Cretaceous phases of extension. This extension is centralized in the Beagle Ridge where significant sedimentary sections were removed. The structure is categorized as elevated ridges and faulted terraces (D'Ercole 2003). The Beagle Ridge constitutes the most uplifted area in the Perth Basin and has a shallow basement. The ridge forms the western boundary of the Cadda Terrace, which is an intermediate terrace of north–south trending shelf between the Beagle Ridge and the Dandaragan Trough in the Northern Perth Basin (Crostella, 1995). The Abrolhos Sub-basin constitutes the western boundary of the Beagle Ridge. The Kockatea Shale sections within this region are severely uplifted and faulted. In addition, significant portions of this formation have been eroded (Song and Cawood 2000).

Geologically, this extension phase caused extensive basin inversion, uplifting as well as the development of structural terraces that step down from the centre of the uplifting in the Beagle Ridge to the Dandaragan Trough in the east (Quaife et al. 1994). The analysis of pore pressure profiles within this region is inferred from well log data, calibrated with some pore pressure measurements and then combined with

the geological, geochemical, geophysical and tectonic conditions. This multidisciplinary study facilitates the formulation of an overall conclusion.

5.3.2.1.1 Well log data

Well log data analysed in this region include Point Louise-1 and Gairdner-1 in the Beagle Ridge, Cadda-1 and Peron-1 in the Cadda Terrace as well as the Cliff Head-1 in the Abrolhos Sub-basin. The locations of these wells are within an area that is located near the centre of the second and major tectonic phase, where major uplifting and subsequent erosion occurred in the late Jurassic to Early Cretaceous. In the following sections, three wells are discussed, namely Point Louise-1 Cadda-1 and Cliff Head-1.

5.3.2.1.1.1 Point Louise-1

The Kockatea Shale in the Point Louise-1 well was intersected at a very shallow depth (43-482 m). However, the well was only logged from the depth of 235 m. Normal pore pressure profile was encountered in the Kockatea Shale in this well (Figure 5-17). There is only one pressure measurement which is the Drill Stem Test (DST) at the base of the Kockatea Shale in this well. This measurement closely matches the predicted pore pressure gradient from sonic transit time (Figure 5-17 top left).

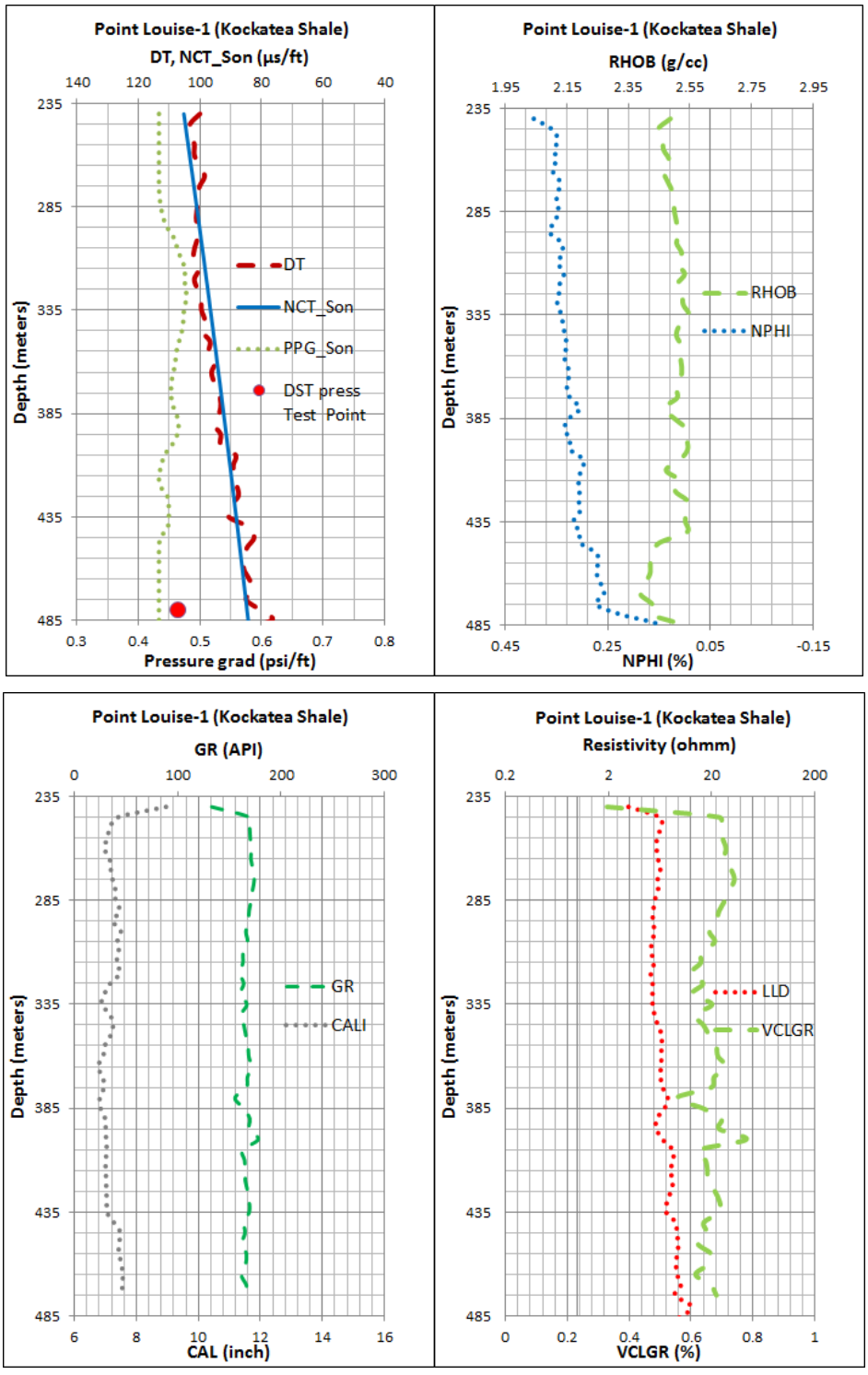

Figure 5-17: Estimated pore pressure and well logs data against depth over the Kockatea Shale in the Point Louise-1 (Beagle Ridge - Perth Basin).

5.3.2.1.1.2 Cadda-1

Furthermore, the Cadda-1 well was spudded in the north-central part of the Perth Basin in the Cadda Terrace. This well is located in a narrow block between the Lesueur and Cadda faults. The Kockatea Shale in this well was expected to be 900

m, but the well went through a normal fault and as such, approximately 450 m is missing (Fig. 7-18). In addition, a continuous dipmeter set of data clearly indicates a faulted zone in the Kockatea Shale. Moreover, a core cut of the top of the Kockatea indicates a highly faulted and fractured zone.

Results obtained from this well indicate normal pore pressure regimes across the whole interval of the Kockatea Shale. No signs of overpressure were observed in the mud logging data. It can be noted that on approaching the center of the uplifting near the township of Jurien, the faulting intensity increases.

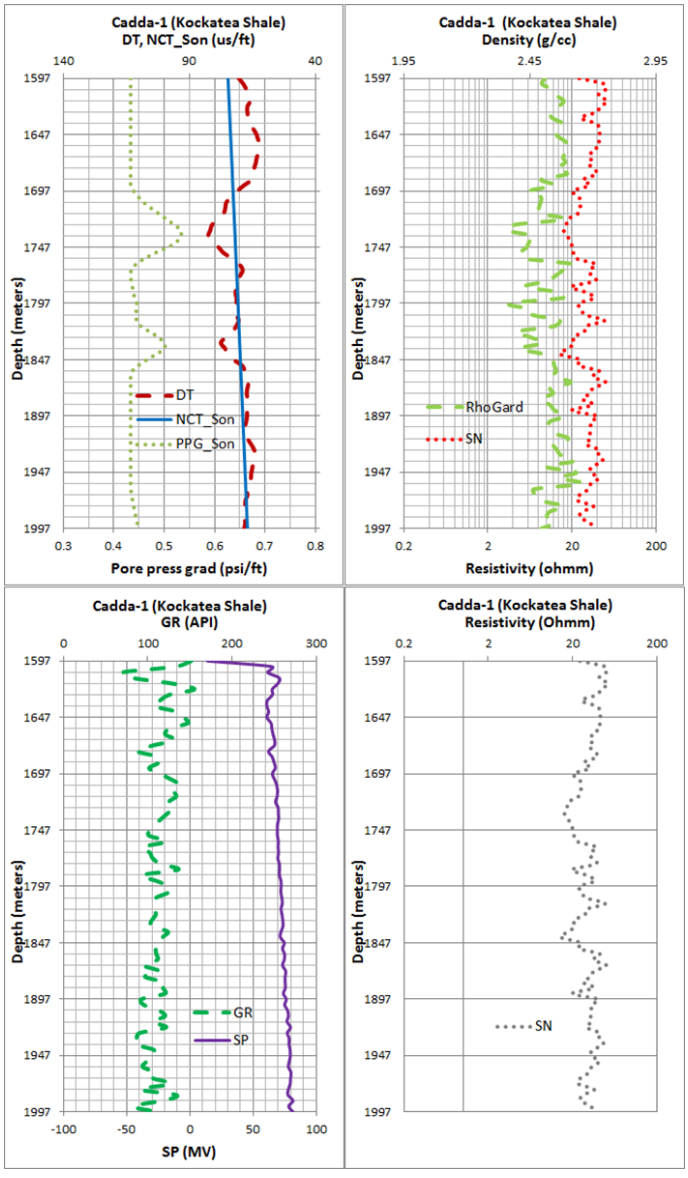

Figure 5-18: Estimated pore pressure and well logs data against depth over the Kockatea Shale in the Cadda-1 well (Cadda Terrace - Perth Basin).

5.3.2.1.1.3 Cliff Head-1

The Cliff Head-1 well is an offshore well which was drilled in the northern part of the Perth Basin in the Abrolhos Sub-basin, off the coast of Western Australia. Structurally, the Cliff Head feature shows that the Cliff Head-1 well is located within a faulted anticline feature with a narrow NW-SE oriented horst block, which has been complexly faulted due to several tectonic episodes (Figure 5-29). The well intersected 297.4 m of the Kockatea Shale from 980.8-1278.3 m. The lithology of this formation comprised of light-grey claystone and siltstone.

Normal pore pressure profile was encountered in the Kockatea Shale in the Cliff Head-1 well (Figure 5-19). Also, there are no abnormalities that were observed in the data cross-plots (Figure 5-20)

There is only one pressure measurement – the Reservoir Description Tool (RDT), at the base of the Kockatea Shale in this well. This measurement closely matches the predicted pore pressure gradient from the sonic transit time as shown in Figure 5-19, Track 7.

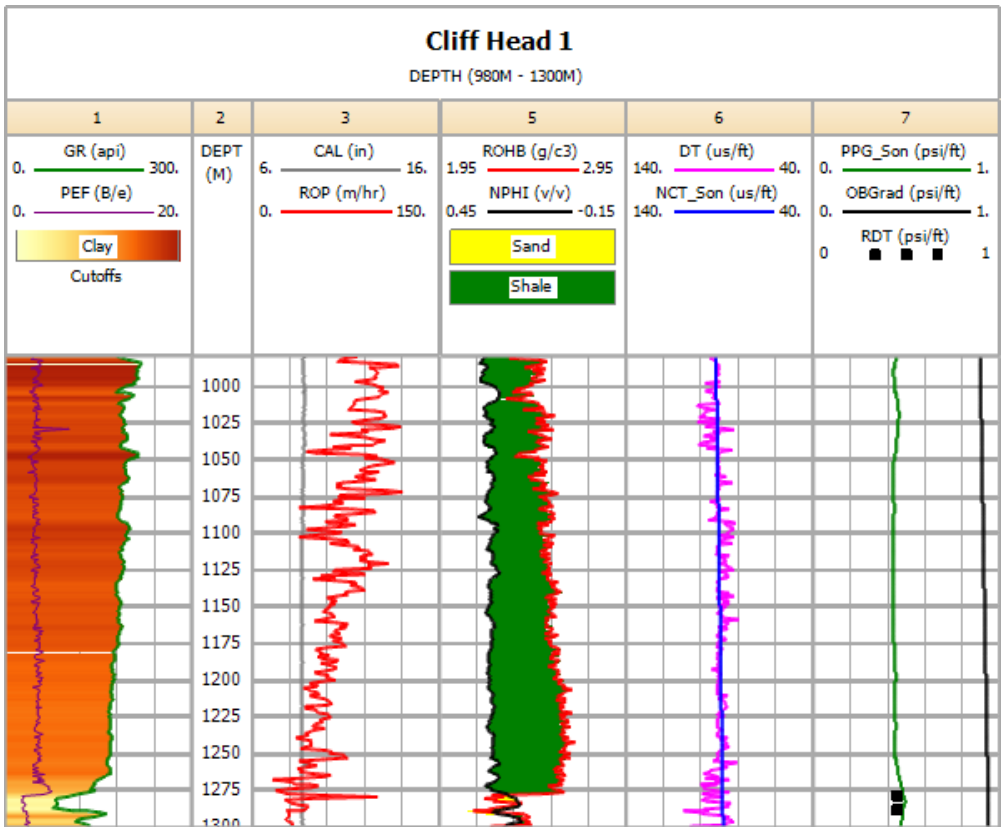

Figure 5-19: Composite well log data and pore pressure profile in the Kockatea Shale in the Cliff Head-1 well.

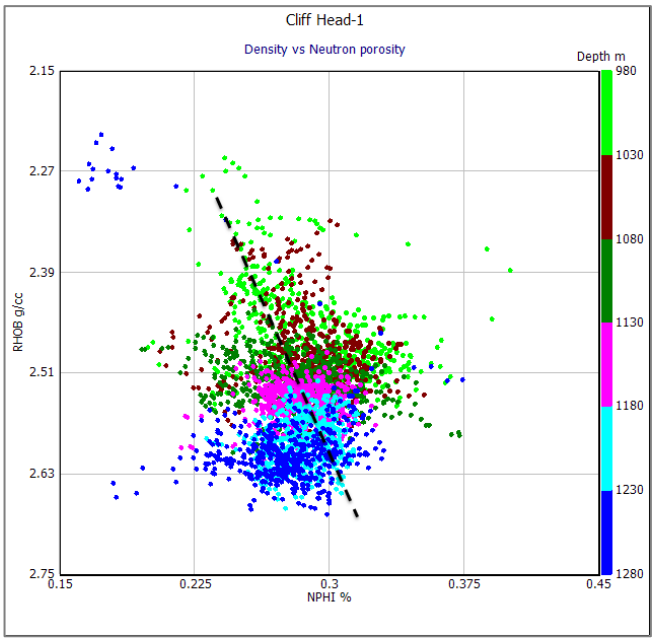

Figure 5-20: Cross-plot of density versus neutron porosity for the Cliff Head-1 well.

5.3.2.1.2 Thermal maturity data

In order to check the shale maturity in this region of the Perth Basin, the major maturity parameter of vitrinite reflectance is studied. The reason for studying thermal maturity in this region is to further examine and narrow down the possible generating mechanisms of overpressures that have been observed elsewhere in the Perth Basin. The analysis is compared with the results obtained within the areas that have encountered overpressure. This will then provide an insight of the overpressure generating mechanisms.

There are only eight wells with vitrinite reflectance data in this region of the Perth Basin i.e. Robb-1, Gairdner-1, Peron 1, Woolmulla-1, Cadda-1, Jurien-1, Beharra-2 and Point Lousie-1 (Figure 5-21).

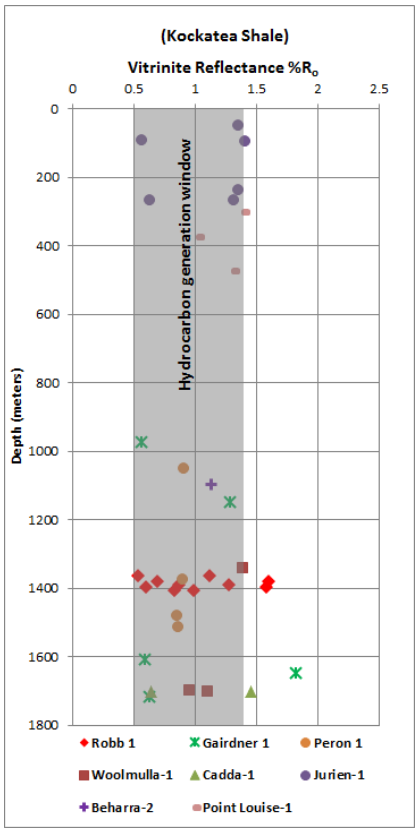

Figure 5-21: Vitrinite reflectance data for the Robb-1, Gairdner-1, Peron 1, Woolmulla-1, Cadda-1, Jurien-1, Beharra-2 and Point Lousie-1 wells. All the vitrinite reflectance data in the respective wells are for the Kockatea Shale intervals, where pore pressure profiles are found to be normal in the Beagle uplift locality (Perth Basin).

The vitrinite reflectance data in Figure 5-21 shows that the Kockatea Shale is within the hydrocarbon generation window (0.5-1.35) and the shales in this area of the Perth Basin are mature for hydrocarbon generation as the vitrinite reflectance is above the onset of oil generation reflectance of 0.5 %. However, even though the vitrinite reflectance data in these wells are above the onset for hydrocarbon generation, no overpressures have been encountered in the Kockatea Shale in this region of the Perth Basin (Figures 5-22 and 5.23). This analysis provides an insight to the possible overpressure generating mechanisms in other parts of the Perth Basin, which will further be explained in Section 5.5.5.

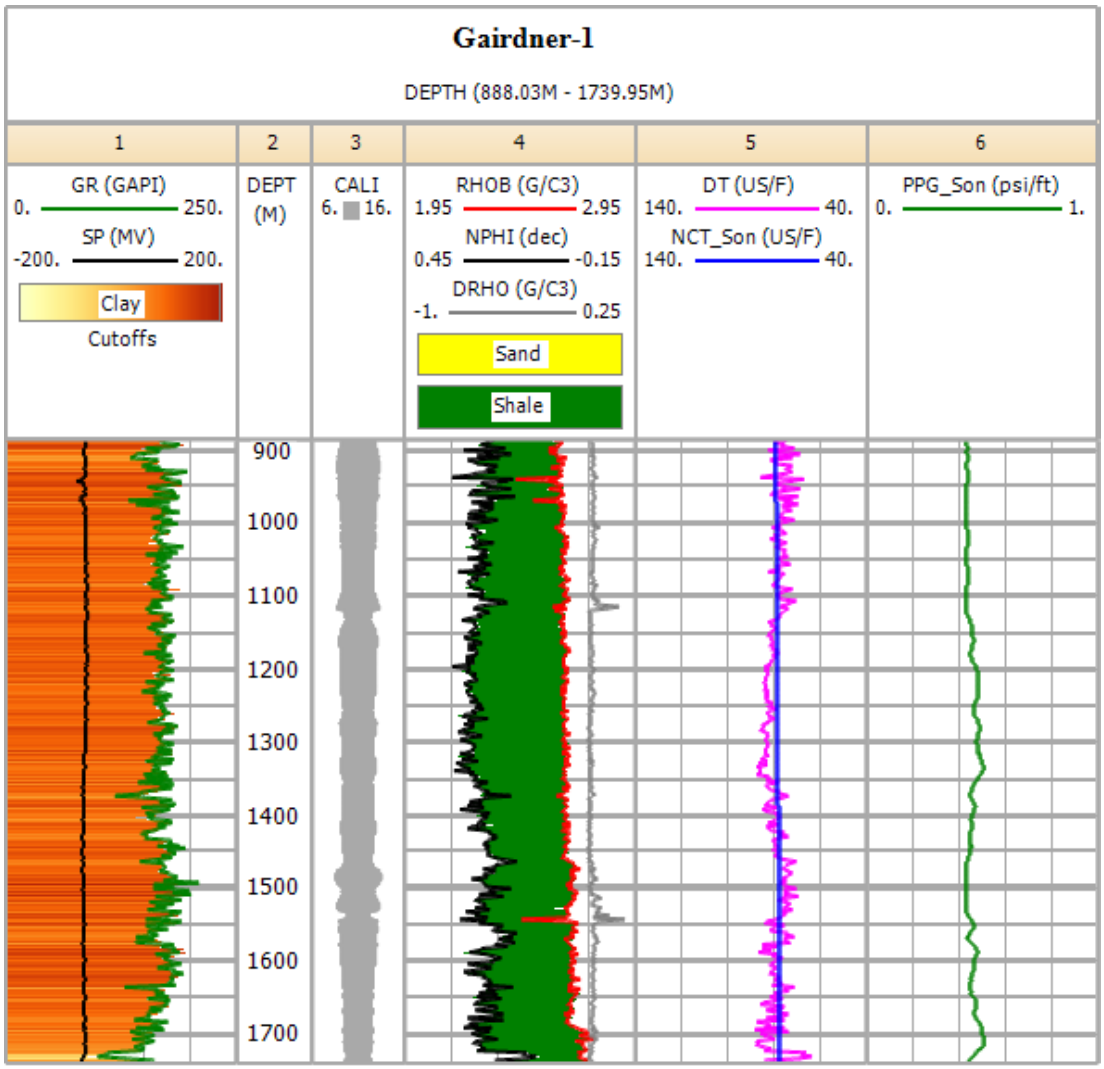

Figure 5-22: Composite well log data and pore pressure profile in the Kockatea Shale in the Gairdner-1 well.

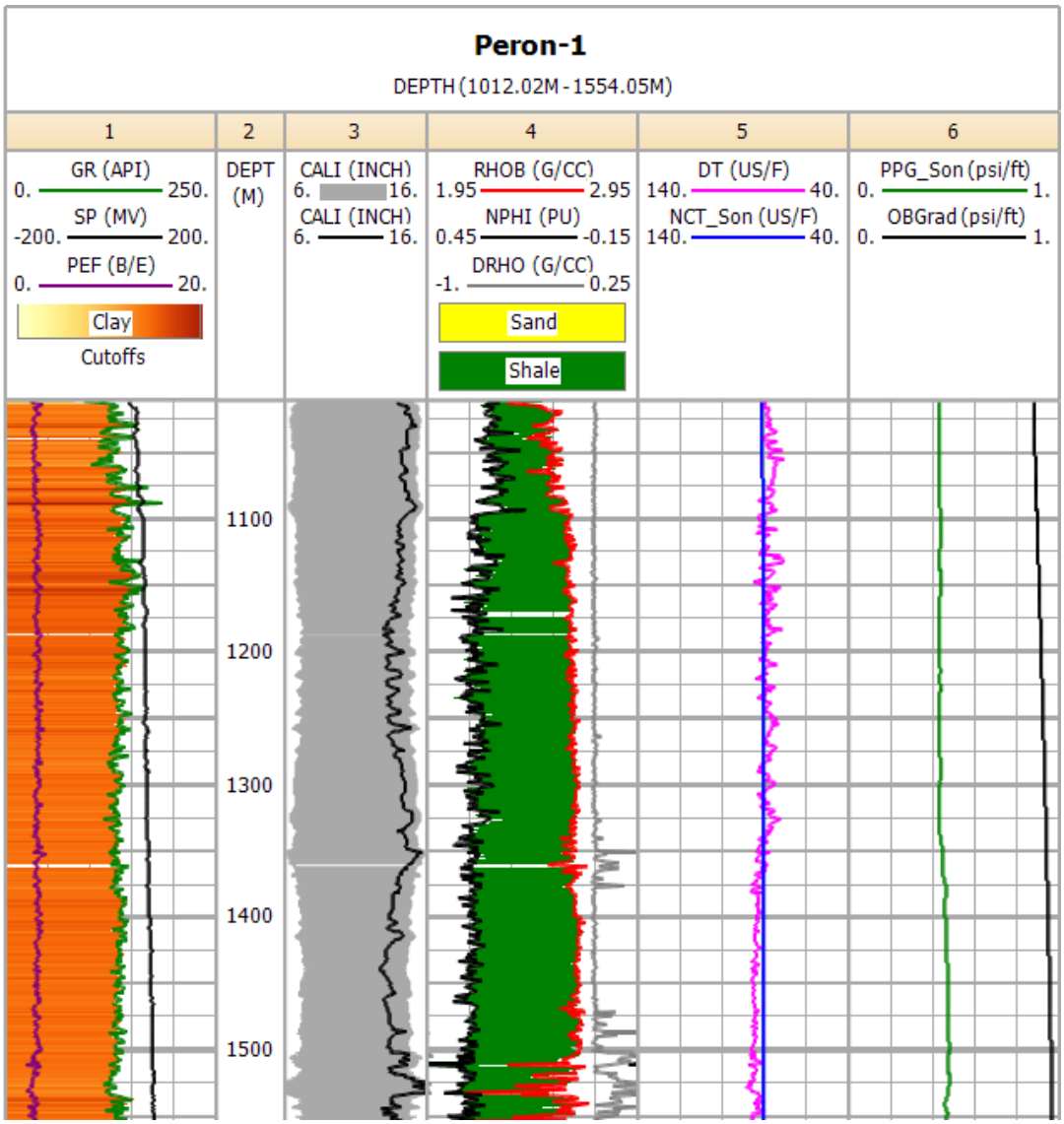

Figure 5-23: Composite well log data and pore pressure profile in the Kockatea Shale in the Peron-1 well.

5.3.2.2 Northampton uplift region

The Abrolhos Sub-Basin, Allanooka High, Bookara Shelf, Greenough Shelf and northern part of the Dongara Saddle are located in the northern boundary of the Perth Basin near the centre of Northampton uplift (Figure 2-1). Throughout the Permian to the Early Cretaceous, the Northern Perth Basin (Figure 2-3) underwent a complex structural history including rifting, inversion, erosion and faulting (D'Ercole 2003).

The structure is highly influenced by the Late Permian phase of extension, where the basement shallows when approaching the centre of the uplifting to the north (Crostella 1995). At the end of Early Triassic, the rifting began to widen, resulting in

the uplift of the basement and regression took place in the north. By the end of Triassic, the basin margins were eroded.

Based on the geographical data and the complex structural history, the Kockatea Shale within this region has been substantially eroded. By way of illustration, the thickness of the Kockatea Shale has been reduced to 45 and 103 m in the Mt Hill-1 and Bookara-1 wells respectively (Figure 5-2).

5.3.2.2.1 Well log data

Well log data that have been analysed in these areas include Bookara-1, Allanooka-1, Allanoka-2, Mooratara-1, Mt Horner-7 and Mt Hill-1. The complete analysis for the Kockatea Shales is shown in Appendix 1b. However, for the purpose of the data analysis, the result from the Mooratara-1 well is discussed.

5.3.2.2.1.1 Mooratara-1

The Mooratara-1 well was drilled onshore in the northern part of the Dongara Saddle area in the Perth Basin. Geologically, the Mooratara feature is situated at the junction of two intersecting fault trends and was most probably formed, as a result of the compressional forces set by the wrench component of the northeast-southwest transfer faults, which bound the feature to the north and south.

The typical stratigraphic section of the Northern Perth Basin was intersected. The well penetrated 200.5 m of the Kockatea Shale from 1095-1295.5 m. The lithology of this formation comprised mainly of claystone with minor interbeds of siltstone and sandstones.

The well exhibited normal pore pressure profile across the whole interval of the Kockatea Shale (Figure 5.24). Also, there are no abnormalities that were observed in the data cross-plots (Figure 5.25). Moreover, no pressure abnormalities were observed in the mud log and drilling data.

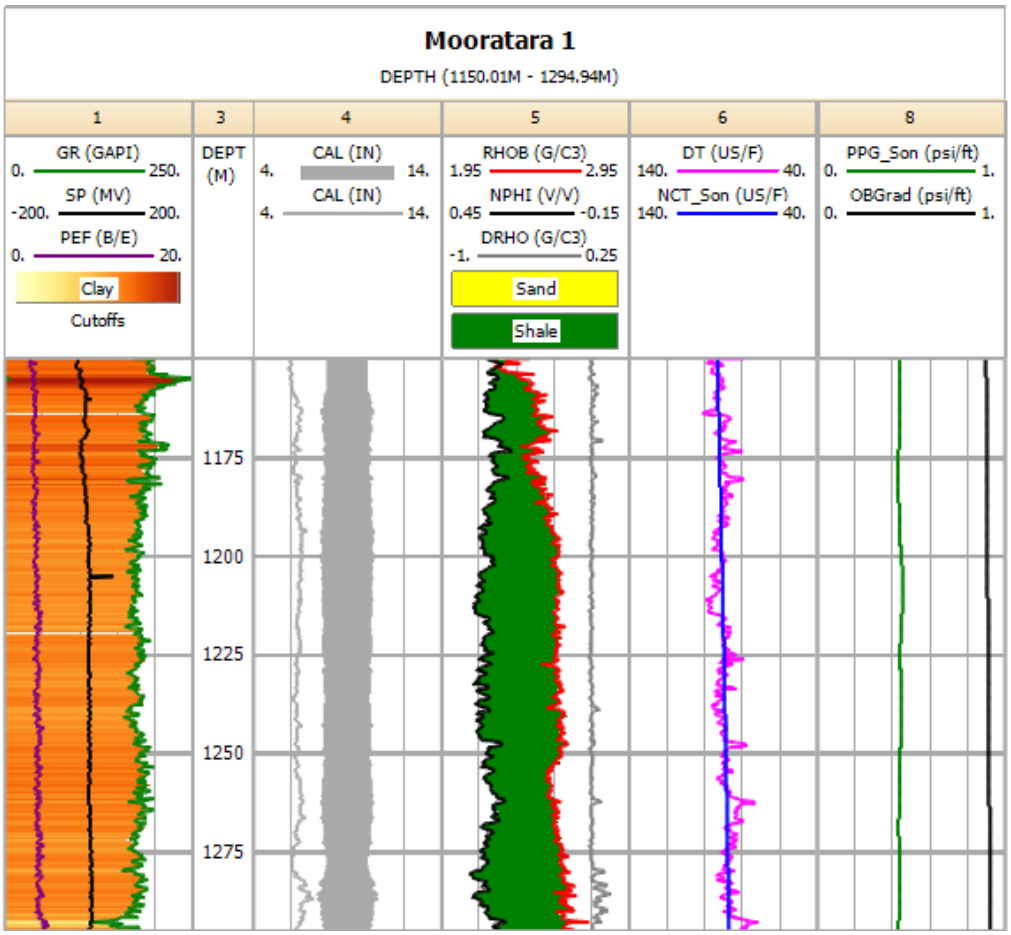

Figure 5-24: Composite well log data and pore pressure profile in the Kockatea Shale in the Mooratara-1 well.

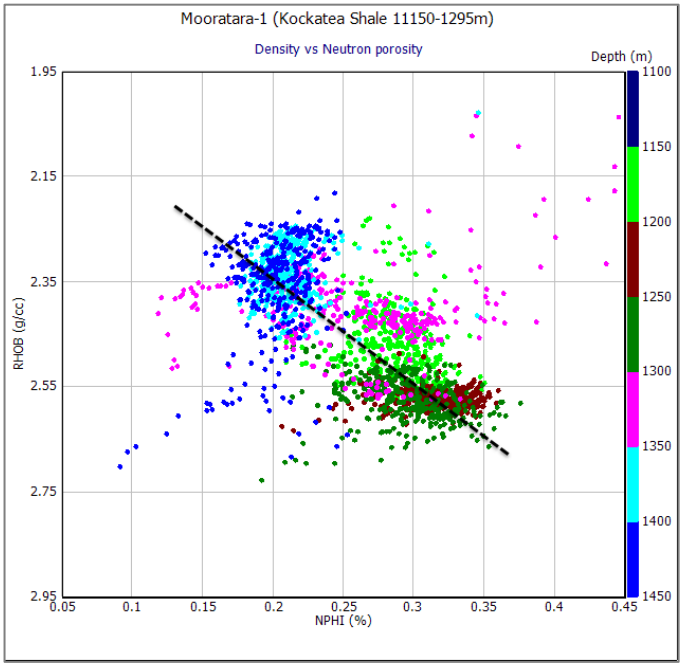

Figure 5-25: Cross-plot of density versus neutron porosity for the Mooratra-1 well.

5.3.3 Pore pressure mapping

The pore pressure gradients for Kockatea Shale were mapped and presented in Figure 5-26. This figure illustrates that moving away from the center of uplifting, pore pressure gradients increase, while pore pressure gradients approach normal toward the centre of the uplifting.

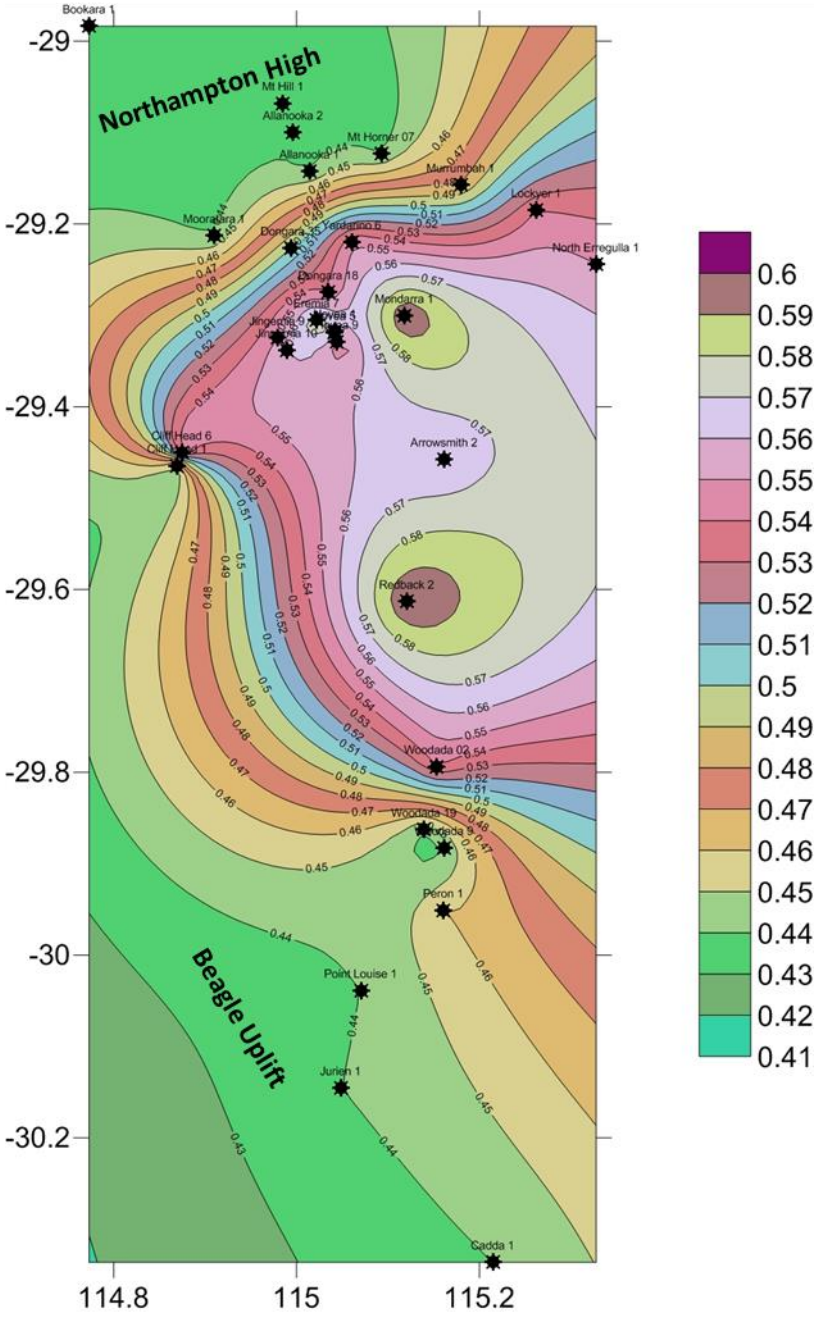

Figure 5-26: Contours of the pore pressure gradients of the Kockatea Shale in the Beagle Ridge, Cadda Terrace, Beharra Spring Terrace, and Dandaragan Trough and adjacent terraces (Northern Perth Basin).

5.4 The role of tectonic activities on pore pressure distribution in shales

This section stresses the importance of the tectonic activities on pore pressure distribution in shale formations. The results of this research have correlated the variations of pore pressure gradients in the Kockatea Shale to the variations of tectonic intensity that took place within the same region.

The investigations on the well log data from the Perth Basin have identified shale intervals which are characterised as overpressured in some parts of the basin, whereas similar shale intervals are found to be normally pressured in other parts of the basin. The phenomena of overpressure have frequently been reported while drilling at the same intervals and from the mud log data as well as in geochemical data analysis. Normal trends of pore pressure gradients were observed in regions that were situated in severely uplifted sections within tectonically active areas. On the other hand, pore pressure gradients increase in the same intervals where there were less intense tectonic activities.

Based on this research, sections with overpressure were observed in the majority of the wells in the Kockatea Shale, where there were less tectonic activities recorded. Regions with less intensity of the tectonic activities showed an increase in the pressure gradients as approaching away from the centre of the two major uplifting phases. On the other hand, normal pore pressure gradients were observed in the Kockatea Shale in shallower wells, which were located within uplifted regions that were more tectonically active. Compressional tectonic activities either induced fracturing in shallower localities as a result of active faulting systems or removed part of the Kockatea Shale as a result of erosion and faulting, resulting in overpressures being released. The data analysed to come up with this newly established theory include well log data, mud log data, drilling reports, seismic data and core images. The well log data indicates that similar lithological sections were examined in the two study cases. However, the results of the pore pressure profiles were significantly different. In addition, seismic characters core images show that the Kockatea Shale has been severely faulted and fractured where normal pore pressure gradients have been observed. On the other hand, overpressure gradients were detected in the Kockatea Shale where the well under examination, has been drilled away from any identifiable faulting.

5.4.1 Interpretation

5.4.1.1 Seismic interpretation for tectonically stable regions

The seismic characters on wells that exhibited overpressure which are available for analysis include the Arrowsmith-2 and Lockyer-1 wells. The Arrowsmith-2 intersected 465.5 m thickness of the Kockatea Shale; whereas approximately half of this thickness was intersected in the Lockyer-1 (222 m).

The Arrowsmith-2 is drilled in the Northern Perth Basin. The chosen location of the Arrosmith-2 was away from any identifiable faults, within an area with a low incidence of fracturing or possible erosion, so that a full interval of the Kockatea Shale can be penetrated and evaluated efficiently. At this well, a typical onshore Northern Perth Basin sedimentation sequence has been encountered. The seismic character of the Arrowsmith-2 well shows the thick and unfaulted Kockatea Shale section (Figure 5-27).

Furthermore, the Lockyer-1 was drilled on the hanging wall side of the southerly downthrown, south-easterly trending North Erregulla Jurassic Fault in the northern section of the Perth Basin (Figure 5-28). Despite the presence of the North Erregulla Fault in this region, it appears from the seismic profile that there is no evidence of active faulting within the Kockatea Shale in the vicinity of the Lockyer-1 well. Also, it seems that the Kockatea Shale in this region of the Perth basin was deposited in a tectonically inactive area (Figure 5-28).

5.4.1.2 Seismic interpretation for tectonically active regions

Seismic characters that are available for analysis on wells that exhibit normal pore pressure within the Kockatea Shale are Cliff Head-1 and Moortara-1. The wells intersected 297.6 and 200 m of the Kockatea Shale respectively.

The three dimensional seismic data within the Cliff Head feature shows that the Cliff Head-1 well is located within a faulted anticline feature with a narrow northwest-southeast oriented horst block, which was complexly faulted because of several tectonic events. As shown in Figure 5-29, the Kockatea Shale has been intersected by two major faults in this area of the Perth Basin. Moreover, it appears from the seismic profile that there is a tectonic event at the top of Permian, which initiates faulting systems that penetrate through the base of the Kockatea Shale. Additionally,

a core cut at the base of the Kockatea Shale in the nearby well of Cliff Head-4 showed that the formation is faulted and naturally fractured (Figure 5-33).

Geologically, the Mooratara feature is situated at the junction of two intersecting fault trends and was most probably formed as a result of the compressional forces set by the wrench component of the northeast-southwest transfer faults, which bounds the feature to the north and south. The interpretation of the seismic character is that the Mooratat-1 well would be drilled on the crest of a large northeast trending fault block complex. In addition, the seismic character clearly indicates that the Kockatea Shale in the Mooratara-1 well has been intersected by a fault line (Figure 5-30). The faulting within the structure might have also contributed to the total absence of the Carynginia formation in the well.

5.4.1.3 Conventional core images in tectonically stable regions

Unfortunately, due to an ignorance of shale formation in the previous era, no cores were cut from the Kockatea Shale in the Arrowsmith-2, Lockyer-1 and Hovea-5 wells to locate evidence of fracturing within. However, cores were cut from the Kockatea Shale in the Redback-2 well as well as from Hovea-3 well, which is a neighbouring well to the Hovea-5 well. The Hovea-3 well exhibited the same abnormalities in log data as the Hovea-5. These wells exhibited abnormal high pressure in the Kockatea Shale. The core images from these two wells show that the intervals of the Kockatea Shale are unaffected by tectonism and there are no signs of fracturing or faulting systems within the formations (Figures 5-31 and 5-32).

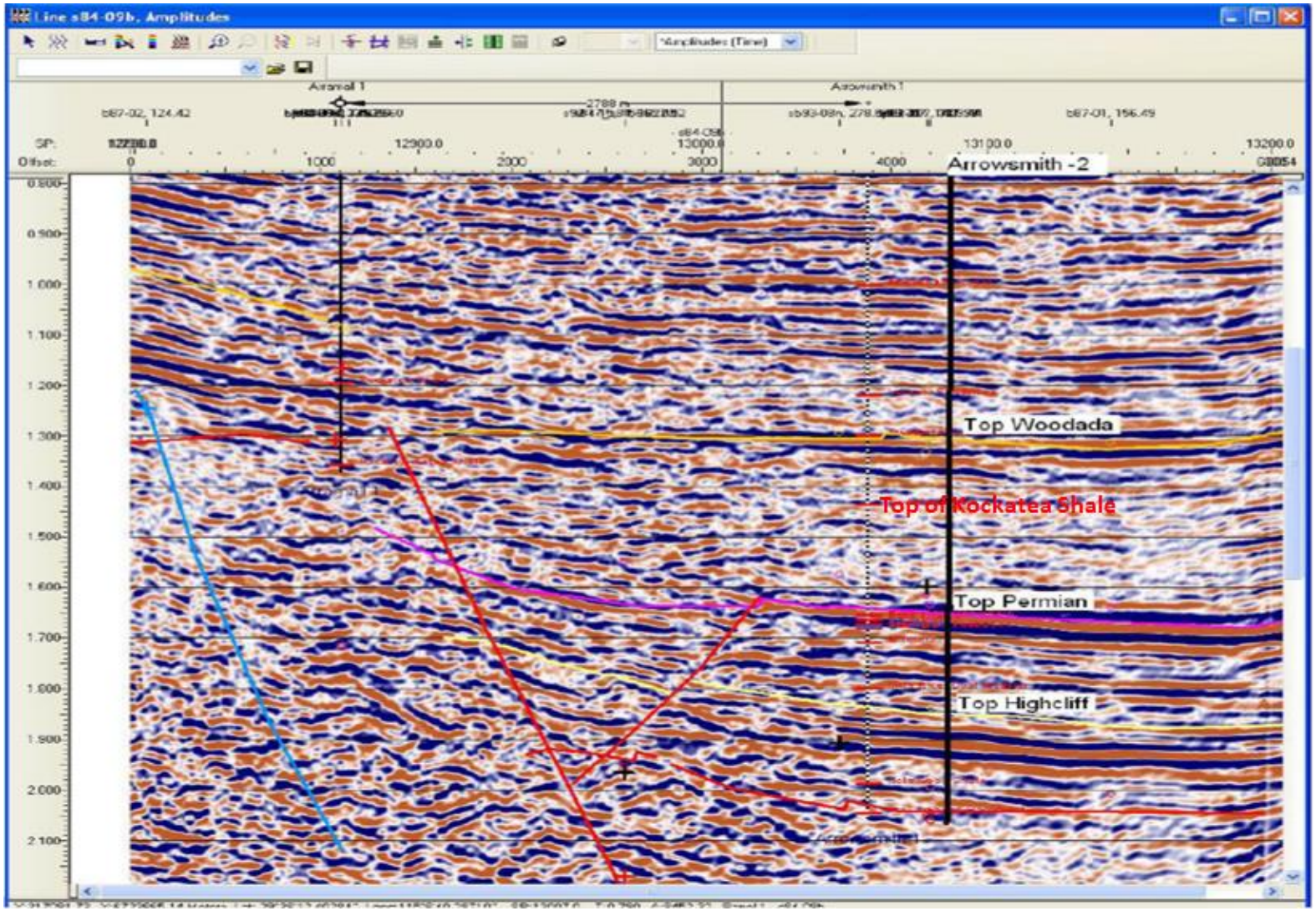

Figure 5-27: Seismic character for the Arrowsmith-2 well (Northern Perth Basin) (Extracted from well completion report)

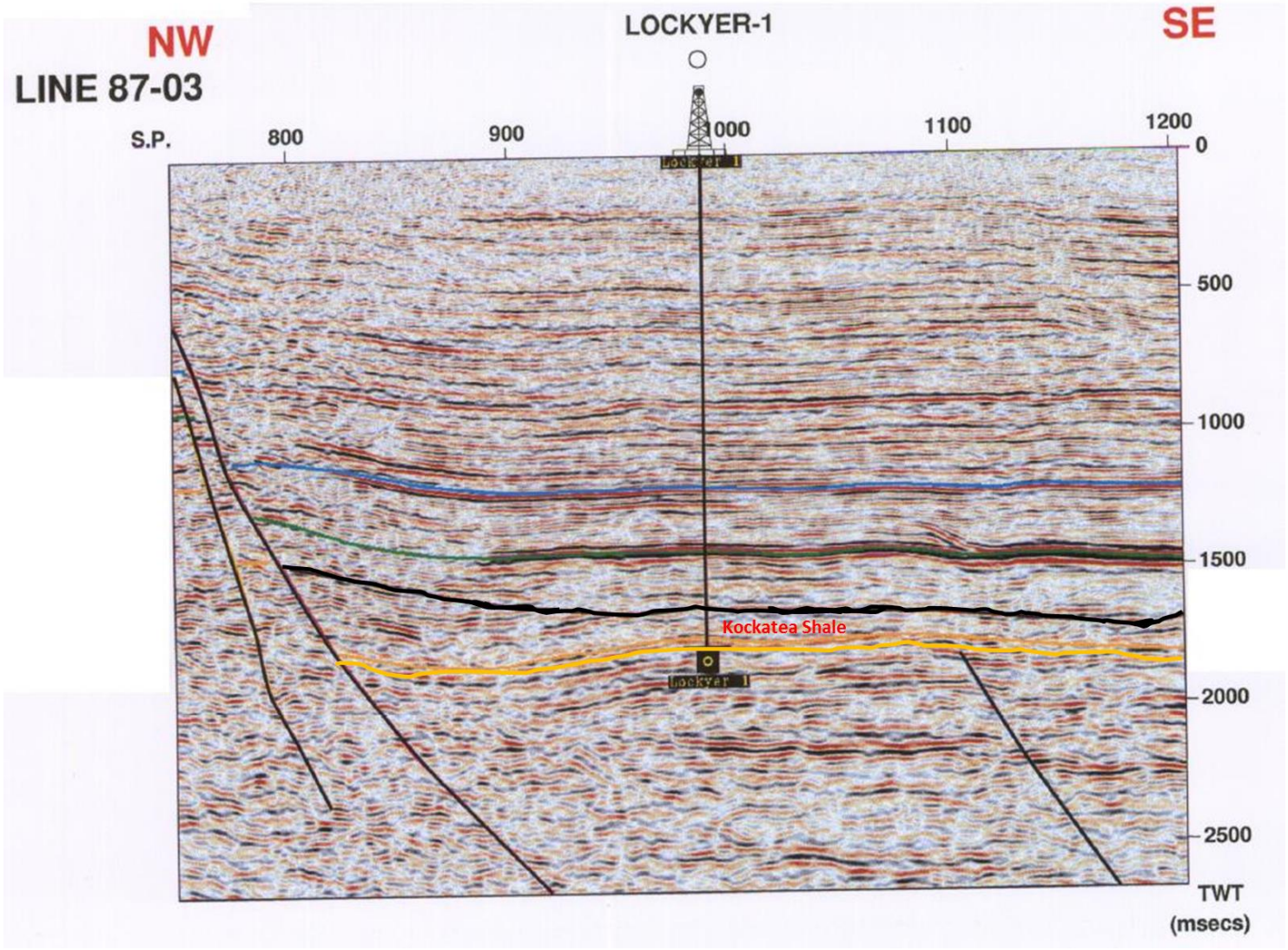

Figure 5-28: Seismic character for the Lockyer-1 well (Northern Perth Basin) (Extracted from well completion report)

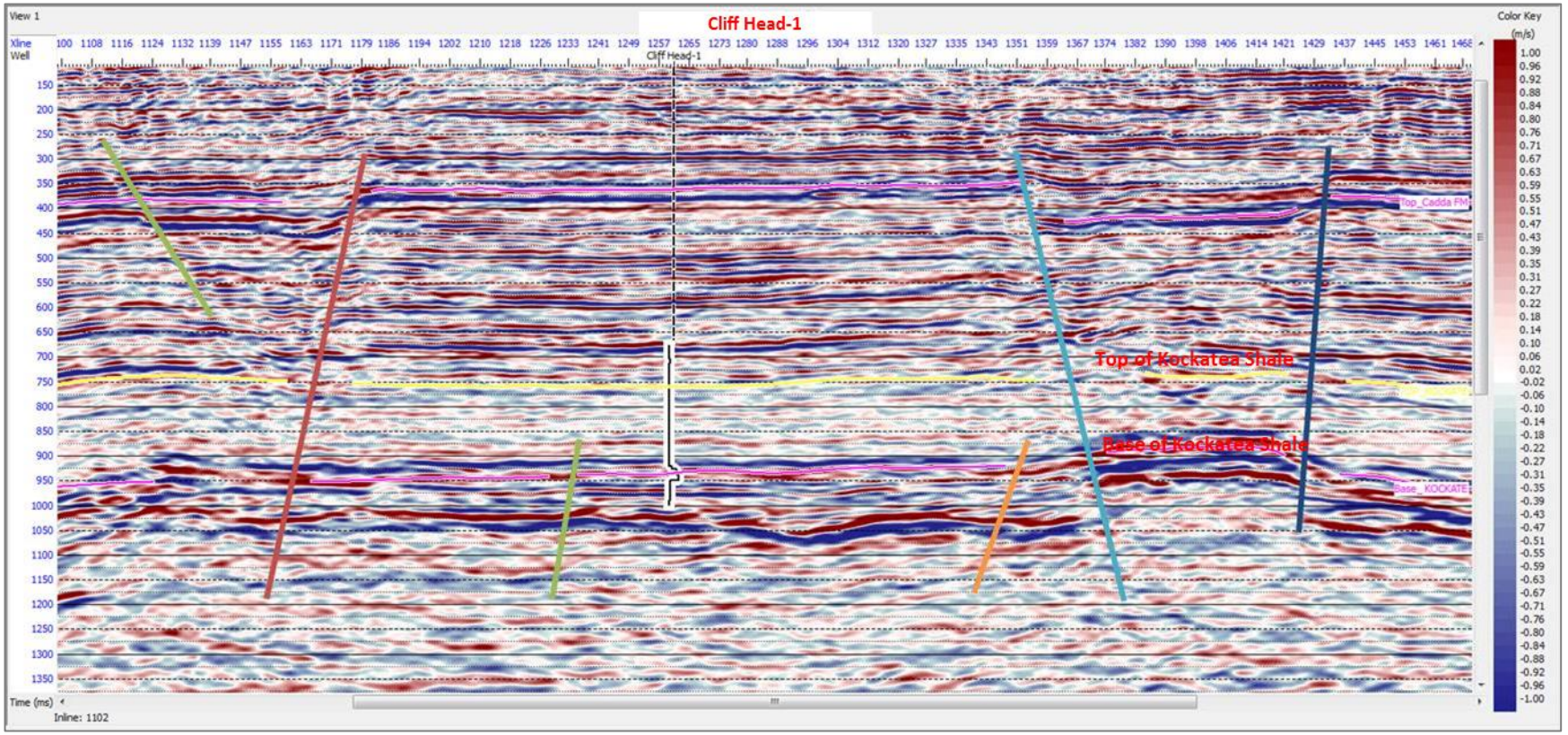

Figure 5-29: Three dimensional seismic character of the Cliff Head-1 well (Perth Basin).

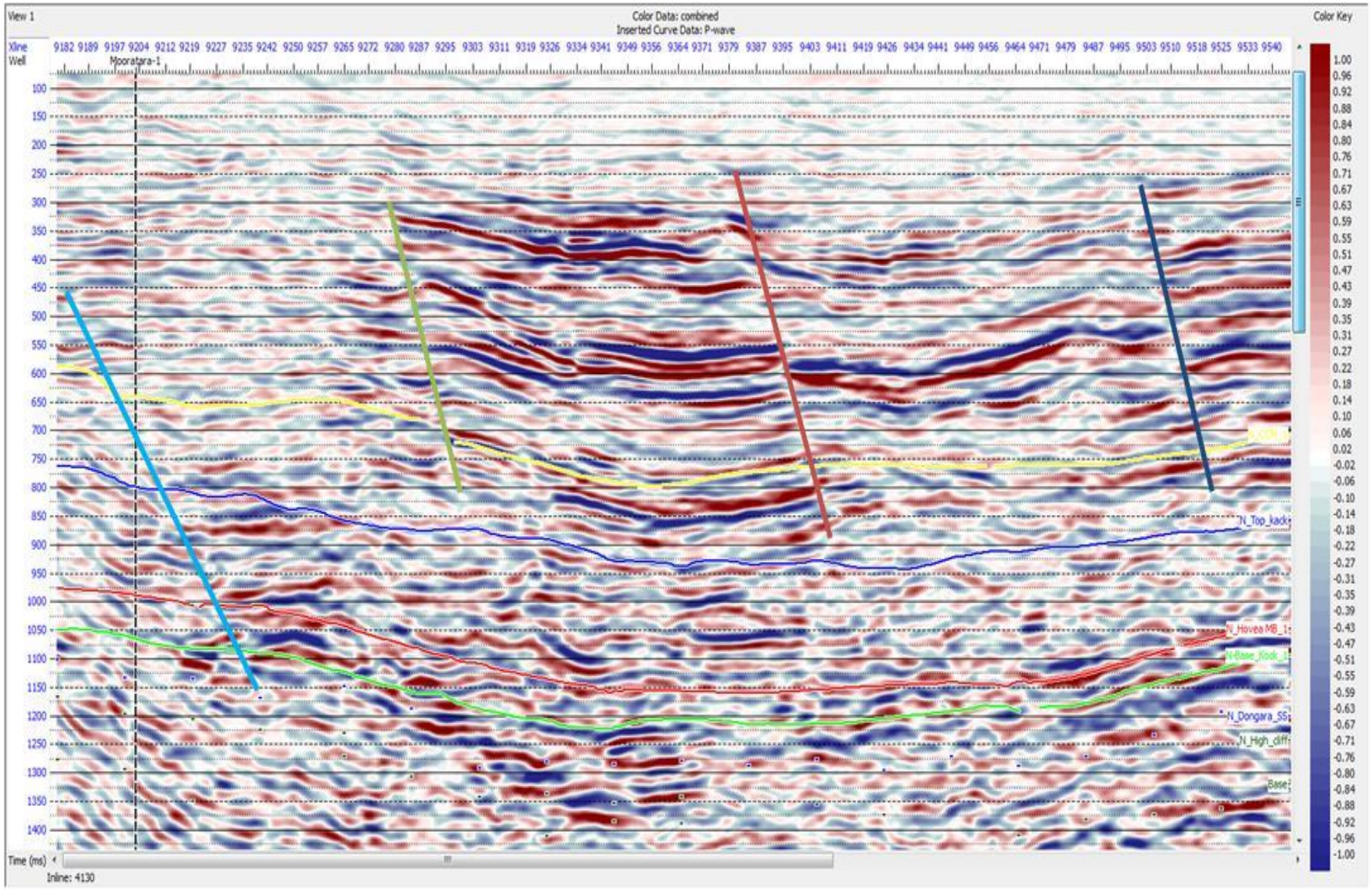

Figure 5-30: Three dimensional seismic character of the Mooratra-1 well (Northern Perth Basin).

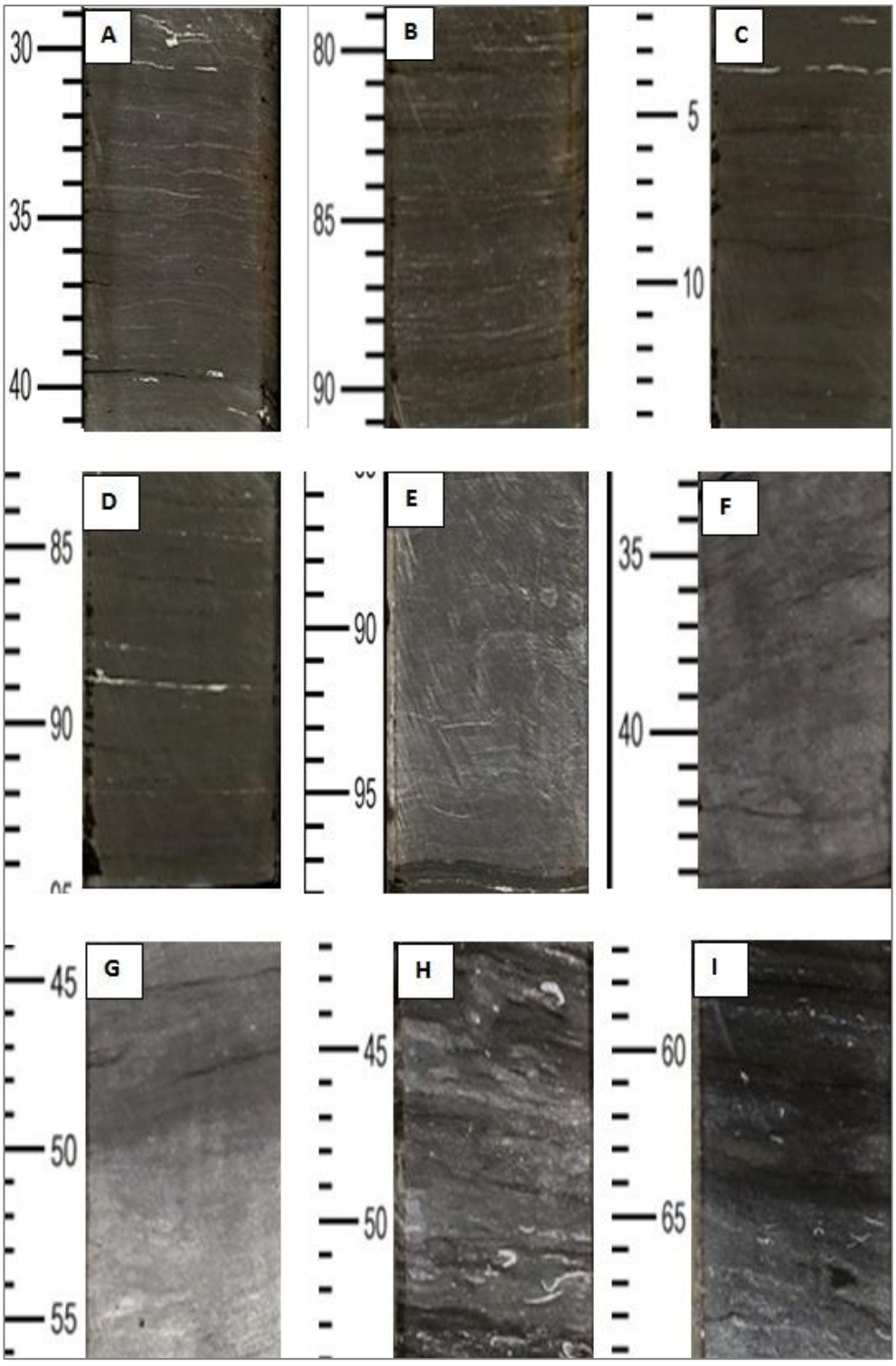

Figure 5-31: Core images showing different sections of the unfaulted Kockatea Shale in the Hovea-3 well (Beharra Springs Terrace) (A) 1973.29-1973.41m, (B) 1974.79-1974.91 m, (C) 1976.02-1976.14 m, (D) 1976.83-1976.95 m, (E) 1977.85-1977.98 m, (F) 1983.33-1983.45 m, (G) 1985.44-1985.56 m, (H) 1986.42-1986.54 m and (I) 1987.56-1987.69 m.

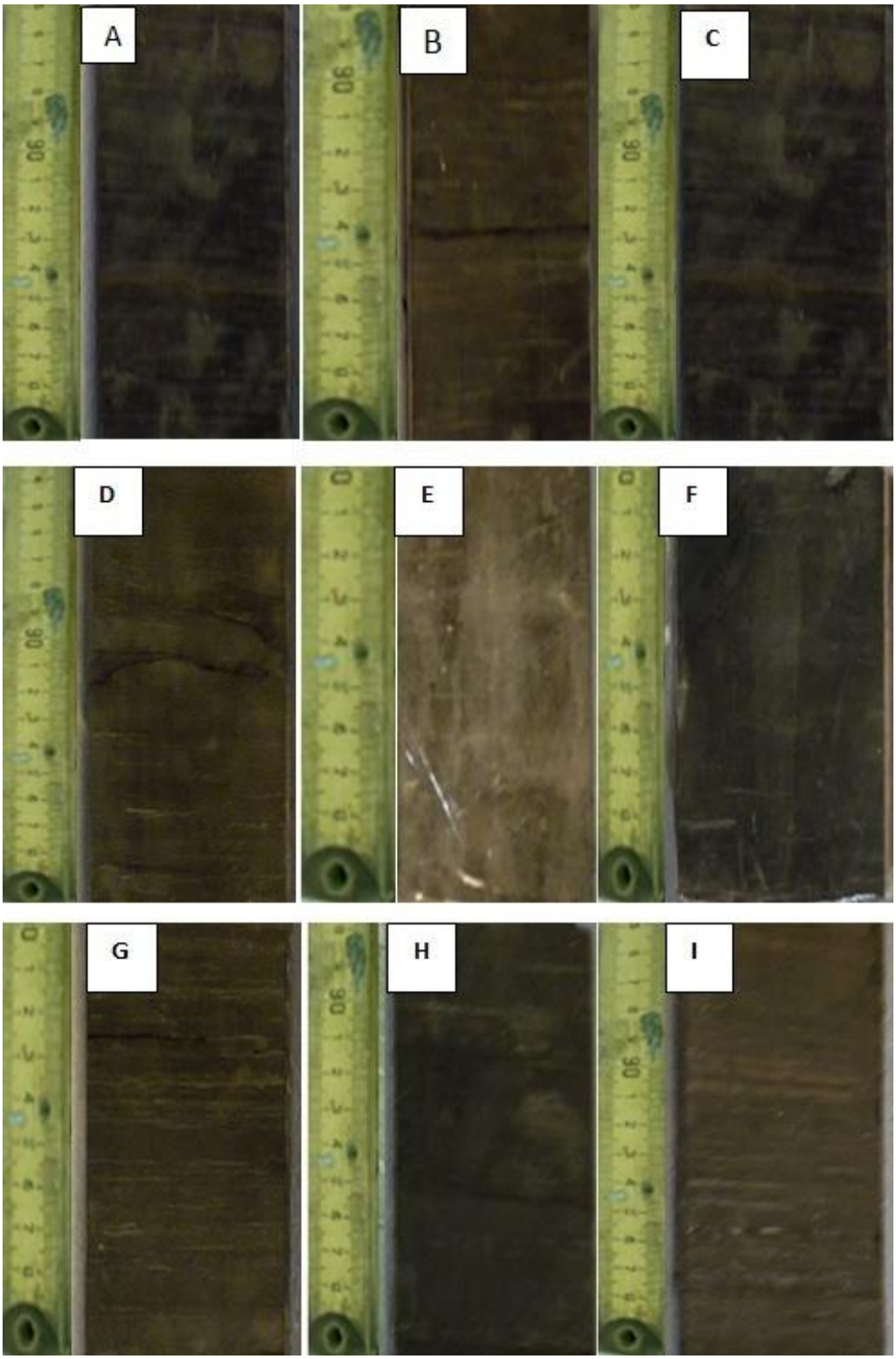

Figure 5-32: Core images showing different sections of the unfaulted Kockatea Shale in the Redback-2 well. (A) 3788.85-3789 m, (B) 3790.63-3790.75 m, (C) 3789.25-2789.40 m, (D) 3791.15-3791.32 m, (E) 3793.55-3793.65, (F) 3797.45-3797.55 m, (G) 3795.21-3975.31 m, (H) 3795.62-3795.74 m and (I) 3803.45-3803.60 m.

5.4.1.4 Conventional core images in tectonically active regions

Within this region, there are not many wells that were cored in the Kockatea Shale. This is due to a lack of interest in the shale during the drilling time. Amongst the wells that exhibited normal pressure in the Kockatea Shale, only the Cadda and Cliff Head-4 wells have been cored. The Cliff Head-4 was cored from 1414 to 1440.35 m (26.35 m). However, the top of the core was cut from the base of the Kockatea Shale. The core image of the Kockatea Shale in this region of the Perth Basin indicates a highly faulted zone and it is naturally fractured (Figure 5-33). The arrows that are shown in the this figure represent the natural fractures that were observed in the sample.

Furthermore, prior drilling the Cadda-1 well, the Kockatea Shale was expected to be 900 m, but the well went through a normal fault and approximately 450 m is missing. In addition, several runs of dipmeter have been made in the Cadda-1 well - two of which were run in the Kockatea Shale. The first one was between 1676.8 and 1884.14 m, which indicates faulted zone with dip reaching 75°, whilst the second was made between 1990.85 and 2027.43 m, which also indicates faulted zone with dip reaching 45° (DMP-WA 2013). Moreover, a core cut of the top of the Kockatea indicates a highly faulted and naturally fractured zone (DMP-WA 2013).

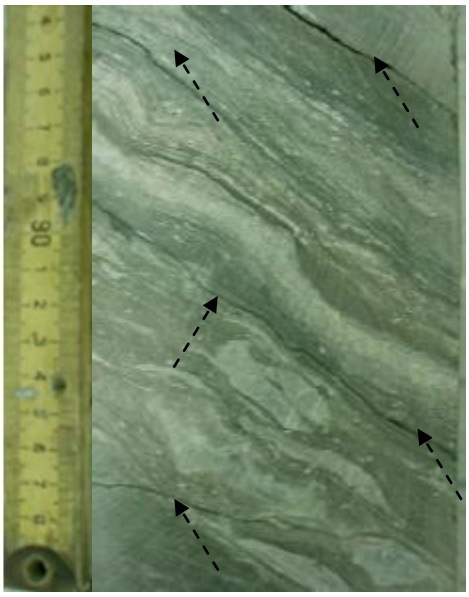

Figure 5-33: A core photograph taken from the Cliff Head-4 well in the base of the Kockatea Shale at depth of 1418.52-1418.682 m MD

5.4.1.5 Well Log data

Data obtained from the Cliff Head-1 and Redback-2 wells indicated that sections of similar lithology in both wells were examined to estimate pore pressure. However, the results were significantly different. The Cliff Head-1 was normally pressured throughout the whole section of the Kockatea Shale, where gamma rays indicated approximately 185 API and the density of 2.55 g/cc (Figure 5-19). On the other hand, in the Redback-2, abnormally high pressure was observed in the Kockatea Shale. The gamma ray analysis indicated approximately 175 API and the density of 2.6 g/cc (Figure 5-13).

Although there is not a large number of measured pore pressure data points for shale intervals in the Perth Basin, the results validation was performed on a few measured pressure data (Figures 5-17 and 519). However, where there was no measured pore pressure data, a different approach was considered which was based on an integration overpressure indicative parameters including the drilling data, mud log data and geochemical analysis and then correlated with the estimated pore pressure profile from log data in the charged zone (Figures 5-9, 5-13 and 5-15).

5.5 The Origins of Overpressure in Kockatea Shale

Overpressure is present in the Perth Basin in the Kockatea Shale throughout the regions that have not experienced major uplifting and erosion, including the Dandaragan Trough and Beharra Springs Terrace. A thorough multidisciplinary study was conducted to examine the cause of overpressure in the Kockatea Shale. The work comprised of the integration of a large geochemical and geological data with the analysis of the well log data response.

This study demonstrated that combination mechanisms contributed to overpressure development driven by the complicated basin geology. Overpressure generating mechanisms for the studied shale formations attributed to the fluid expansion and later tectonic loading. Both mechanisms have contributed at different extents to overpressure development.

5.5.1 Wireline logs responses

The wireline logs available for analysis include the density, neutron density, sonic transit time, resistivity and gamma ray logs.

The responses of well logs to overpressure reveal that fluid expansion mechanisms contributed to overpressure development in the Kockatea Shale. There is a clear reversal in sonic transit time, resistivity and neutron porosity logs within the Kockatea Shale which caused the reversal in vertical effective stress in all the wells where overpressure is observed. The density log remains fairly constant as opposed to a normal trend of continuous increase. These responses constitute evidence of unloading which causes the vertical effective stress to reverse (Figure 5-34). Interestingly, the same behaviour is observed in other wells that have encountered overpressure with the top of the data diversion from the normal trends varying according to the top depth of the Kockatea Shale. It is unfortunate that there are no pore pressure measurements in the Kockatea Shale due to several operational difficulties. These problems are discussed in detail in Section 3.3.

Further investigations were needed to examine which mechanism amongst the fluid expansion mechanisms generated overpressure in the Kockatea Shale. These investigations include: the analysis of Sonic-Density Cross-plot, X-Ray Diffraction, Natural Gamma Ray Spectrometry logs (NGS) and Geochemical and Gas Composition.

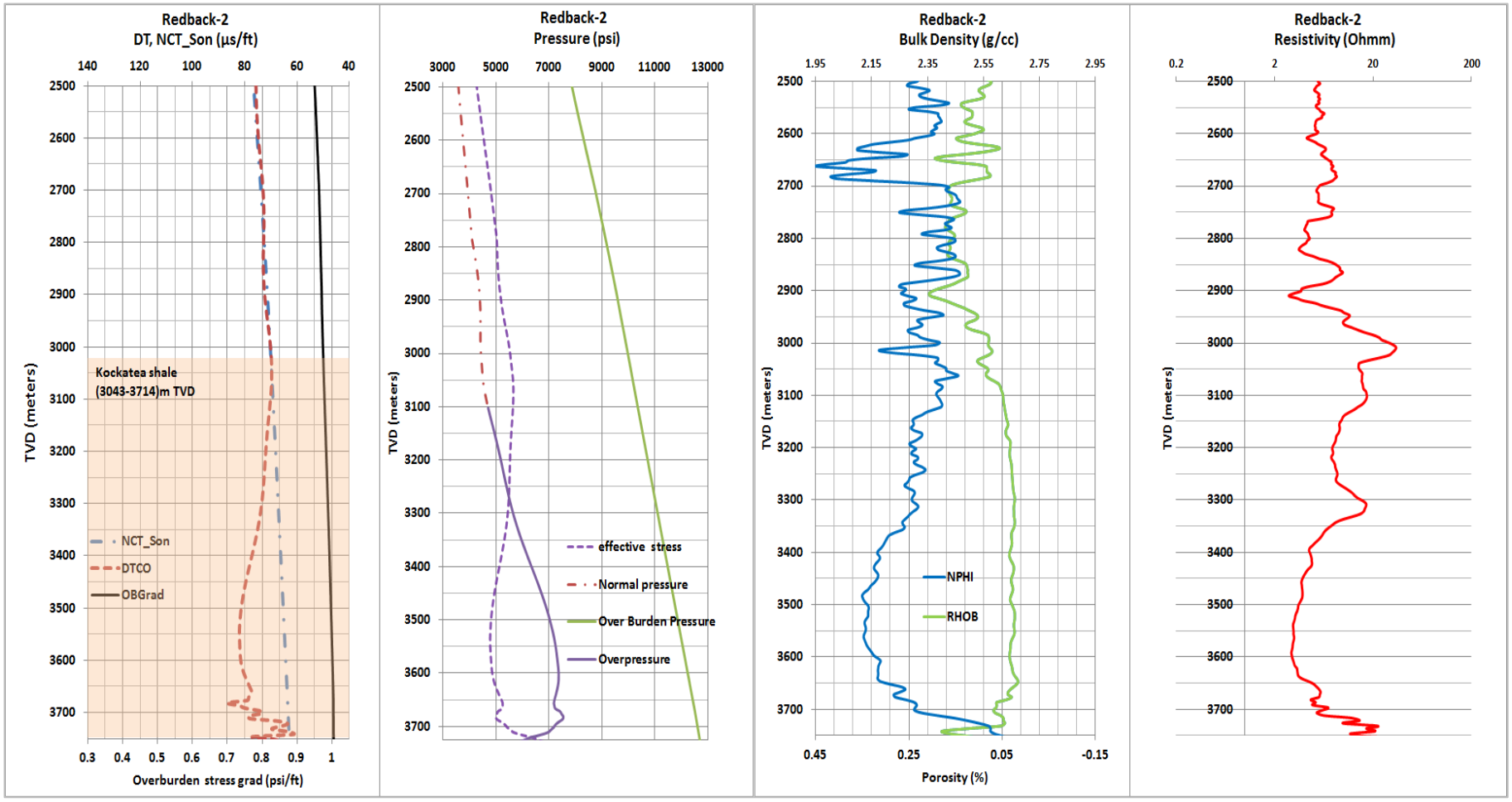

Figure 5-34: Well logs data responses to overpressure across the Kockatea Shale in the Redback-2 well (Perth Basin).

5.5.2 Sonic-Density Cross-plots

This study used the conventional well logs data to identify the mineralogy and to quantify the possible fluid expansion mechanism for overpressure in the Kockatea Shale. A study conducted by Dutta (2002) that discussed the impact of smectite diagenesis on compaction profiles and compaction disequilibrium, study proposed two limiting compaction profiles; one for smectite and one for illite. Based on Dutta's study, the smectite and illite curves were used in this study for another purpose, other than the one which they initially proposed for. The two profiles were used herein to identify the causes of overpressure in the Kockatea Shale in the Perth Basin. To demonstrate this, a cross-plot of Sonic Transit Time versus Density in the shale intervals was analysed to see where the overpressured data points fall. Figure 5-35 shows the points of higher difference between neutron porosity and density porosity fall farther from the smectite-rich trend. It has been noticed that as depth increases, the difference of neutron porosity-density porosity increases and the ratio of smectite to illite decreases (illite percentage increases) along with increases in the pore pressure gradients (unloading increase).

The observations provide clear evidence that the overpressure generating mechanism is the clay diagenesis processes. Amongst the clay diagenesis processes, the transformation of smectite to illite or mixed-layer (illite and smectite) seems to be dominant.

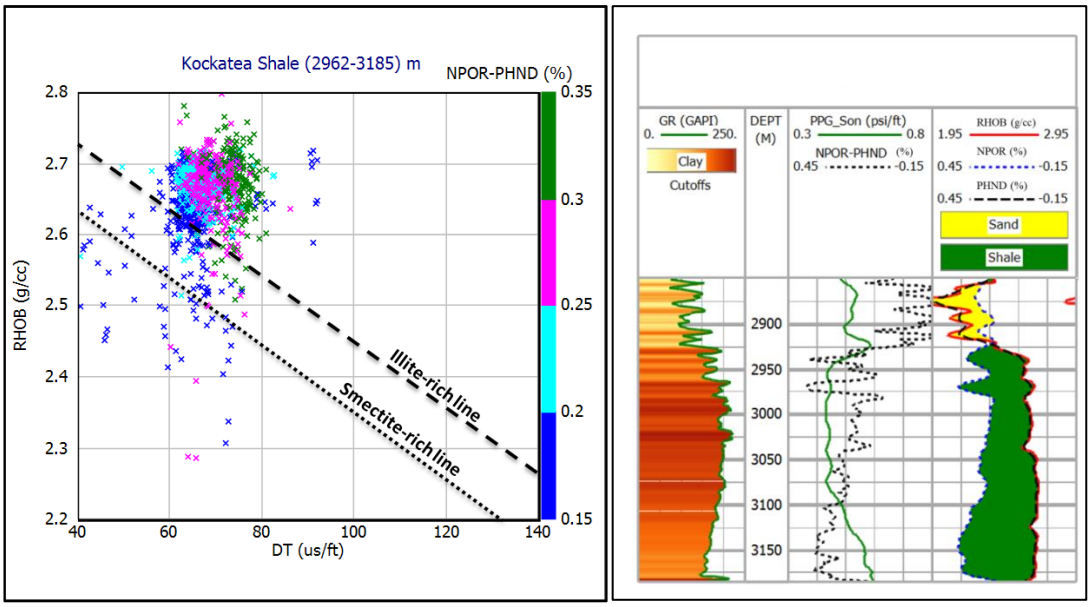

Figure 5-35: Sonic-density cross-plot for Kockatea Shale in the Lockyer-1 well (left), (Neutron porosity - density porosity) is shown in colour. The dotted line is the smectite-rich trend and the dashed line is the illite-rich trend. Well logs plot and pore pressure profile versus depth for the same well is shown on the right.

Further investigations were needed to ensure whether the patterns in Figure 5-35 are due to load transfer through clay transformation (unloading), rather than just variations in clay compositions. In order to do this, clay compositions were examined through the X-Ray Diffraction study.

5.5.3 X-Ray Diffraction

The proportions of different minerals in the Kockatea Shale were further determined by examining x-ray diffraction on rock samples taken from the wells. The results presented in the Tables 5-2 and 5-3 show that as depth increases, the proportion of illite and mixed-layer (illite-smectite) clays increases in the samples with a minor or no presence of smectite clay. These results can be interpreted by consistent transformation of smectite clay to illite and mixed-layer (illite-smectite) clays.

Remarkably, as depth increases, the clay compositions are consistent with the process of clay transformations from smectite to either illite or to mixed-layer clay (illite-smectite) rather than a random variation of clay composition within the formations under examination. In addition, the temperatures and the burial depths for the Kockatea Shale in these two wells are in the range at which the processes of the

mentioned clay transformations occur. The average geothermal gradient is around 3.42°C/100 m and with surface temperature of 21°C, it gives an estimated temperature of approximately 103°C at 2400 m depth in the Arrowsmith-2 well and 151°C in the Redback-2 well at 3792 m. This temperature is adequate for smectite to have disappeared or transformed into illite or mixed layer (illite and smectite) (Hower et al., 1976; Boles and Franks, 1979).

Table 5-2: X-Ray Diffraction data from the Arrowsmith-2 well (Kockatea Shale).

X-RAY DIFFRACTION DATA - Clay Mineralogy (Weight %) Well Arrowsmith-2							
Relative Clay Abundance (<4 Microns)							
Dapth (m)	% I/S EXPANDABILITY	SMECTITE	ILLITE-SMECTITE	ILLITE	KAOLINITE	CHLORITE	TOTAL CLAY
2400	40	1	19	19	38	23	100
2645	45	1	29	16	33	21	100
2677	45	5	33	31	20	11	100

Table 5-3: X-Ray Diffraction data from the Redback-2 well (Kockatea Shale).

WHOLE ROCK MINERALOGY (Weight %) Well Redback-2 (Kockatea Shale)																			
SAMPLE ID	DEPRH (M)	QUARTZ	K-FELDSPAR (MICROCLINE)	PLAGIOCLASE (ALBITE)	CALCITE	AMORPHOUS	GYPSUM	DOLOMITE (CALCITE MAGNESIUM)	PYRITE	FLUORAPATITE	BARITE	MAGNETITE	TOTAL NON-CLAY	SMECTITE	ILLIT-SMECTITE	ILLITE	KAOLINITE	CHLORITE	TOTAL CLAY	GRAND TOTAL
RB-F1	3792	50	-	7.3	-	3	-	-	1.3	-	-	-	62	-	32	-	-	6.1	38	100
RB-F2	3798	20	-	10	9.7	3	-	-	4.3	-	-	-	47	-	35	-	16	1.6	53	100
RB-F3	3819	42	-	6.1	-	3	-	-	0.7	-	-	-	52	-	41	-	-	7.1	48	100
RB-F4	3834	18.2	-	7.1	-	7	3.9	-	15	-	-	-	51	-	35	-	11.8	2.8	49	100

5.5.4 Natural Gamma Ray Spectrometry logs (NGS)

Minerals identification was further investigated by analysing the Natural Gamma Ray Spectrometry Logs (NGS). The total gamma ray spectrum is resolved into three naturally radioactive constituents- Thorium, Potassium and Uranium (Th, K, and U respectively). In general, gamma ray spectrometry logs provide only qualitative information about the mineralogy, since the minerals composition and the porosity of clays may vary. Therefore, they can only provide supportive analysis.

Analysis of NGS plots from the Arrowsmith-2 well indicates a higher percentage of illite clay in the overpressured section of the Kockatea Shale. The cross-plot of Thorium versus Potassium illustrates that illite is the principal clay contained in the examined interval of the Kockatea Shale.

It can be seen from Figures 5-36 and 5-9, that the majority of the overpressured points are plotted in the illite segment of the chart, which further supports the hypothesis of the possible complete transformation of smectite to illite. The conversion of smectite to illite eliminates considerable amount of smectite interlayer surface, which was hydrated when the clay was in smectite phase. Consequently, the amount of bound water decreases and the amount of intergranular water increases. As a result of volume increases in the intergranular water, pore pressure builds up.

However, clay transformation from smectite to illite and illite-smectite is not considered as a significant mechanism that produces a high magnitude of overpressure (Osborne and Swarbrick, 1997). This is due to the fact that the maximum volume changes between interlayer and intergranular water only increases the volume of intergranular water by an insignificant amount. In fact, the overpressure observed in the Kockatea Shale is noticeably in high magnitudes as noticed from the reversals of the vertical effective stress. As such, compaction disequilibrium is eliminated and the clay transformation mechanism could be combined with other overpressure-generating mechanisms. In order to ascertain, geochemical and gas composition data as well as the stress data were analysed.

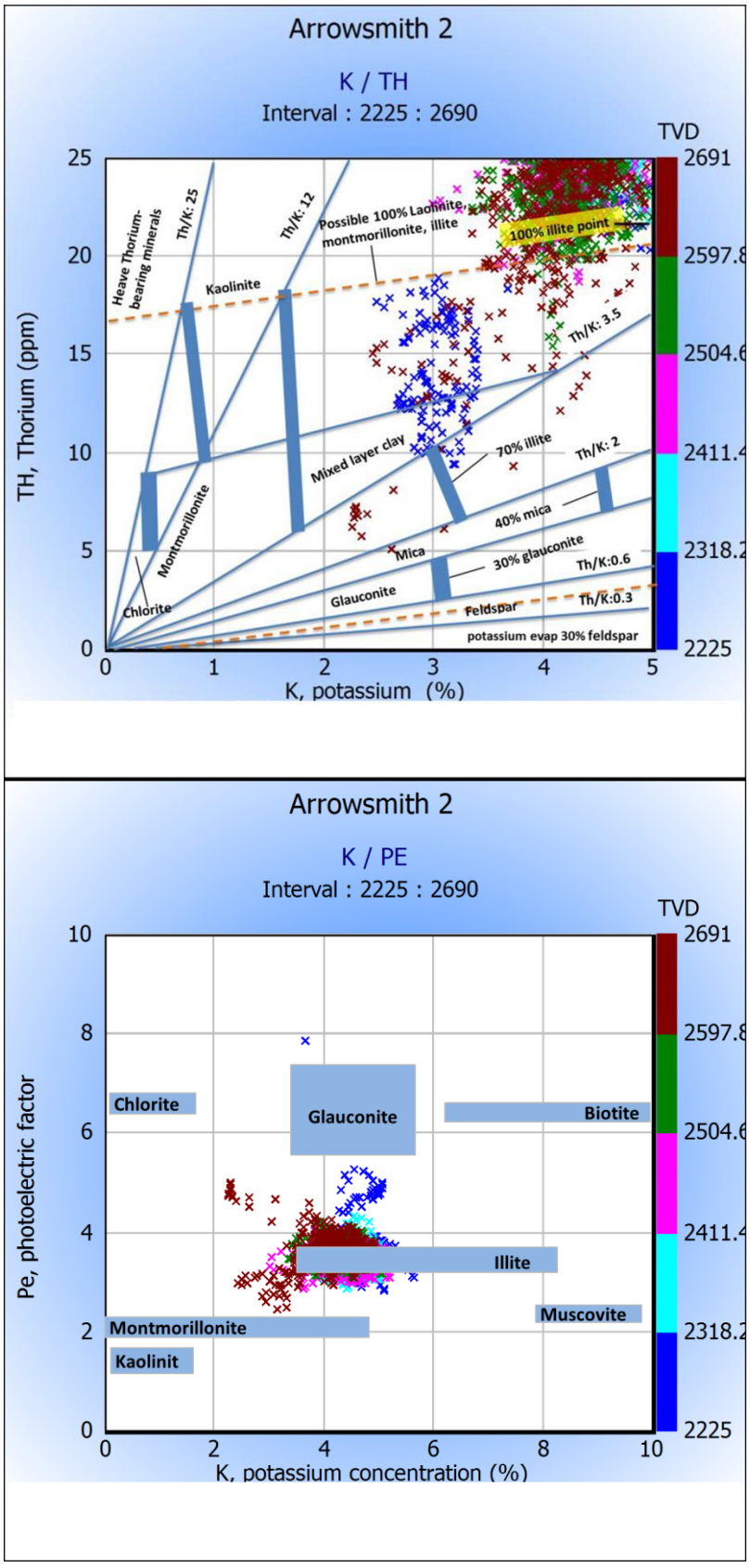

Figure 5-36: Natural Gamma Ray Spectrometry logs (NGS) for the Kockatea Shale in the Arrowsmith-2 well (Perth Basin).

5.5.5 Geochemical and gas composition analysis

Geochemical and thermal studies show consistent increase of gas wetness with the Ethane ratio increasing at exactly the same depth at the top of overpressure. Below the top of overpressure, there is a break in the slope in the Ethane and gas wetness ratios. At the top of the overpressure zone, these ratios decrease at a slower pace and then reverse to increase, before it returns to decrease when the pore pressure profile returns to the normal gradient (Figure 5-38). On the other hand, the gas dryness ratio deviated from its trend within the same zone.

With the high thermal maturity of the Kockatea Shale, Tmax> 400 °C (Figure 5-37), the responses in Figure 5-38 can be explained by more in situ cracking of the ethane and higher hydrocarbons, to the extent that the friction of light hydrocarbon (i.e. methane) is lessened, causing the composition of gas to become increasingly wet. Furthermore, the Ethane Isotope (Figure 5-7) shows a normal increase as depth increases, but when intersecting the overpressured zone, it deviates from the normal trend but returns to be normal as the pore pressure approaches the normal gradients. In addition, the tops of gas wetness increase and the dryness ratio decrease are consistent with the top depth of overpressure.

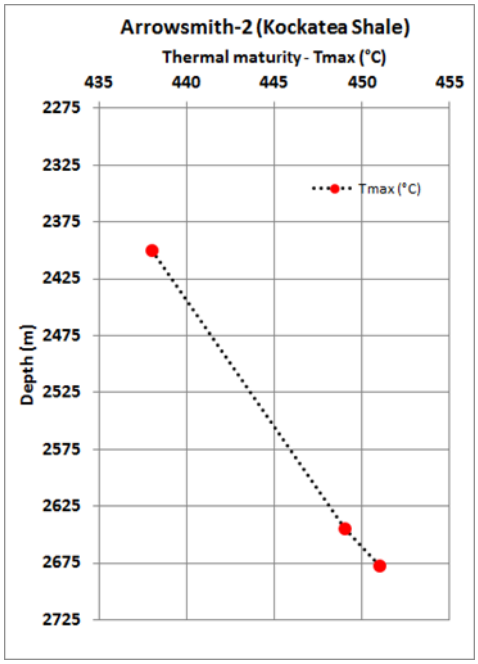

Figure 5-37: Thermal maturities in the Kockatea Shale in the Arrowsmith-2 well (Perth basin).

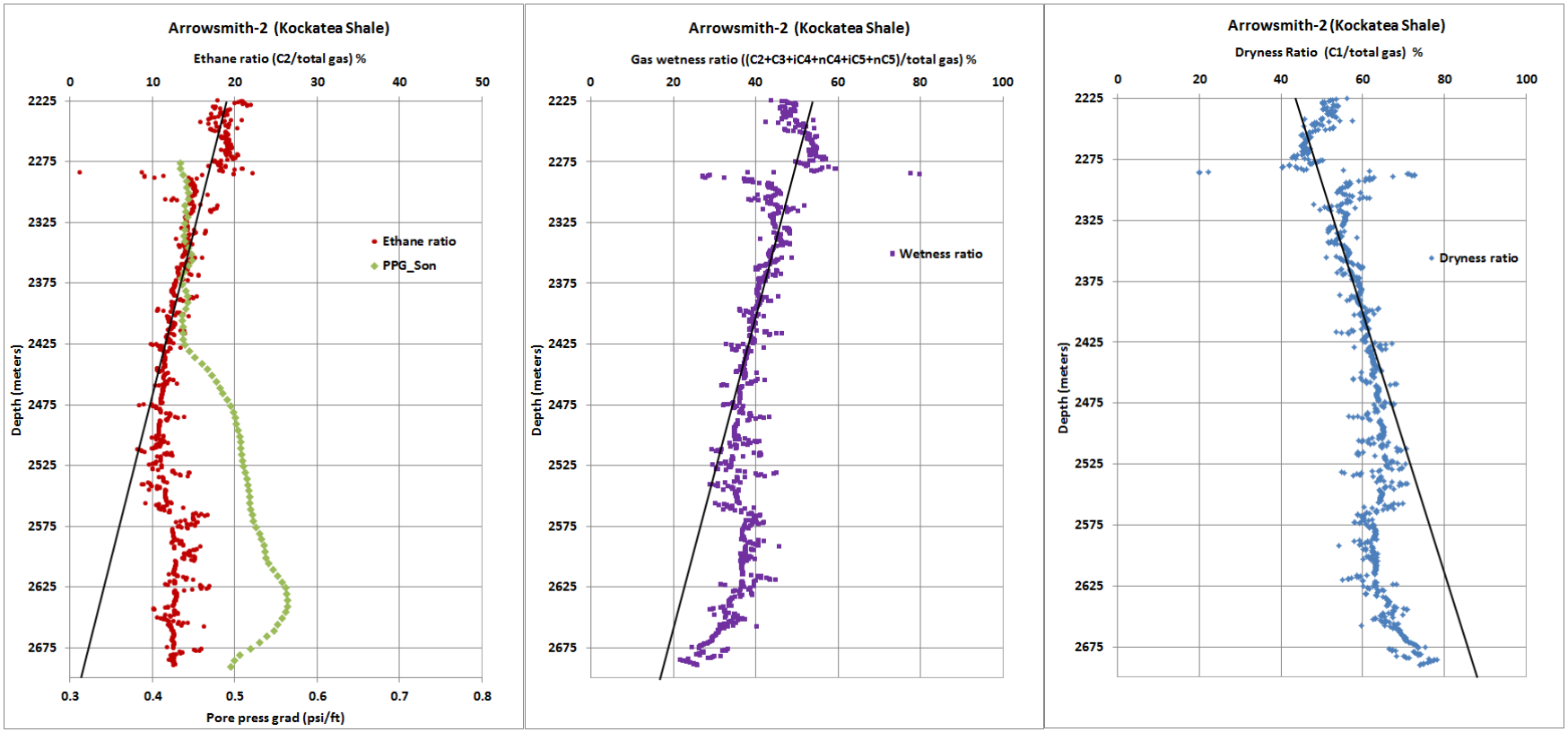

Figure 5-38: Gas wetness and dryness ratios in the Kockatea Shale in the Arrowsmith-2 well (Perth Basin).

In an attempt to add certainty and bring an additional advantage to the analysis, the thermal maturity parameter (vitrinite reflectance) is correlated with the gas composition analysis. The vitrinite reflectance data within the Kockatea Shale showed that the Kockatea Shale within both the overpressured and normally pressured regions of the Perth Basin are mature for kerogen cracking into hydrocarbons.

Unfortunately, there are no sufficient vitrinite reflectance data in a single well to quantify the type of hydrocarbon generations, whether it is gas or oil. However, the data scattered above and even beyond the onset of gas generation. This indicates that the Kockatea Shale is mature and the cracking of kerogen and hydrocarbon is taking place in both regions of the Perth Basin (Figure 5-39). Interestingly, both regions showed high maturity for hydrocarbon generation in the Kockatea Shale, but overpressures were only observed where the tectonic activities were less intense. The tectonically active regions showed normal pressure gradients in the Kockatea Shale. Therefore, the mechanism of hydrocarbon generation may or may not be a significant factor in the overpressure development in the Kockatea Shale.

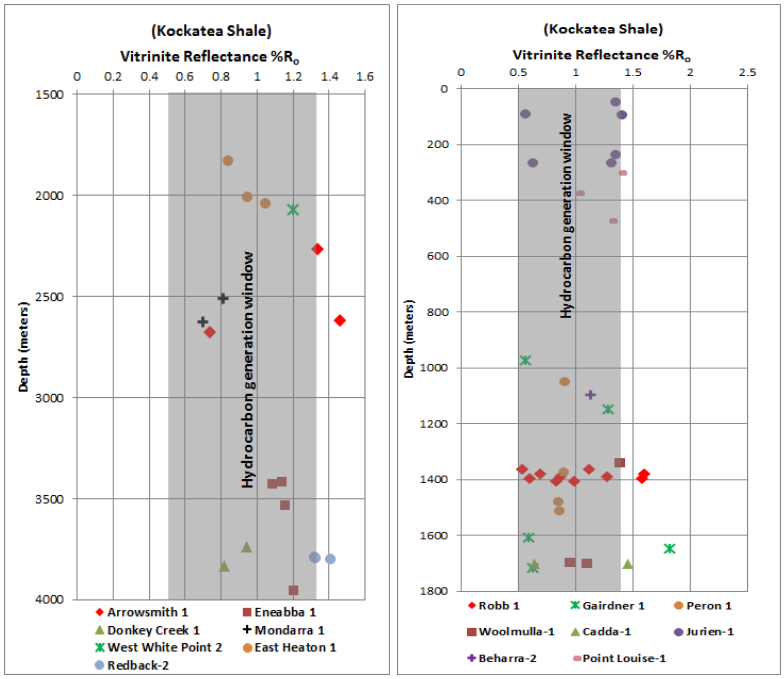

Figure 5-39: The vitrinite reflectance data for the Kockatea Shale in a number of wells in the Perth Basin. The vitrinite reflectance data plot in the right is for the wells where pore pressure profile are found to be normal and the left for the wells where pore pressure profile are found to be abnormally high.

5.5.6 Lateral tectonics compression

Upon an intensive evaluation that entailed tectonic stress data and the complicated geology of the study area, in conjunction with the trajectory of the principal stress S_{hmax}), there is strong evidence that the most likely mechanism associated with the clay transformation is the lateral tectonics compression. The main reasons for this deduction are: (1) the forces induced by the principal stress (S_{hmax}) where $S_{hmax} > S_v \approx S_{hmin}$ and it acts in a horizontal plane east-west perpendicular to the main north–south and northwest–southeast faults trends (see Section 2.4), (2) the positions and the trends of the main faults that showed a progressive down dip - decrease of dip angle as depth increases (see Section 2.3.4 and Figure 2.3) and (3) the main transfer faults providing efficient lateral seals for the overpressure that was developed in the Kockatea Shale (see Section 2.3).

The lateral tectonics explains the high magnitude of overpressure observed as the diagenesis effects cannot produce high overpressure. Lateral tectonics compression would have caused the vertical effective stress to reverse and density log to reverse slightly or remain at a reasonably constant value, because the compaction is not reversible. The slight reversal on density logs may be due to the load transfers to pore fluids as a result of clay diagenesis and cracks opening to permit transmission of pore fluids.

Chapter 6 Pore pressure and its relation to the local tectonic activities in the Laurel Formation (Canning Basin)

Several organic-rich shale formations were identified in the Canning Basin, including but not limited to the Laurel Formation. The pore pressure of these formations is poorly defined and the purpose of this study is to study pore pressure and draw up an overview of the pressure regime that exists in the Laurel Formation. The other objective is to analyse whether the effects of tectonic activities on the distribution of pore pressure in the Kockatea Shale of the Perth Basin (Section 5.4) is applicable for the Laurel Formation in the Canning Basin. This study was limited to the two main sub-basins in the Canning Basin, namely the Fitzroy Trough and the Lennard Shelf, where the Laurel Formation was deposited. The study focused on the Fitzroy Trough because the deposition environment and characterizations of the Laurel Formation are similar across the trough. However, the structural framework and tectonic elements are different. The pore pressure in the Lennard Shelf was studied due to its tectonic nature as severe uplifting and erosion have taken place in this region. As such, a valid comparison of pore pressure profiles of different regions of the basin can be made. Therefore, appropriate correlations can be established in line with the findings obtained from the Perth Basin.

The chapter starts with a section of informational background on the Laurel Formation in Section 6.1. Thereafter, the data in the Fitzroy Trough is analysed, examining different structural anticlines and moving from the Yulleroo Anticline in Section 6.2.1 to St George Range Anticline and Christmas Creek Structure in Section 6.2.2. The pore pressure analysis of the Laurel Formation in the Lennard Shelf is presented in Section 6.2.3. The effect of tectonic activities on pore pressure is discussed within Sections 6.2 and 6.3.

6.1 The Laurel formation

The Laurel formation is a Lower Carboniferous unit that is deposited in the Northern Canning Basin, mainly in the Fitzroy Trough and the Lennard Shelf. It is classified as a potential shale gas formation. The lithology of the unit comprises mainly of sandstone, shale and carbonate. The thickness varies significantly from the Fitzroy Trough to the Lennard Shelf. This variation was driven by the major tectonic features such as the growth of the Fenton Fault that was associated with the subsidence of the

Fitzroy Trough. As a result, the Laurel Formation maintained a significantly thick section in the Fitzroy Trough (Cadman et al. 1993). However, Guppy (1958) mentioned that due to further uplifting and erosion of the northern margin of the Canning Basin during the mid-Carboniferous period, a considerable section of the Laurel formation was eroded (Figure 2.8). DMPa (2014) has also stated that the northern part of the Canning basin is more intensely deformed than the southern, due to the movement of the major faults.

This chapter focuses on examining the pore pressure of the Laurel Formation in specific areas such as the Fitzroy Trough and the Lennard Shelf. The studied regions have experienced a series of different syn- and post-depositional tectonic events which have influenced various features such as the formation tops, thicknesses and pore pressure profiles. Figures 6-1 and 6-2 show the formation top and thickness of the Laurel Formation in the studied areas.

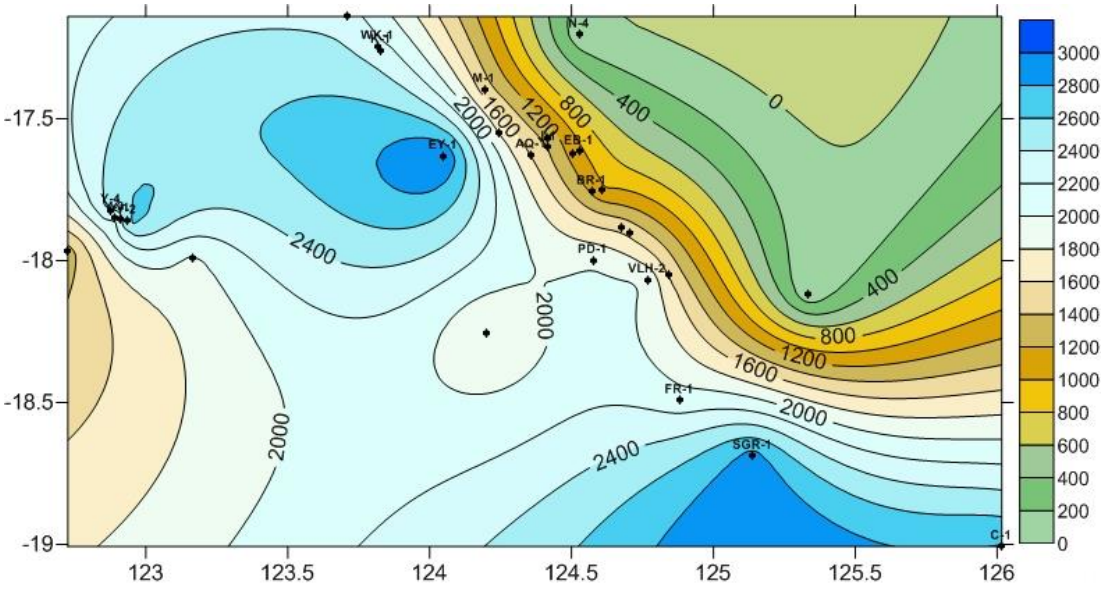

Figure 6-1: Depth contours for the top of the Laurel formation in the Canning Basin. The Top right section of the figure defines the Lennard Shelf whilst the top left and the bottom right show the Fitzroy Trough.

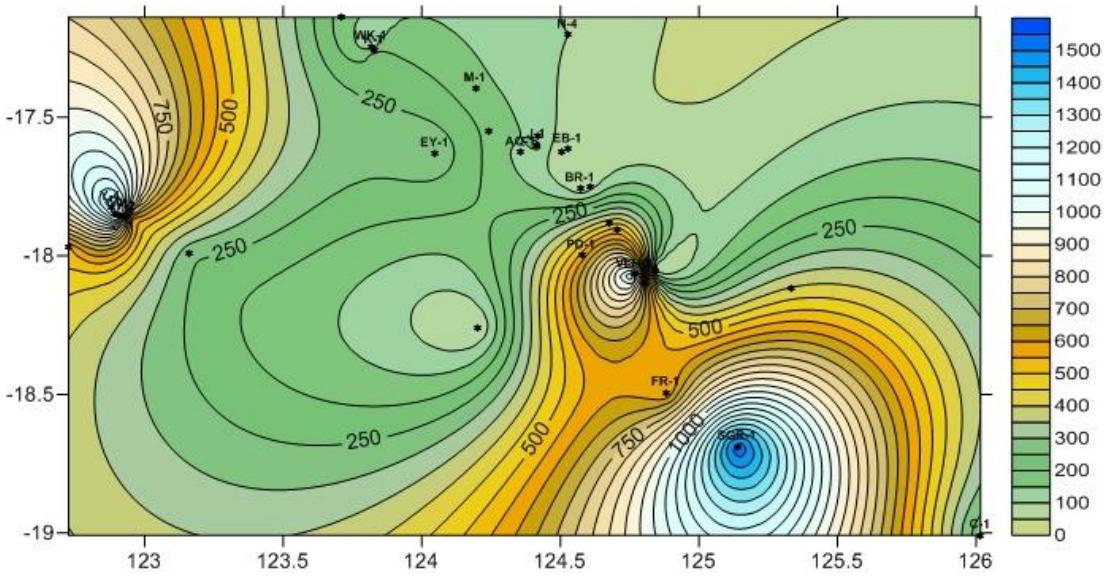

Figure 6-2: Isopach map for the Laurel formation in the Northern Canning Basin. The Top right section of the figure defines the Lennard Shelf whilst the top left and the bottom right display the Fitzroy Trough.

Data from 19 wells in the Northern Canning Basin were examined. Within the Fitzroy Trough, this study has looked at pore pressure in various regions that have different structural features within the Fitzroy Trough. These areas include the Yulleroo, Valhalla, St George Range and Christmas Creek Anticlines.

6.2 Data analysis

6.2.1 Yulleroo Anticline and regional structures (Fitzroy Trough)

The Fitzroy Trough constitutes the main structural feature in the Northern Canning Basin (Ellyard 1982). The Yulleroo structure is a major anticline situated in the south-western, deeper and thicker portion of the Fitzroy Trough. The horizontal extent of the anticline covers approximately 120 square kilometres with a vertical closure within the uppermost part of the Carboniferous of approximately 600 meters. The overall structural style of this part of the Fitzroy Trough is extensional with minor compressional elements. The Trough is bounded by major faults with lesser interior faults within the Yulleroo structure (Bischoff 1968). Within this area of the Canning Basin, a gentle folding appears to have taken place, partially as a result of anticlinal structure initiation (Guppy 1958). On the downthrown side of the Fenton

fault and within the Yulleroo Anticline, four wells were drilled, namely Yulleroo-1, Yulleroo -2, Yulleroo-3 and Yulleroo-4.

Based on structural data, this region of the Canning Basin neither has geo-mechanical hazards nor a presence of any potential faulting penetrating the wells. As such, the pore pressure can be efficiently studied. This in turns allows a valid comparison, with the pore pressure study that was conducted in the Perth Basin, to be made; particularly in the localities of the Dandaragan trough and the Beharra Springs Terrace which experienced similar tectonic features (Section 5.3.1).

6.2.1.1 Log data

Well log data from the studied wells in this region of the Canning Basin that exhibited overpressure include Yullerro-1, Yulleroo-2, Yulleroo-3 and Yulleroo-4, together with a pore pressure measurement; mud logs data and ethane isotope data analysis. Complete results are shown in Appendix 2a. In this section, results from the Yulleroo-1 and Yulleroo-4 wells are discussed.

In the Yulleroo-1 well, deviations from the normal trends were observed in the sonic transit time and density log at a depth of around 3000 m. These log responses comprise evidence of overpressure which is validated by a DST pressure test point (0.6 psi/ ft) that was conducted within the data deviation window and set on the estimated pore pressure profile from sonic log (Figure 6-3).

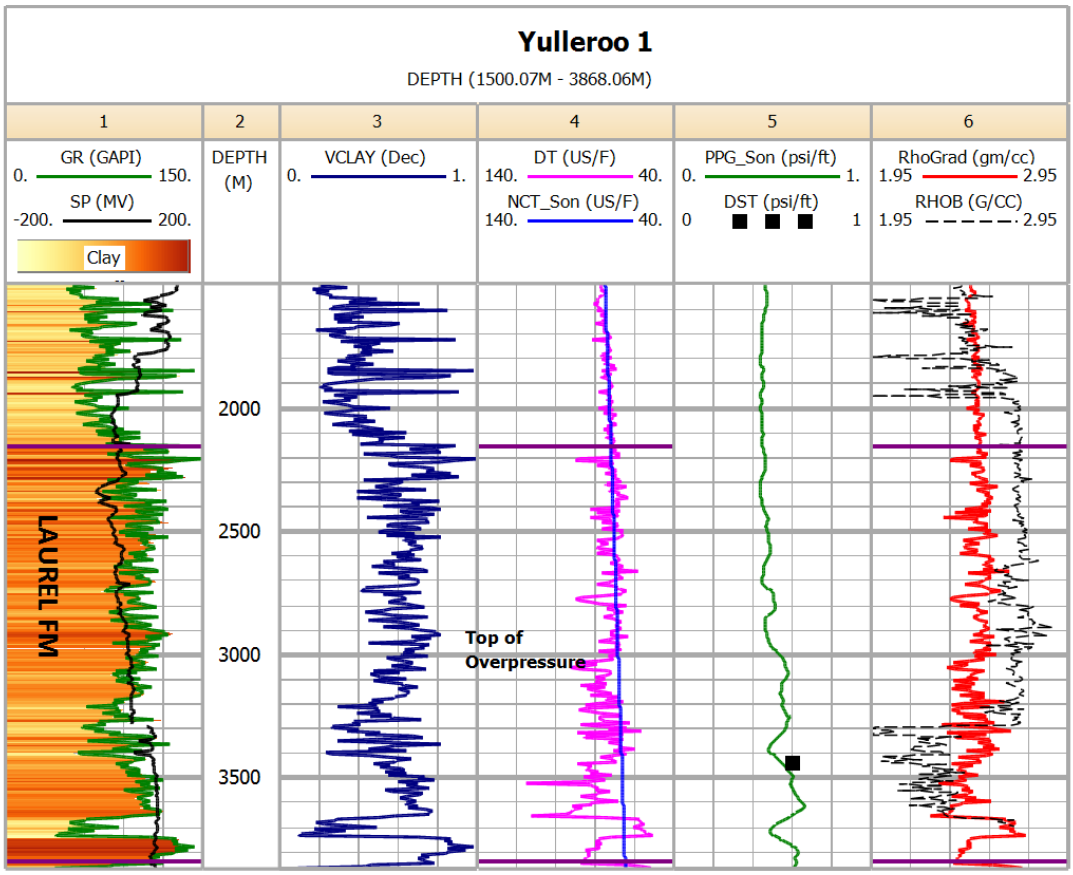

Figure 6-3: Composite logs for the well log data parameters and pore pressure profile in the Yulleroo-1 well (Canning Basin).

As seen in Figure 6-4, the vertical effective stress remains fairly constant in the overpressured section. This constitutes clear evidence that the loading mechanism is the cause of overpressure generation. However, given that the temperature gradient in this region of the Canning Basin is 2.39°C/ 100 m plus the average surface temperature of 23.9 °C (Figure 6-5), this gives an approximate temperature at the depth of 2500 m to be 83.6°C. This temperature range is above the range at which the smectite is transformed to illite (see Section 3.2.2.2). As such, the data below 2500 m is used to create a trend of differentiation, below which significant amounts of smectite are transformed to illite. The purpose of creating such a trend is to examine the overpressure generating mechanism. This trend which correlates the density to sonic transit time is presented in Equation 6.1 and Figure 6-6 shows an illustration of such a trend. As the Yulleroo-1 well has low quality data of the density

log, this trend was created from the density data obtained from the Yulleroo-4 well. Also, the appropriate density for the Yulleroo-1 well was thus estimated from the sonic log using the Gardner method (Gardner et al. 1974) (Equation 6-2).

$$\rho_b = 2.86834 - 0.003639 * DT \qquad Equation\ 6-1$$

$$\rho_b = 0.23 * (v)^{0.25} \qquad Equation\ 6-2$$

Where ρ_b is the density given in (g/cc) and DT is the sonic transit time given in µs/ ft, v is the velocity which is the inverse of sonic transit time and it is given in *ft/ s*, and the constants *0.23* and *0.25* are derived empirically.

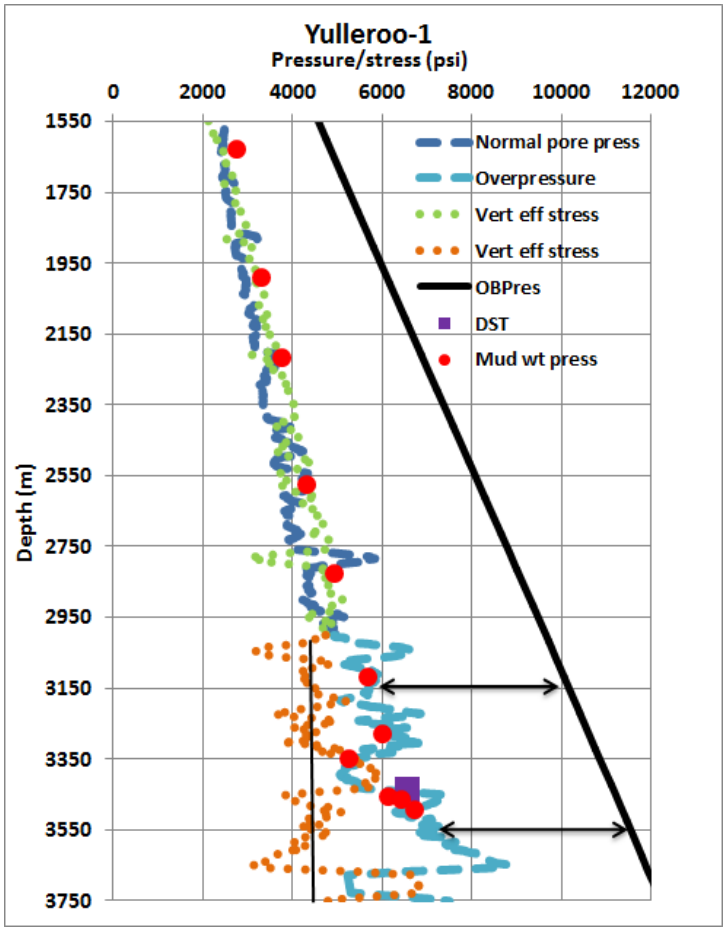

Figure 6-4: Pore pressure and vertical stresses profiles in the Yulleroo-1 well (Canning Basin).

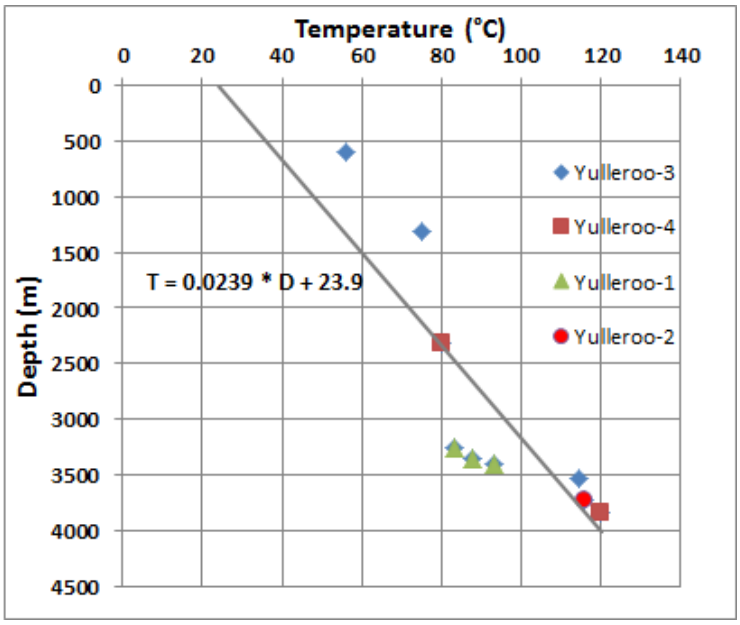

Figure 6-5: Geothermal gradient in the Yulleroo wells (Canning Basin).

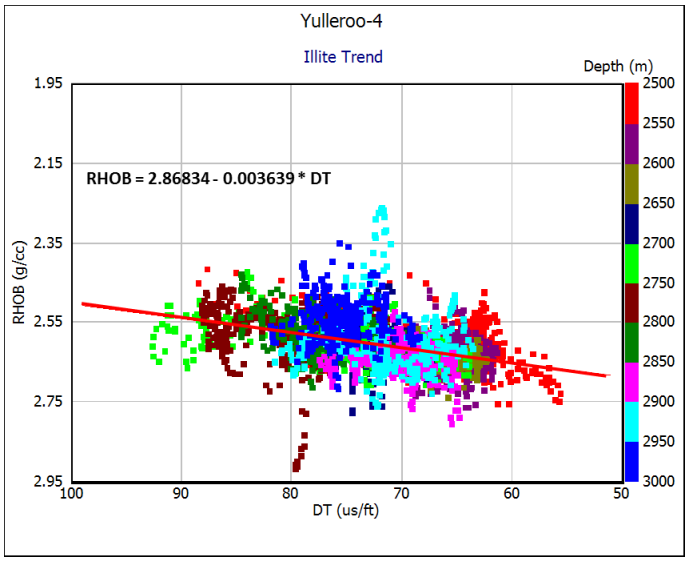

Figure 6-6: A cross-plot of density versus sonic transit time showing the trend below, where a significant amount of smectite is transformed to illite (Data taken from the Yulleroo-4 well). Most of the data are plotted on red-line smectite trend.

The same phenomenon of the Yulleroo-1 well was also observed in the Yulleroo-4 well (i.e., the deviation of sonic transit time, resistivity, neutron porosity and constant density, except that the top of the deviation from the normal trend is at a depth of approximately 2680 m (Figure 6-7)). Unfortunately, there is no pore pressure test data within the deviation window of the well log data parameters. However, the overpressure existence in this well was confirmed by analysing Ethane isotope data

from this well. The deviations of well log data parameters occur around the same depth as the reversal in the Ethane isotope, which is an indication of overpressure.

On cross-plots of density against sonic transit time and density against resistivity (Figure 6-8), the overpressured data points below 2680 m fall within the segments of the plots that have constant density-high sonic transit time and constant density-low resistivity. The regression lines shown on the cross-plots were created based on data between 1600 – 2600 m, for the interval that overlays the overpressured section. This is so as to create a normal compaction trend that can be used to examine the overpressure generation mechanism. Once again, this is clear evidence of the loading mechanism.

It was difficult to show the same trends on cross-plots of the Yulleroo-1 well due to poor quality density log and the used density for pore pressure estimation is estimated from the sonic log using Gardner's method.

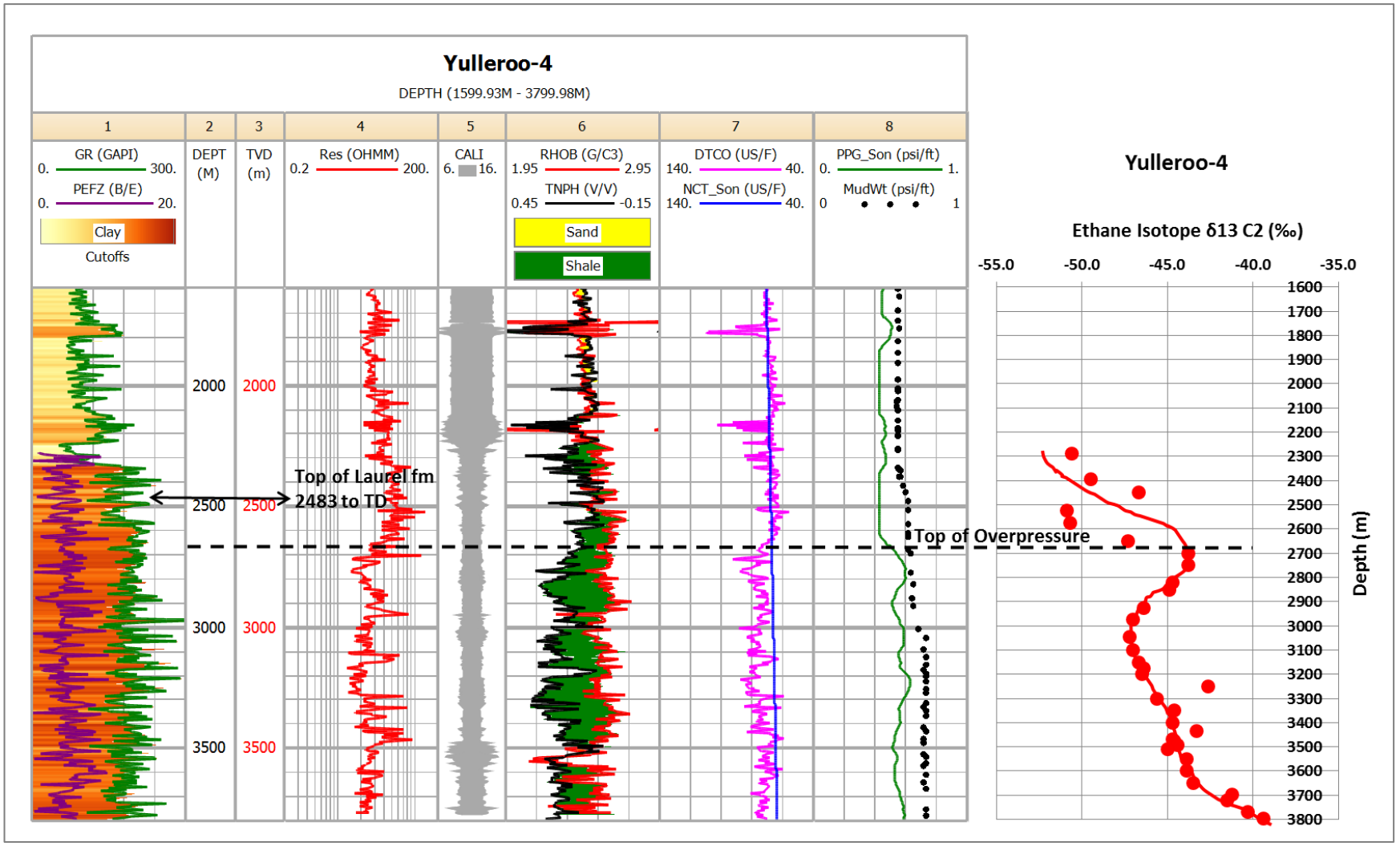

Figure 6-7: Composite logs for the well log parameters, pore pressure profile and Ethane isotope data for the Yulleroo-2 well, showing that the top of overpressure coincides with the reversal in the Ethane isotope.

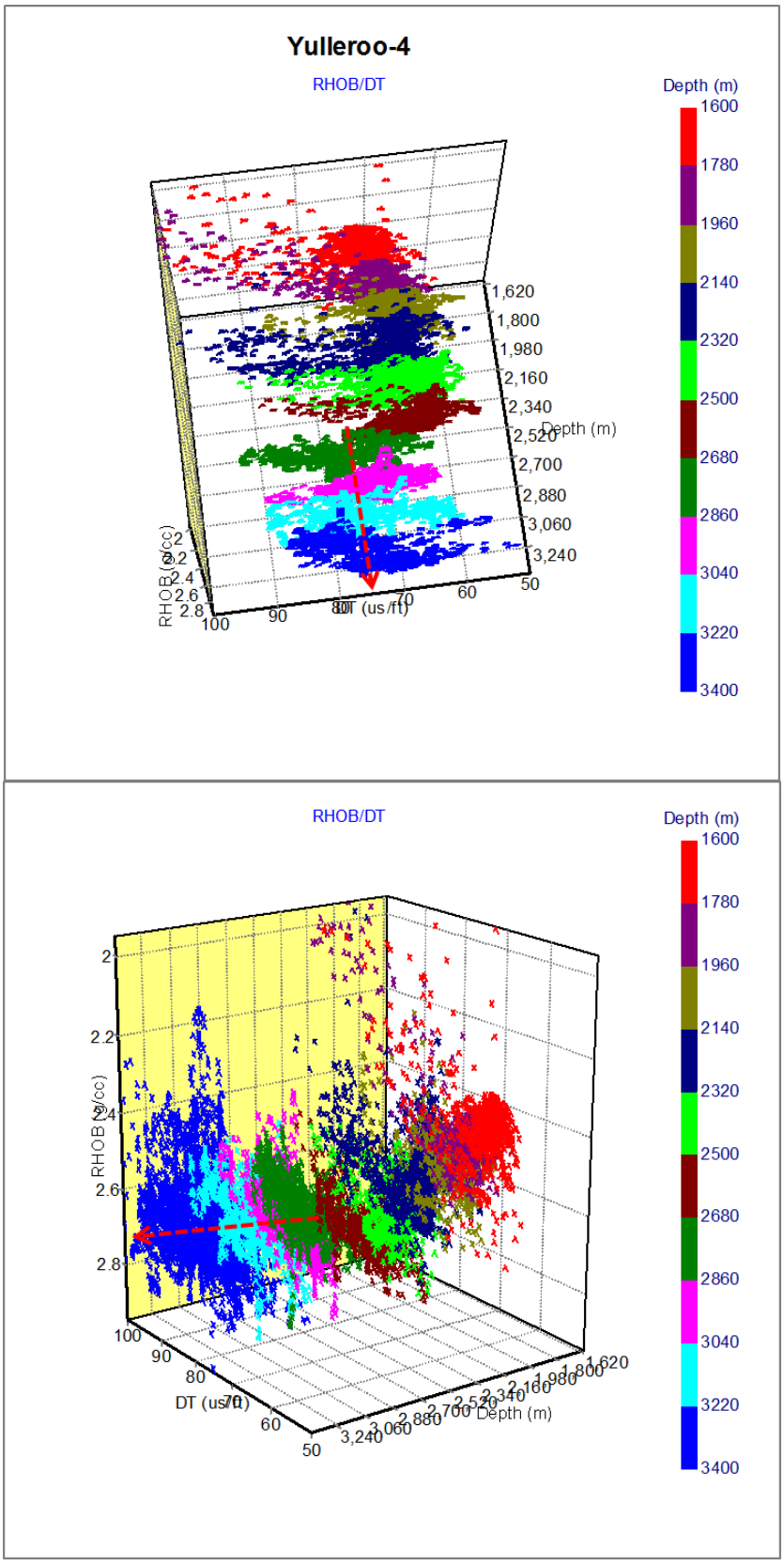

Figure 6-8: Cross-plots of density versus sonic transit time in the Yulleroo-4 well showing that the sonic and density remain fairly constant in the overpressured zone (Canning Basin).

As the Yulleroo wells penetrated thick sections of the Laurel Formation, it was mandatory to examine pore pressure in other wells within the same region that have less thickness of the Laurel Formation. Therefore, the East Yeeda-1 well was a potential candidate to examine in this category.

Geologically, the well is located in the eastern section of the Fitzroy Trough, south of the Pinnacle Fault which defines the border between the Trough and the high basement of the Lennard Shelf. The well was drilled within less severely faulted, northwest trending elongate anticline (Bridge 1985). The well has penetrated 289 m of the Laurel Formation (3012 – 3301 m). The well penetrated a stratigraphic sequence similar to the Yulleroo wells. However, the thickness of the Laurel Formation is substantially less than the Yulleroo-1 and Yulleroo-4 wells.

As shown in Figures 6-9 and 6-10, the well log data parameters followed the normal trends until the depth of approximately 3200 m. At this depth, the sonic, neutron porosity and resistivity logs started to deviate. In addition, there was a slight increase in the mud weight. However, the weight of the mud remained below the pore pressure profile. With the mud weight remaining slightly less than the pore pressure profile curve; there are no risks regarding the overpressure estimation and evaluation. This is due to the fact that the Equivalent Circulating Density (ECD) would be higher than the used mud weight.

Indeed, the East Yeeda-1 indicates the dependency of overpressure occurrence and preservation on the geological structure and tectonic elements with the potential origins other than the thickness of the formation. It is clear that despite the low thickness of the formation, the East Yeeda-1 well exhibits overpressure within the basal section of the Laurel Formation. The preservation of overpressure seems to be influenced by the nature of the tectonics in this region of the Fitzroy Trough.

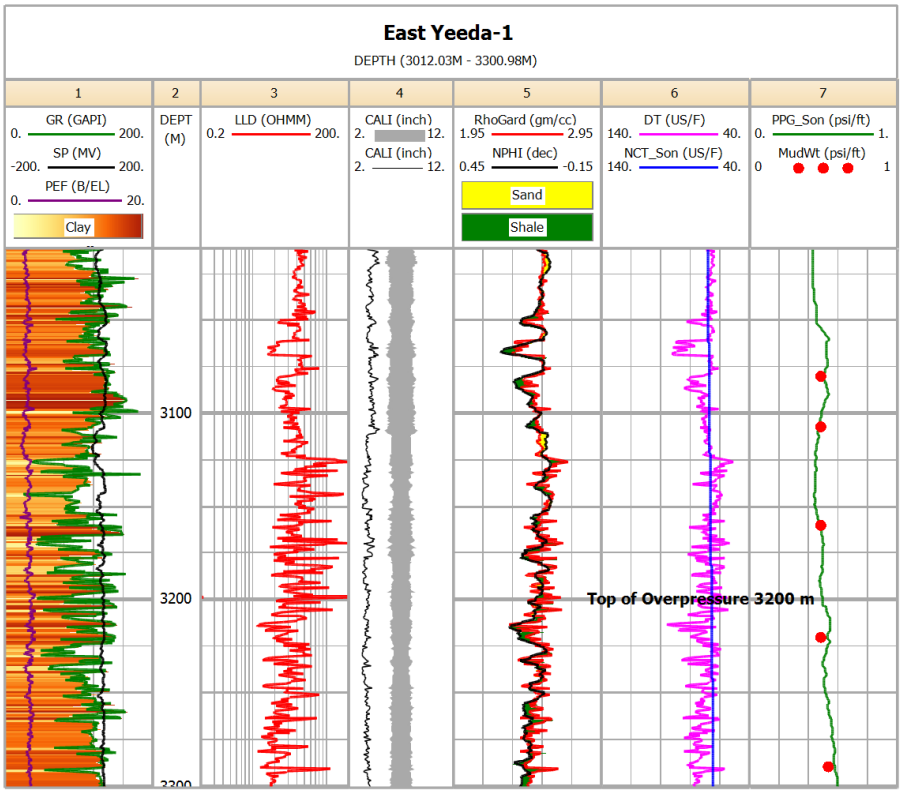

Figure 6-9: Composite logs for the well log parameters and pore pressure profile for the East Yeeda-1 well.

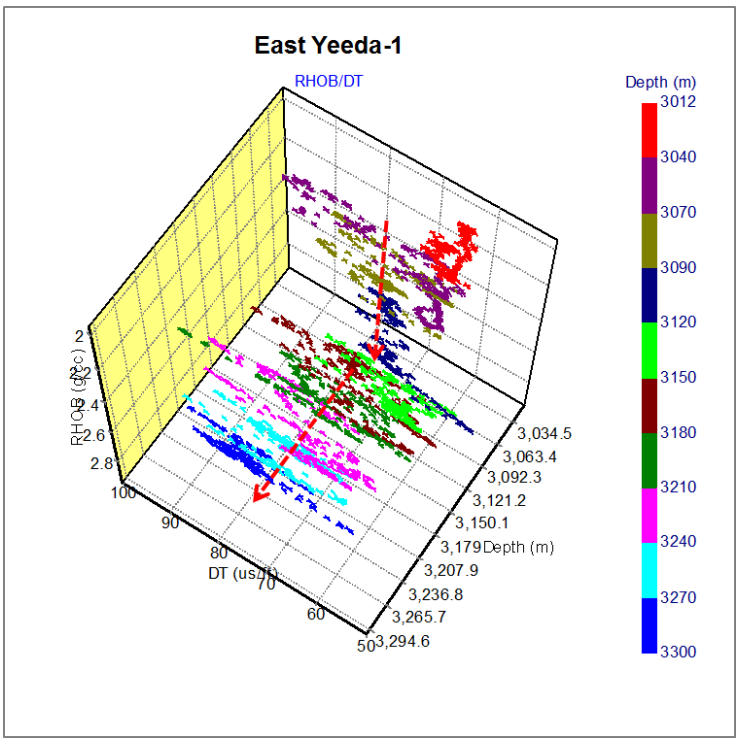

Figure 6-10: Cross-plots of density versus sonic transit time in the Yulleroo-4 well showing that the sonic and density remain fairly constant in the overpressured zone (Canning Basin).

6.2.1.2 Geochemistry

The thermal maturity data (Tmax) and Vitrinite Reflectance (VR) taken from the Laurel Formation in the Yulleroo-1, Yulleroo-2 and Yulleroo-3 wells indicate that the formation is in the window of gas generation (Figure 6-11). In addition, the analysis of gas composition from the Yulleroo-3 and Yulleroo-4 wells depict that there is a break in the slope of gas wetness and gas dryness ratios at approximately the same depth at the top of overpressure (Figures 6-12 and 6-13). The data presented in these two figures show approximate values consistent with the gas composition ratios in these two wells. With the thermal maturity data (Tmax) values above 400 °C (Figure 6-11 left), the responses in Figures 6-12 and 6-13 constitute a clear evidence of over maturity of the Laurel Formation for gas generation, particularly the cracking of the Ethane and higher hydrocarbons, to the extent that the friction of light hydrocarbon (i.e. Methane) is reduced, causing the composition of the gas to become increasingly wet within the overpressured section and reverting back to being drier below the charged zones.

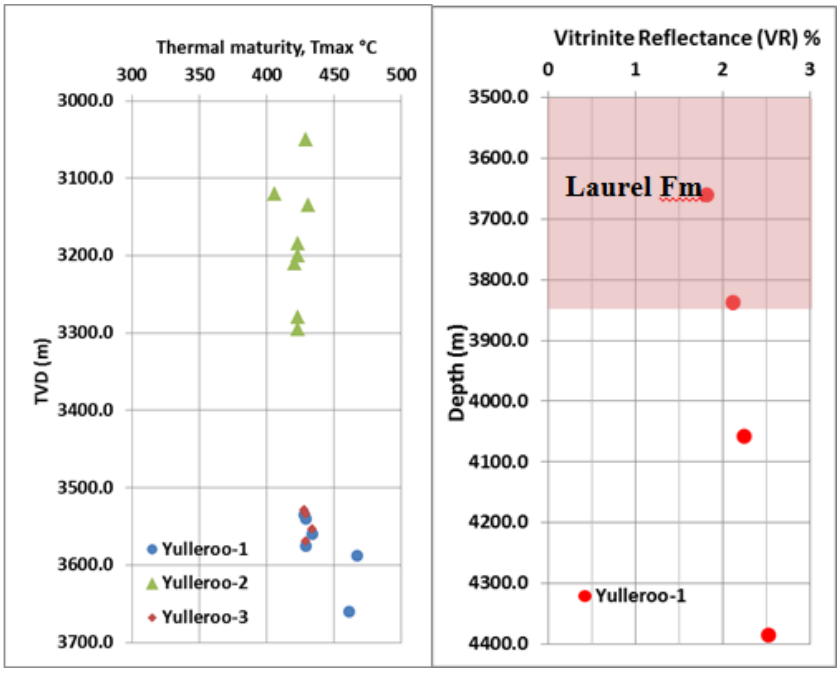

Figure 6-11: Geochemical data for Yulleroo wells: the left is the thermal maturity data (Tmax) taken from the Laurel Formation in the Yulleroo-1 (2150-3832 m), Yulleroo-2 (2700 – 3300 m) and Yulleroo-3 (2208 – 3580 m), whilst the right is the Vitrinite Reflectance data taken from Yulleroo-1 well.

However, it seems that the gas generation mechanism is a secondary mechanism for generating overpressure in the Laurel Formation. This derivation is due to the response of the vertical effective stress to overpressure (Figure 6-4). If gas generation was meant to be the prime overpressure mechanism, the vertical effective stress would have been reversed. Instead, it remains fairly constant within the overpressured section of the Laurel Formation. Another point with regards to the overpressure generating mechanism is that the composition of gas within the charged intervals are not sufficient to generate high magnitudes of overpressure that would cause the vertical effective stress to reverse.

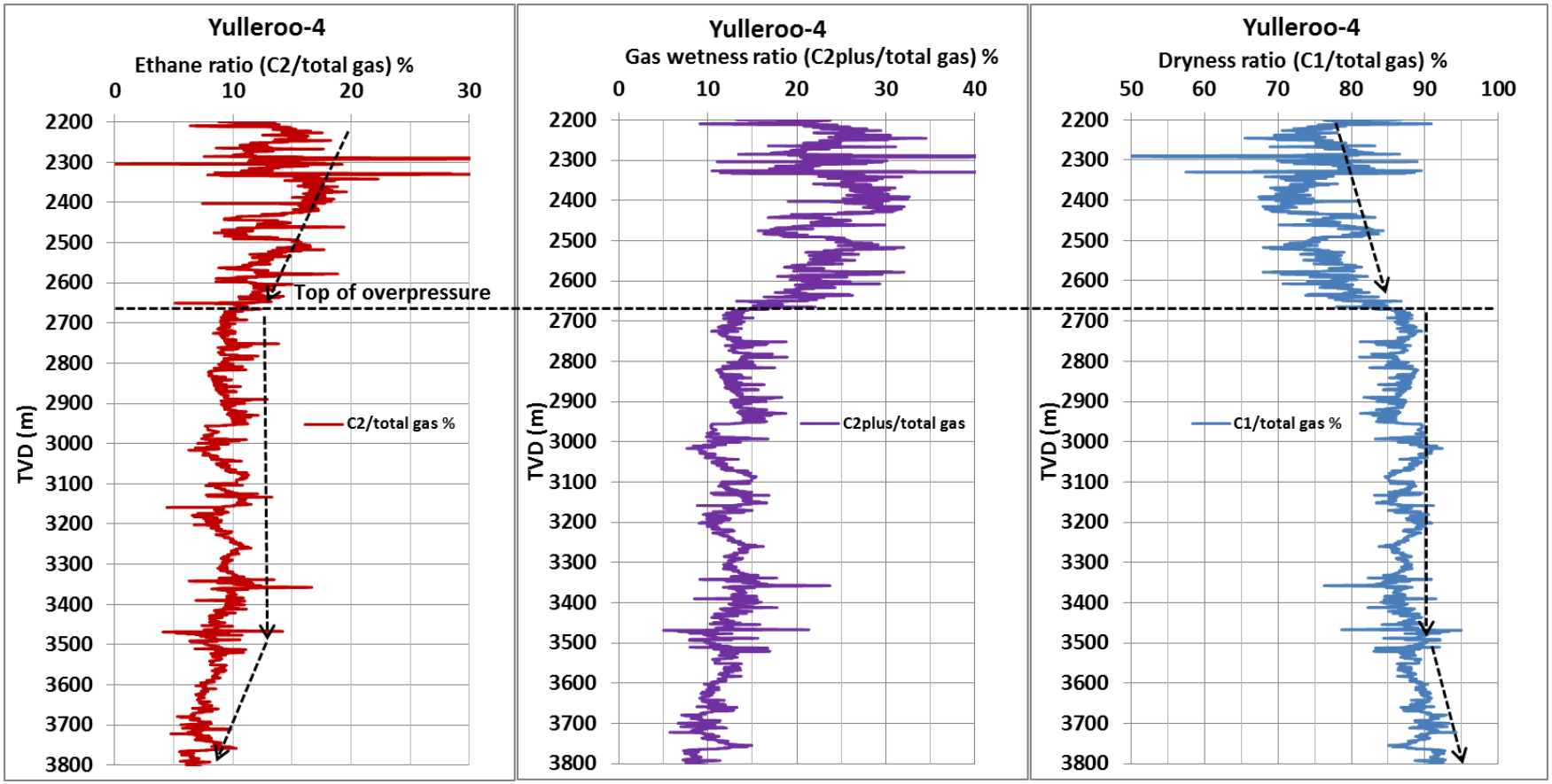

Figure 6-12: Gas wetness and dryness ratios in the Yulleroo-4 well (Canning Basin).

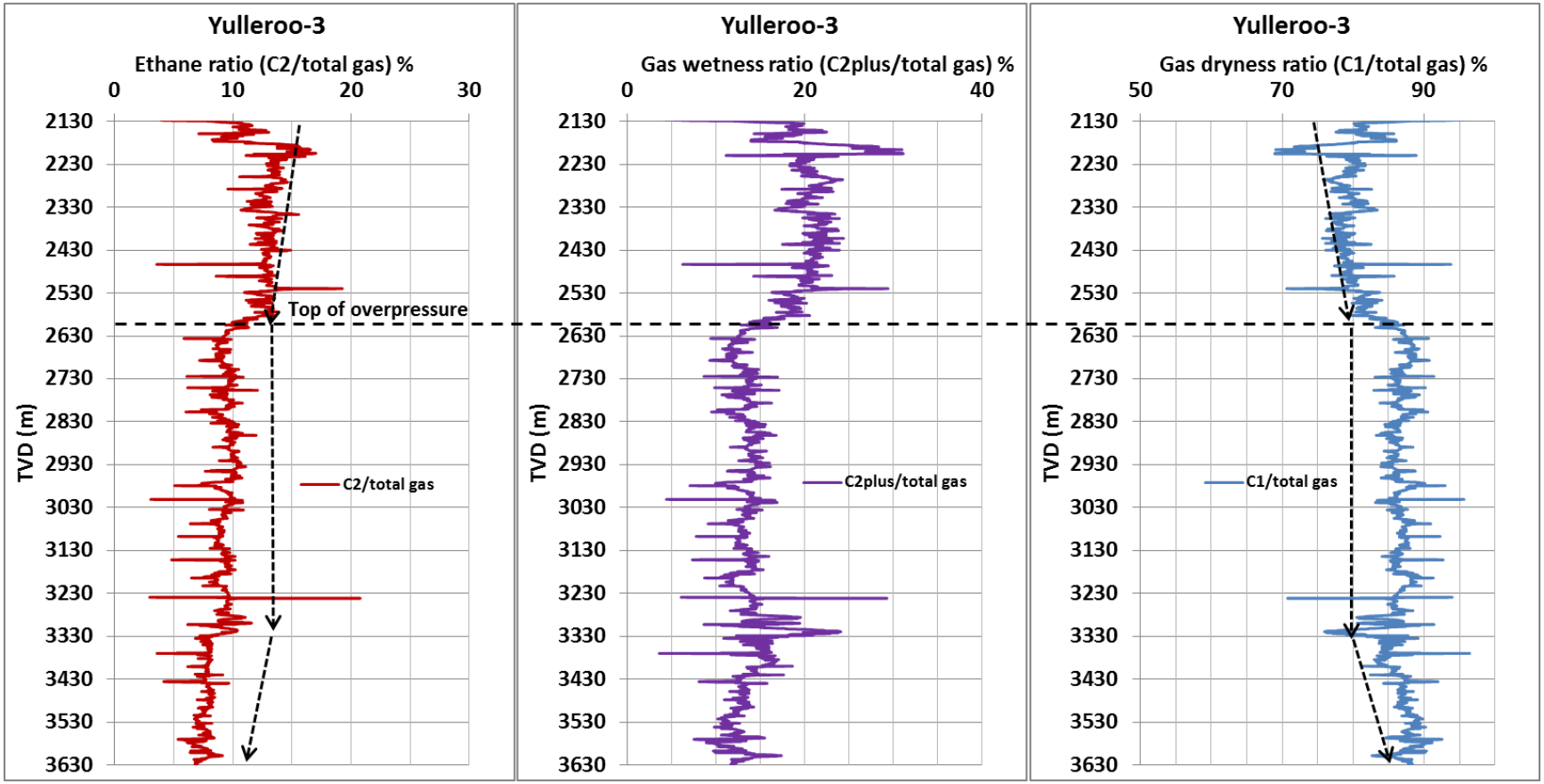

Figure 6-13: Gas wetness and dryness ratios in the Yulleroo-3 well (Canning Basin).

6.2.1.3 Mineralogical analysis

In order to examine every potential cause of overpressure in the Laurel Formation, the mineralogical compositions of the formation are studied in terms of analysing X-ray diffraction (XRD). Results from 11 samples taken from the Yulleroo-1 well have been evaluated against the criteria of clay transformation as a potential origin of overpressure (Table 6-1). The samples from 1 to 8 are taken from the normally pressured section above the overpressure interval of the Laurel Formation. However, the samples from 9 to 11 are from the overpressured section. Table 6.1 shows that the smectite clay is still the principal clay contained in the samples with minor increases in the kaolinite clay in the samples of overpressured interval.

Further to analysing the X-ray diffraction data and in order to bring an additional advantage to the analysis, the Natural Gamma Ray Spectrometry has also been analysed. However, there was no single well within the Yulleroo structure that has such data in the Laurel Formation. Despite that, this study has evaluated the data found in the nearby area (Valhalla-2 well) and thus exhibited overpressure within the Laurel Formation. As depicted in Figure 6-14, it is clear that most of the data points fall in the montmorillonite clay segment of the plot. It has been stated by Varma (2002) that the montmorillonite clay is a member of the smectite group.

In relation to the overpressure generation mechanism in the Laurel Formation, the results presented in Table 6.1 and Figure 6-14 can be interpreted such that the diagenesis effect has no significance on the overpressure development. Presently, there is a high percentage of smectite clay found in the samples and the percentage even show a relative increase in the overpressured zone. In addition, the percentage of illite and kaolinite clays are scarce. As such, the processes of smectite transformation into illite or kaolinite are eliminated as a possible cause of overpressure.

Table 6-1: Mineralogical composition determined by X-ray diffraction analysis (XRD) from the Yulleroo-1 well (Canning Basin).

Mineralogical composition from Yulleroo-1 well															
Sample No.	Depth (m)		Quartz	Illite	Koalin	Smectite	Chlorite	Total clay	Albite	Microcline/ Orthoclase	Pyrite	Siderite	Dolomite	Calcite	Total
	Top	Bottom													
1	2280.49	2283.54	57	5	4	17	<1	26	4	8	1	2	2	-	100
2	2378.05	2381.10	58	4	4	14	<1	22	6	11	1	<1	3	-	100
3	2487.80	2490.85	49	5	4	22	<1	31	6	9	<1	<1	4	-	100
4	2576.22	2579.27	40	6	10	28	1	45	6	8	<1	<1	1	-	100
5	2698.17	2701.22	44	5	8	28	<1	41	7	6	<1	<1	-	1	100
6	2795.73	2798.78	40	5	9	31	1	46	6	6	<1	2	-	<1	100
7	2875.46	2879.12	48	7	1	27	1	36	8	7	-	<1	-	-	100
8	2914.63	2917.68	41	6	9	28	<1	43	7	6	<1	2	-	1	100
9	3028.51	3032.16	26	8	13	42	1	64	5	4	<1	1	-	-	100
10	3036.59	3039.63	34	7	11	32	1	51	7	5	<1	2	-	1	100
11	3131.10	3134.15	36	6	9	32	1	48	7	5	<1	1	-	2	100

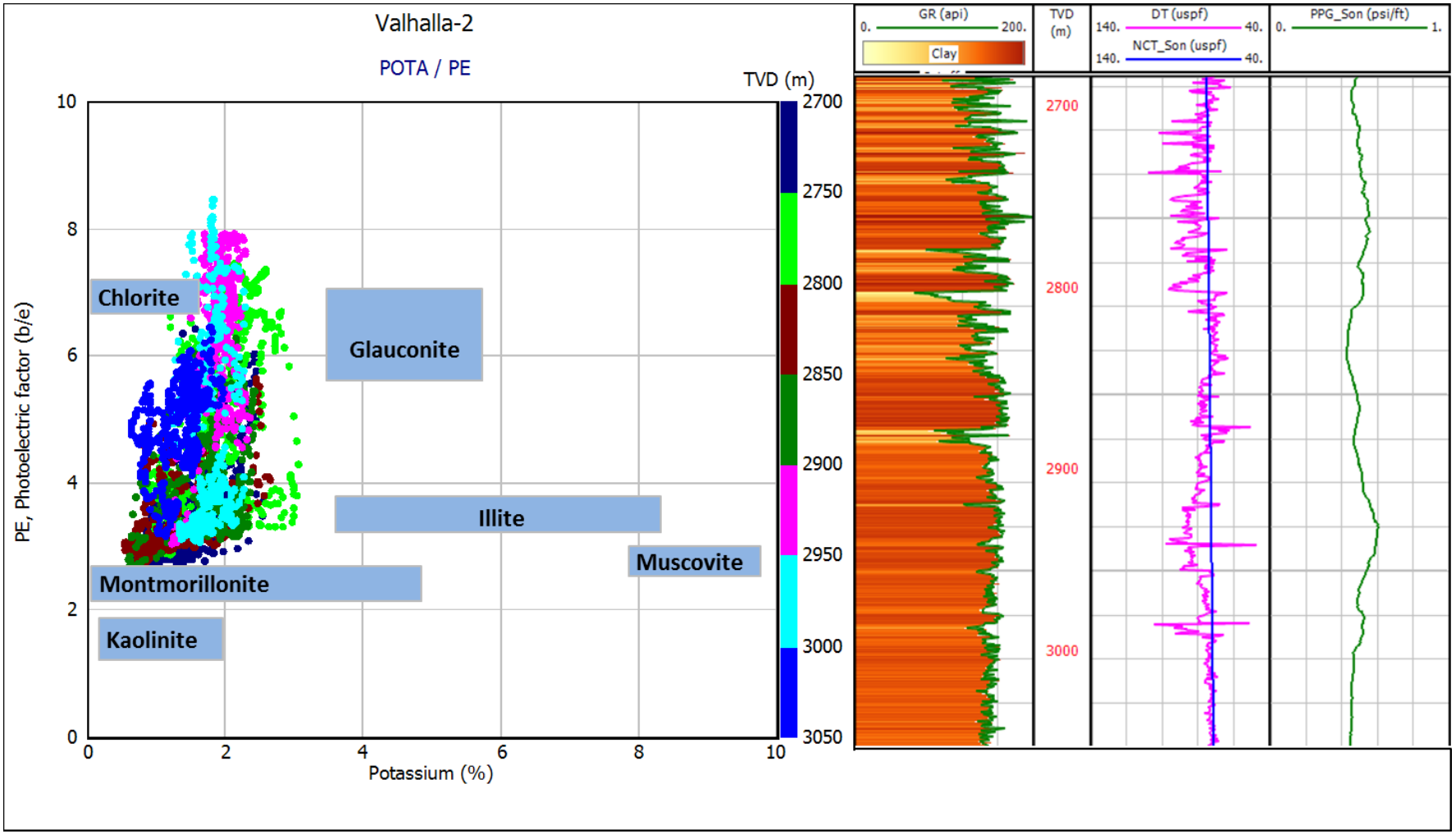

Figure 6-14: Natural Gamma Ray Spectrometry log (NGS) for the Laurel Formation (lower clastic) in the Valhalla-2 well (Canning Basin).

It is worth mentioning that the same overpressure phenomenon in the Laurel Formation was observed in the Valhalla and Paradise prospects, which have similar structural features as the Yulleroo structure. The pore pressure profiles in these areas are presented in Appendix 2a.

6.2.2 St George Range Anticline and Christmas Creek Structure (Fitzroy Trough)

6.2.2.1 St George Range Anticline

St George Range anticline constitutes the largest identified anticline in the Canning Basin. It is located in the south eastern portion of the Fitzroy Trough. The anticline extends to approximately 58 km in the east west orientation; with a variation in width of 25 – 32 km. The vertical closure of the anticline is about 915 m within an area of 1680 square kilometres (Forman et al. 1981).

Shannon and Henderson (1966) stated that syndepositional faulting systems were formed within the Laurel Formation in this area of the Fitzroy Trough. These faults accompanied the structural growth of this period and continued through the Mid-Carboniferous. The structural development throughout the Carboniferous period provided a further structural growth and significantly influenced the depositional features of the Laurel formation. Moreover, Guppy (1958) stated that a substantial part of the upper Laurel formation was eroded during the periodic uplifting and erosion, resulting in the "Alice Springs Orogeny" during the Mid-Carboniferous time. The next major tectonic feature took place during the Triassic period. During this period, the St George Range Anticline experienced major uplifting and compression, caused by a right lateral wrenching along the marginal faults of the Fitzroy Trough.

It is unfortunate that the seismic profile was limited only to the flanks of the anticline. However, several data extracted from boreholes that were drilled in the anticline indicate the presence of thrust faults and fractures in both the Lower and Upper Carboniferous. These faults seem to have influenced pore pressure profiles within this structure. St George Range-1 and Fitzroy River-1 wells provide examples of such boreholes. Shannon and Henderson (1966) stated that there are vertical

fractures present throughout the whole section of the Laurel Formation. For instance, a vertical fracture was observed in a core that was cut at a depth of 3181.4 - 3183.23 m from St George Range-1 well. In addition, the bottom of the core (3275.6 - 3278.65 m) contains several open fractures. These fractures might have resulted from the displacement of the thrust-faults that are present in the well.

The thickness of the Laurel Formation within this area of the Canning Basin varies significantly to over 1550 m around the axis of the anticline (e.g. St George range-1 well), to approximately 700 m in the western end of the anticline (e.g. Fitzroy river-1 well) and 206 m in the Cycas-1 well of the nearby Christmas Creek Anticline (Figure 6-2). The lithology of the Laurel Formation within the anticline is classified as limestone, shale and sandstone.

In light of the aforementioned structural framework of the St George Range Anticline, the pore pressure in this region of the Fitzroy Trough is studied. This allows for a valid comparison, with the pore pressure study that was conducted in the Perth Basin, to be made (particularly the Beagle uplift and Northampton uplift regions in Section 5.3.2). Therefore, an appropriate conclusion can be reached.

6.2.2.2 The Christmas Creek Anticline

The Christmas Creek structure is a large elongated north-south trending and Palaeozoic age anticline that is situated east of the St George Range anticline in the north-eastern portion of the Fitzroy Trough (Canning Basin). It has a closure that extends to an area of 40 square kilometres and is approximately 11 kilometres long and 4 kilometres wide (Ellyard 1983).

Forman, et al. (1981) also mentioned that the structure is believed to have first been formed during the Ordovician. However, its present shape is formed as a result of major extension that was initiated in the middle Devonian and resumed episodically through to the Middle Triassic period, According to Ellyard (1983), the older extensional boundaries of the Fitzroy Trough were reactivated during an episode of wrench tectonics during the Late Triassic. In addition, Brown, et al. (1984) stated that large north-south trending hinge line faults exist in this region and parallel the structure to the east and are considered to be genetically related.

The Laurel Formation within this structure dominantly comprises of shale, siltstone with minor interbedded sandstone and limestone. Above the top of the Laurel Formation, there is a low angle structural dip (1° to 4°). However, there is an overall

increase in dip angle to 10° in deeper formations such as the Anderson and Laurel Formations as shown in Table 6-2. According to Bengtson (1981) and Devilliers and Werner (1990), a sudden change in dipmeter is interpreted as either some sort of distortion near the fault plane or that one fault block is tilted more than the other. Therefore, a pore pressure study in this region provides an insight to the effects of tectonic compression on the pore pressure regime. Hence, a valid comparison can once again be made with the pore pressure studies in the Beagle uplift and Northampton uplift regions (Perth Basin) (Section 5.3.2), which further allows for an appropriate correlation.

Table 6-2: Structural dip from the Cycas-1 well (Canning Basin).

Depth Interval (m)	Formation/unit	Structural dip
248-440	Noonkanbah Formation	2-3°
475-554	Poole Sandstone	2°
774-1697	Grant Formation	1°
1702.5-2115	Upper Pre-Glacial Unit	2-3°
2142-2272	Lower Pre-Glacial Unit	3°
2314-2352	Anderson Formation	4-5°
2440	Anderson Formation	4°
2440-2454	Anderson Formation	3°
2476-2499	Anderson Formation	4°
2579-2596	Anderson Formation	5°
2643-2659	Anderson Formation	7-8°
2720-2733	Anderson Formation	9-10°
2836	Laurel Formation	10°

6.2.2.3 Log data

Well log data from the wells studied in the St George Range Anticline of Canning Basin include St George Range-1 and Fitzroy River-1. These wells were drilled around the axis, in the western margin of the anticline respectively. In addition, the log data from the Cycas-1 well was studied to examine the pore pressure regime in the Laurel Formation in the Christmas Creek Anticline.

Within the Laurel Formation, neither of the examined boreholes had any pore pressure related abnormalities from well log data, nor did they have any signs of overpressure while drilling.

In St George Range-1 well, a thick section of the Laurel Formation was encountered (1554) m, with the formation top is being intersected at a depth of 2884 m (Figure 6-185). The values of the well log data parameters within the Laurel Formation are comparable and closely matching the log data values in the Yulleroo wells. However, there were no reversals as observed in the Yulleroo structure. Instead, the parameters continued to follow the normal trends throughout the whole well. As such, the pore pressure is characterized as normal at the gradient of 0.44 psi/ ft across the whole section of the Laurel Formation.

In addition, Figures 6-16, 6-17 and 6-18 show composite logs and pore pressure profiles in the Fitzroy River-1 and Cycas-1 well. The first borehole was also drilled within the western edge of the St George Range Anticline, whilst the Cycas-1 was spudded in the Christmas Creek Anticline. Likewise, these wells depict normal pore pressure regimes across the whole section of the Laurel Formation. It is noticeable that the thickness of the Laurel Formation decreased as moving to the east and west from the axis of the St George Range Anticline. The Fitzroy River-1 well intersected approximately 545 m of the Laurel Formation, whilst the Cycas-1 well intersected at about 206 m. Yet again, the well log data parameters are within the same range as the wells in the Yulleroo structure, which is an illustration of examining intervals with similar classifications. However, the different structures as well as the tectonic features seem to be the foremost factors of having overpressure in the Laurel Formation within the Yulleroo region on one hand, and normal pore pressure within the area of St George Range on the other hand.

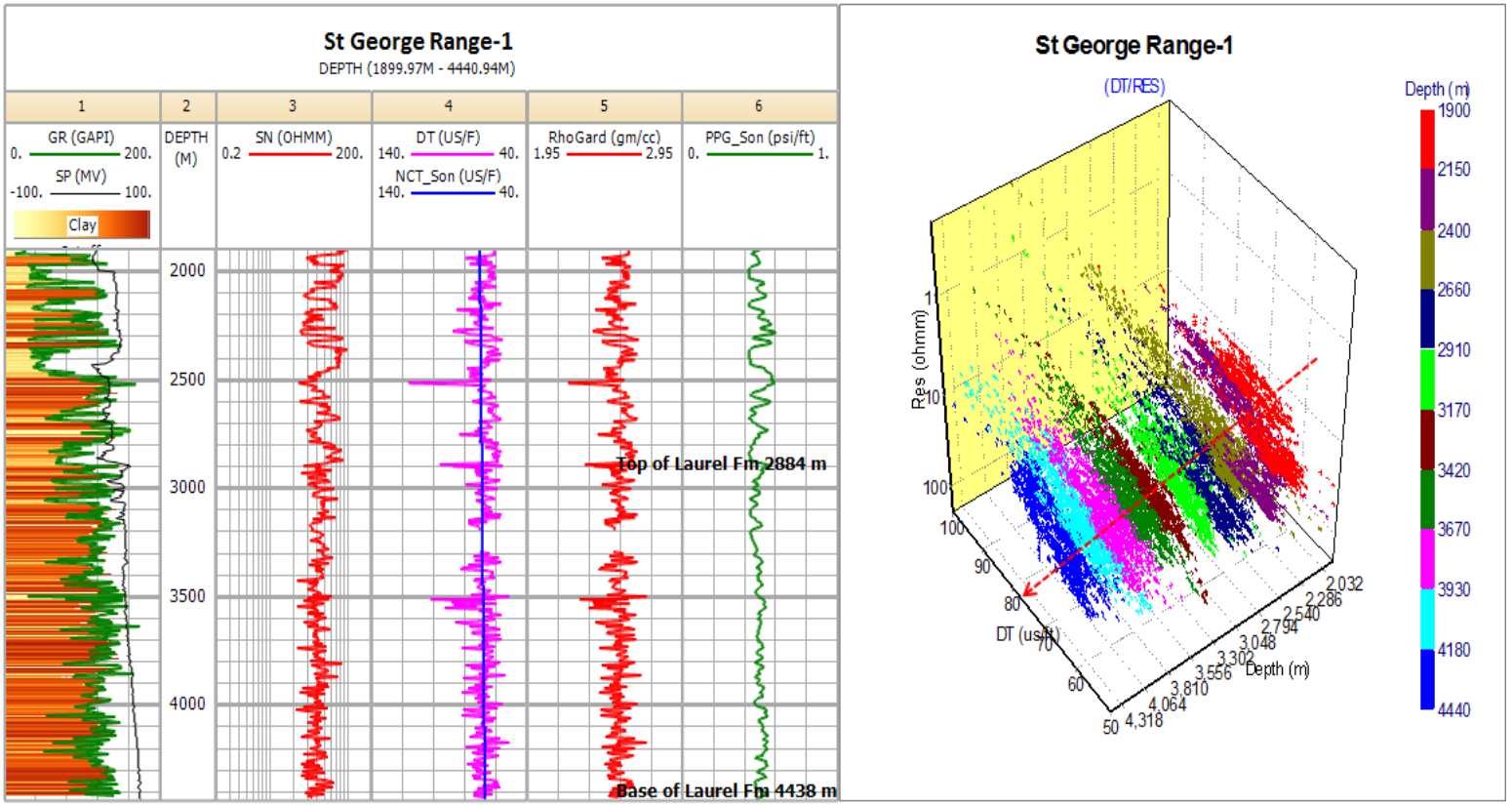

Figure 6-15: Well log data, and pore pressure profile (left) and cross-plot of sonic transit time versus resistivity (right) for the Laurel Formation in St George Range-1 well.

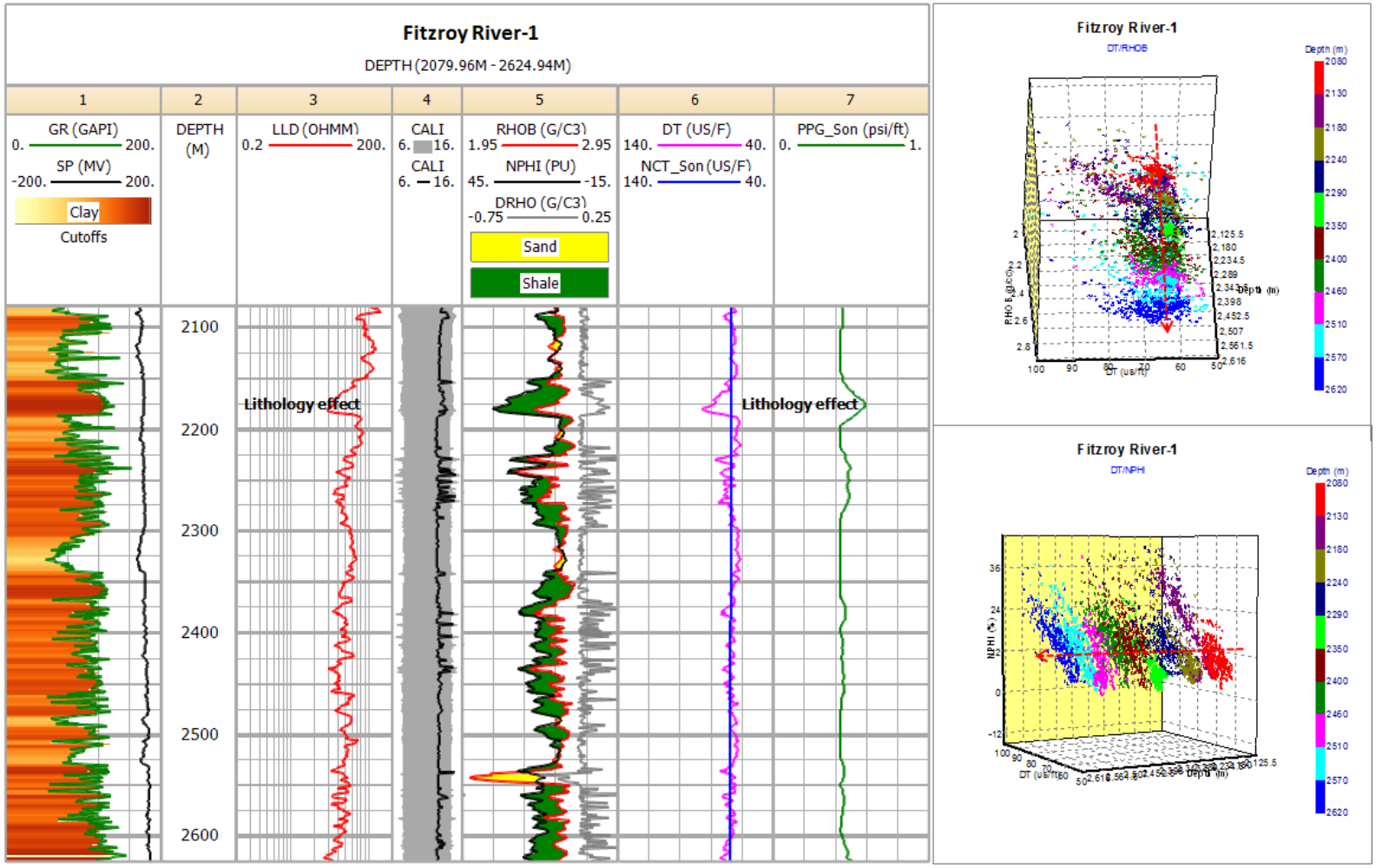

Figure 6-16: Well log data, and pore pressure profile as well as data cross-plots for the Laurel Formation in the Fitzoy River-1 well (Canning Basin).

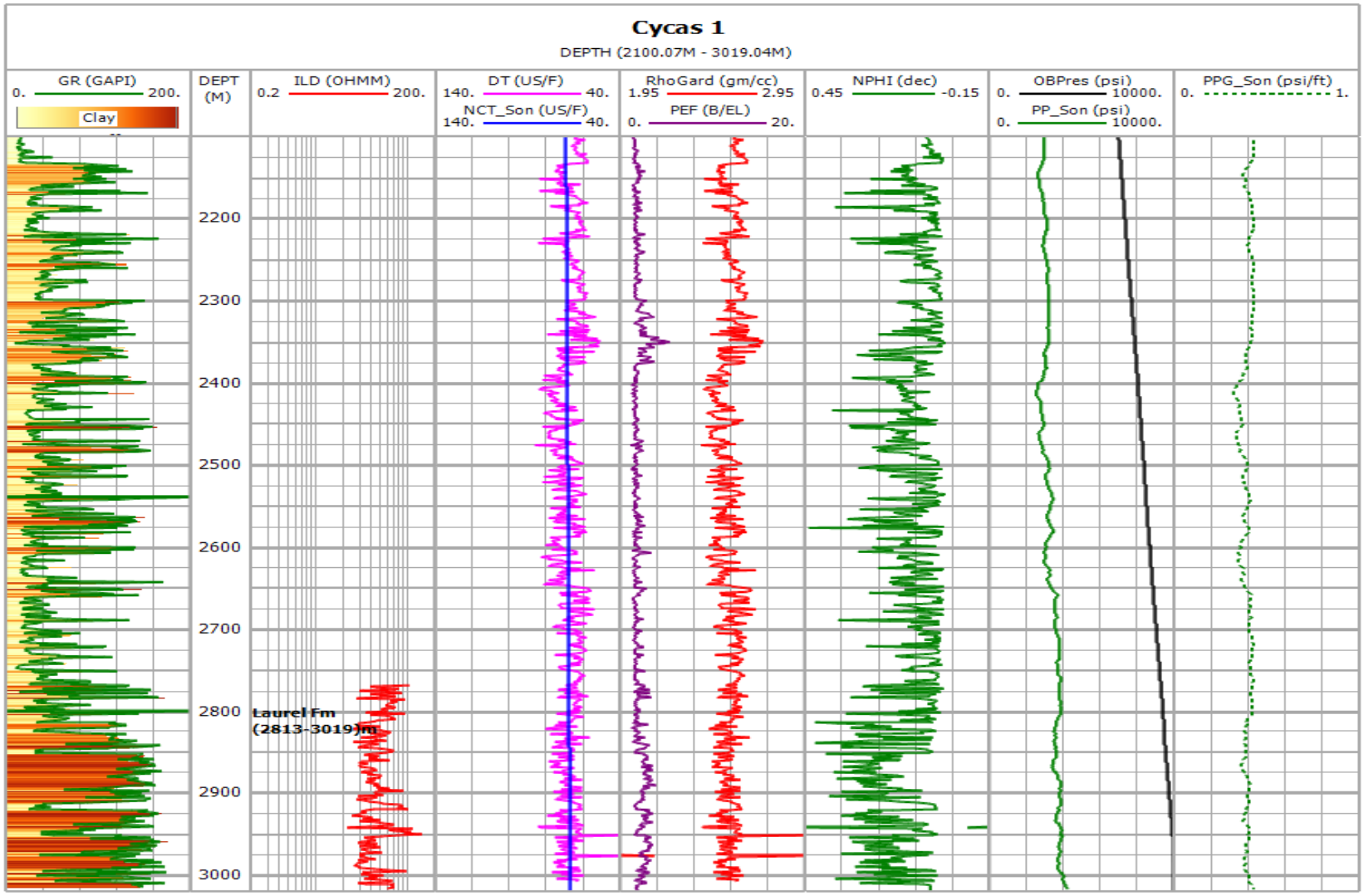

Figure 6-17: Pore pressure profile for the Laurel formation in the Cycas-1 well (Canning Basin).

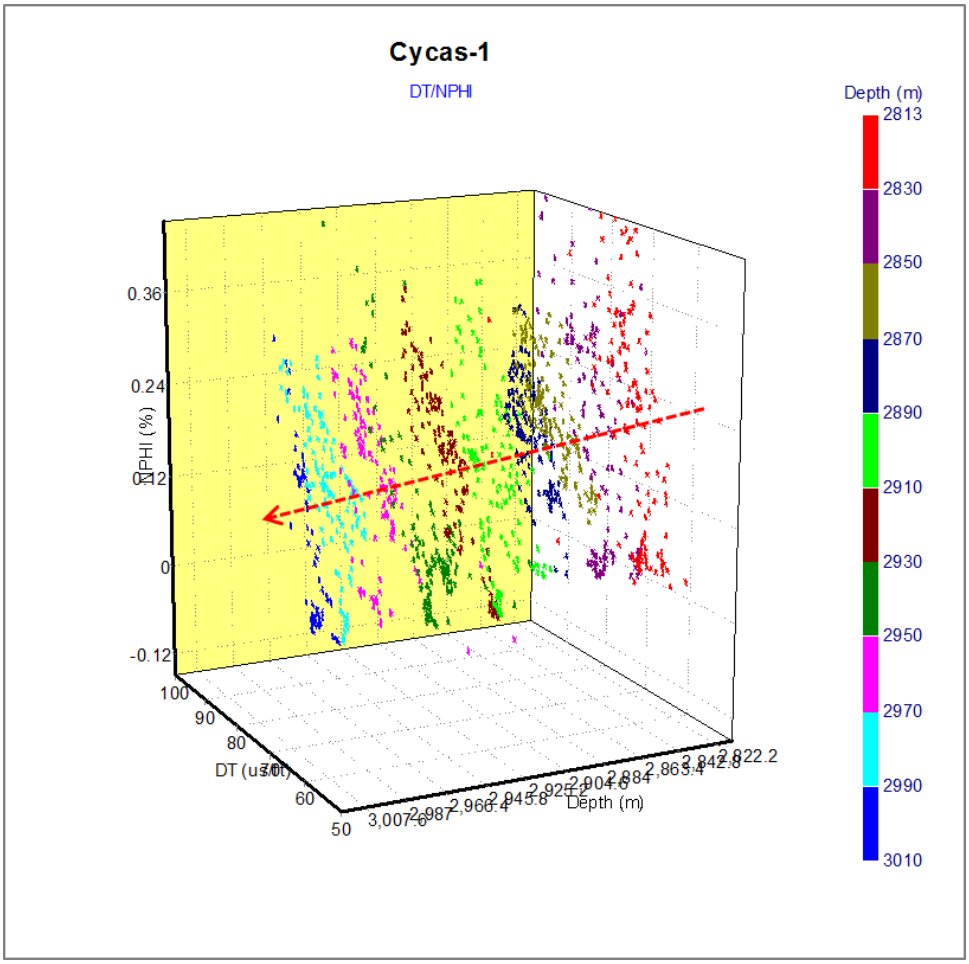

Figure 6-18: Cross-plot of sonic transit time versus neutron porosity for the Laurel formation in the Cycas-1 well (Canning Basin).

6.2.2.4 Geochemistry

The Vitrinite Reflectance (Ro %) data taken from the Cycas-1 well in formations above the Laurel Formation were within the oil generation window (Ro range of 0.5 - 1.35 %). However, a high level of organic maturity was observed at the top of the Laurel Formation (Ro = 2.2%) as shown in Figure 6-19. This suggests that the sediments below this depth are beyond the oil generation range and are within the gas generation window.

The Ro data within the Laurel Formation indicate that the formation is mature for gas generation in this area of the Fitzroy Trough (Canning Basin). However, the formation has exhibited normal pore pressure profile (Figure 6-17) as opposed to the western margin of the Trough (Yulleroo structure). This in turn highlights the significance of the local tectonic elements on the preservation of overpressure and possibly endorses the methodology that was established in Chapter 5 as stated in

Section 5.4. If sufficient seal had provided, the generated gas would have caused a high magnitude of overpressure in the Laurel Formation within the Christmas Creek Structure. Instead, the interior faults and induced fractures as stated in Section 6.2.2.2 and Table 6-2 could possibly have acted as conduits for the generated gas to be disseminated to the surrounding formations, leading to the equalization of the pore pressure with hydrostatic.

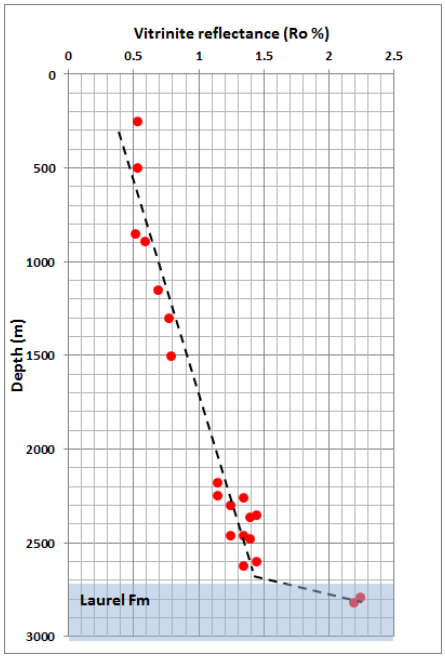

Figure 6-19: Vitrinite Reflectance data against depth from the Cycas-1 well (Canning Basin).

Furthermore, a couple of thermal maturity data at the top of the Laurel Formation in the Fitzroy River-1 well showed high thermal maturity of Tmax > 460 °C (Table 6-3). This maturity range is still higher than the onset of hydrocarbon generation for most Kerogen types (McCarthy et al. 2011).

Table 6-3: Thermal maturity data from the top of the Laurel Formation in the Fitzroy River-1 and St George Range-1 wells (St George Range Anticline).

Well Name	Depth (m)	Tmax (°C)
Fitzroy River-1	2160	466
Fitzroy River-1	2180	462
St George Range-1	3745.9	477

6.2.3 Lennard shelf

6.2.3.1 Structural features

The Lennard Shelf is an area of relatively shallow basement that forms the northern margin of the Fitzroy Trough (Figure 2-6). The Shelf contains sediments of approximately 4000 m, ranging from the Ordovician period and younger sections (Figure 2-8). It is structurally controlled by a complex series of northwest fault systems and northeast transfer zones (Crostella 1998). These faults include the Blackstone, Sundown, Meda, and Mount Percy Transfer Zones (Middleton 1991).

This area of the Canning Basin is featured by an uplifting event that took place in the Late Carboniferous, which focused on the Lennard Shelf and the mid-basin Arch (Dorling et al. 1998). Ellyard (1982) has also mentioned that the uplifting has resulted in significant erosion that caused a complete removal of the Anderson Formation and significantly down-cut into the Lower Carboniferous unit of the Laurel Formation below the Anderson Formation. A further uplifting event that took place in the Late Triassic period resulted in the Lennard Shelf to remain elevated and undergo further erosion (Arne et al. 1989). In addition, various dipmeter data obtained from various wells that were drilled in the Lennard Shelf indicated an increase in the structural dip, which in turn reflect the presence of interior faulting and associated fracturing within the structure (Table 6-4).

Table 6-4: Structural dipmeters dips from various wells drilled within the Lennard Shelf (Northern Canning Basin).

Well Name	Formation/unit	Structural dip
Aquanita-1	Noonkanbah Formation	2-20°
Aquanita-1	Poole Sandstone	2-30°
Aquanita-1	Grant Formation	0-30°
Aquanita-1	Laurel Fomation	0-30°
Aquanita-1	Yellow Drum Equ	0-30°
Aquanita-1	Gumhole Formation	2-30°
Aquanita-1	May River Unit	9-22°
Janpam-1	Noonkanbah Formation	0-5°
Janpam-1	Poole Sandstone	0-14°
Janpam-1	Grant Formation	0-64°
Janpam-1	Laurel Fomation	0-30°
Janpam-1	Yellow Drum Equ	0-22°
Janpam-1	Gumhole Formation	0-7°
Janpam-1	May River Unit	1-8°
Boronia-1	Grant	2°
Boronia-1	Laurel	10-12°
Boronia-1	Luluiqui Shelf	6°
Boronia-1	Clanmeyer	7°
Boronia-1	Pillara	23°
Meda-1	Grant Formation	30°
Meda-1	Devonian Sequence	25°

6.2.3.2 Log data

The lithological description, thickness and formation tops of the Laurel Formations varies from one well to another within the region of the Lenard Shelf (Figures 6-1, 6-2 and 6-20). The generalized lithological description of the formation can be classified as the Upper Carbonate, Middle Shale and Lower Carbonate. However, the formation underwent significant erosion that has caused the removal of significant sections. As a result, the thickness of the Laurel Formation has been lessened to an extent that makes it very difficult to efficiently evaluate pore pressure via the compaction trend method.

Figure 6-20 shows well log data, lithological description and pore pressure profile for the Boronia-1 and Aquanita-1 wells, which represent examples for the complexity of pore pressure evaluation within this locality.

Due to the aforementioned complications, it was difficult to establish a reliable normal compaction trend that can be used for pore pressure estimation. However, navigating through the database of this research indicates no signs of overpressure nor any abnormalities observed in the well log data parameters (Figure 6-20). As such, the pore pressure regime of the Laurel Formation in the Lennard Shelf is characterized as normal.

6.2.3.3 Geochemistry

It is unfortunate that there are not much of geochemical data that were obtained for the Laurel Formation in the Lennard Shelf. However, very limited thermal maturity data points are gained from the Kora-1 and Valentine-1 wells (Table 6-5). These data points indicate that the formation is mature for hydrocarbon generation that might generate overpressure if sufficient seal was provided. However, with reference to Section 6.2.3.1, the interior faulting and associated fracturing within the structure could possibly have acted as conduits for the generated fluid to be dissipated to the surrounding sediments, re-equilibrating the pore pressure back to normal gradients.

Table 6-5: Thermal maturity data from the Laurel Formation in the Kora-1 and Valentine-1 wells (Lennard Shelf).

Well Name	Depth (m)	Tmax (°C)
Kora-1	2515	486
Valentine-1	2290	431
Valentine-1	2340	430
Valentine-1	2450	432

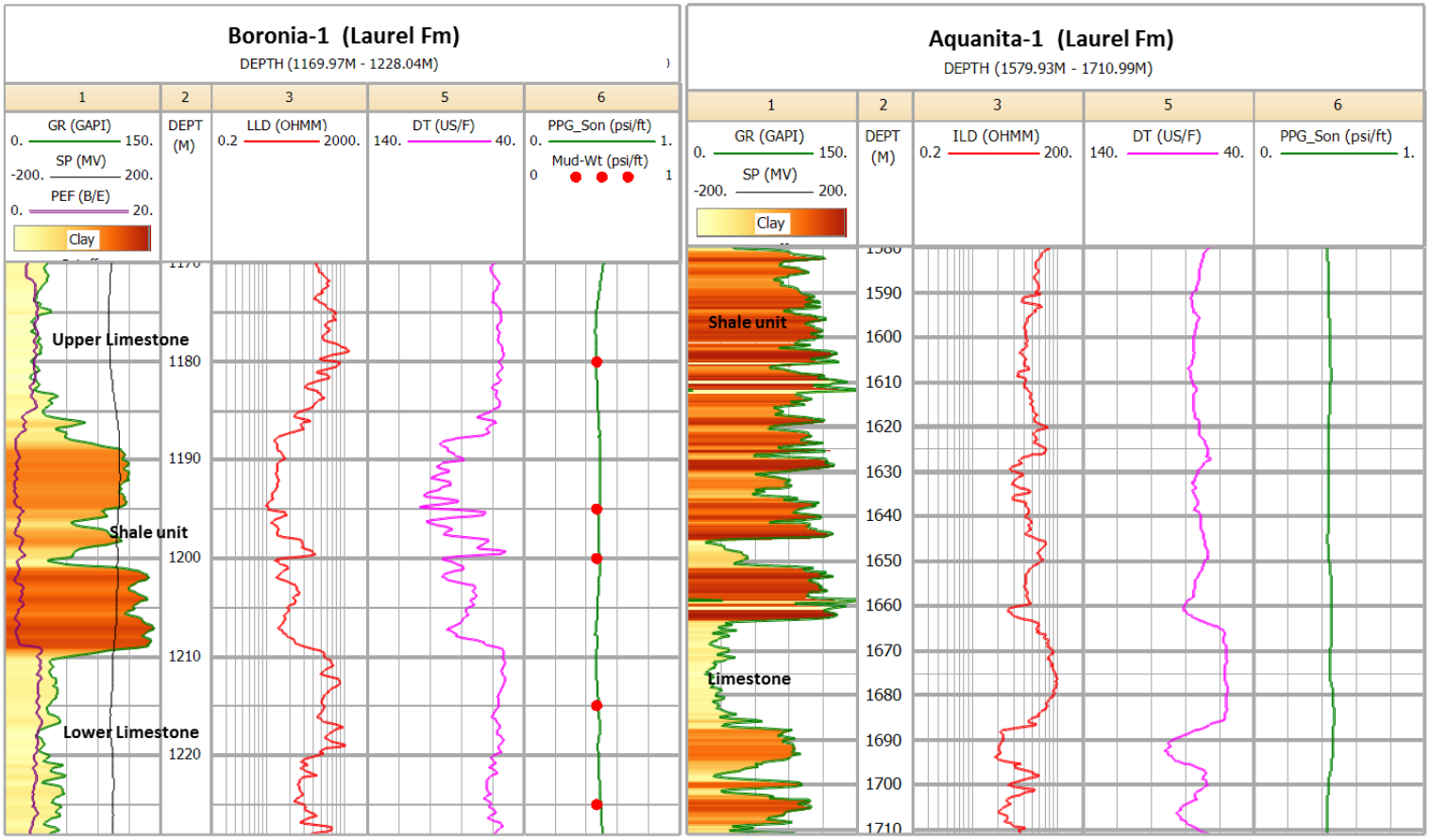

Figure 6-20: Examples of pore pressure profile for the Laurel Formation in the Lennard Shelf (Canning Basin) taken from the Boronia-1 well (left) and Aquanita-1 well (right).

Chapter 7 Discussions, conclusions and recommendations

7.1 Discussions

The significance of pore pressure study for potential gas shale intervals is discussed in Section 7.1.1. The overpressure detection and estimation methods in the shale intervals are discussed in Section 7.1.2. In addition, the relationship between the occurrence and preservation of overpressure in gas shale intervals and the tectonic activities that took place in the Perth and Canning Basins is discussed in Section 7.1.3. Furthermore, the origins of overpressure in the Kockatea Shale of the Perth Basin and the Laurel Formation of the Canning Basin are discussed in Section 7.1.4. The validity of the results is provided within Sections 7.1.2, 7.1.3 and 7.1.4.

7.1.1 Significance of pore pressure study for gas shale intervals

Pore pressure evaluation in sedimentary rocks is not only significant for safe drilling operation and appropriate completion planning, but it is also important for formation evaluation analysis for gas shale intervals. Therefore, it is essential to discuss the reasons why pore pressure study in shales is important.

Several researches concerning pore pressure in sedimentary basins have indicated that the higher the gas saturation in shales, the greater the potential to induce overpressure; resulting in a greater possibility for commercial production (Fertl 1973; Chatellier et al. 2011).

The pore pressure for gas shale intervals is an important factor in the evaluation of the candidate formations. This is mainly when the study of pore pressure is conducted together with other shale parameters such as thermal maturity and total organic content (TOC). A joined study of gas shale characteristics would certainly assist for a better understanding and assessment of the candidate formations. As a result, the shale sweet spots can be identified.

In the Perth and Canning Basins, only a few wells were drilled to evaluate gas shale intervals. As such, pore pressure regimes in these formations are poorly defined. In addition, various parts of the basins have experienced different tectonic activities. These tectonic features include uplifting, erosion and subsidence. More importantly, no previous research has been conducted to study the effects of tectonic activities on pore pressure profiles in shale intervals. As such, this study has addressed this issue

and provided an appropriate correlation. Moreover, as different origins of overpressure have different implications on the direction of future investment and appraisal of gas shale layers, the possible causes of overpressure that have been encountered in the studied formations were extensively examined using a multi-disciplinary approach, building on a methodology that was proposed by previous researchers.

7.1.2 Overpressure detection and estimation

In total, data from 43 and 19 boreholes were evaluated in the Perth and Canning Basins respectively. The Normal Compaction Trend Method (NCT) was implemented to predict the pore pressure of the Perth and Canning Basins in Western Australia. Well log and mud log data were the basis of this study. In general, pore pressure was inferred indirectly using Eaton's method (Equation 4-1) and utilizing the Interactive Petrophysics software. Overpressures were observed by the diversion of the porosity-dependent parameters from their normal trends. These data parameters include sonic transit time, resistivity, porosity and density. Sonic transit time was preferred for pore pressure estimation of shales, mainly due to the fact that it is less affected by bad borehole conditions, as compared to resistivity and density logs.

In addition, drilling, mud log and geochemical data, as well as limited pore pressure measurements, were extensively reviewed for evidence of overpressure. In turn, these data were used to validate the results and replaced the absence of direct pressure measurements such as Repeated Formation Tester (RFT) and Drill Stem Test (DST). In locations where there were diversions of the porosity-dependent parameters from their normal trends, the aforementioned data on these sections showed every indication of overpressure. The obtained overpressure related parameters included: continuous increase in the rate of penetration (ROP), mud weight and gas-while-drilling within these intervals, as well as a reversal in the Ethane isotope. It can also be noted that there were no changes in the other drilling parameters such as weight on bit (WOB), bit and surface rotations (RPM), mud flow rate and mud pump pressure (Figure 5-16).

However, there were some challenges concerning the implementation of the NCT method to estimate pore pressure. These limitations include some lithology complexity in the studied intervals, as well as a lack of regional experience regarding

the evaluation of overpressure in gas shale intervals in this part of the world. Nevertheless, these challenges were resolved by precisely smoothing the data parameters. In addition, Eaton (1975) proposed using an exponent of 3 for Equation 4-1. However, when an exponent of 3 was used, overpressure was overestimated. Since the magnitude of overpressure is relatively low, the exponent was fine-tuned and finally adjusted to 2, which then provided the best match between the predicted overpressure and the pore pressure measurement (Figure 6-3) and other mud log data parameters such as the mud weights (Figures 5-9, 5-13 and 5-15).

7.1.3 Pore pressure and tectonics activities

Within the Perth and Canning Basins, there are different tectonic features such as uplifting, erosion and subsidence. With some maturity data that have become available, it is significant to study the type of pore pressure regime in place for the studied formations and the effects the tectonic features have on pore pressure regimes. Several sets of data were studied to validate the results, so as to formulate the most suitable correlation. These data include well log data, seismic interpretation, conventional core images and structural features of the studied areas.

7.1.3.1 Perth Basin

Investigations on the Perth Basin have characterised the Kockatea Shale in some parts of the Perth basin to be overpressured. On the other hand, like sections in similar formations were found to be normally pressured in other parts of the basin. It can be assumed that the severe uplifting and the subsequent erosion caused by compressional tectonics had great impacts on the pore pressure distribution in the Kockatea Shale (Section 5.4).

Normal pore pressure regimes were observed in the Kockatea Shale in areas that were rigorously uplifted and eroded (Figure 5-26). Uplifting and subsequent erosion due to tectonics compression removed significant portions of the Kockatea Shale in some regions and induced fractures within other areas. This took place in localities within an immediate vicinity of the centres of the two major uplifting and tectonic phases. The first phase of tectonics is an Early Permian phase that created half-grabens that hinge around the Northampton High. The second and more extensive occurred in the Late Jurassic to Early Cretaceous periods. The centre of the second

uplifting phase is near the coastal town of Jurien in the Beagle Ridge, where up to eight kilometres of sections were removed.

Normal pore pressures were observed mainly in wells where the Kockatea Shale was intersected at a shallower depth in localities of the Beagle Ridge, Cadda Terrace and around the Northampton uplift region. Overpressures in these areas may have developed and as a result of the faults and induced fractures which acted as conduits, overpressures were released through. The removal of significant parts of the formation may also have facilitated a re-equilibration of the pore pressure back to the normal condition.

On the other hand, overpressures were observed in the Kockatea mainly in regions where there were less intense tectonic activities; particularly in wells where the Kockatea Shale was intersected at deeper depths. Regions with tectonic activities of less intensity showed an increase in pressure gradients, when moving away from the centre of the uplift (Figure 5-26). The areas where overpressures were observed include the Dandaragan Trough and adjacent terraces that have similar structures. The phenomenon of overpressure has been observed by the diversion of the effective stress-dependent parameters from their normal trends. The top of overpressure zones are the depths where the diversion occurred and overpressures were confirmed by cross-checking the available data such as drilling reports, mud log data and gas geochemistry (Figures 5-7, 5-9, 5-13 and 5-15).

7.1.3.2 Canning Basin

The results obtained from the study that was conducted on the Laurel Formation in the Canning Basin (Chapter 6) confirmed the theory that was established in the Perth Basin. In particular, the study was limited to two main sub-basins, namely the Fitzroy Trough and the Lennard Shelf.

Various data were examined to correlate the findings of the Canning Basin to those obtained from the Perth Basin. These data include structural, well log and geochemical data (Section 6.2).

Comparable to the Perth Basin, the pore pressure profile in the Laurel Formation varies significantly in different areas of the Canning Basin. Overpressure was observed in some regions, while other areas showed trends of normal pore pressure. It is apparent that overpressure has been encountered in the Laurel Formation where there is no evidence of faulting or fractures that have intersected the formation, e.g.

the Yulleroo Anticline (Section 6.2.1). In contrast, normal pore pressure was observed in the Laurel Formation, where the interval is located within the faulted region and the formation was intersected by faulting systems, e.g. St George Range Anticline (Section 6.2.2). The faulting and induced fractures could possibly had effects on the geological environment that would have otherwise led to a preservation of the possibly generated overpressure due to various generating mechanisms.

Although the maturity of the rocks is quite significant in generating hydrocarbons, that could possibly lead to overpressure development for the Laurel Formation in the St George Range and Christmas Creek Anticlines (Sections 6.2.2.3 and 6.2.2.4), maintaining overpressure involves variables such as the local tectonics and structural elements. These features are very important in constraining overpressure within the shales. Otherwise, it will be disseminated to the surrounding sediments. More importantly, it is obvious that the effects of tectonic elements are similar in the Perth and Canning Basins as the research has observed the same phenomenon in both basins. As such, this philosophy can seemingly be universalized.

7.1.4 Overpressure generating mechanisms

Overpressure was observed within the two studied formations in certain regions of the Perth and Canning Basins. However, different origins of overpressure exist for each of the studied formations. Interpretations are first provided for each basin, before the comparison and contrasting points are highlighted.

7.1.4.1 Perth Basin

There is clear evidence that the overpressure generating mechanisms in the Kockatea Shale are fluid expansion and lateral tectonic compression. Amongst the fluid expansion mechanisms, there are two potential mechanisms, namely the clay diagenesis and hydrocarbon generation. Among the clay diagenesis processes, the transformation of smectite to illite or mixed-layer (illite-smectite) seems to be dominant. This claim has been determined from the analysis of results, obtained from the wireline log responses, Sonic-Density Cross-plots, X-Ray Diffraction and Natural Gamma Ray Spectrometry logs (NGS) and the complicated geology of the Perth Basin (Section 5.5). However, since the normally pressured regions also exhibited high maturity capable for hydrocarbon generation as shown in Figure 5-39, the

hydrocarbon generating mechanism may be ruled out as a major cause of overpressure. It may however, have had insignificant contributions in the pore pressure build-up.

The shale in Figure 5-35 is of depth and temperature that is likely for the smectite to be mostly transformed to illite. From the figure, it is apparent that points with higher differences between neutron porosity and density porosity fall farther away from the smectite - rich trend. It has been observed that as depth increases, the difference between neutron porosity and density porosity increases, while the ratio of smectite to illite decreases. Therefore, there is an increase in the pore pressure gradients (unloading increase). Although there are a few data points where the difference of neutron porosity - density porosity approaches the smectite rich trend (the ratio of smectite to illite increases), these data are not representative of the whole shale interval, but rather, correspond solely to the inter-bedded sandstone sections within the Kockatea Shale. The present-day pressure of the upper section of Kockatea Shale exhibits normal pressure gradients. Overpressure in this section may have been developed and then released, due to the high permeability of the overlaying Woodada sandstone sections, which have not allowed overpressures to be preserved within the shales (Figure 2-5). Additionally, this stratigraphical sequence suggests that overpressure have been generated internally (clay transformation). The system may have been pressurized and then re-equilibrated back to the normal conditions. Incomplete clay transformations could be a possible explanation to the normal pore pressure in the upper section of the Kockatea Shale.

In fact, clay transformation from smectite to illite is not considered to be a significant mechanism that produces high magnitudes of overpressure (Osborne and Swarbrick 1997). This is as the maximum volume changes between interlayer and intergranular water increase the volume of intergranular water by an insignificant amount. In addition, the overpressure identified in the Kockatea Shale is noticeably high as noticed from the reversal of the vertical effective stress (Figure 5-34). As such, the clay transformation mechanism could be combined with other overpressure generating mechanisms.

Moreover, the later tectonic loading is also believed to have a significant role in the overpressure generation. This belief has been derived from analysing the complicated geology of the study area, in conjunction with the trajectory of the principal stress (S_{hmax}) and combined with the analysis of well log data responses and the high

magnitude of overpressure that caused a reversal in the vertical effective stress. The reasoning for the above derivation are: (1) the forces induced by the principal stress (S_{hmax}) which act in a horizontal plane east-west perpendicular to the main north-south and northwest-southeast faults trends (Figure 2-4) and (2) the positions and trends of the main faults and the main transfer faults, provided efficient lateral seals for the developed overpressure in the Kockatea Shale. The lateral tectonics explains the observed high magnitude of overpressure as the diagenesis effects cannot produce high overpressure. Lateral tectonics compression would have allowed the vertical effective stress to be reversed and the density log to change slightly or remain reasonably at a constant value because compaction is not reversible. Additionally, lateral tectonics causes an increase in neutron porosity (Figure 5-34).

With the available data, it is tricky to deduce whether the lateral tectonic compression, clay transformation or hydrocarbon generation is the major overpressure generating mechanism contributing to the development of overpressure in the Kockatea Shale. However, all aforementioned processes have contributed at different extents to overpressure development, with the lateral tectonic compression and clay transformation processes being the most prevalent. Therefore, more investigations are required to ascertain whether clay transformation or lateral compression was the primary mechanism for generating overpressure.

7.1.4.2 Canning Basin

The results suggest that the prime origin of overpressure that was observed in the Laurel Formation is the Loading Mechanism (under-compaction), with hydrocarbon generation being a secondary mechanism.

Figures 6-3 and 6-4 comprise of clear evidence of under-compaction. As clearly seen, there was no reversal in the sonic transit time, density logs as well as the vertical effective stress. These parameters remained fairly constant in the overpressure section of the Laurel Formation. However, the under-compaction alone cannot cause high magnitudes of overpressure as the DST data point shows 0.6 psi/ ft. As such, it was mandatory to examine other possible causes of overpressure. It was observed that the hydrocarbon generation may have caused the high overpressure. The maturity data of the Laurel Formation is within the gas generation window (Figure 6-11).

In addition, Figures 6-12 and 6-13 constitute clear evidence of over maturity of the Laurel Formation for gas generation, particularly the cracking of Ethane and higher hydrocarbons, to the extent that the friction of the light hydrocarbon (i.e. methane) is reduced.

Hence, it seems that the gas generation mechanism is a secondary mechanism for generating overpressure in the Laurel Formation. This deduction is due to the response of vertical effective stress to overpressure (Figure 6-4). If gas generation was meant to be the prime overpressure mechanism, the vertical effective stress would have been reversed. Instead, it remained fairly constant within the overpressure section of the Laurel Formation.

In an attempt to examine whether clay transformation processes contributed to overpressure build-up, the mineralogical composition was examined through XRD analysis. The observations indicate that clay transformation can be ruled out as a possible cause for overpressure generation. Detailed interpretation for this analysis is provided in Section 6.2.1.3.

7.1.4.3 Comparison and contrasting of the basins

A few contrasting points can be made in relation to overpressure generating mechanisms in the Kockatea Shale (Perth Basin) and the Laurel Formation (Canning Basin). Firstly, the isotope responses to overpressure differ between the Kockatea Shale and the Laurel Formation. In the Kockatea Shale, the isotope deviated from its normal trend in the overpressure section and returned to normal trend below the charged zone, but there was no reversal (Figure 5-7). This is attributed to the fact that gas generation is not considered as a major mechanism for overpressure generation. On the other hand, the response of isotope to overpressure in the Laurel Formation showed a clear reversal in the overpressured zone (Figure 6-7). This is due to the significant contribution of gas generation to overpressure development in the Canning Basin. The mineralogical analysis showed some discrepancy. The illite clay is the principal clay in the Kockatea Shale (Perth Basin) (Tables 5-2 and 5-3), whilst the smectite clay is still considered as the major clay elements in the Laurel Formation (Canning Basin) (Table 6-1). Furthermore, the responses of the vertical effective stress in the Kockatea Shale differ from the Laurel Formation. In the Kockatea Shale, there was a reversal, whereas in the Laurel Formation, it remained fairly constant.

7.2 Conclusions

Several sets of data were analysed to conduct a comprehensive pore pressure study on two potential gas shale intervals in the Perth and Canning Basins. Different aspects of pore pressure, as well as the influences of structural elements and tectonic on pore pressure distribution were examined. The following points can be concluded from the results of this research:

1. Normal pore pressure profiles were observed in the Kockatea Shale of the Perth Basin in areas that have been rigorously uplifted, eroded and where there were severe tectonic activities. Uplifting and erosion due to tectonics compression removed significant portions of the Kockatea Shale in some areas and induced fractures in others. The removal of significant parts of the formation, as well as the induced faulting and fractures, have acted as communication channels and facilitated a re-equilibration of the pore pressure back to the normal condition.
2. Overpressures were observed in the Kockatea, mainly in areas where there were less intense tectonic activities and the intersections of the formation were at deeper depths. Regions with tectonic activities of less intensity showed an increase in pressure gradients as approaching away from the centres of the two major uplifting phases. The top depth of the overpressure zone is linearly related to the top depth of the Kockatea Shale.
3. There is a great correlation between the occurrence and preservation of overpressure and the local tectonic and structural elements. The faulting and fracture-induced tectonics would have prevented the pressure build-up or facilitated re-equilibrium to normal pressure. The severe tectonic activities are responsible for most of the major structural features of the Perth Basin and the distribution of pore pressure in the basin.
4. The occurrence of overpressures in the Kockatea Shale that were buried to deeper depths and the analysis of data suggest that the built-up overpressure is due to a number of mechanisms.
5. The overpressures in the lower section of the Kockatea Shale were developed internally due to the dehydration of the shale. It was mainly due to the

transformation of smectite clay to illite and mixed layer clay (smectite-illite). This conclusion was reached by analysing well logs, clay compositional variations and the stratigraphical sequence. On the other hand, the upper section of the Kockatea Shale showed normal pressure profile as a result of either incomplete clay transformations or overpressures that were initially developed and then re-equilibrated back to the normal conditions, through overlaying high permeability Woodada sandstone. The permeable Woodada Formation did not allow overpressure to develop and thus normal pressure was maintained in the upper section of the Kockatea shale. The thick overpressured shale intervals exhibit systematic variations of smectite to illite percentages as well as the relationships between neutron porosity-density porosity differences (Figure 5-35).

6. The principal stress direction and the complicated structure of northern Perth Basin indicate that the lateral tectonics compression mechanism has associated with the clay transformation mechanism. The main reasons for this claim are: (i) the forces induced by the principal stress (S_{hmax}) act in a horizontal plane east west, perpendicular to the main north-south and northwest-southeast faults trends, (ii) the positions and trends of the main faults and main transfer faults provided efficient lateral seals for the developed overpressure in the Kockatea Shale and (iii) the observed high magnitude of overpressure suggests that the lateral tectonics compression has contributed significantly to overpressure development, as the diagenesis effects cannot produce high overpressure.
7. Similar to the Kockatea Shale (Perth Basin), the pore pressure profile in the Laurel Formation varies significantly in different areas of the Canning Basin. Overpressure was observed in some regions and other areas showed normal trends of pore pressure regimes.
8. Normal pore pressure was observed in the Laurel Formation, where the interval is located within the faulted region and the formation was intersected by faulting systems, e.g. St George Range Anticline. On the other hand, overpressure was encountered in the Laurel Formation, where there is no evidence of faulting or fractures that have intersected the formation, e.g. the Yulleroo Anticline.

9. The faulting and fracture-induced tectonics have affected the geological environment as alternatively, there would be a preservation of the possibly generated overpressure due to various generating mechanisms.
10. It is obvious that the effects of tectonic elements are similar in the Perth and Canning Basins, as this study has observed the same phenomenon in both basins. As such, there is a great possibility to generalize this philosophy.
11. Although the maturity of the rocks is quite significant in generating hydrocarbons (that could possibly lead to overpressure development in shale gas reservoirs), maintaining overpressure is a function of variables such as the local tectonics and structural elements. These features are very important in constraining overpressure within the shales. Otherwise, it will be disseminated to the surrounding sediments.
12. The prime origin of overpressure observed in the Canning Basin is under-compaction, with hydrocarbon generation being a secondary mechanism.

7.3 Recommendations for future researches

1- Study the tectonic stress in the study areas and examine whether or not the same stress regime has been existed over the long geological times and correlate that to sealing properties of the bounding faults.
2- Investigate the timing of overpressuring and its relations with faulting and fault sealing behaviour over the geological time and compare the timing of overpressuring with the timing of faulting
3- Since not all faults and fractures will be leaking, it is recommended to assess fault sealing from both juxtaposition and geomechanical aspects.

References

Alixant, J.-L. and R. Desbrandes (1991). "Explicit Pore-Pressure Evaluation: Concept and Application." SPE Drilling Engineering **6**(3).

Alixant, J.-L. and R. Desbrandes (1991). "Explicit pore-pressure evaluation: Concept and application." SPE Drilling Engineering **6**(03): 182-188.

Apak, S. N. and G. Carlsen (1997). A compilation and review of data pertaining to the hydrocarbon prospectivity in the Canning Basin, Geological Survey of Western Australia, Department of Minerals and Energy.

Arne, D., P. Green, et al. (1989). "Regional thermal history of the Lennard shelf, Canning Basin, from apatite fission track analysis: Implications for the formation of Pb-Zn ore deposits." Australian Journal of Earth Sciences **36**(4): 495-513.

Athy, L. F. (1930). "Density, porosity, and compaction of sedimentary rocks." AAPG bulletin **14**(1): 1-24.

Bengtson, C. (1981). "Statistical curvature analysis techniques for structural interpretation of dipmeter data." AAPG Bulletin **65**(2): 312-332.

Bigelow, E. (1994). "Well logging methods to detect abnormal pressure." Developments in Petroleum Science **38**: 187-187.

Bischoff, G. (1968). "Online Systems - Petroleum and Geothermal Information (WAPIMS), Well Completion Report, Yulleroo-1 , Government of Western Australia."

Bois, M., Y. Grosjean, et al. (1994). "Shale compaction and abnormal pressure evaluation application to the offshore Mahakam."

Boles, J. R. and S. G. Franks (1979). "Clay diagenesis in Wilcox sandstones of southwest Texas: implications of smectite diagenesis on sandstone cementation." Journal of Sedimentary Research **49**(1).

Bowers, G. (1995). "Pore pressure estimation from velocity data: Accounting for overpressure mechanisms besides undercompaction." SPE Drilling & Completion **10**(2): 89-95.

Bowers, G. and T. J. Katsube (2002). "The role of shale pore structure on the sensitivity of wire-line logs to overpressure." MEMOIRS-AMERICAN ASSOCIATION OF PETROLEUM GEOLOGISTS: 43-60.

Bowers, G. L. (2002). "Detecting high overpressure." The Leading Edge **21**(2): 174-177.

Bridge, O. (1985). Online Systems - Petroleum and Geothermal Information (WAPIMS), Well Completion Report, East Yeeda-1, Government of Western Australia

Brown, S., I. Boserio, et al. (1984). The geological evolution of the Canning Basin—implications for petroleum exploration. The Canning Basin, WA: Proceedings of the Geological Society of Australia and the Petroleum Exploration Society of Australia, Canning Basin Symposium, Perth Western Australia.

Buick, I., A. Storkey, et al. (2008). "Timing relationships between pegmatite emplacement, metamorphism and deformation during the intra-plate Alice Springs Orogeny, central Australia." Journal of Metamorphic Geology **26**(9): 915-936.

Cadman, S., L. Pain, et al. (1994). Perth Basin, Western Australia, Department of Primary Industries and Energy, Bureau of Resources Sciences.

Cadman, S., L. Pain, et al. (1993). "Canning Basin." Western Australia: Australian Petroleum Accumulations Report **9**: 81.

Cadman, S., V. Vuckovic, et al. (1993). Australian Petroleum Accumulation Report 9-Canning Basin, WA, Petroleum Resource Branch, Department of Primary Industries and Energy.

Cadman, S. J., Pain, L. and Vuckovi V. (1994). Perth Basin, W.A., Australian Petroleum Accumulations Report 10, Bureau of Resource Sciences, Canberra.

Cadman, S. P., L Vuckovic, V le Poidevin, SR (1993). Canning Basin, WA, Bureau of Resource Sciences.

Carey, S. (1976). The expanding Earth: developments in geotectonics, vol. 10, Amsterdam: Elsevier.

Chatellier, J., K. Ferworn, et al. (2011). Overpressure in shale gas—When geochemistry and engineering data meet and agree: AAPG, Search and Discovery Article# 40767 Adapted from an oral presentation including slides, Houston Texas, June 30, 2011.

Cheng, C. H. and M. N. Toksöz (1979). "Inversion of seismic velocities for the pore aspect ratio spectrum of a rock." Journal of Geophysical Research: Solid Earth (1978–2012) **84**(B13): 7533-7543.

Colten-Bradley, V. A. (1987). "Role of pressure in smectite dehydration--effects on geopressure and smectite-to-illite transformation." AAPG Bulletin **71**(11): 1414-1427.

Condon, M. A. and J. N. Casey (1958). "Alternative Interpretation of Fenton and Pinnacle Faults." Bureau of Minerals and Resources Australia **Bulk 36 Appendix IV**.

Crostella, A. (1995). An evaluation of the hydrocarbon potential of the onshore northern Perth Basin, Western Australia, Geological Survey of Western Australia.

Crostella, A. (1998). A review of oil occurrences within the Lennard Shelf, Canning Basin, Western Australia, Geological Survey of Western Australia.

Crostella, A. and J. Backhouse (2000). Geology and petroleum exploration of the central and southern Perth Basin, Western Australia, Geological Survey of Western Australia.

Curtis, J. B. (2002). "Fractured shale-gas systems." AAPG bulletin **86**(11): 1921-1938.

D'Ercole, C., A. J. Mory, et al. (2003). Leads and prospects within tenements of the Northern Perth Basin Western Australia, 2002, Geological Survey of Western Australia.

D'Ercole, C. (2003). The rejuvenation of the northern Perth Basin. GSWA 2003 SEMINAR Extended abstracts.

Devilliers, M. and P. Werner (1990). "Example of fault identification using dipmeter data." Geological Society, London, Special Publications **48**(1): 287-295.

DICKINSON, G. n. (1951). Geological aspects of abnormal reservoir pressures in the Gulf Coast region of Louisiana, USA. 3rd World Petroleum Congress.

DMP-WA (2013). "Online Systems - Petroleum and Geothermal Information (WAPIMS), Well Completion Report, Cadda No.1, Government of Western Australia." Retrieved 15 Feb, 2014, from http://dmp.wa.gov.au/.

DMP-WA (2012). "Online Systems - Petroleum and Geothermal Information (WAPIMS), Well Completion Report, Government of Western Australia." Retrieved 15 Feb, 2014, from http://dmp.wa.gov.au/.

DMP (2014). "Natural Gas from Shale and Tight Rocks - An overview of Western Australia's regulatory framework." Retrieved 02 Jan, 2015, from http://www.dmp.wa.gov.au/documents/Natural_Gas_from_Shale_and_Tight_Rocks_-_An_overview_of_Western_Australia_regulatory_framework.pdf.

DMPa (2014). Summary of Petroleum Prospectivity: Canning Basin. Government of Western Australia, Department of Mines and Petroleum, Petroleum Division.

Dorling, S., D. Groves, et al. (1998). "Lennard Shelf Mississippi Valley-type (MVT) Pb-Zn deposits, Western Australia." AGSO Journal of Australian Geology and Geophysics **17**: 115-120.

Draou, A. and S. O. Osisanya (2000). New Methods for Estimating of Formation Pressures and Fracture Gradients from Well Logs. SPE Annual Technical Conference and Exhibition. Dallas, Texas.

Druce, E. C. and B. Radke (1979). The geology of the Fairfield Group, Canning Basin, Western Australia, Australian Government Pub. Service.

Dutta, N. (2002). "Deepwater geohazard prediction using prestack inversion of large offset P-wave data and rock model." The Leading Edge **21**(2): 193-198.

Eaton, B. (1975). The equation for geopressure prediction from well logs. Fall Meeting of the Society of Petroleum Engineers of AIME.

Eaton, B. A. (1975). The Equation for Geopressure Prediction from Well Logs. Fall Meeting of the Society of Petroleum Engineers of AIME. Dallas, Texas.

Ellyard, E. J. (1982). Online Systems - Petroleum and Geothermal Information (WAPIMS), Well Completion Report, Boronia -1, Government of Western Australia, from http://dmp.wa.gov.au/

Ellyard, E. J. (1983). Online Systems - Petroleum and Geothermal Information (WAPIMS), Well Completion Report, Cycas -1, Government of Western Australia, from http://dmp.wa.gov.au/.

Fertl, W. and D. Timko (1971). Parameters for identification of overpressure formations. Drilling and Rock Mechanics Conference.

Fertl, W. H. (1973). Significance of shale gas as an indicator of abnormal pressures. SPE Drilling and Rock Mechanics Conference, Society of Petroleum Engineers.

Fertl, W. H. (1979). "Gamma ray spectral data assists in complex formation evaluation." Log Anal.;(United States) **20**(5).

Ferworn, K., J. Zumberge, et al. (2008). "Gas character anomalies found in highly productive shale gas wells." Technical presentation, GeoMark Research, Houston.

Forman, D. J. (1981). Geological evolution of the Canning Basin, Western Australia.

Forman, D. J., D. W. Wales, et al. (1981). Geological Evolution of the Canning Basin, Western Australia. Bureau of Mineral Resources., Australian Government Pub. Service.

Gardner, G., L. Gardner, et al. (1974). "Formation velocity and density-the diagnostic basics for stratigraphic traps." Geophysics **39**(6): 770-780.

GeoscienceAustralia (2003). "Oil and Gas Resources of Australia 2003." Geoscience Australia, http://www.ga.gov.au/products-services/publications/oil-gas-resources-australia/2003.html#a.

Gretener, P. E. (1979). Pore Pressure: fundementals, general, ramifications, and implications for structural geology (revised). Oklohoma, AAPG

Guppy, D. J. (1958). The geology of the Fitzroy Basin, Western Australia, Department of National Development, Bureau of Mineral Resources, Geology and Geophysics.

Haines, P. (2004). "Depositional facies and regional correlations of the Ordovician Goldwyer and Nita Formations." Canning Basin, Western Australia, with implications for petroleum exploration: Geological Survey of Western Australia, Record **7**.

Hall, R. L. (1989). "Lower Bajocian ammonites (Middle Jurassic; Soninniidae) from the Newmarracarra Limestone, Western Australia." Alcheringa **13**(1): 1-20.

Hansom, J. and M.-K. Lee (2005). "Effects of hydrocarbon generation, basal heat flow and sediment compaction on overpressure development: a numerical study." Petroleum Geoscience **11**(4): 353-360.

Harris, L. (1994). "Structural and tectonic synthesis for the Perth Basin, Western Australia." Journal of Petroleum Geology **17**(2): 129-156.

Haworth, J. (2013). US Gas industry a learning opportunity for Western Australia. Petroleum and Geothermal Petroleum Division. Petroleum in Western Australia, Western Australia's digests of petroleum exploration, development and production, 7.

Hermanrud, C., L. Wensaas, et al. (1998). "Memoir 70, Chapter 4: Shale Porosities from Well Logs on Haltenbanken (Offshore Mid-Norway) Show No Influence of Overpressuring

".

Hillis, R. R. and S. D. Reynolds (2000). "The Australian stress map." Journal of the Geological Society **157**(5): 915-921.

Holditch, S., Ayers, WB., McVay, DA., Lee, JW., Bickley, JA., Blasingame, TA., Perry, KF (2007). "Topic paper# 29." National Petroleum Council Unconventional Gas Subgroup of the Technology Task Group of the NPC Committee on Global Oil and Gas.

Holditch, S. A. (2006). "Tight gas sands." Journal of Petroleum Technology **58**(6): 86-93.

HOWER, J., E. V. ESLINGER, et al. (1976). "Mechanism of burial metamorphism of argillaceous sediment: 1. Mineralogical and chemical evidence." Geological Society of America Bulletin **87**(5): 725-737.

Iasky, R. and A. Mory (1993). "Structural and tectonic framework of the onshore northern Perth Basin." Exploration Geophysics **24**(3/4): 585-592.

Iasky, R. and A. Mory (1994). "Structural and tectonic framework of the Onshore Northern Perth Basin." Exploration Geophysics **24**(4): 585-592.

Jarvie, D. M., R. J. Hill, et al. (2007). "Unconventional shale-gas systems: The Mississippian Barnett Shale of north-central Texas as one model for thermogenic shale-gas assessment." AAPG Bulletin **91**(4): 475-499.

Jonasson, Karina E Ellis, et al. (2001). Western Australia Atlas of Petroleum Fields: Onshore Canning Basin, Department of Minerals and Energy WA Petroleum Division.

Jonasson, K. E. (2001). Western Australia Atlas of Petroleum Fields, Onshore Canning Basin, Petroleum Division, Mineral and Petroleum Resources Western Australia.

Jones, D. and G. Pearson (1972). "The tectonic elements of the Perth Basin." APEA Journal **12**(1): 17-22.

Jorden, J. and O. Shirley (1966). "Application of drilling performance data to overpressure detection." Journal of Petroleum Technology **18**(11): 1387-1394.

Katahara, K. (2008). "What is shale to a petrophysicist?" The Leading Edge **27**(6): 738-741.

Kawata, Y. and K. Fujita (2001). Some predictions of possible unconventional hydrocarbons availability until 2100. SPE Asia Pacific Oil and Gas Conference and Exhibition, Society of Petroleum Engineers.

Khaksar, A. and C. Griffiths (1996). Influence of effective stress on the acoustic velocity and log derived porosity. SPE Asia Pacific Oil and Gas Conference, Society of Petroleum Engineers.

King, R. C., R. R. Hillis, et al. (2008). "In situ stresses and natural fractures in the Northern Perth Basin, Australia." Australian Journal of Earth Sciences **55**(5): 685-701.

Kuuskraa, V. A. and S. H. Stevens (2009). "Worldwide gas shales and unconventional gas: A status report." American Clean Skies Foundation (ACSF), and the Research Partnership to Secure Energy for America (RPSEA).

Lesso, J. W. G. and T. M. Burgess (1986). Pore Pressure and Porosity From MWD Measurements. SPE/IADC Drilling Conference. Dallas, Texas.

Lewis, C. R. and S. Rose (1970). "A theory relating high temperatures and overpressures." Journal of Petroleum Technology **22**(1): 11-16.

Luo, X. and G. Vasseur (1992). "Contributions of Compaction and Aquathermal Pressuring to Geopressure and the Influence of Environmental Conditions (1)." AAPG bulletin **76**(10): 1550-1559.

Magoon, L. B. (1988). "The petroleum system—a classification scheme for research, exploration, and resource assessment." Petroleum systems of the United States: US Geological Survey Bulletin **1870**: 2-15.

McCarthy, K., K. Rojas, et al. (2011). "Basic petroleum geochemistry for source rock evaluation." Oilfield Review **23**(2): 32-43.

McWhae, J. R. H., P. Playford, et al. (1956). "The stratigraphy of western Australia." Journal of the Geological Society of Australia **4**(2): 1-153.

Medlock, K. B., A. M. Jaffe, et al. (2011). Shale gas and US national security, James A. Baker III Institute for Public Policy of Rice University.

Middleton, M. F. (1991). "Seismic stratigraphy, structural analysis, and tectonic evolution of the northern Canning Basin, Western Australia." Western Australia Geological Survey **5**: 70.

Miller, T. W. (1995). "New insights on natural hydraulic fractures induced by abnormally high pore pressures." AAPG bulletin **79**(7): 1005-1018.

Mory, A., D. Haig, et al. (2005). "Geology of the northern Perth Basin, Western Australia—a field guide." Geological Survey of Western Australia Record **2005**: 9.

Mory, A. J. and R. P. Iasky (1996). Stratigraphy and structure of the onshore northern Perth Basin, Western Australia, Geological Survey of Western Australia.

Mouchet, J.-P. and A. F. Mitchell (1989). Abnormal Pressures While Drilling: Origins, Prediction, Detection, Evaluation, Editions Technip.

Muir, W. (2013). "Shale Gas In Australia, Drivers And Roadblocks." Retrieved 24/06, 2013, from http://www.pnronline.com.au/article.php/99/1234.

Naik, G. (2003). "Tight Gas Reservoirs–An Unconventional Natural Energy Source for the Future." www. sublette-se. org/files/tight_gas. pdf. Accessado em **1**(07): 2008.

Osborne, M. J. and R. E. Swarbrick (1997). "Mechanisms for generating overpressure in sedimentary basins: a reevaluation." AAPG Bulletin **81**(6): 1023-1041.

Owad-Jones, D. and G. Ellis (2000). Western Australia atlas of petroleum fields. Onshore Perth Basin, Department of Minerals and Energy, Petroleum Division Perth. **1**.

Passmore, V. (1991). "Promising hydrocarbon potential seen in Canning Basin off Australia." Oil and Gas Journal;(United States) **89**(34).

Pikington, P. E. (1988). "Uses of Pressure and Temperature Data in Exploration and Now Developments in Overpressure Detection." SPE Journal of Petroleum Technology **40**(5).

Playford, P. E. (1989). "Reefal platform development, Devonian of the Canning Basin, western Australia."

Playford, P. E., A. E. Cockbain, et al. (1976). Geology of the Perth Basin, Western Australia, Geological Survey of Western Australia Perth.

Powell, D. (1976). "The geological evolution of the continental margin off northwest Australia." APEA J **16**(1): 13-23.

Quaife, R., J. Rosser, et al. (1994). The structural architecture and stratigraphy of the offshore northern Perth Basin. The Sedimentary Basins of Western Australia: Proceedings of the Petroleum Exploration Society of Australia Symposium, Perth.

Ramdhan, A. M. (2010). Overpressure and compaction in the lower Kutai Basin, Indonesia, Durham University.

Ratner, M. and M. Tiemann (2013). "An overview of unconventional oil and natural gas: resources and federal actions." Congressional Services Report.

Read, S. M., PJ (1991). Classification of New Zealand soft sedimentary rock materials. 7th ISRM Congress, International Society for Rock Mechanics.

Rogner, H.-H. (1997). "An assessment of world hydrocarbon resources." Annual review of energy and the environment **22**(1): 217-262.

Rubey, W. W. and M. K. Hubbert (1959). "Role of fluid pressure in mechanics of overthrust faulting II. Overthrust belt in geosynclinal area of western Wyoming in light of fluid-pressure hypothesis." Geological Society of America Bulletin **70**(2): 167-206.

Schenk, C. J. (2004). "Geologic Definition and Resource Assessment of Continuous (Unconventional) Gas Accumulations—the US Experience." Website, http://aapg. confex. com/aapg/cairo2002/techprogram/paper—66806. htm, printed Nov **16**: 1.

Schmoker, J. W. (1995). "Method for assessing continuous-type (unconventional) hydrocarbon accumulations." DL Gautier, GL Dolton, KI Takahashi, and KL Varnes, eds **1995**.

Schmoker, J. W. and T. R. Klett (1999). US Geological Survey Assessment Model for Undiscovered Conventional Oil, Gas, and NGL Resources--the Seventh Approximation, US Department of the Interior, US Geological Survey.

Scott, J. (1991). "The occurrence of oil-prone source rocks in continental half grabens: APEA Journal, v. 18."

Shannon, P. H. and S. W. Henderson (1966). Online Systems - Petroleum and Geothermal Information (WAPIMS), Well Completion Report, St George Range-1 , Government of Western Australia." Retrieved 27 March, 2014, from http://dmp.wa.gov.au/.

Song, T. and P. A. Cawood (2000). "Structural styles in the Perth Basin associated with the Mesozoic break-up of Greater India and Australia." Tectonophysics **317**(1): 55-72.

Song, T. and P. A. Cawood (2000). "Structural styles in the Perth Basin associated with the Mesozoic break-up of Greater India and Australia." Tectonophysics **317**(1–2): 55-72.

Tanguy, D. R. and W. A. Zoeller (1981). APPLICATIONS OF MEASUREMENTS WHILE DRILLING. SPE Annual Technical Conference and Exhibition. San Antonio, Texas.

Terzaghi, K., R. B. Peck, et al. (1996). Soil mechanics in engineering practice, Wiley-Interscience.

Thomas, B. (1979). "Geochemical analysis of hydrocarbon occurrences in northern Perth Basin, Australia." AAPG Bulletin **63**(7): 1092-1107.

Tingay, M. R. P., R. R. Hillis, et al. (2003). "Variation in vertical stress in the Baram Basin, Brunei: tectonic and geomechanical implications." Marine and Petroleum Geology **20**(10): 1201-1212.

Towner, R. R. and D. L. Gibson (1983). Geology of the onshore Canning Basin, Western Australia, Australian Government Pub. Service.

Van Ruth, P., R. Hillis, et al. (2003). "The origin of overpressure in 'old' sedimentary basins: an example from the Cooper Basin, Australia." Geofluids **3**(2): 125-131.

Varma, R. S. (2002). "Clay and clay-supported reagents in organic synthesis." Tetrahedron **58**(7): 1235-1255.

Veevers, J. J. and A. T. Wells (1961). The geology of the Canning basin, Western Australia, Bureau of Mineral Resources, Geology and Geophysics.

Wallace, W. E. (1965). "Abnormal Subsurface Pressures Measured From Conductivity Or Resistivity Logs." The Log Analyst **V**(4).

Watts, E. (1948). "Some Aspects of High Pressures in the D-7 Zone of the Ventura." Transactions of the AIME **174**(01): 191-205.

Yeates, A., D. Gibson, et al. (1984). Regional geology of the onshore Canning Basin, WA. The Canning Basin, WA Proceedings of the Geological Society of Australia & Petroleum Exploration Society of Australia Symposium, Perth.

'Every reasonable effort has been made to acknowledge the owners of all copyright material. I would be pleased to hear from any copyright owner who has been omitted or incorrectly acknowledged.'

Appendices

Appendix **1 Perth Basin**

Appendix 1a Pressure-depth plots, well lo data and cross-plots for the wells that exhibited overpressure in the Kockatea Shale and drilled in the locality of Dandaragan Trough & Adjacent terraces

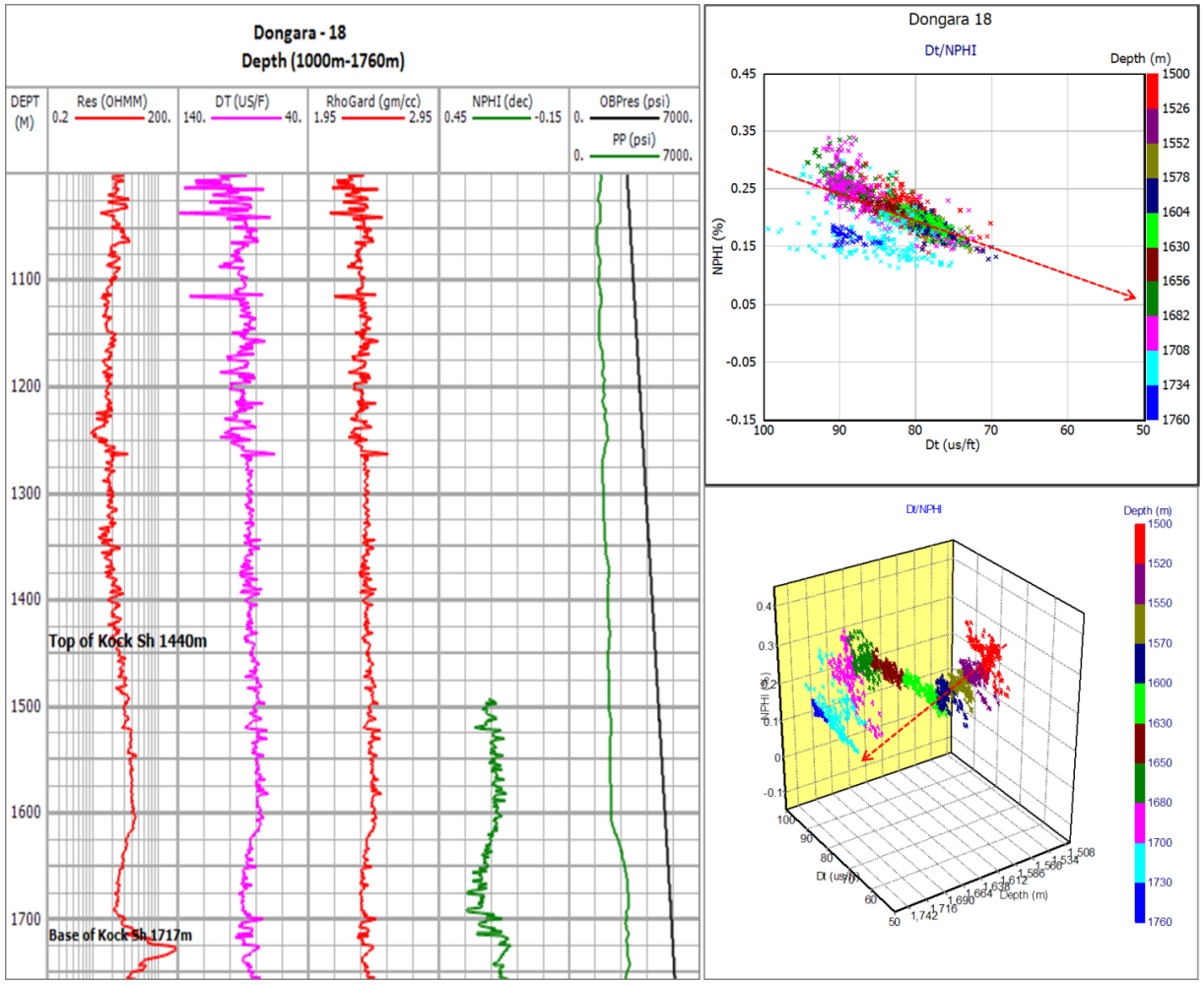
Dongara - 18
Depth (1000m-1760m)
DEPT (M)
Res (OHMM) 0.2 200.
DT (US/F) 140. 40.
RhoGard (gm/cc) 1.95 2.95
NPHI (dec) 0.45 -0.15
OBPres (psi) 0. 7000.
PP (psi) 0. 7000.
1100
1200
1300
1400
1500
1600
1700
Top of Kock Sh 1440m
Base of Kock Sh 1717m
Dongara 18
Dt/NPHI
Depth (m)
NPHI (%)
Dt (us/ft)
Depth (m)

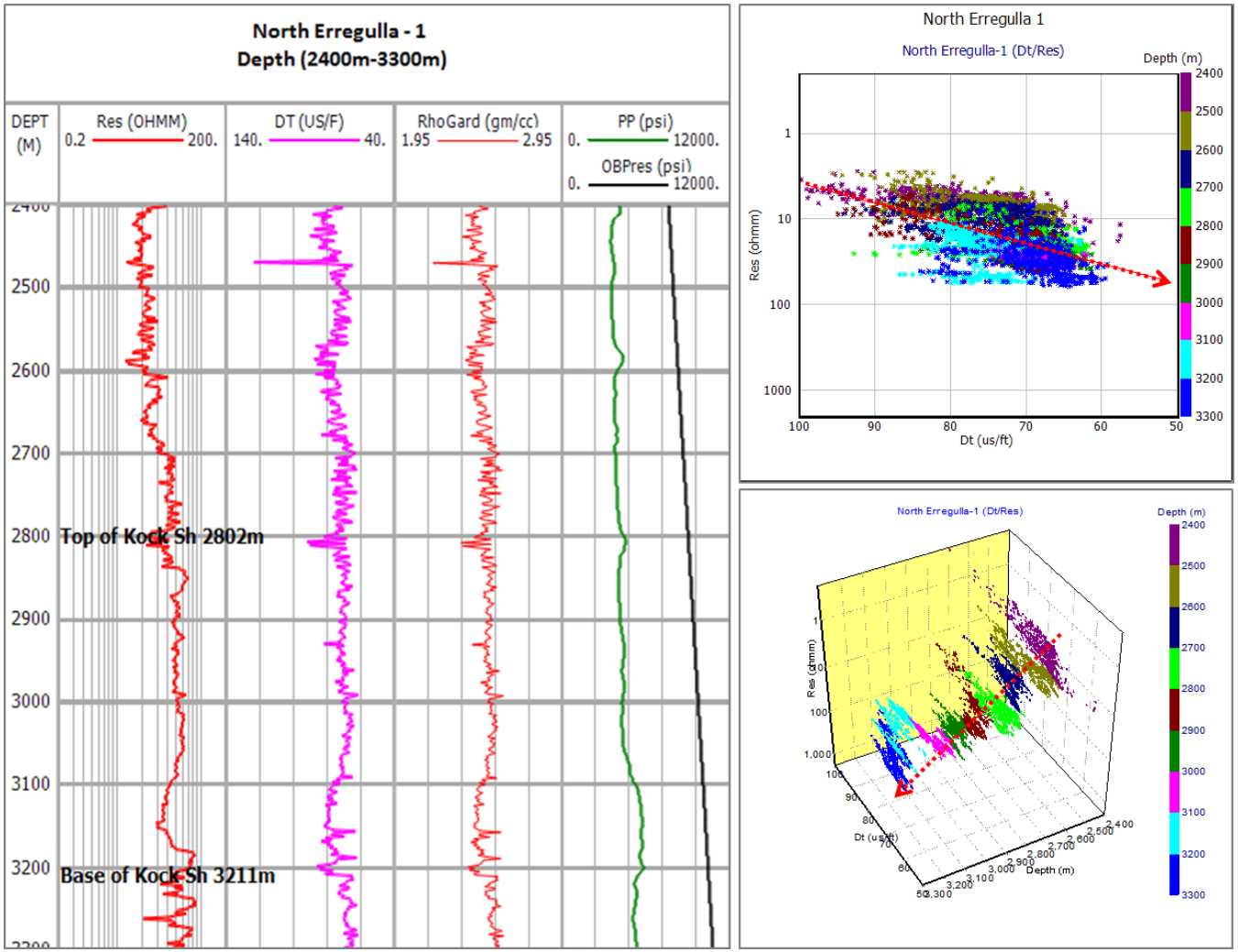
North Erregulla - 1
Depth (2400m-3300m)
DEPT (M)
Res (OHMM) 0.2 200.
DT (US/F) 140. 40.
RhoGard (gm/cc) 1.95 2.95
PP (psi) 0. 12000.
OBPres (psi) 0. 12000.
2500
2600
2700
2800
3000
3100
3200
Top of Kock Sh 2802m
Base of Kock Sh 3211m
North Erregulla 1
North Erregulla-1 (Dt/Res)
Depth (m)
Res (ohmm)
Dt (us/ft)
North Erregulla-1 (Dt/Res)
Depth (m)
Res (ohmm)
Dt (us/ft)
Depth (m)

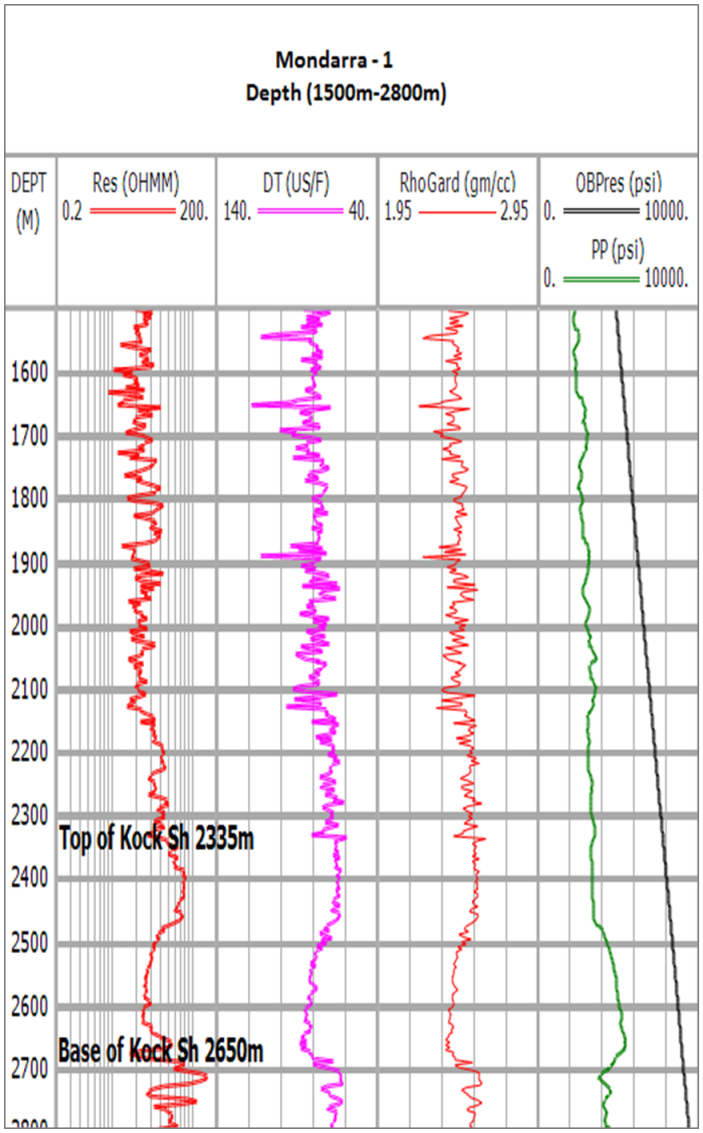
Mondarra - 1
Depth (1500m-2800m)
DEPT (M)
Res (OHMM) 0.2 200.
DT (US/F) 140. 40.
RhoGard (gm/cc) 1.95 2.95
OBPres (psi) 0. 10000.
PP (psi) 0. 10000.
1600
1700
1800
1900
2000
2100
2200
2300
2400
2500
2600
2700
Top of Kock Sh 2335m
Base of Kock Sh 2650m

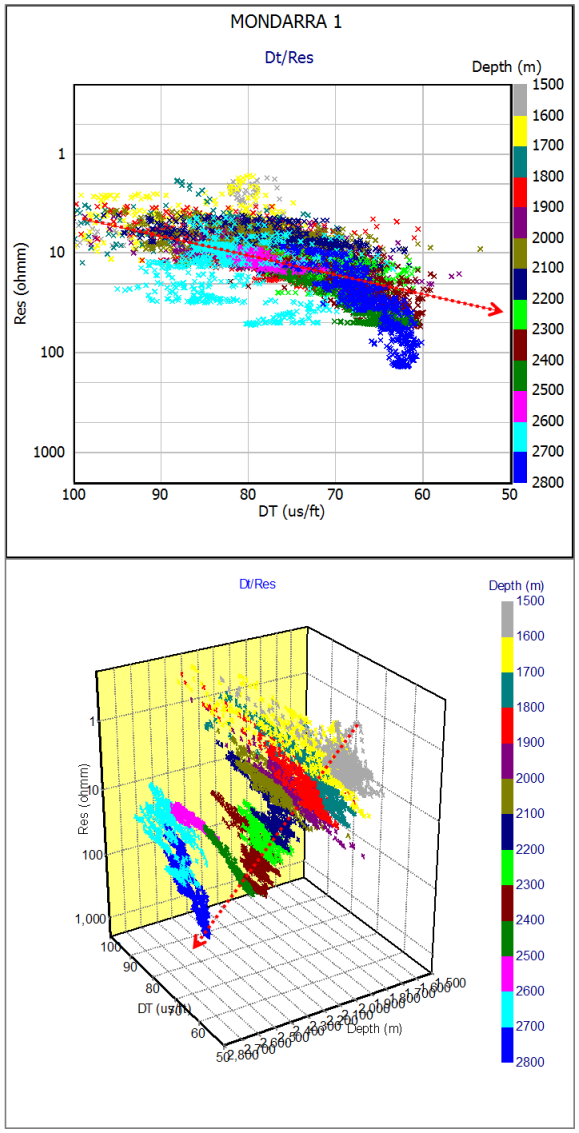
MONDARRA 1
Dt/Res
Depth (m)
Res (ohmm)
1
10
100
1000
100
90
80
70
60
50
DT (us/ft)
1500
1600
1700
1800
1900
2000
2100
2200
2300
2400
2500
2600
2700
2800
Dt/Res
Depth (m)
Res (ohmm)
1
10
100
1,000
100
90
80
DT (us/ft)
60
50
Depth (m)
1500
1600
1700
1800
1900
2000
2100
2200
2300
2400
2500
2600
2700
2800

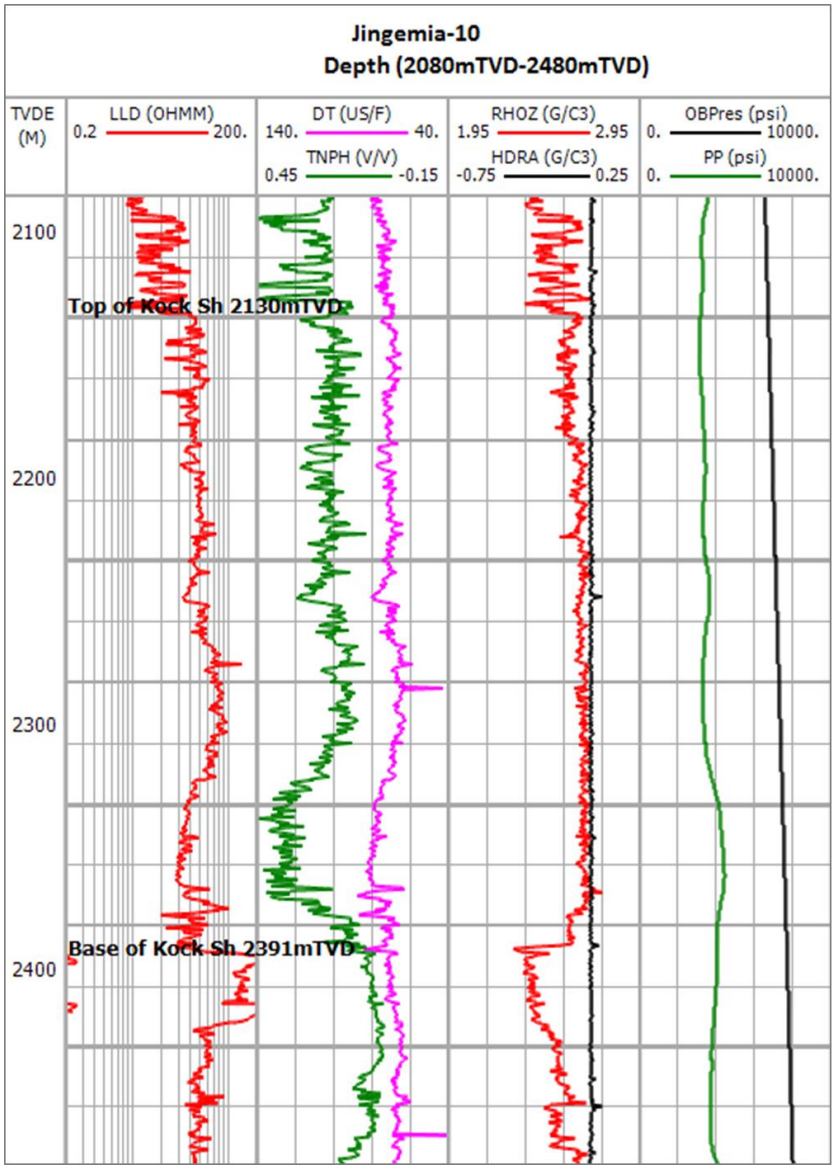
Jingemia-10
Depth (2080mTVD-2480mTVD)
TVDE (M)
LLD (OHMM)
0.2
200.
DT (US/F)
140.
40.
TNPH (V/V)
0.45
-0.15
RHOZ (G/C3)
1.95
2.95
HDRA (G/C3)
-0.75
0.25
OBPres (psi)
0.
10000.
PP (psi)
0.
10000.
2100
2200
2300
2400
Top of Kock Sh 2130mTVD
Base of Kock Sh 2391mTVD

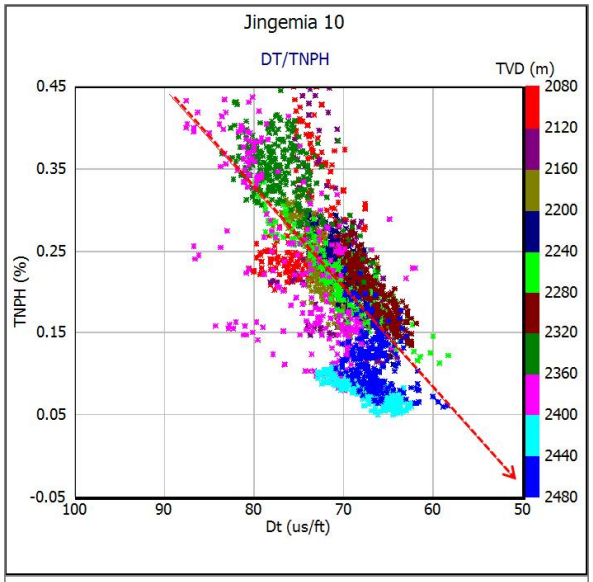
Jingemia 10
DT/TNPH
TVD (m)
TNPH (%)
Dt (us/ft)
0.45
0.35
0.25
0.15
0.05
-0.05
100
90
80
70
60
50
2080
2120
2160
2200
2240
2280
2320
2360
2400
2440
2480

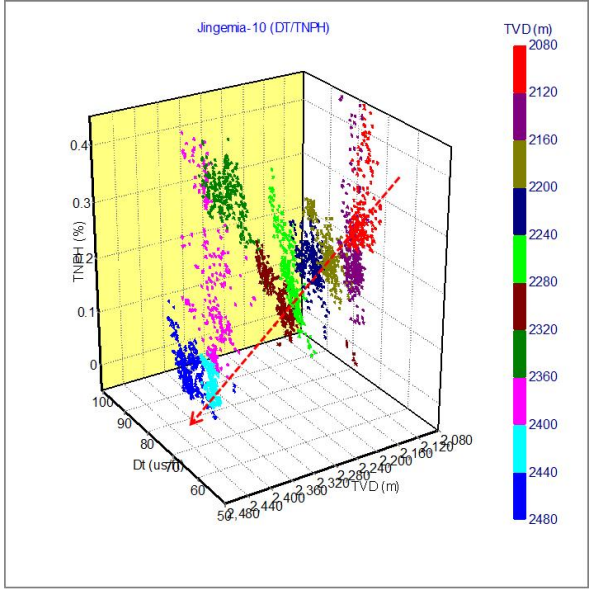
Jingemia-10 (DT/TNPH)
TVD (m)
TNPH (%)
Dt (us/ft)
TVD (m)
0.4
0.3
0.2
0.1
0
100
90
80
60
50
2080
2120
2160
2200
2240
2280
2320
2360
2400
2440
2480

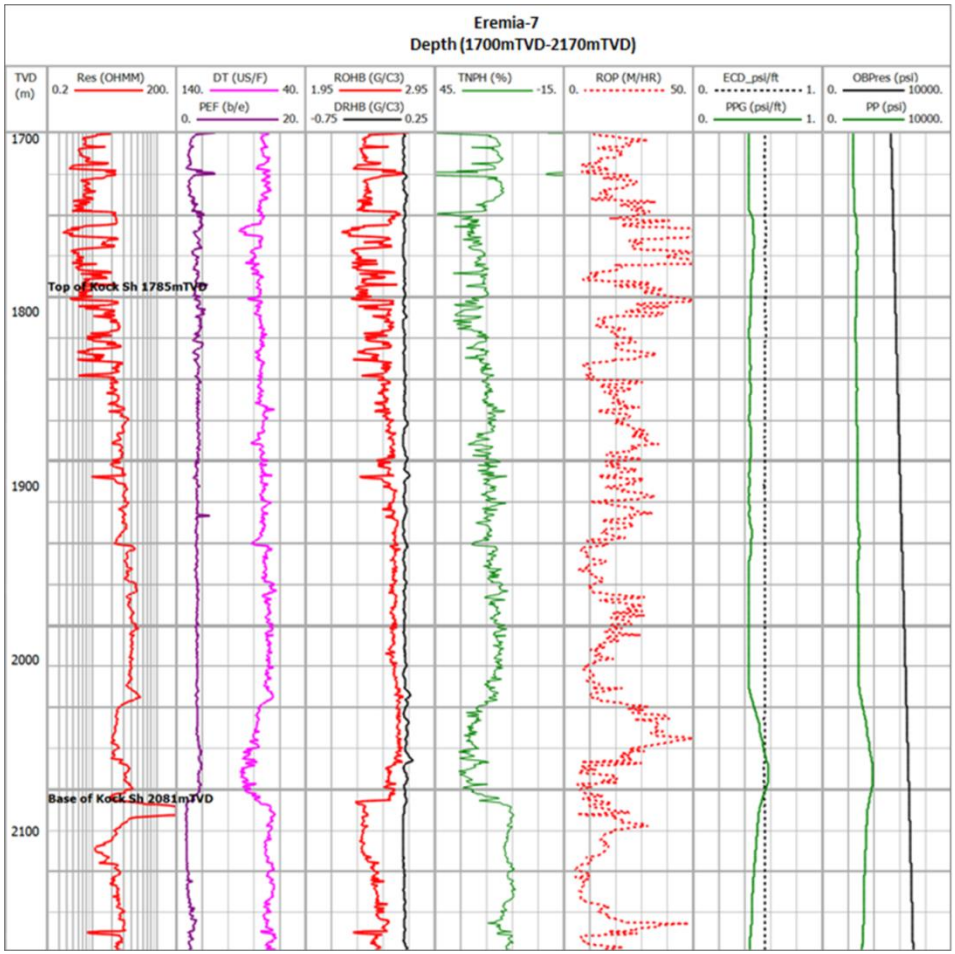
Eremia-7
Depth (1700mTVD-2170mTVD)
TVD (m)
Res (OHMM)
0.2
200.
DT (US/F)
140.
40.
PEF (b/e)
0.
20.
ROHB (G/C3)
1.95
2.95
DRHB (G/C3)
-0.75
0.25
TNPH (%)
45.
-15.
ROP (M/HR)
0.
50.
ECD_psi/ft
0.
1.
PPG (psi/ft)
0.
1.
OBPres (psi)
0.
10000.
PP (psi)
0.
10000.
1700
1800
1900
2000
2100
Top of Kock Sh 1785mTVD
Base of Kock Sh 2081mTVD

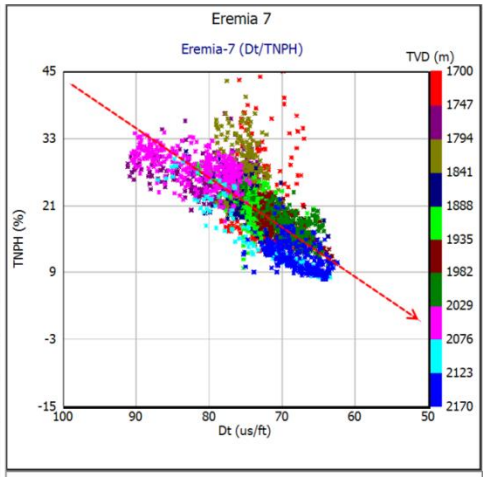
Eremia 7
Eremia-7 (Dt/TNPH)
TVD (m)
1700
1747
1794
1841
1888
1935
1982
2029
2076
2123
2170
TNPH (%)
45
33
21
9
-3
-15
100
90
80
70
60
50
Dt (us/ft)

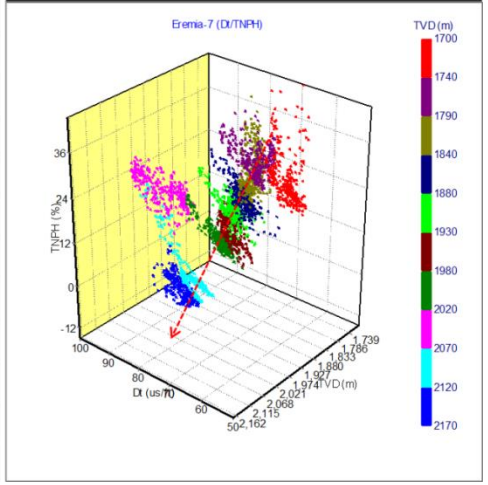
Eremia-7 (Dt/TNPH)
TVD (m)
1700
1740
1790
1840
1880
1930
1980
2020
2070
2120
2170
TNPH (%)
36
24
12
0
-12
100
90
80
Dt (us/ft)
60
50
1,739
1,786
1,833
1,880
1,927
1,974
2,021
2,068
2,115
2,162
TVD (m)

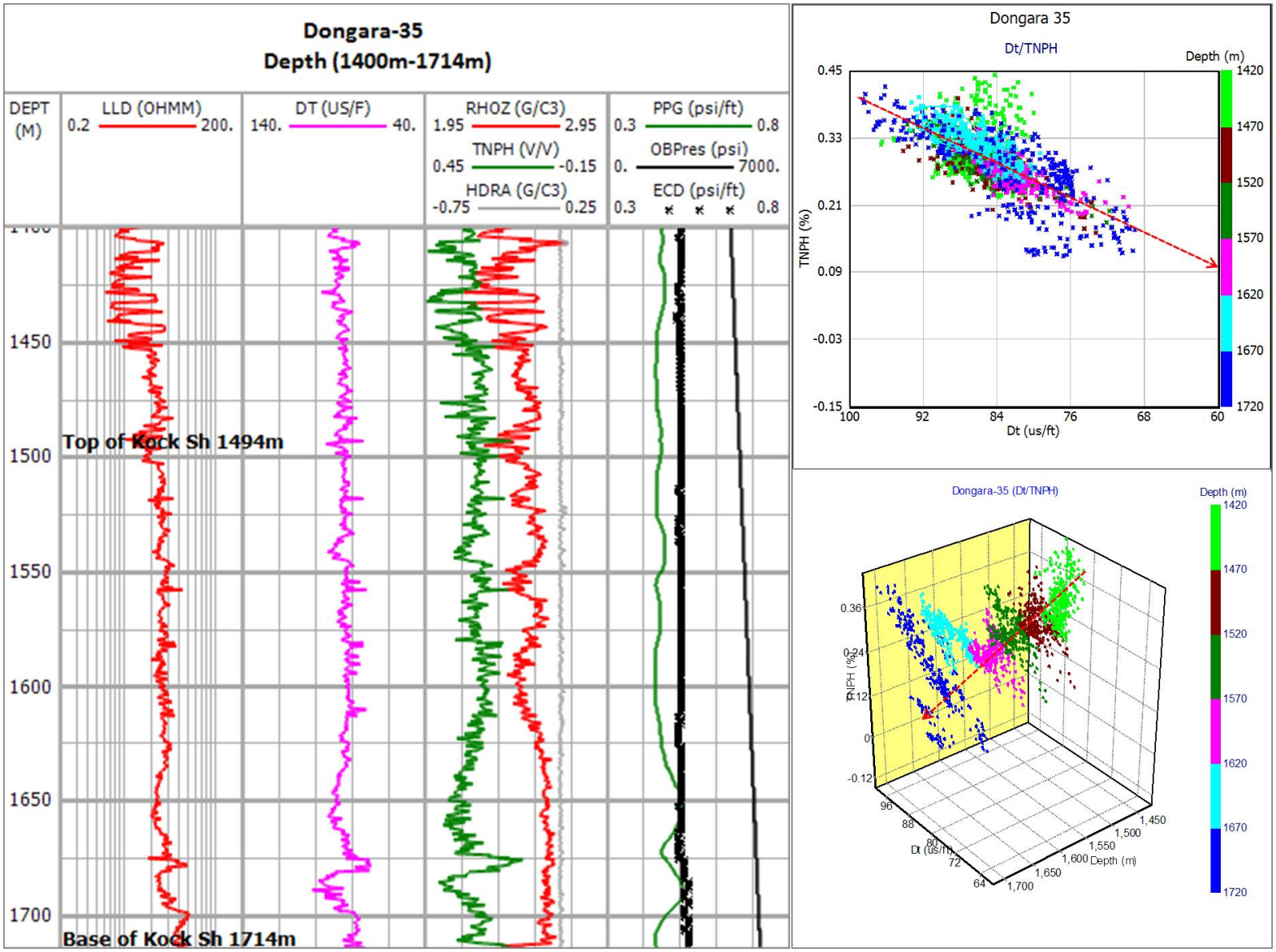
Dongara-35
Depth (1400m-1714m)
DEPT (M)
LLD (OHMM) 0.2 200.
DT (US/F) 140. 40.
RHOZ (G/C3) 1.95 2.95
TNPH (V/V) 0.45 -0.15
HDRA (G/C3) -0.75 0.25
PPG (psi/ft) 0.3 0.8
OBPres (psi) 0. 7000.
ECD (psi/ft) 0.3 0.8
1450
1500
1550
1600
1650
1700
Top of Kock Sh 1494m
Base of Kock Sh 1714m
Dongara 35
Dt/TNPH
Depth (m)
TNPH (%)
Dt (us/ft)
Dongara-35 (Dt/TNPH)
Depth (m)
TNPH (%)
Dt (us/ft)
Depth (m)

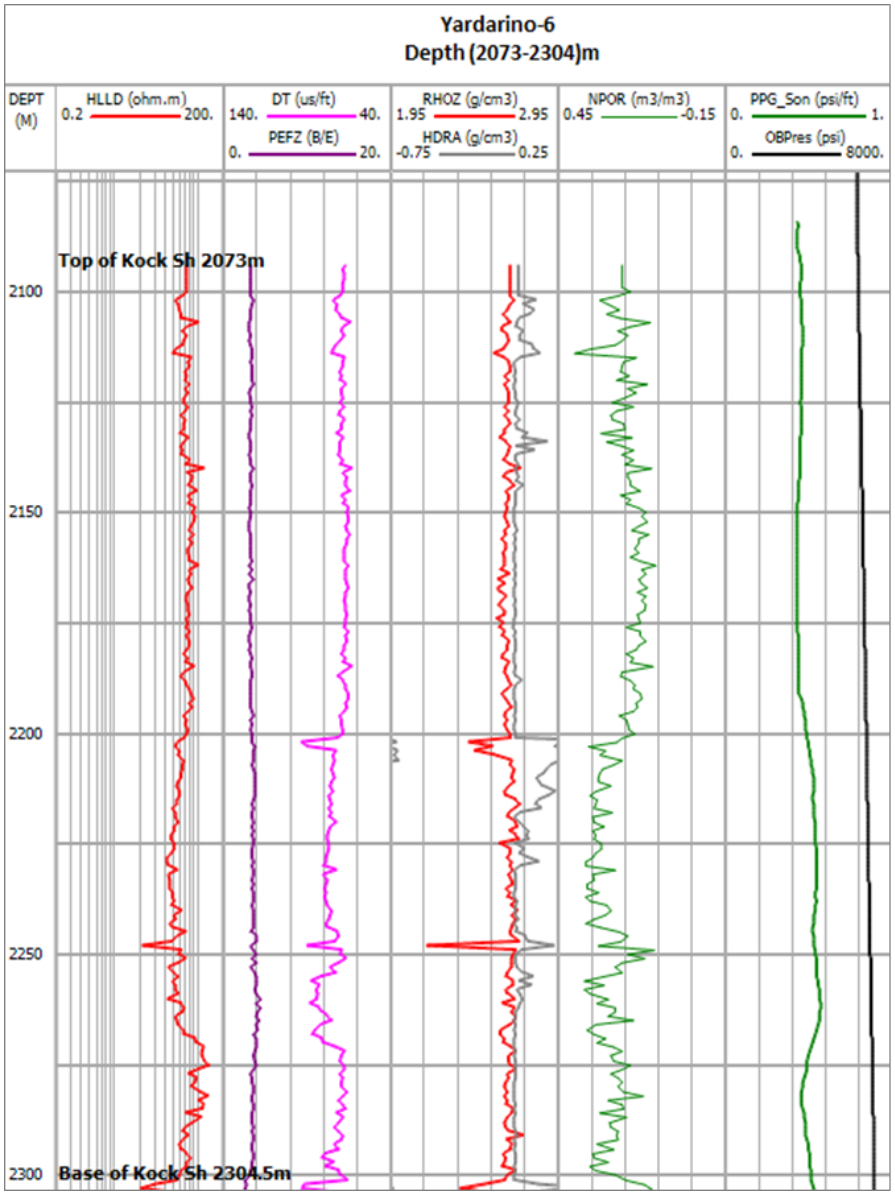
Yardarino-6
Depth (2073-2304)m
DEPT (M)
HLLD (ohm.m) 0.2 200.
DT (us/ft) 140. 40.
PEFZ (B/E) 0. 20.
RHOZ (g/cm3) 1.95 2.95
HDRA (g/cm3) -0.75 0.25
NPOR (m3/m3) 0.45 -0.15
PPG_Son (psi/ft) 0. 1.
OBPres (psi) 0. 8000.
Top of Kock Sh 2073m
Base of Kock Sh 2304.5m
2100
2150
2200
2250
2300

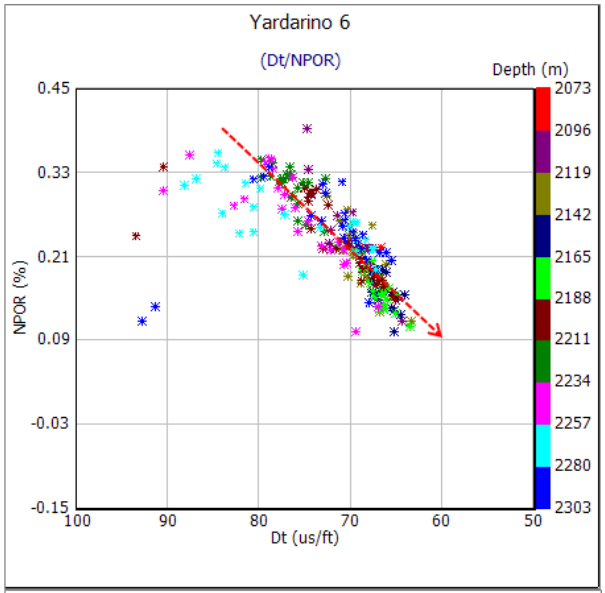
Yardarino 6
(Dt/NPOR)
Depth (m)
NPOR (%)
Dt (us/ft)
0.45
0.33
0.21
0.09
-0.03
-0.15
100
90
80
70
60
50
2073
2096
2119
2142
2165
2188
2211
2234
2257
2280
2303

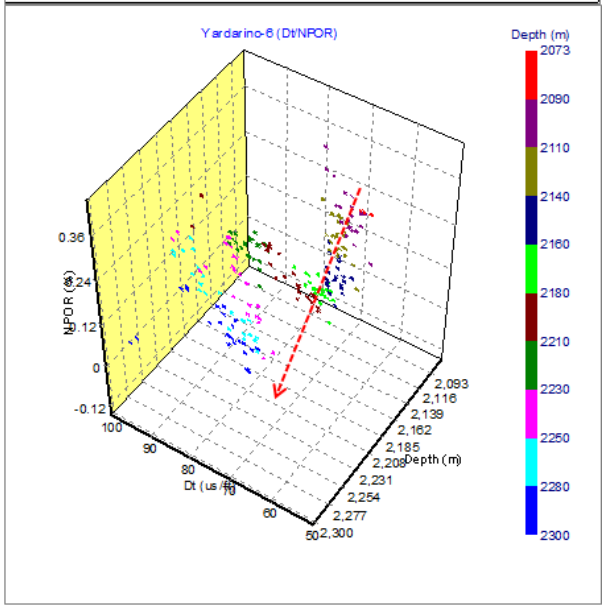
Yardarino-6 (Dt/NPOR)
Depth (m)
NPOR (%)
Dt (us/ft)
Depth (m)
0.36
0.24
0.12
0
-0.12
100
90
80
70
60
50
2,093
2,116
2,139
2,162
2,185
2,208
2,231
2,254
2,277
2,300
2073
2090
2110
2140
2160
2180
2210
2230
2250
2280
2300

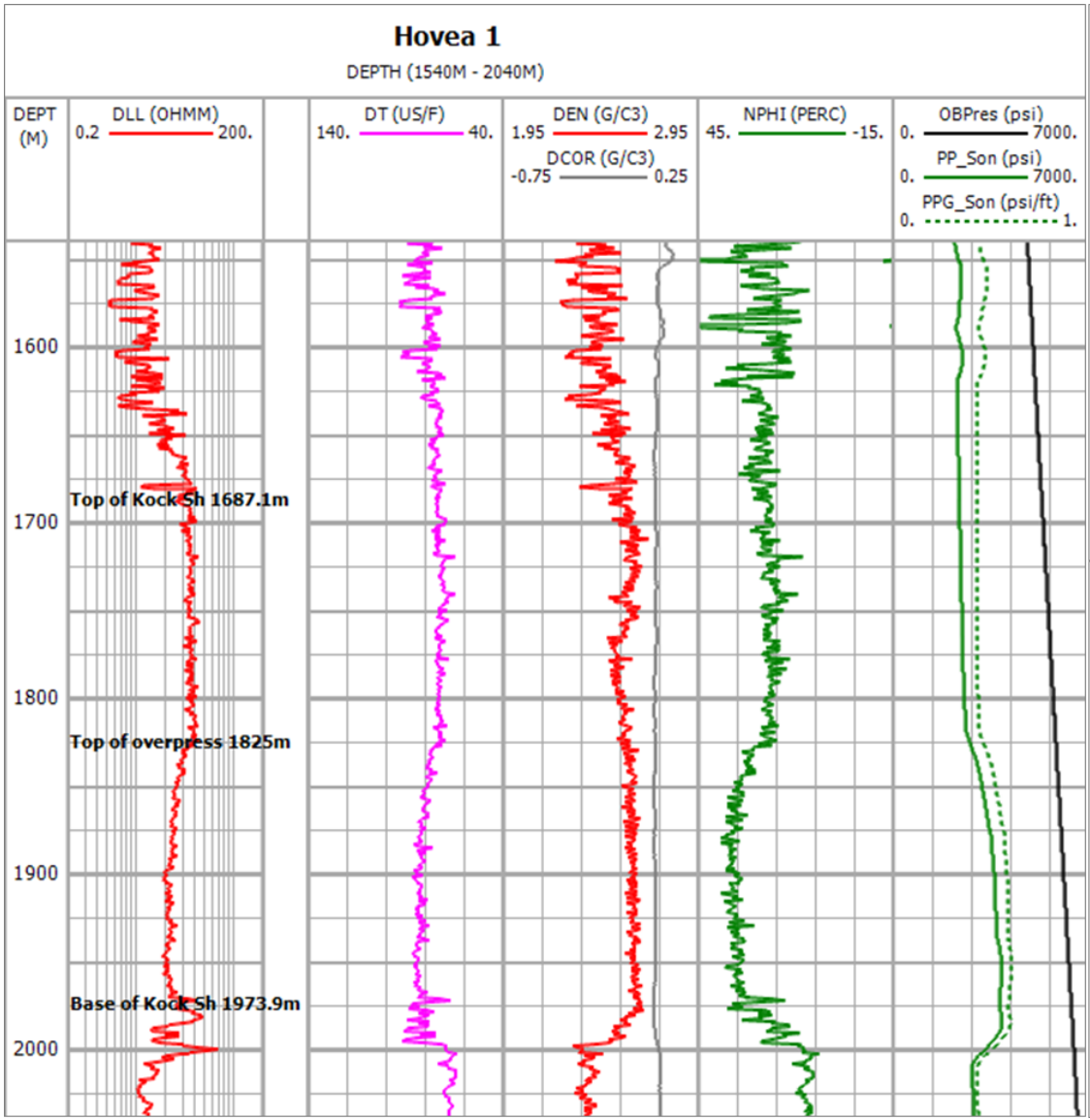
Hovea 1
DEPTH (1540M - 2040M)
DEPT (M)
DLL (OHMM) 0.2 200.
DT (US/F) 140. 40.
DEN (G/C3) 1.95 2.95
DCOR (G/C3) -0.75 0.25
NPHI (PERC) 45. -15.
OBPres (psi) 0. 7000.
PP_Son (psi) 0. 7000.
PPG_Son (psi/ft) 0. 1.
1600
1700
1800
1900
2000
Top of Kock Sh 1687.1m
Top of overpress 1825m
Base of Kock Sh 1973.9m

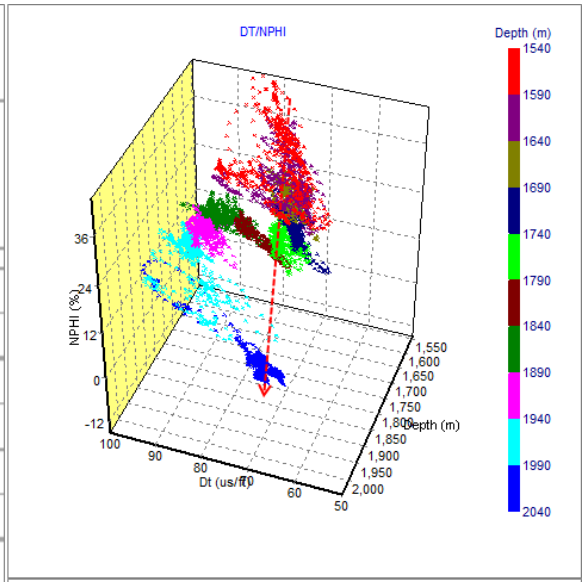
DT/NPHI
Depth (m)
1540
1590
1640
1690
1740
1790
1840
1890
1940
1990
2040
NPHI (%)
36
24
12
0
-12
100
90
80
Dt (us/ft)
60
50
1,550
1,600
1,650
1,700
1,750
1,800
1,850
1,900
1,950
2,000
Depth (m)

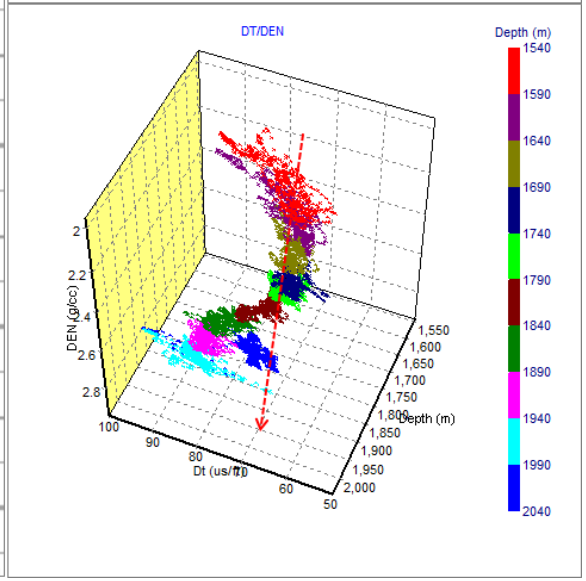
DT/DEN
Depth (m)
1540
1590
1640
1690
1740
1790
1840
1890
1940
1990
2040
DEN (g/cc)
2
2.2
2.4
2.6
2.8
100
90
80
Dt (us/ft)
60
50
1,550
1,600
1,650
1,700
1,750
1,800
1,850
1,900
1,950
2,000
Depth (m)

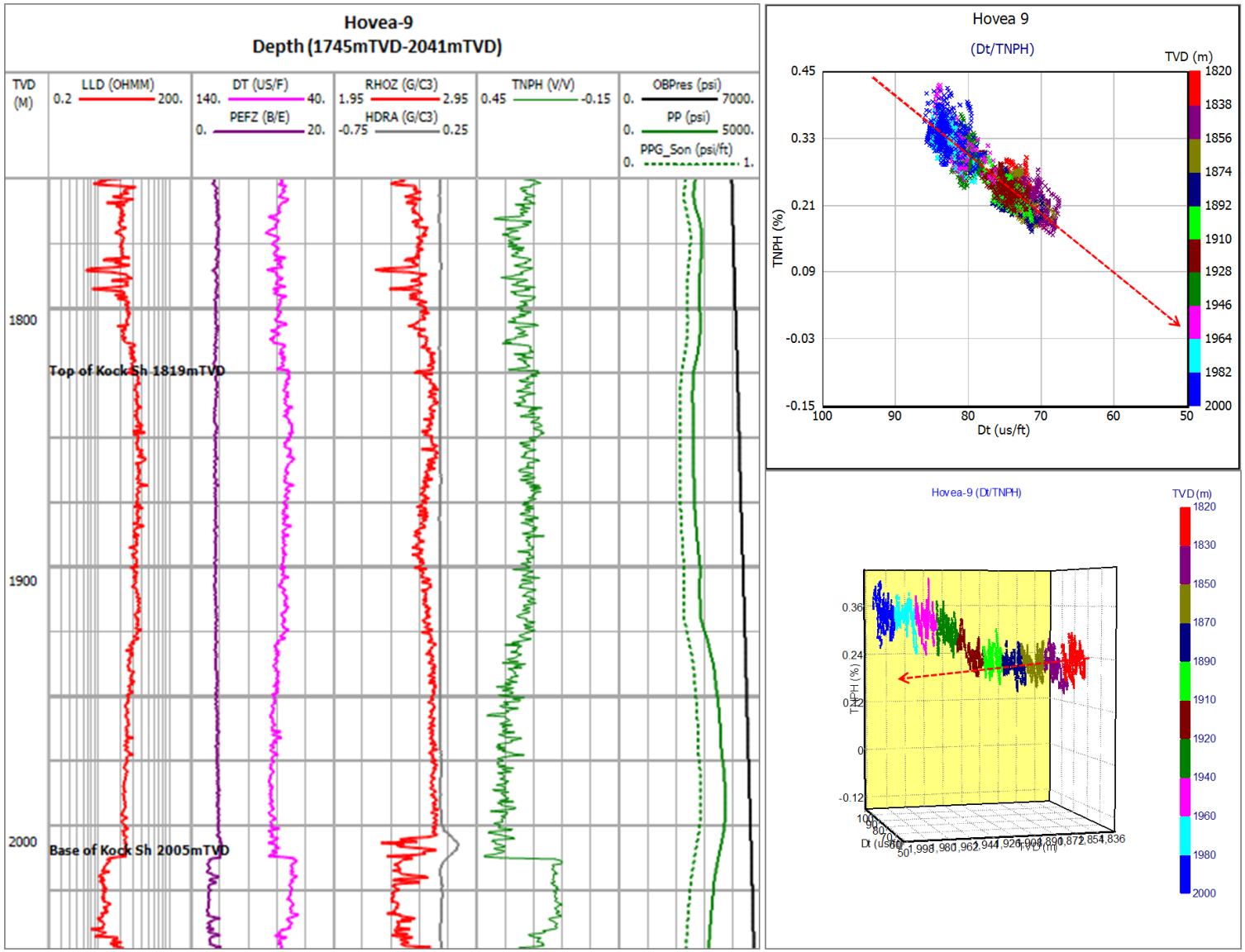
Hovea-9
Depth (1745mTVD-2041mTVD)
TVD (M)
LLD (OHMM)
0.2
200.
DT (US/F)
140.
40.
PEFZ (B/E)
0.
20.
RHOZ (G/C3)
1.95
2.95
HDRA (G/C3)
-0.75
0.25
TNPH (V/V)
0.45
-0.15
OBPres (psi)
0.
7000.
PP (psi)
0.
5000.
PPG_Son (psi/ft)
0.
1.
1800
1900
2000
Top of Kock Sh 1819mTVD
Base of Kock Sh 2005mTVD
Hovea 9
(Dt/TNPH)
TVD (m)
TNPH (%)
Dt (us/ft)
Hovea-9 (Dt/TNPH)
TVD (m)
TNPH (%)
Dt (us/ft)
TVD (m)

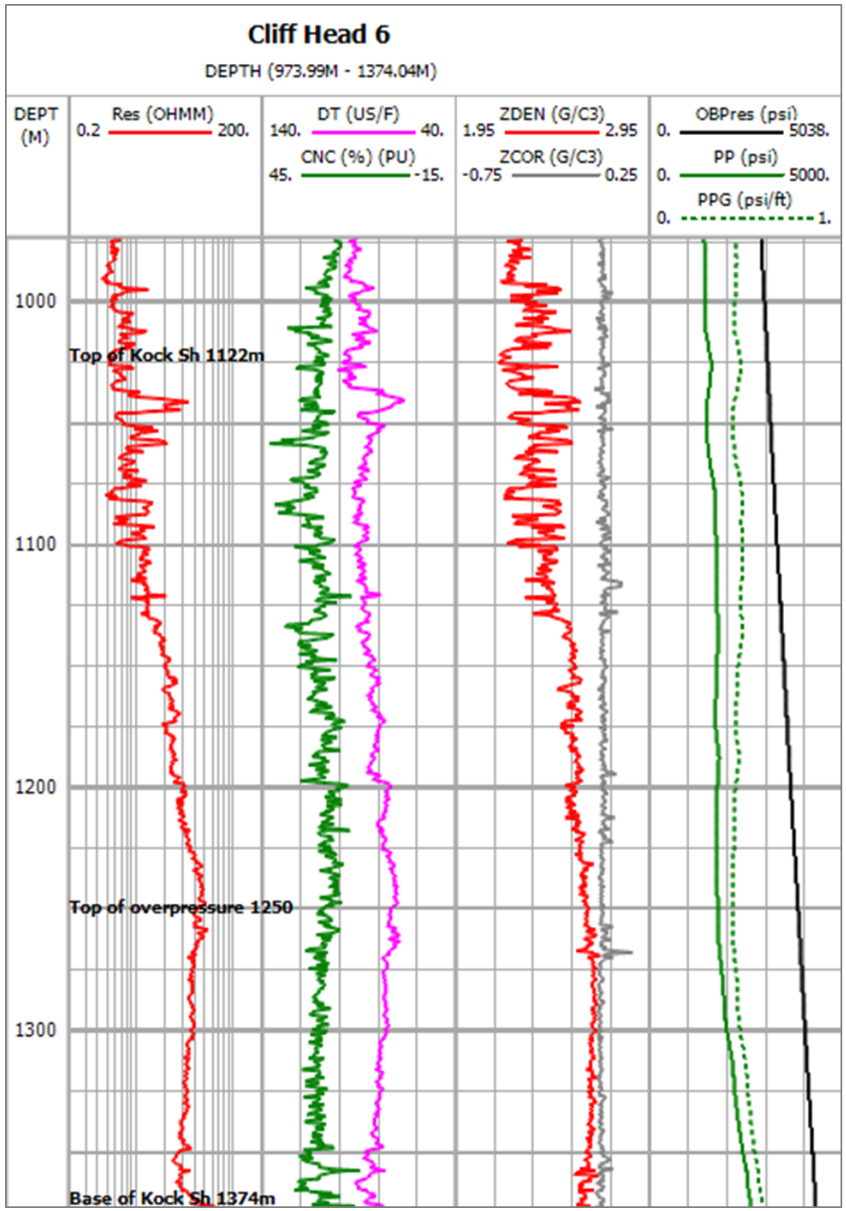
Cliff Head 6
DEPTH (973.99M - 1374.04M)
DEPT (M)
Res (OHMM) 0.2 200.
DT (US/F) 140. 40.
CNC (%) (PU) 45. -15.
ZDEN (G/C3) 1.95 2.95
ZCOR (G/C3) -0.75 0.25
OBPres (psi) 0. 5038.
PP (psi) 0. 5000.
PPG (psi/ft) 0. 1.
1000
1100
1200
1300
Top of Kock Sh 1122m
Top of overpressure 1250
Base of Kock Sh 1374m

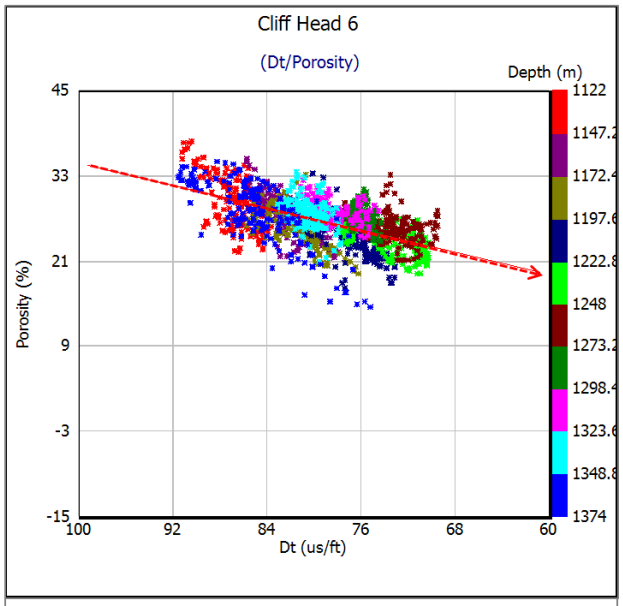
Cliff Head 6
(Dt/Porosity)
Depth (m)
Porosity (%)
45
33
21
9
-3
-15
100
92
84
76
68
60
Dt (us/ft)
1122
1147.2
1172.4
1197.6
1222.8
1248
1273.2
1298.4
1323.6
1348.8
1374

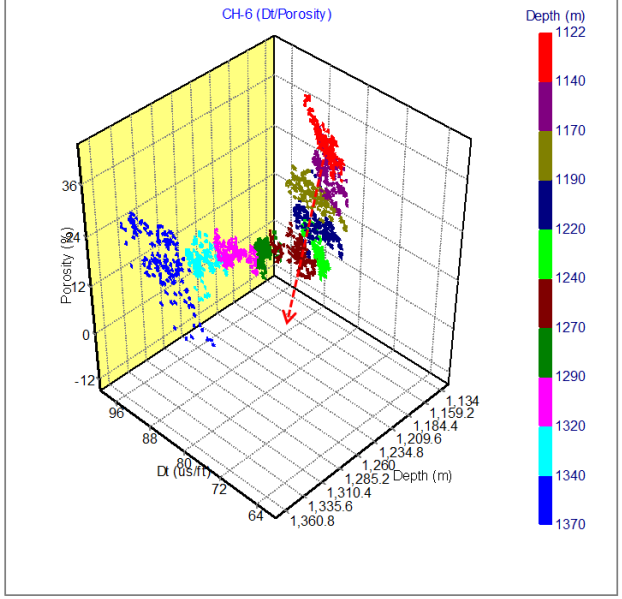
CH-6 (Dt/Porosity)
Depth (m)
Porosity (%)
36
24
12
0
-12
96
88
80
72
64
Dt (us/ft)
1,134
1,159.2
1,184.4
1,209.6
1,234.8
1,260
1,285.2
1,310.4
1,335.6
1,360.8
Depth (m)
1122
1140
1170
1190
1220
1240
1270
1290
1320
1340
1370

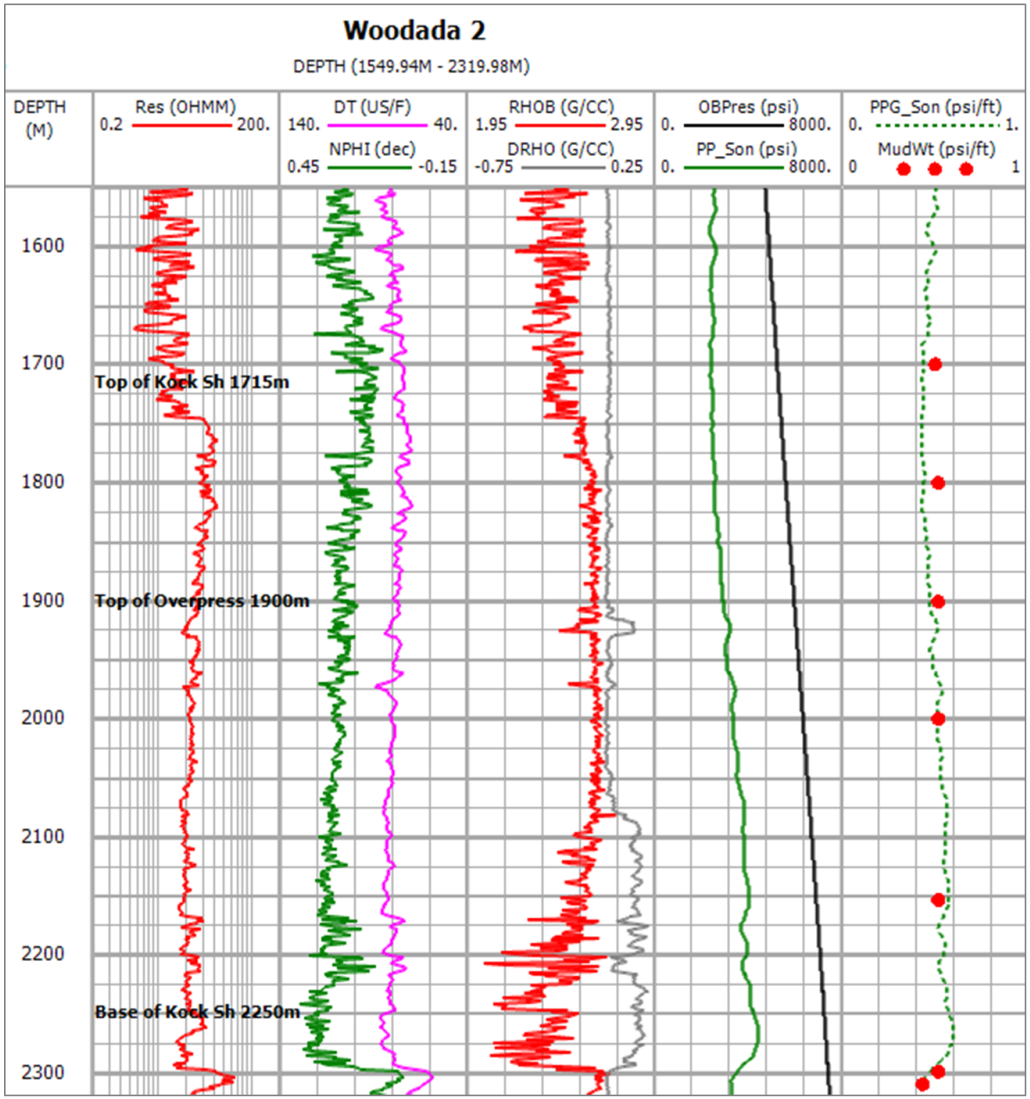
Woodada 2
DEPTH (1549.94M - 2319.98M)
DEPTH (M)
Res (OHMM)
0.2
200.
DT (US/F)
140.
40.
NPHI (dec)
0.45
-0.15
RHOB (G/CC)
1.95
2.95
DRHO (G/CC)
-0.75
0.25
OBPres (psi)
0.
8000.
PP_Son (psi)
0.
8000.
PPG_Son (psi/ft)
0.
1.
MudWt (psi/ft)
0
1
1600
1700
1800
1900
2000
2100
2200
2300
Top of Kock Sh 1715m
Top of Overpress 1900m
Base of Kock Sh 2250m

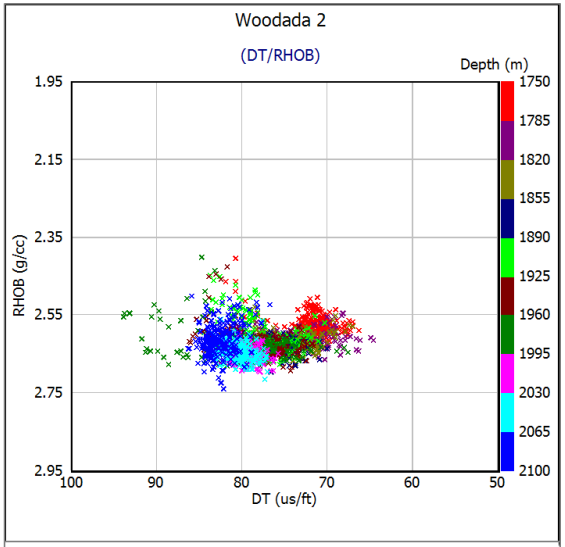
Woodada 2
(DT/RHOB)
Depth (m)
RHOB (g/cc)
DT (us/ft)
1.95
2.15
2.35
2.55
2.75
2.95
100
90
80
70
60
50
1750
1785
1820
1855
1890
1925
1960
1995
2030
2065
2100

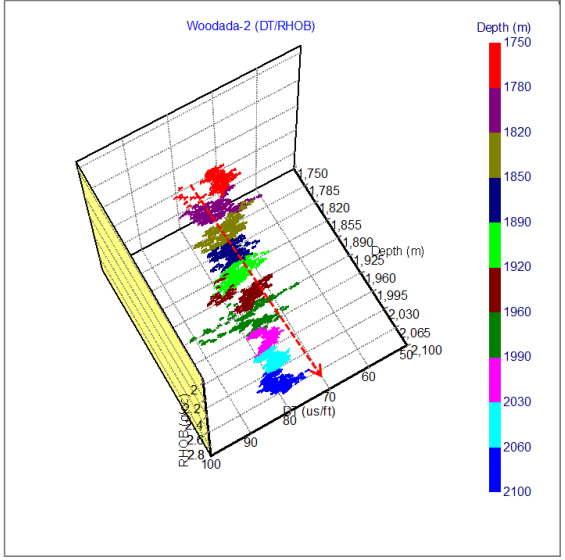
Woodada-2 (DT/RHOB)
Depth (m)
1750
1780
1820
1850
1890
1920
1960
1990
2030
2060
2100
DT (us/ft)
RHOB (g/cc)

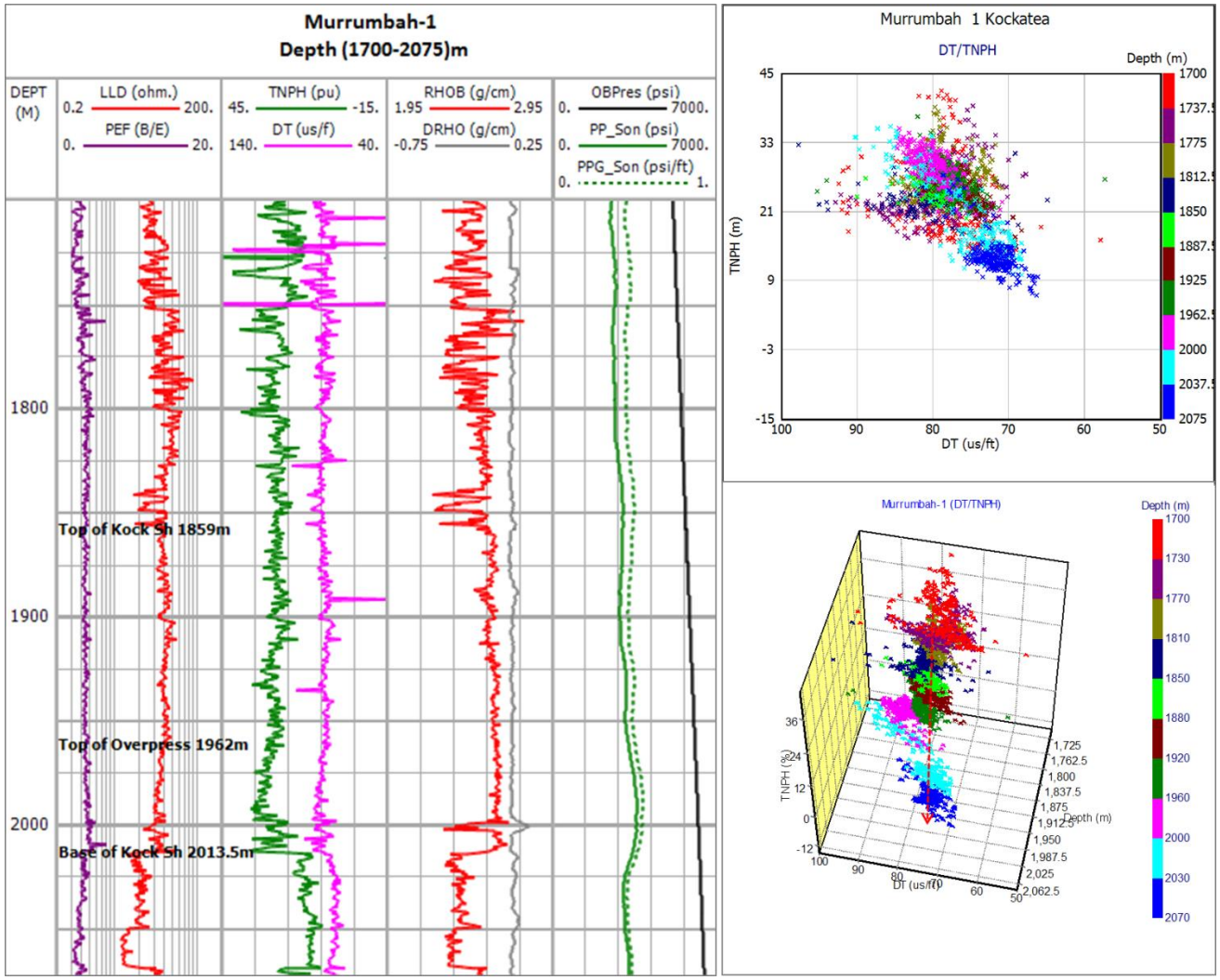
Murrumbah-1
Depth (1700-2075)m
DEPT (M)
LLD (ohm.) 0.2 200.
PEF (B/E) 0. 20.
TNPH (pu) 45. -15.
DT (us/f) 140. 40.
RHOB (g/cm) 1.95 2.95
DRHO (g/cm) -0.75 0.25
OBPres (psi) 0. 7000.
PP_Son (psi) 0. 7000.
PPG_Son (psi/ft) 0. 1.
1800
1900
2000
Top of Kock Sh 1859m
Top of Overpress 1962m
Base of Kock Sh 2013.5m
Murrumbah 1 Kockatea
DT/TNPH
Depth (m)
TNPH (m)
DT (us/ft)
Murrumbah-1 (DT/TNPH)
TNPH (%)
DT (us/ft)
Depth (m)

Appendix 1b Pressure-depth plots, well lo data and cross-plots for the wells that exhibited normal pore pressure in the Kockatea Shale and drilled around Beagle and Northampton uplift areas (Perth Basin)

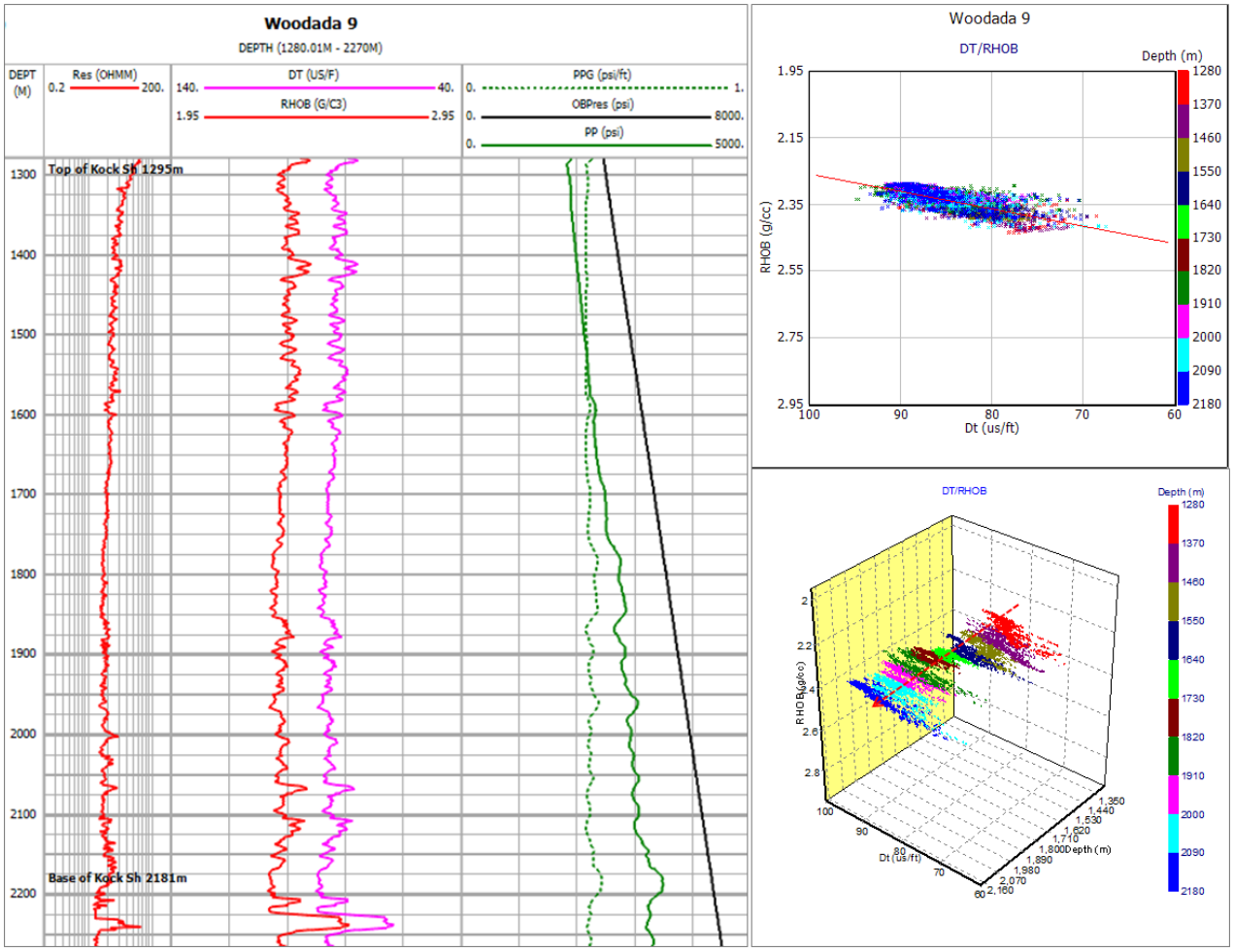
Woodada 9
DEPTH (1280.01M - 2270M)
DEPT (M)
Res (OHMM)
0.2
200.
DT (US/F)
140.
40.
RHOB (G/C3)
1.95
2.95
PPG (psi/ft)
0.
1.
OBPres (psi)
0.
8000.
PP (psi)
0.
5000.
Top of Kock Sh 1295m
Base of Kock Sh 2181m
1300
1400
1500
1600
1700
1800
1900
2000
2100
2200
Woodada 9
DT/RHOB
Depth (m)
RHOB (g/cc)
Dt (us/ft)
1.95
2.15
2.35
2.55
2.75
2.95
100
90
80
70
60
1280
1370
1460
1550
1640
1730
1820
1910
2000
2090
2180
DT/RHOB
Depth (m)
RHOB(g/cc)
Dt (us/ft)
Depth (m)
2
2.2
2.4
2.6
2.8
100
90
80
70
60
1,350
1,440
1,530
1,620
1,710
1,800
1,890
1,980
2,070
2,160

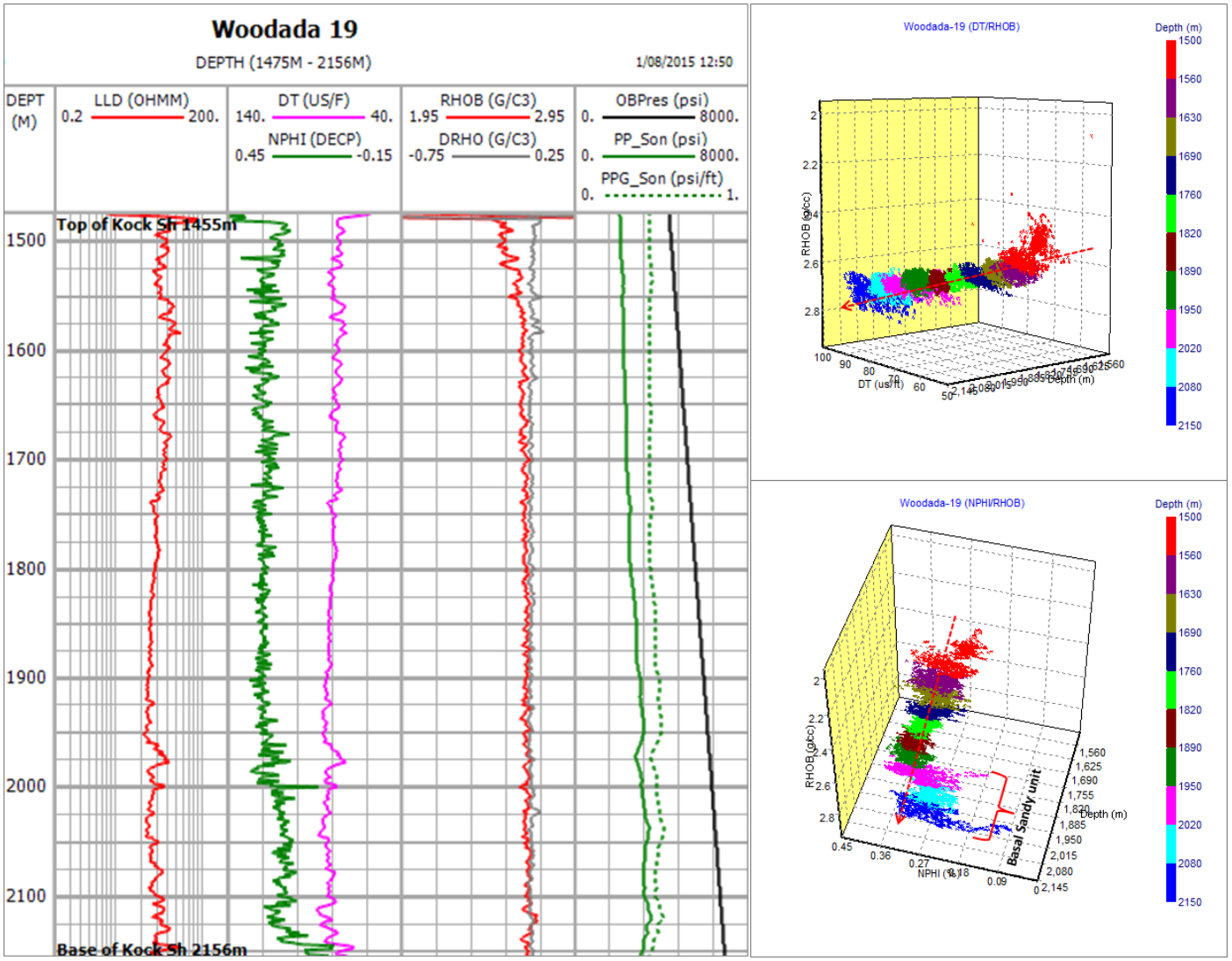
Woodada 19
DEPTH (1475M - 2156M)
1/08/2015 12:50
DEPT (M)
LLD (OHMM) 0.2 200.
DT (US/F) 140. 40.
NPHI (DECP) 0.45 -0.15
RHOB (G/C3) 1.95 2.95
DRHO (G/C3) -0.75 0.25
OBPres (psi) 0. 8000.
PP_Son (psi) 0. 8000.
PPG_Son (psi/ft) 0. 1.
Top of Kock Sh 1455m
Base of Kock Sh 2156m
1500
1600
1700
1800
1900
2000
2100
Woodada-19 (DT/RHOB)
Depth (m)
RHOB (g/cc)
DT (us/ft)
Depth (m)
Woodada-19 (NPHI/RHOB)
Depth (m)
RHOB (g/cc)
NPHI (%)
Depth (m)
Basal Sandy unit

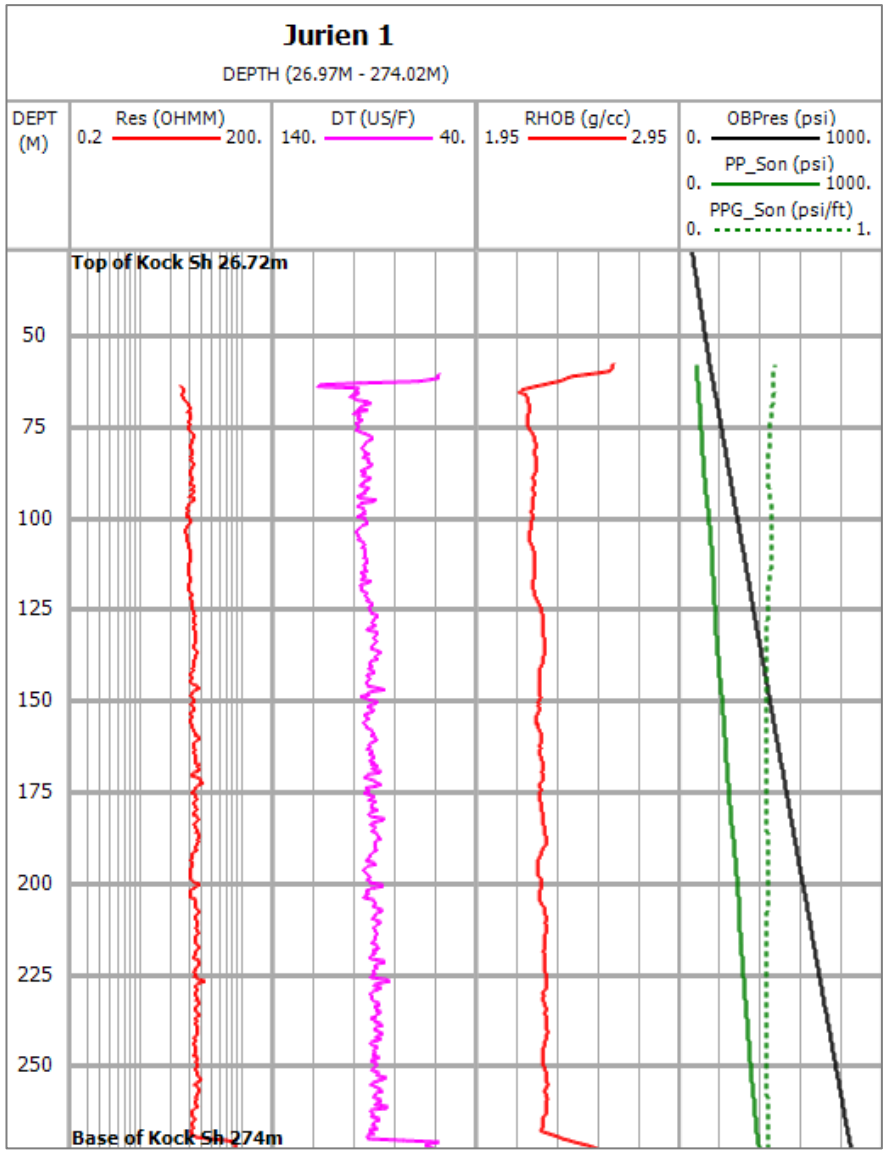
Jurien 1
DEPTH (26.97M - 274.02M)
DEPT (M)
Res (OHMM)
0.2
200.
DT (US/F)
140.
40.
RHOB (g/cc)
1.95
2.95
OBPres (psi)
0.
1000.
PP_Son (psi)
0.
1000.
PPG_Son (psi/ft)
0.
1.
Top of Kock Sh 26.72m
50
75
100
125
150
175
200
225
250
Base of Kock Sh 274m

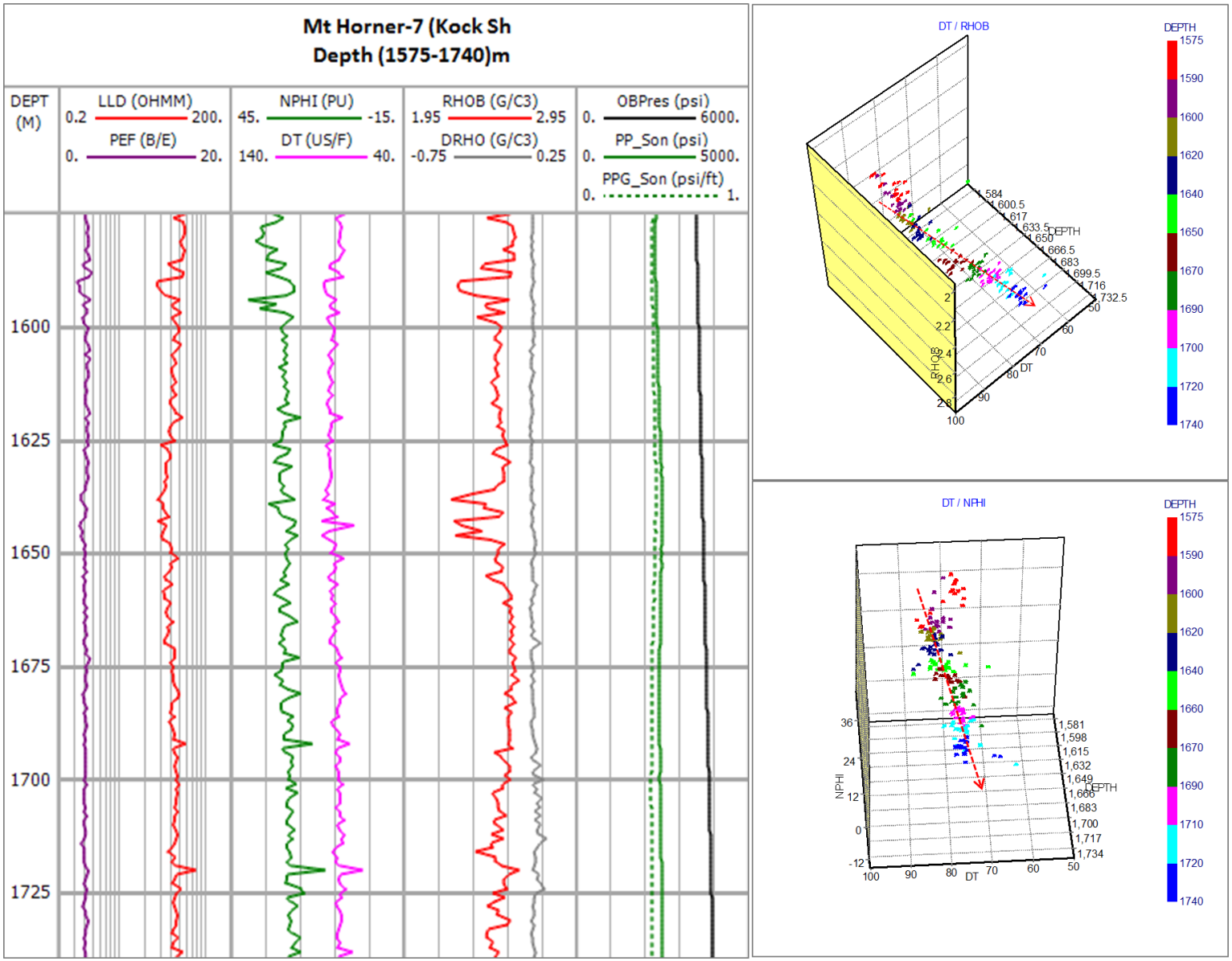
Mt Horner-7 (Kock Sh
Depth (1575-1740)m
DEPT (M)
LLD (OHMM) 0.2 200.
PEF (B/E) 0. 20.
NPHI (PU) 45. -15.
DT (US/F) 140. 40.
RHOB (G/C3) 1.95 2.95
DRHO (G/C3) -0.75 0.25
OBPres (psi) 0. 6000.
PP_Son (psi) 0. 5000.
PPG_Son (psi/ft) 0. 1.
1600
1625
1650
1675
1700
1725
DT / RHOB
DEPTH
RHOB
DT
DT / NPHI
NPHI
DEPTH

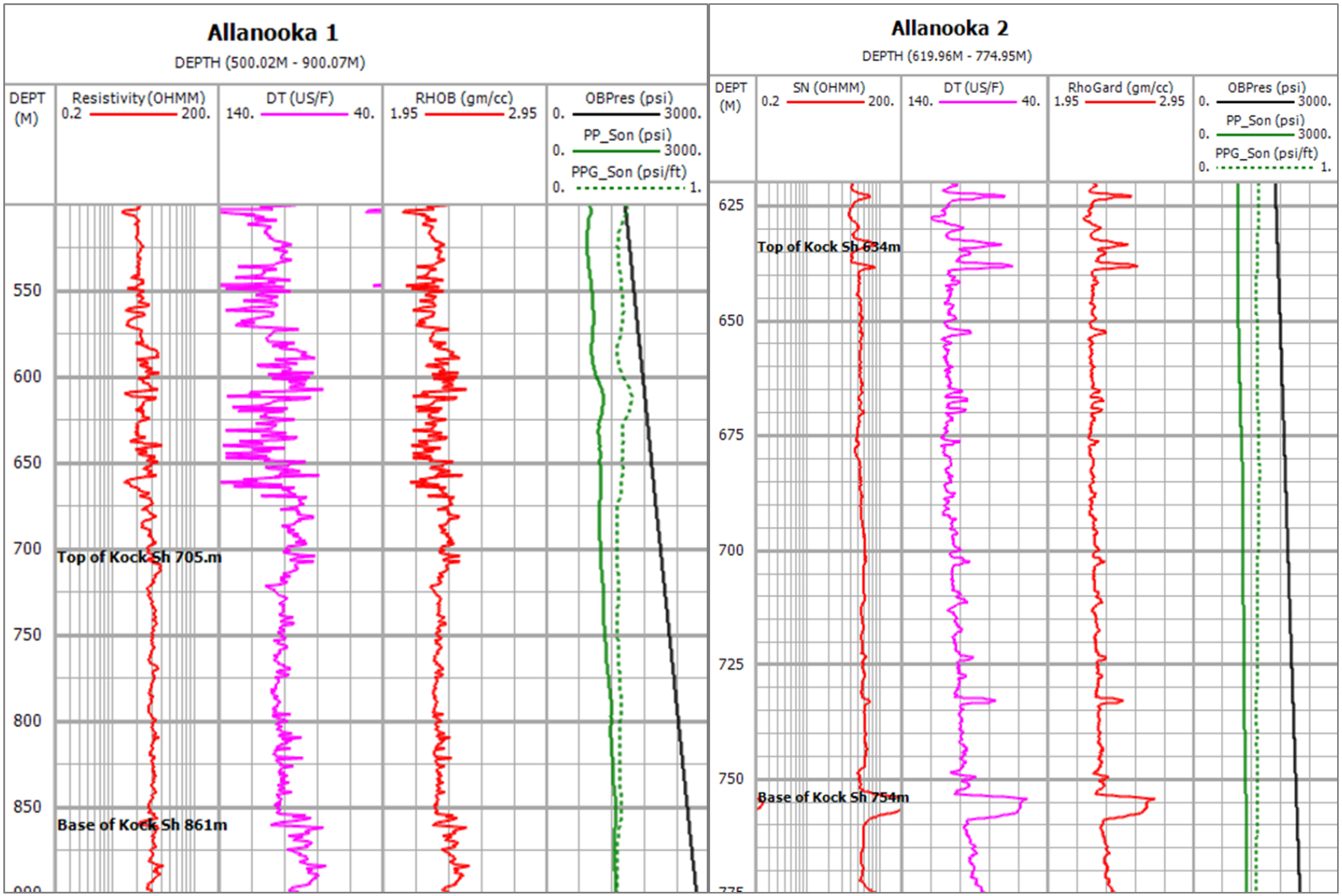
Allanooka 1
DEPTH (500.02M - 900.07M)
DEPT (M)
Resistivity (OHMM) 0.2 200.
DT (US/F) 140. 40.
RHOB (gm/cc) 1.95 2.95
OBPres (psi) 0. 3000.
PP_Son (psi) 0. 3000.
PPG_Son (psi/ft) 0. 1.
550
600
650
700
750
800
850
Top of Kock Sh 705.m
Base of Kock Sh 861m
Allanooka 2
DEPTH (619.96M - 774.95M)
DEPT (M)
SN (OHMM) 0.2 200.
DT (US/F) 140. 40.
RhoGard (gm/cc) 1.95 2.95
OBPres (psi) 0. 3000.
PP_Son (psi) 0. 3000.
PPG_Son (psi/ft) 0. 1.
625
650
675
700
725
750
Top of Kock Sh 634m
Base of Kock Sh 754m

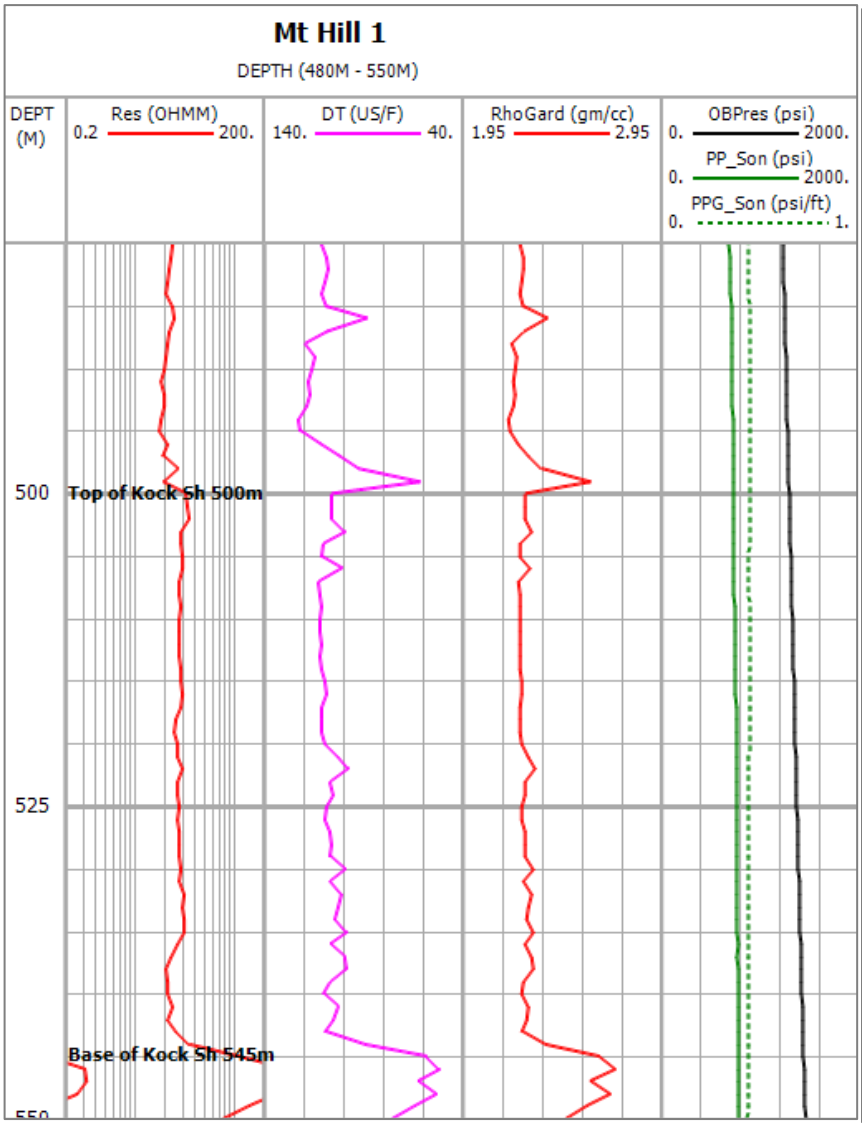
Mt Hill 1
DEPTH (480M - 550M)
DEPT (M)
Res (OHMM) 0.2 200.
DT (US/F) 140. 40.
RhoGard (gm/cc) 1.95 2.95
OBPres (psi) 0. 2000.
PP_Son (psi) 0. 2000.
PPG_Son (psi/ft) 0. 1.
500
525
Top of Kock Sh 500m
Base of Kock Sh 545m

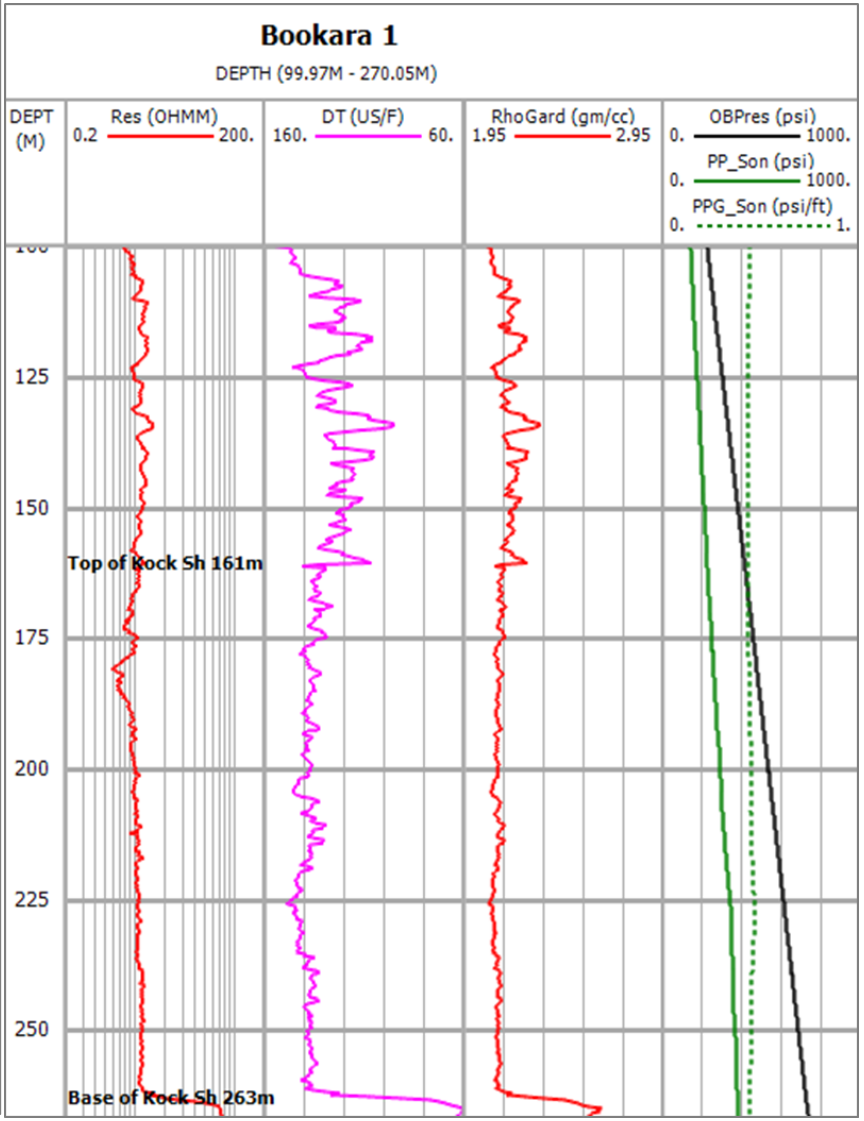
Bookara 1
DEPTH (99.97M - 270.05M)
DEPT (M)
Res (OHMM) 0.2 200.
DT (US/F) 160. 60.
RhoGard (gm/cc) 1.95 2.95
OBPres (psi) 0. 1000.
PP_Son (psi) 0. 1000.
PPG_Son (psi/ft) 0. 1.
125
150
175
200
225
250
Top of Kock Sh 161m
Base of Kock Sh 263m

Appendix 2 Canning Basin

Appendix 2a Pressure-depth plots, well lo data and cross-plots for the wells that exhibited overpressure in the Laurel Formation and drilled in the Yulleroo Anticline and regional structures

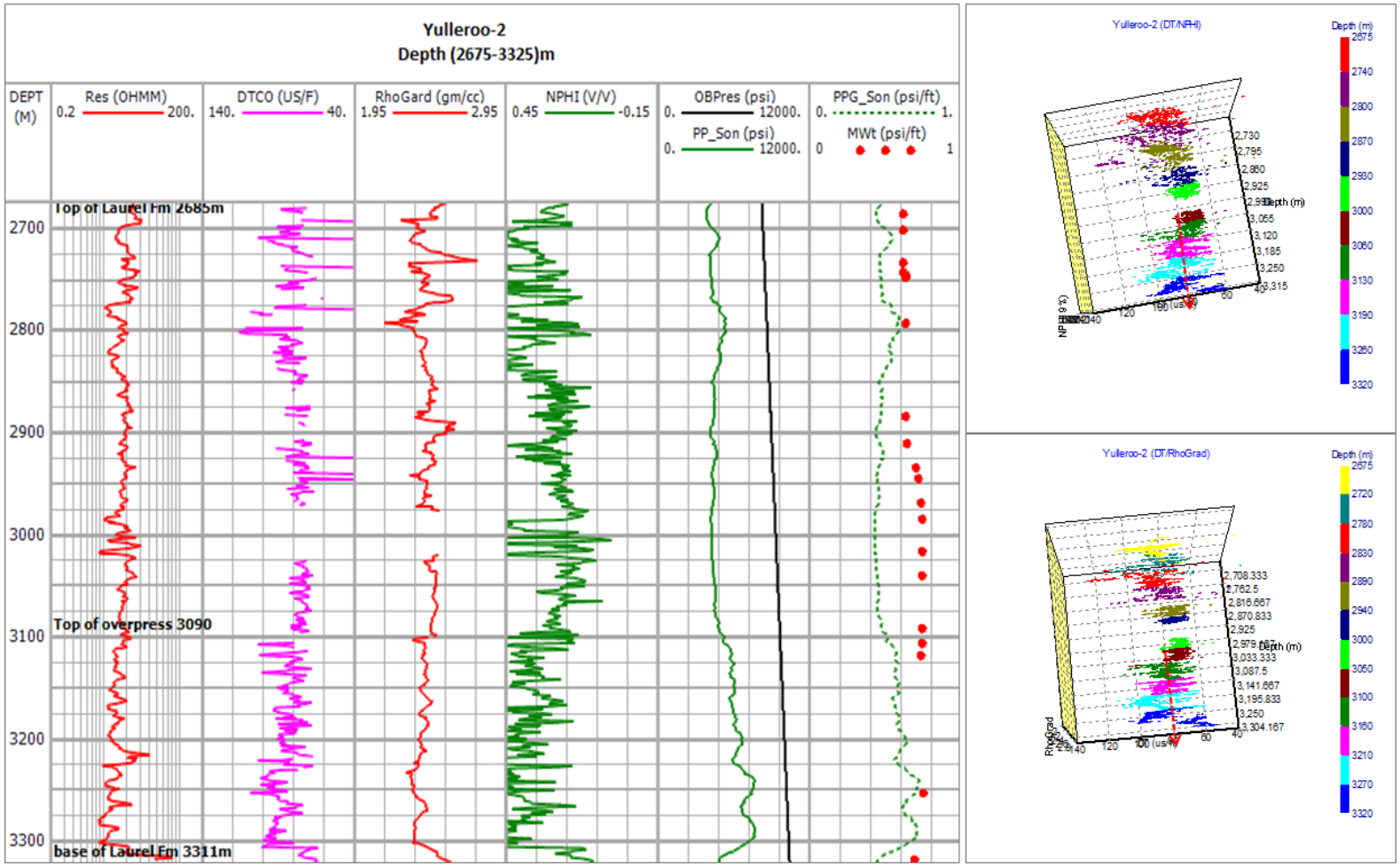
Yulleroo-2
Depth (2675-3325)m
DEPT (M)
Res (OHMM) 0.2 200.
DTCO (US/F) 140. 40.
RhoGard (gm/cc) 1.95 2.95
NPHI (V/V) 0.45 -0.15
OBPres (psi) 0. 12000.
PP_Son (psi) 0. 12000.
PPG_Son (psi/ft) 0. 1.
MWt (psi/ft) 0 1
Top of Laurel Fm 2685m
Top of overpress 3090
base of Laurel Fm 3311m
2700
2800
2900
3000
3100
3200
3300
Yulleroo-2 (DT/NPHI)
Depth (m)
Yulleroo-2 (DT/RhoGrad)
Depth (m)

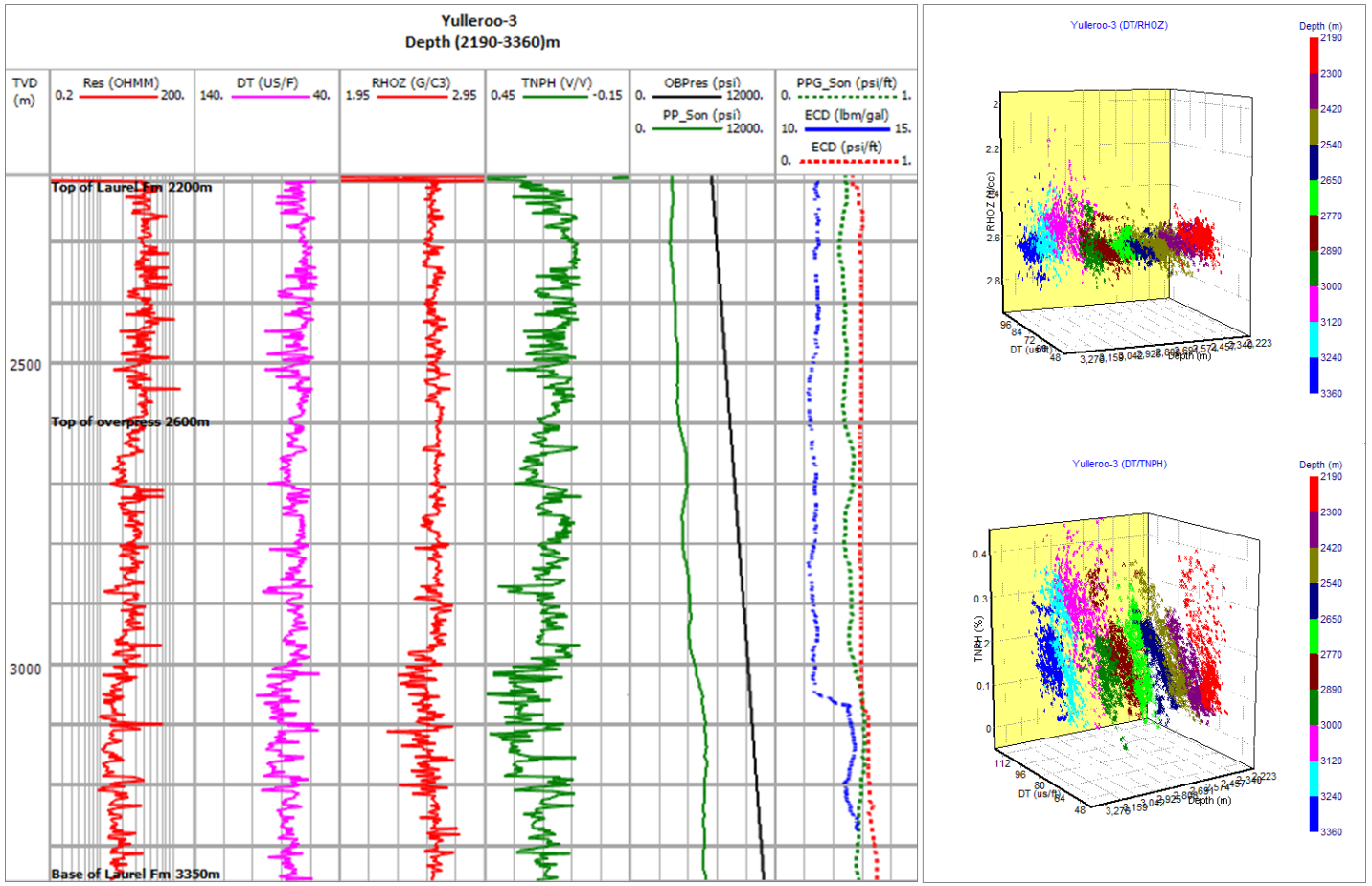
Yulleroo-3
Depth (2190-3360)m
TVD (m)
Res (OHMM) 0.2 200.
DT (US/F) 140. 40.
RHOZ (G/C3) 1.95 2.95
TNPH (V/V) 0.45 -0.15
OBPres (psi) 0. 12000.
PP_Son (psi) 0. 12000.
PPG_Son (psi/ft) 0. 1.
ECD (lbm/gal) 10. 15.
ECD (psi/ft) 0. 1.
Top of Laurel Fm 2200m
Top of overpress 2600m
Base of Laurel Fm 3350m
2500
3000
Yulleroo-3 (DT/RHOZ)
Depth (m)
RHOZ (g/cc)
DT (us/ft)
Depth (m)
Yulleroo-3 (DT/TNPH)
Depth (m)
TNPH (%)
DT (us/ft)
Depth (m)

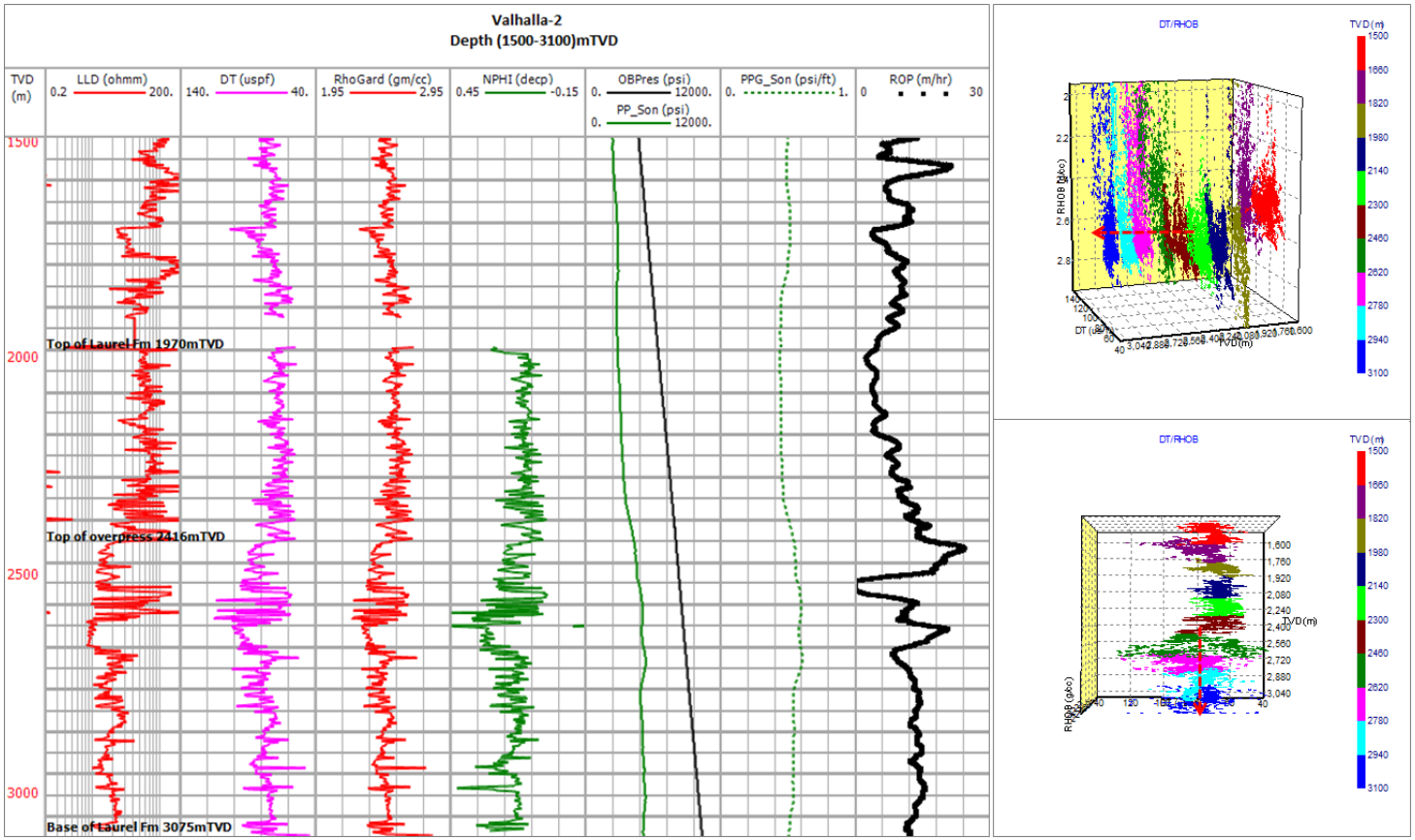
Valhalla-2
Depth (1500-3100)mTVD
TVD (m)
LLD (ohmm) 0.2 200.
DT (uspf) 140. 40.
RhoGard (gm/cc) 1.95 2.95
NPHI (decp) 0.45 -0.15
OBPres (psi) 0. 12000.
PP_Son (psi) 0. 12000.
PPG_Son (psi/ft) 0. 1.
ROP (m/hr) 0 30
1500
2000
2500
3000
Top of Laurel Fm 1970mTVD
Top of overpress 2416mTVD
Base of Laurel Fm 3075mTVD
DT/RHOB
TVD(m)
RHOB (gpc)
DT (uspf)

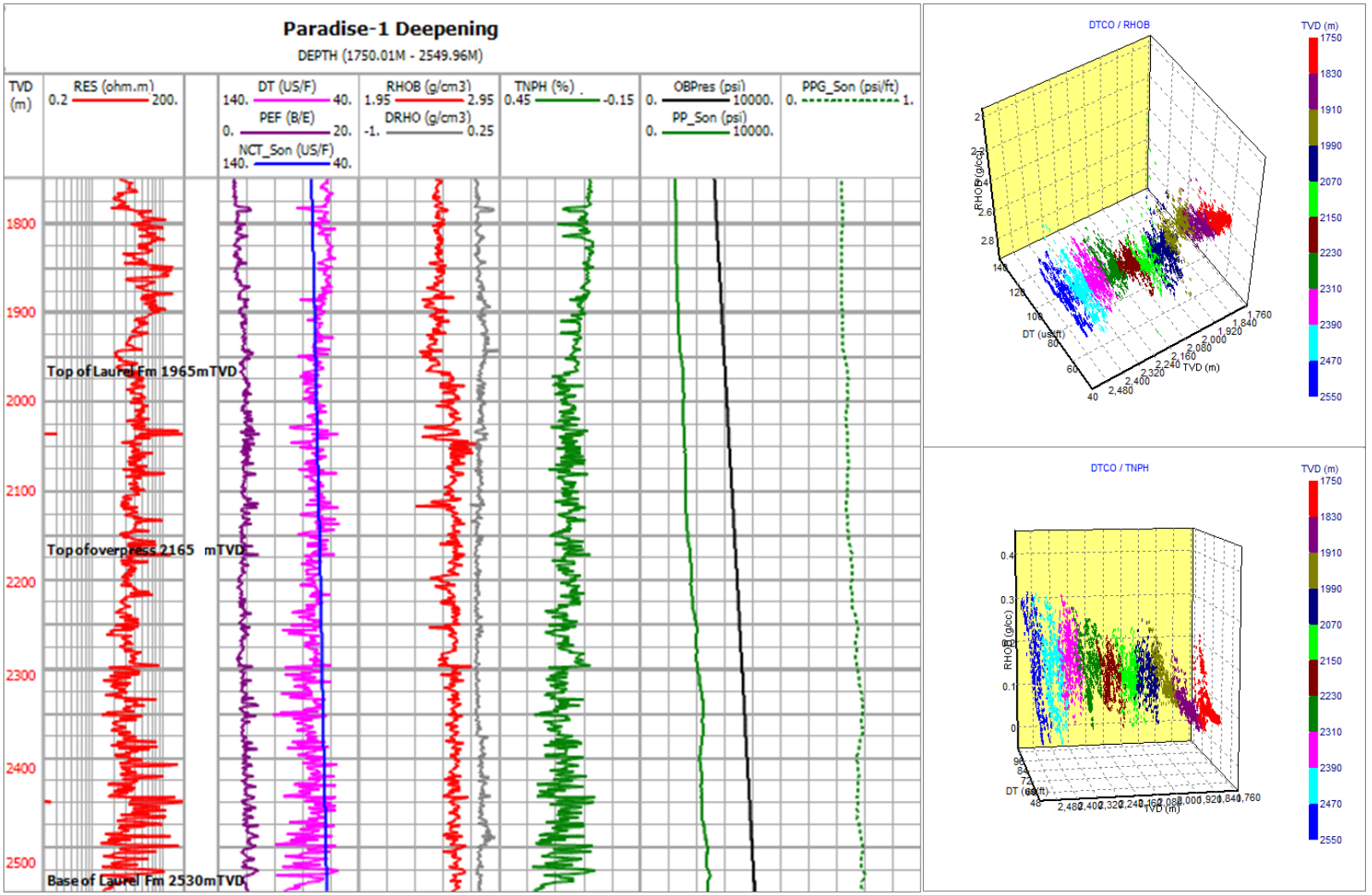
Paradise-1 Deepening
DEPTH (1750.01M - 2549.96M)
TVD (m)
RES (ohm.m) 0.2 200.
DT (US/F) 140. 40.
PEF (B/E) 0. 20.
NCT_Son (US/F) 140. 40.
RHOB (g/cm3) 1.95 2.95
DRHO (g/cm3) -1. 0.25
TNPH (%) 0.45 -0.15
OBPres (psi) 0. 10000.
PP_Son (psi) 0. 10000.
PPG_Son (psi/ft) 0. 1.
1800
1900
2000
2100
2200
2300
2400
2500
Top of Laurel Fm 1965mTVD
Top of overpress 2165 mTVD
Base of Laurel Fm 2530mTVD
DTCO / RHOB
TVD (m)
RHOB (g/cc)
DT (us/ft)
TVD (m)
DTCO / TNPH
TVD (m)
RHOB (g/cc)
DT (us/ft)
TVD (m)

Appendix 2b Pressure-depth plots, well lo data and cross-plots for the wells that exhibited normal pore pressure in the Laurel Formation and drilled in the Lennard Shelf Area

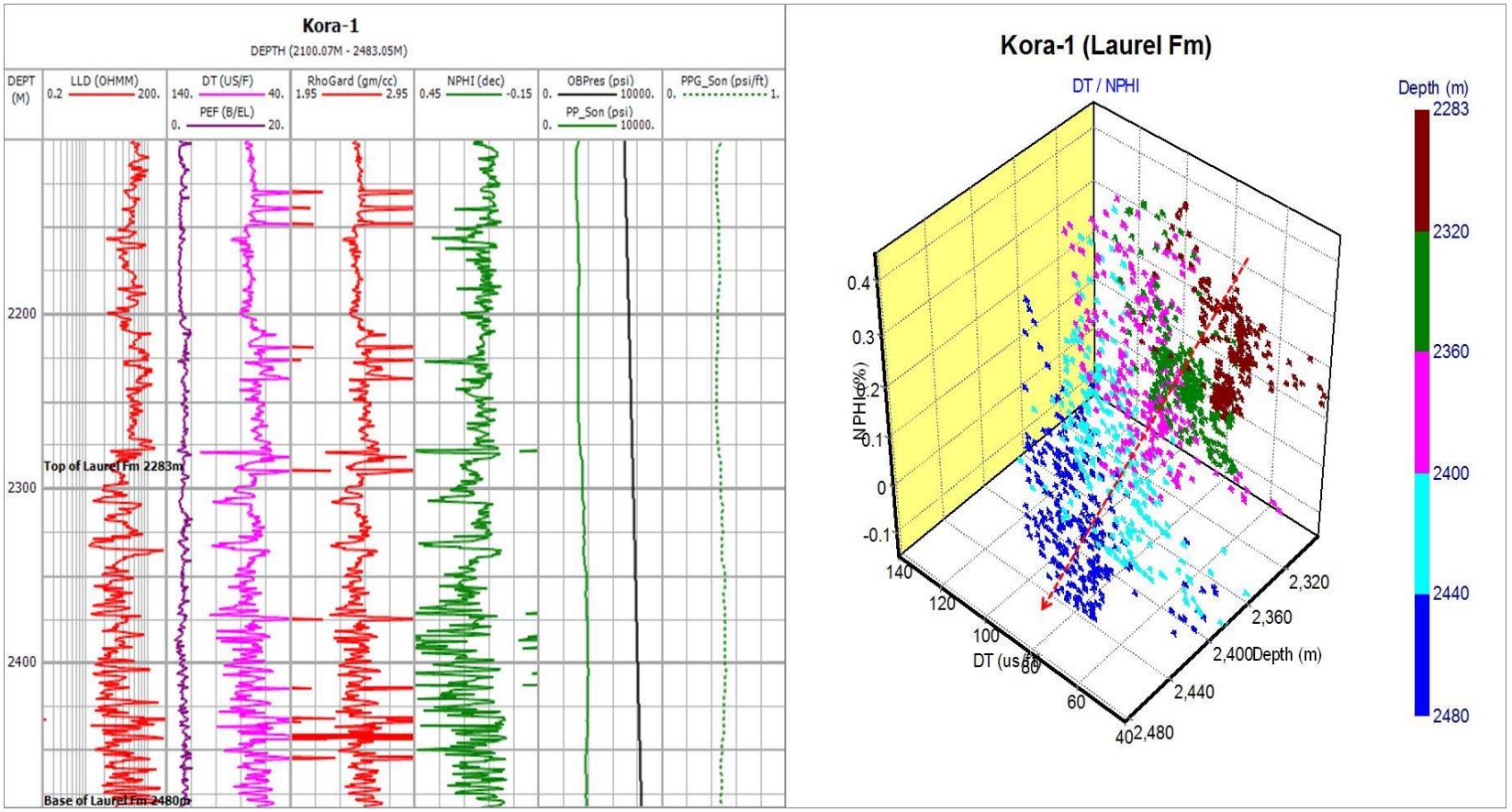
Kora-1
DEPTH (2100.07M - 2483.05M)
DEPT (M)
LLD (OHMM)
0.2
200.
DT (US/F)
140.
40.
PEF (B/EL)
0.
20.
RhoGard (gm/cc)
1.95
2.95
NPHI (dec)
0.45
-0.15
OBPres (psi)
0.
10000.
PP_Son (psi)
0.
10000.
PPG_Son (psi/ft)
0.
1.
2200
2300
2400
Top of Laurel Fm 2283m
Base of Laurel Fm 2480m
Kora-1 (Laurel Fm)
DT / NPHI
Depth (m)
2283
2320
2360
2400
2440
2480
NPHI (%)
0.4
0.3
0.2
0.1
0
-0.1
140
120
100
DT (us/ft)
80
60
40
2,320
2,360
2,400
Depth (m)
2,440
2,480

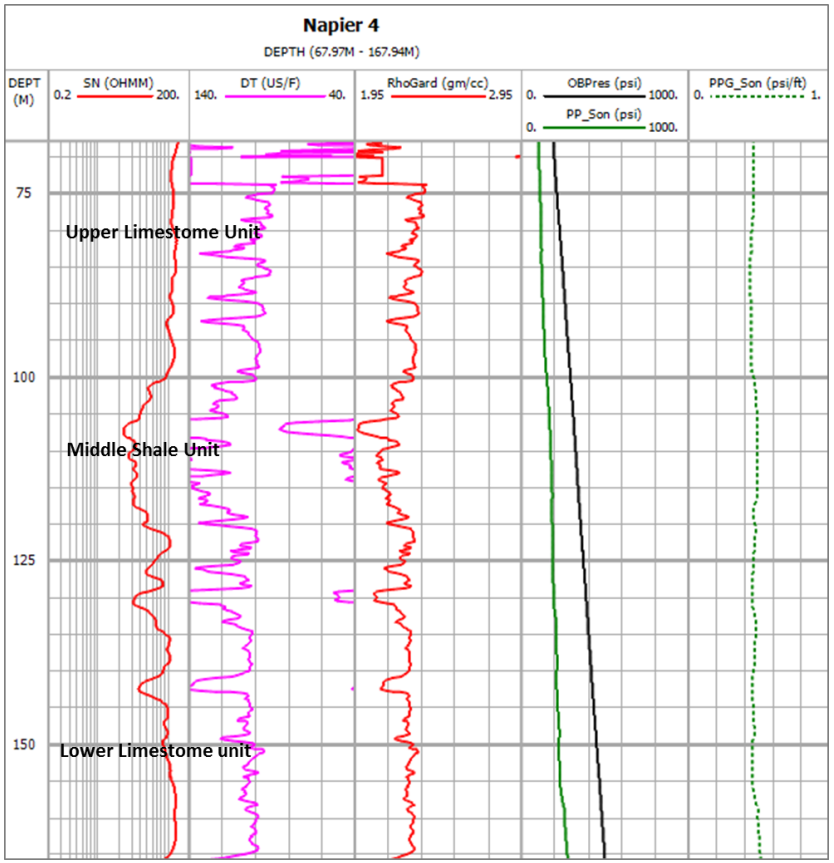
Napier 4
DEPTH (67.97M - 167.94M)
DEPT (M)
SN (OHMM) 0.2 200.
DT (US/F) 140. 40.
RhoGard (gm/cc) 1.95 2.95
OBPres (psi) 0. 1000.
PP_Son (psi) 0. 1000.
PPG_Son (psi/ft) 0. 1.
75
100
125
150
Upper Limestome Unit
Middle Shale Unit
Lower Limestome unit

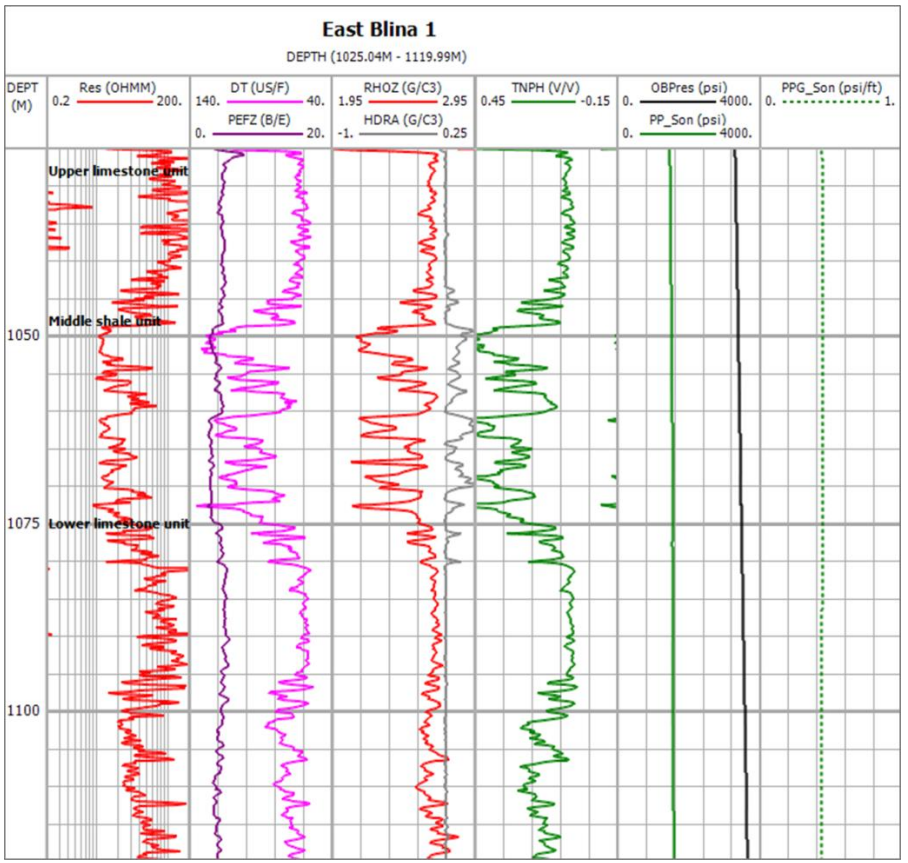
East Blina 1
DEPTH (1025.04M - 1119.99M)
DEPT (M)
Res (OHMM) 0.2 200.
DT (US/F) 140. 40.
PEFZ (B/E) 0. 20.
RHOZ (G/C3) 1.95 2.95
HDRA (G/C3) -1. 0.25
TNPH (V/V) 0.45 -0.15
OBPres (psi) 0. 4000.
PP_Son (psi) 0. 4000.
PPG_Son (psi/ft) 0. 1.
1050
1075
1100
Upper limestone unit
Middle shale unit
Lower limestone unit

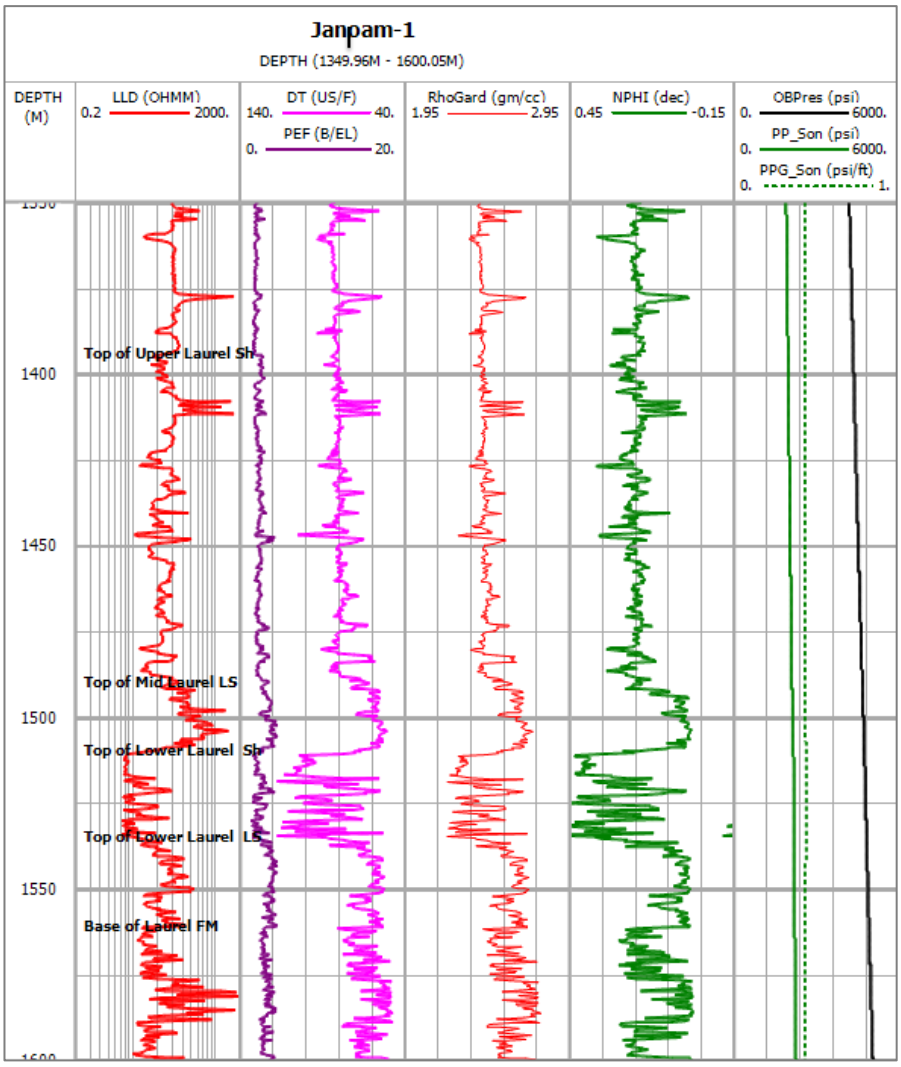
Janpam-1
DEPTH (1349.96M - 1600.05M)
DEPTH (M)
LLD (OHMM)
0.2
2000.
DT (US/F)
140.
40.
PEF (B/EL)
0.
20.
RhoGard (gm/cc)
1.95
2.95
NPHI (dec)
0.45
-0.15
OBPres (psi)
0.
6000.
PP_Son (psi)
0.
6000.
PPG_Son (psi/ft)
0.
1.
1400
1450
1500
1550
Top of Upper Laurel Sh
Top of Mid Laurel LS
Top of Lower Laurel Sh
Top of Lower Laurel LS
Base of Laurel FM

Appendix 2c geochemical data from various wells drilling in the Caning Basin

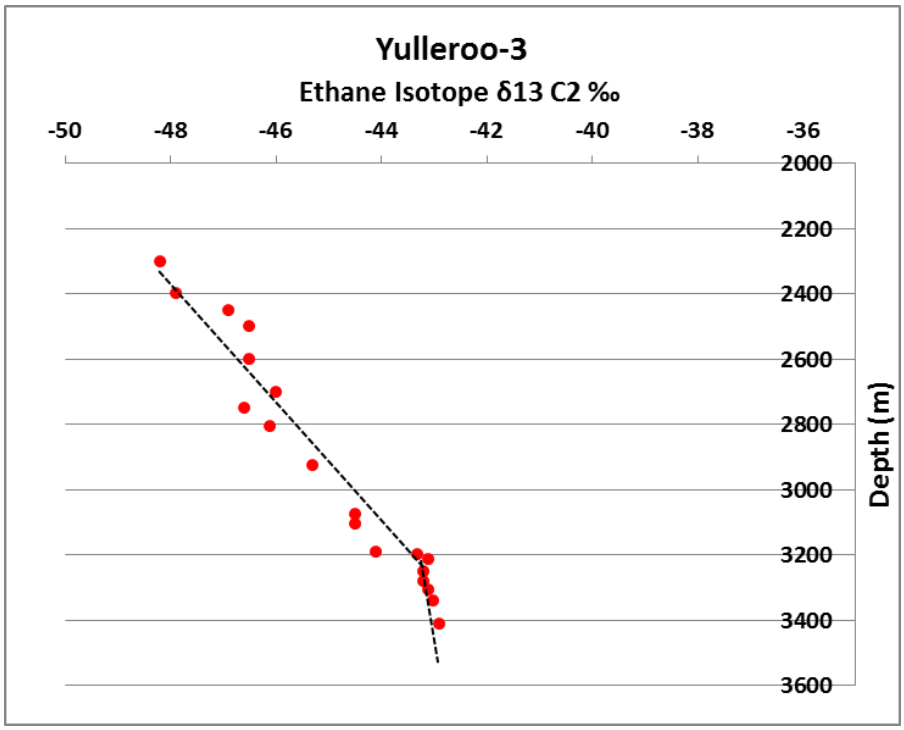

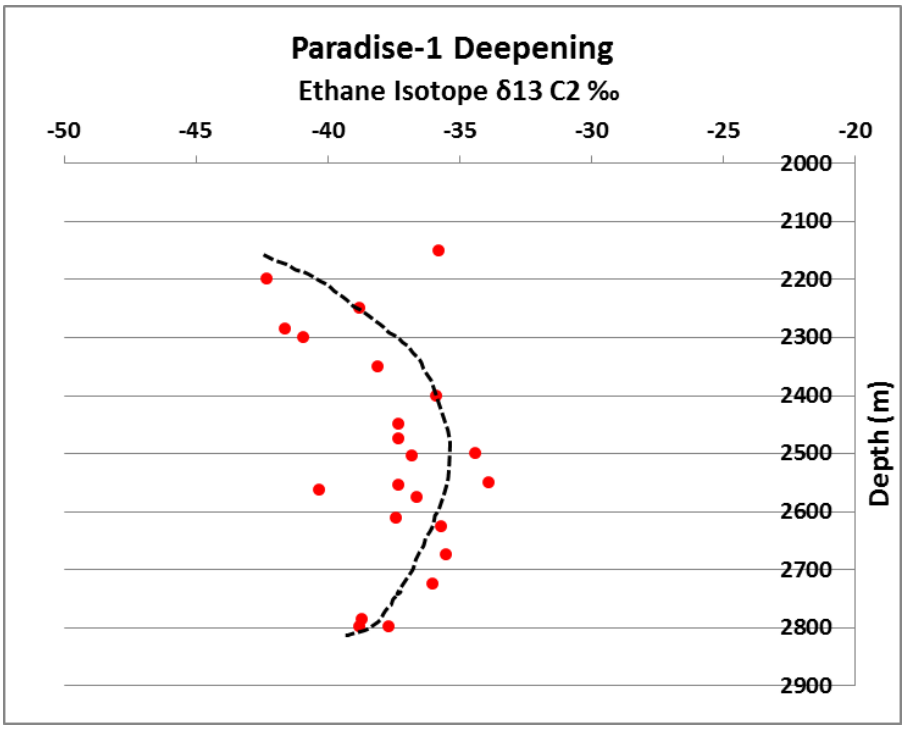

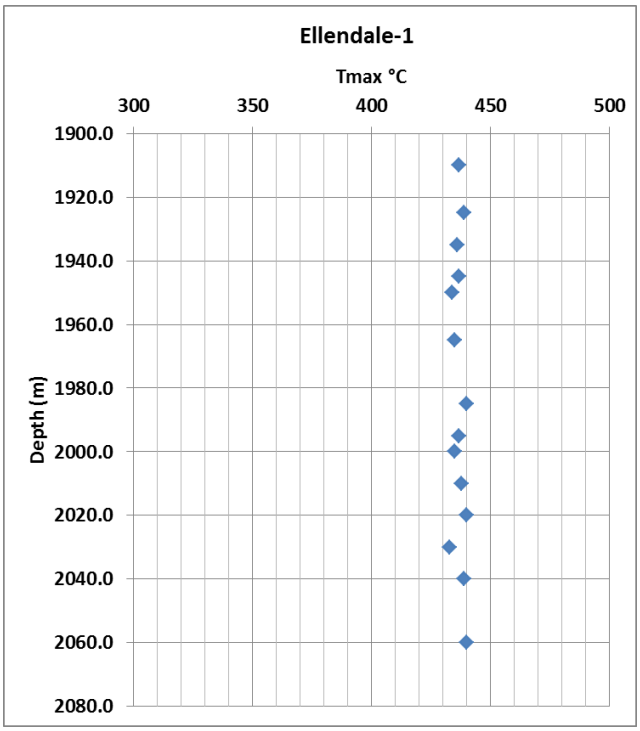
Ellendale-1
Tmax °C
300
350
400
450
500
Depth (m)
1900.0
1920.0
1940.0
1960.0
1980.0
2000.0
2020.0
2040.0
2060.0
2080.0